

Advanced Photovoltaic Solar Array Design

Final Technical Report (CDRL 008)

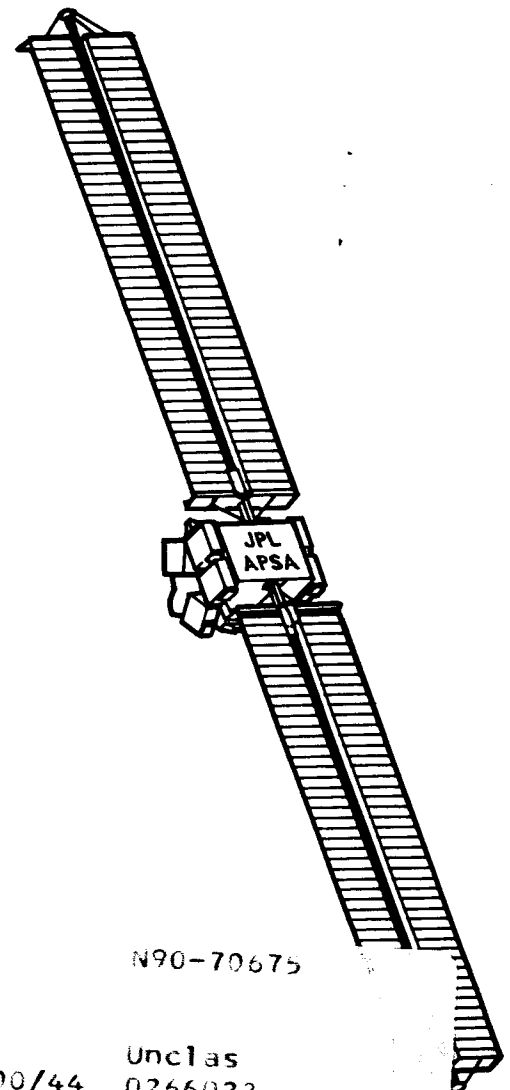
3 November 1986

Prepared by:
Engineering and Test Division
TRW Space & Technology Group
One Space Park
Redondo Beach, CA 90278

JPL Contract No. 957358 (NAS7-918)
TRW Report No. 46810-6004-UT-00

Prepared for:
Jet Propulsion Laboratory
California Institute of Technology
4800 Oak Grove Drive
Pasadena, CA 91109

(NASA-CR-186345) ADVANCED PHOTOVOLTAIC
SOLAR ARRAY DESIGN Final Technical Report
(TRW Space Technology Labs.) 272 p



N90-70675

00/44 Unclass 0266022

Advanced Photovoltaic Solar Array Design

Final Technical Report (CDRL 008)

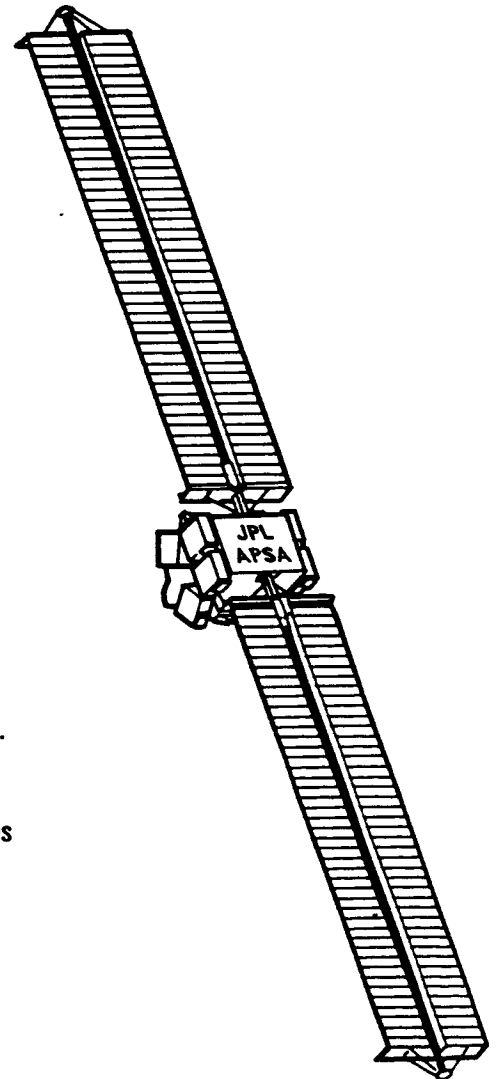
3 November 1986

Prepared by:
Engineering and Test Division
TRW Space & Technology Group
One Space Park
Redondo Beach, CA 90278

JPL Contract No. 957358
TRW Report No. 46810-6004-UT-00

This work was performed for the Jet Propulsion Laboratory, California Institute of Technology, sponsored by the National Aeronautics and Space Administration, under Contract NAS7-918. Reference herein to any specific commercial product, process, or service by trade name, trademark, manufacturer, or otherwise, does not constitute or imply its endorsement by the United States Government, TRW, or the Jet Propulsion Laboratory, California Institute of Technology

The results and conclusions in this report are those of the author, and should not be interpreted as an endorsement by the United States Government or the Jet Propulsion Laboratory, California Institute of Technology.



ABSTRACT

The objective of this study was to define the design of an ultralightweight, high-performance, advanced photovoltaic solar array that would be suitable for all shuttle-launched, long-term, non-Space Station missions for NASA and U.S. commercial space organizations. The array design had the following performance goals: (1) beginning-of-life (BOL) power output of 8 to 12 kW at a specific power greater than 130 W/kg in a geosynchronous orbit, (2) end-of-life (EOL) specific power greater than 105 W/kg after 10 years of operation, (3) EOL power density greater than 110 W/m², (4) a design based on a technology maturity such that a prototype wing could be built within 15 months after the completion of the design definition study.

Through a series of design trades and an evaluation of existing and near-term photovoltaic component and structural systems technology, a design for a two-wing flatpack, foldout, flexible blanket solar array was developed that utilized thin (63 μ m) silicon cell modules and a canister-deployed continuous longeron lattice mast system. The estimated performance of the baseline design was as follows: (1) 10.4 kW (BOL) array with a BOL specific power of 136 W/kg; (2) an EOL specific power of 96.7 W/kg with an EOL power density of 95 W/m²; (3) deployed frequency and strength of 0.10 Hz and 0.015 g, respectively. An implementation plan was developed for the fabrication of a prototype wing including engineering design drawings and budgetary and planning (B&P) schedule and cost. The prototype wing can be constructed within a 10-month period. System-level design verification tests can be completed within a subsequent 5-month period.

The array design can be utilized for other orbital missions (near earth orbit and interplanetary) or meet other functional requirements with minimum modifications. The modifications will not significantly decrease specific power, power density, strength, or stiffness characteristics.

FOREWORD

This is the final technical report on the Advanced Photovoltaic Solar Array (APSA) Design Definition Study, prepared by TRW Space & Technology Group (S&TG), Redondo Beach, California, for the California Institute of Technology, Jet Propulsion Laboratory (JPL), Pasadena, California, under JPL Contract 957358 (NAS7-918). The JPL technical monitor was Mr. P. Stella. This report covers the entire Phase I program conducted over the period October 1985 through August 1986.

The program at TRW S&TG was performed under the auspices of the Controls and Mechanical Systems Operation (CMSO) of the Engineering and Test Division, Mr. C. D. Kirby, CMSO Manager. TRW Program Manager was Mr. R. M. Kurland. Principal Engineer for Mechanical Design was Mr. W. J. Skinner. Principal Engineer for Electrical Design was Mr. M. E. Williams. Key subcontract support came from AEC-Able Engineering, Goleta, California (Mr. M. D. Benton) and Astro Aerospace Corporation, Carpinteria, California (Mr. N. Peterson), for the design of deployable mast systems.

Several key engineers at TRW contributed to the success of the study. Their contributions are acknowledged below:

I. L. Allard	Mechanical Manufacturing Technology
J. M. Allen	Harness Design
K. S. Anderson	Dynamics Analysis
M. D. Cannady	Electrical Design
F. D. Cottrell	Materials Engineering
A. J. Daniels	Harness Design
E. G. Dodge	Product Design
C. M. Donovan	Materials Engineering
A. Kaplan	Structures Analysis
H. G. Mesch	Electrical Manufacturing Technology
M. W. Mills	Electrical Design Technology
G. Pul	Structures Analysis
C. E. Smoot	Mechanical Design
N. J. Stevens	Environmental Compatibility
C. S. Susskind	Assembly and Test
C. S. Underwood	Environmental Compatibility
P. J. Walters	Product Design
R. S. Wolf	Structures Analysis

REPORT ORGANIZATION

The report consists of six main sections. Nomenclature and Terminology are contained on pages immediately following the list of Illustrations and Tables. Sections 1 and 2, Introduction and Summary, respectively, provide the reader with an overview of the program background and key results. Section 2 includes a brief description of the array design and its predicted electrical and mechanical performance, the utility of the array design for a variety of missions and functional requirements, and a description of the recommended prototype wing configuration to be fabricated and tested under Phases II and III of the APSA program. Subsequent report sections provide details of trade studies and analyses performed in defining the array design and an implementation plan for the prototype wing.

Section 3, Preliminary design Results, presents the results of the electrical, mechanical, and configurational trade studies and analyses on all aspects of the array design, the selection and rationale for the preferred options, and the initial estimates of array performance in terms of weight, size, specific power, and power density for the baseline mission (10 kW [BOL] array for a 10-year geosynchronous mission). These results were presented in the Preliminary Design Review Data Package (Reference 1).

Section 4, Baseline Design Definition, presents details of the recommended array design and a revised estimate of array performance. These results, along with the information in Section 5, were presented in the Final Design Review Data Packages (References 2 and 3). Engineering drawings of the array components and layout are contained in Volume 2 of the Final Design Review Data Package (Reference 3). The utility of the array design for other near-earth or planetary missions is briefly discussed along with the accommodation of other functional requirements. Advanced technology items are also indentified that have the potential to improve the present estimates of array performance.

Section 5, Prototype Wing Implementation Plan, presents details of the recommended prototype wing design needed to demonstrate the feasibility and performance characteristics of the array configuration. The approach to fabrication, assembly, and integration of the wing is discussed, along with recommended component development tests and an implementation schedule to fabricate the prototype wing (Phase II of APSA) and to test the prototype wing (Phase III of APSA).

Section 6, Conclusions and Recommendations, presents the key conclusions drawn form the Phase I study and makes recommendations for future activities. Section 7 identifies any new technology developed under the study. The Appendix summarizes the results of a market survey, concerning the utility of an array of this type, that was undertaken as part of the study.

CONTENTS

	Page
ABSTRACT	iii
FOREWORD	iv
REPORT ORGANIZATION	vii
NOMENCLATURE AND TERMINOLOGY	xxiii
1. INTRODUCTION	1-1
1.1 Background	1-1
1.2 Scope	1-2
1.3 Array Performance Goals	1-3
1.4 Technical Approach	1-7
2. SUMMARY	2-1
2.1 Array Design	2-11
2.2 Array Performance	2-11
2.3 Design Utility	2-11
2.4 Prototype Wing Description	2-18
2.5 Design Implementation Risk	2-20
3. PRELIMINARY DESIGN RESULTS	3-1
3.1 Array Configuration	3-1
3.2 Mechanical Design Trades	3-5
3.2.1 Blanket Assembly	3-5
3.2.2 Blanket Housing Assembly	3-17
3.2.3 Blanket Deployment System	3-34
3.2.4 Wing Integration Hardware	3-46
3.2.5 Wing Dynamic Characteristics	3-49
3.2.6 Wing Deflection Characteristics	3-56
3.3 Electrical Design Trades	3-61
3.3.1 Power Element Definition	3-61
3.3.2 Solar Cell Stack	3-61
3.3.3 Circuitry Layout	3-72

CONTENTS (Continued)

	Page
3.3.4 Blanket Electrical Harness	3-77
3.3.5 Circuit Protection	3-80
3.3.6 Environmental Interactions	3-83
3.4 Weight Trends	3-85
3.5 Array Performance Trends	3-91
3.5.1 Specific Power	3-91
3.5.2 Power Density	3-94
4. BASELINE DESIGN DEFINITION	4-1
4.1 Array Configuration	4-1
4.2 Mechanical Design	4-5
4.2.1 Blanket Assembly	4-5
4.2.2 Blanket Housing Assembly	4-10
4.2.3 Blanket Deployment System	4-16
4.2.4 Wing Integration Hardware	4-19
4.3 Electrical Design	4-25
4.3.1 Solar Panel Assembly	4-25
4.3.2 Blanket Electrical Harness	4-30
4.3.3 Circuit Protection	4-35
4.4 Array Performance	4-41
4.4.1 Electrical Output	4-41
4.4.2 Dynamics and Strength Characteristics	4-47
4.4.3 Specific Power and Power Density	4-49
4.5 Design Maturity/Equipment List	4-54
4.6 Utility to Other Missions/Requirements	4-56
4.6.1 Scalability to Other Power Levels	4-56
4.6.2 Accommodation of Advanced Photovoltaic Technology Components	4-58
4.6.3 Interplanetary Mission Performance	4-63
4.6.4 Low Earth Orbit Mission Performance	4-66
4.6.5 Spacecraft Integration Issues	4-76
4.6.6 Automatic Retraction Capability	4-76
4.7 Risk Assessment	4-78

CONTENTS (Continued)

	Page
5. PROTOTYPE WING IMPLEMENTATION PLAN	5-1
5.1 Prototype Wing Description	5-1
5.2 Fabrication Flow Plans	5-3
5.2.1 Mechanical Subassemblies	5-3
5.2.2 Electrical Subassemblies	5-6
5.2.3 Wing Integration	5-10
5.3 Component Development Tests	5-13
5.4 Development Schedule	5-14
6. CONCLUSIONS AND RECOMMENDATIONS	6-1
6.1 Conclusions	6-1
6.2 Recommendations	6-3
7. NEW TECHNOLOGY	7-1
APPENDIX	A-1
REFERENCES	R-1

ILLUSTRATIONS

	Page
i Generic Wing Structure (Rear Side Shown)	xxiv
1-1 Advanced Photovoltaic Solar Array Design Development Flow Plan	1-8
1-2 Nominal 5 kW (BOL) Wing Sizes and Aspect Ratios Used in Trade Studies	1-10
2-1 5.2 kW (BOL) GEO Deployed Solar Array Wing Configuration	2-2
2-2 Detail of Accordion Folding and Definition of Solar Panel Assembly	2-3
2-3 Stowed Configuration of 5.2 kW (BOL) GEO Solar Array Wing (Viewed from Lid Structure)	2-4
2-4 Stowed Configuration of 5.2 kW (BOL) GEO Solar Array Wing (Viewed from Pallet with Latching/Release Mechanism)	2-5
2-5 Blanket Deployment Mast System	2-6
2-6 Schematic of Solar Panel Assembly Circuitry with Summary Designs Features	2-8
2-7 Typical Solar Panel Showing Layout of Solar Cell Modules and Electrical Harness	2-9
2-8 BOL and EOL Solar Array Electrical Performance (Two Wings), 10-Year Geosynchronous Mission	2-12
2-9 Effect of Array Power Level on BOL and EOL Specific Power	2-15
2-10 Impact of Gallium Arsenide Solar Cell Modules on EOL Wing Performance	2-16
2-11 Impact of Thin Film Amorphous Silicon Solar Cell on BOL and EOL Wing Performance	2-17
2-12 Prototype Wing for Phases II and III of APSA Program (Option A Shown)	2-19
3-1 Stowed Wing Configuration Options	3-2
3-2 Wing Blanket/Mast Arrangement Options	3-3
3-3 Spacecraft/Wing Integration Options, 2.0 m (80 Inches) Wide Spacecraft Body, Horizontal Shuttle Stowage Mode	3-6
3-4 Spacecraft/Wing Integration Options, 2.5 m (100 Inches) Wide Spacecraft Body, Horizontal Shuttle Stowage Mode	3-7

ILLUSTRATIONS (Continued)

	Page
3-5 Other Spacecraft/Wing Integration Options, 2.0 to 2.5 m (80 and 100 Inches) Wide Spacecraft, Horizontal Shuttle Stowage Mode	3-8
3-6 Other Spacecraft/Wing Integration Options, Horizontal Shuttle Stowage Mode	3-9
3-7 Spacecraft/Wing Integration Options, Vertical Shuttle Stowage Mode	3-10
3-8 Accordion-Folded Blanket Assembly	3-12
3-9 Candidate Blanket Assembly Hinge Designs	3-16
3-10 Conceptual Configuration of Housing Structure	3-18
3-11 Required Sandwich Core Thickness for Lid and Pallet Structure of Tiedown Spacing and Design Criteria, 0.25 mm (10 mil) GY70 Graphite/Epoxy Facesheets	3-21
3-12 Required Sandwich Core Thickness for Lid and Pallet Structure as a Function of Tiedown Spacing, 0.25 m (10 mil) Facesheets Thickness	3-22
3-13 Areal Weight Trends for Lid and Pallet Structure as a Function ₃ of Tiedown Spacing, 0.25 mm (10 mil) Thick Facesheets, 50 kg/m ³ (3.1 pcf) Aluminum Honeycomb Core	3-23
3-14 Weight Trends for Mid Aspect Ratio Wing Blanket Housing Assembly as a Function of Number of Tiedown Pairs, Graphite/Epoxy Facesheet Sandwich Housing Construction	3-24
3-15 Stowed Pressure Relaxation Characteristics for Candidate Polyimide Foam Padding	3-26
3-16 Pushrod Stowed Blanket Preload Mechanism Concept	3-29
3-17 Torque Tube Stowed Blanket Preload Mechanism Concept	3-30
3-18 Blanket Tension System (Four to Eight Units per Blanket Assembly)	3-32
3-19 Blanket Guidewire Mechanism Concept	3-33
3-20 Principal Mast System Options	3-40
3-21 Other mast System Options	3-41
3-22 ABLEMAST System Weight versus Deployed Wing Fundamental Frequency, Preliminary Estimates (Fiberglass Mast, Graphite/Epoxy Canister)	3-44

ILLUSTRATIONS (Continued)

	Page
3-23 ABLEMAST System Eight versus Deployed Wing Strength, Preliminary Estimates (Fiberglass Mast, Graphite/Epoxy Canister)	3-45
3-24 Attachment of Blanket Housing Assembly to Mast System	3-47
3-25 Mast Tip Fitting Connecting Lid Structure to Outboard End of Mast	3-48
3-26 NASTRAN Finite Element Models Used for Dynamic and Deflection Analyses	3-50
3-27 Effect of Blanket Tension and Mast Stiffness on Deployed Wing Frequency, 4.34 Aspect Ratio Wing	3-51
3-28 Cantilevered Deployed Mode Shapes for 4.34 Aspect Ratio Wing (Blanket Tension = 18 N [4 pounds]; $EI_m = 1.18 \times 10^3 \text{ N-m}^2$ [$0.64 \times 10^6 \text{ lb-in}^2$]; $GJ_m = 86 \text{ N-m}^2$ [$3 \times 10^4 \text{ lb-in}^2$])	3-53
3-29 Effect of Mast Stiffness on Deployed Wing Frequency (4.34 Aspect Ratio Wing)	3-54
3-30 Effect of Number of Blanket/Mast Intermediate Attachments on Wing Frequency; 10 kW (BOL) Wing; AR - 7:1, 0.36 m (14 inches) Diameter Mast; 90 N (20 pounds) Blanket Tension. (Note: Only Full Integer Conditions Apply.)	3-55
3-31 Deployed Wing Modal Frequency vs. Blanket Cant Angle (Blanket Tension = 18.0 N [4 pounds], $EI_m = 1.8 \times 10^3 \text{ N-m}^2$ [$0.64 \times 10^6 \text{ lb-in}^2$], $GJ_m = 86 \text{ N-m}^2$ [$3 \times 10^4 \text{ lb-in}^2$] Blanket Tensioning Device Spring Constant = 1760 N/m [10 lb/in])	3-57
3-32 Deployed Wing Modal Frequency vs. Tensioning Device Spring Constant (Blanket Tension = 18.0 N [4 pounds], $EI_m = 1.8 \times 10^3 \text{ N-m}^2$ [$0.64 \times 10^6 \text{ lb-in}^2$], $GJ_m = 86 \text{ N-m}^2$ [$3 \times 10^4 \text{ lb-in}^2$], 15-degree Cant Angle)	3-57
3-33 Cantilevered Equilibrium Shape of Wing	3-58
3-34 Cantilevered Deflected Shape of Wing (0.02 g Quasi-Static Uniformly Distributed Load Normal to Blanket Plane)	3-58
3-35 Cantilevered Mast Tip Deflection Versus Mast Bending Stiffness (0.02 g Quasi-Static Uniformly Distributed Load Normal to Blanket Plane)	3-59

ILLUSTRATIONS (Continued)

	Page
3-36 Deflection of Center Region of Blanket Relative to Its Ends Versus Blanket Tension (0.02 g Quasi-Static) Uniformly Distributed Load Normal to Blanket Plane)	3-59
3-37 Primary Electrical Power Elements	3-62
3-38 Primary Electrical Power Flow	3-63
3-39 The Effect of Silicon Cell Thickness on Specific Power and Power Density Characteristics	3-66
3-40 In-Plane Single Loop Discrete Interconnector	3-73
3-41 Blanket Circuit Configuration, Wing Aspect Ratio = 2.40 (BOL/EOL Wing Power = 4800/3500 Watts for 24-Cell-Covered Panel Wing)	3-74
3-42 Blanket Circuit Configuration, Wing Aspect Ratio = 5.0 (BOL/EOL Wing Power = 4800/3500 Watts for 36-Cell-Covered Panel Wing)	3-75
3-43 Blanket Circuit Configuration, Wing Aspect Ratio = 8.5 (BOL/EOL Wing Power = 4800/3500 Watts for 48-Cell-Covered Panel Wing)	3-76
3-44 Comparative Thickness of Solar Cell Stack and Flexible Printed Circuit Electrical Harness Using 2-Ounce Copper	3-81
3-45 Harness Hinge and Splice Details	3-81
3-46 Conceptual Arrangement of Diode Box/Blanket Harness/SADA Harness Interface	3-82
3-47 Conceptual Implementation of Flatpack Bypass Diodes for Shadow Protection on Panel Layout	3-84
3-48 NASCAP Array Charging Analysis Model	3-86
3-49 Negative Voltages Computed Under Moderate GEO Substorm Environment (Sunlight Charging)	3-87
3-50 Negative Voltages Computed Under Severe GEO Substorm Environment (Sunlight Charging)	3-87
3-51 Effect of Key Array Design Parameters on Specific Power Performance	3-93
4-1 5.2 kW (BOL) GEO Deployed Solar Array Wing Configuration	4-2
4-2 Stowed Configuration of 5.2 kW (BOL) GEO Solar Array Wing (Viewed from Lid Structure)	4-3

ILLUSTRATIONS (Continued)

	Page
4-3 Stowed Configuration of 5.2 kW (BOL) GEO Solar Array Wing (Viewed from Pallet Structure with Latching/Release Mechanism)	4-4
4-4 Installation of Solar Array on Spacecraft	4-6
4-5 Flexible Blanket Solar Panel Assembly (SPA) Substrate	4-7
4-6 SPA Substrate Details	4-8
4-7 Flexible Blanket Leader Panel Assemblies	4-9
4-8 Blanket Housing Lid Panel Assembly Structure GY70 (Graphite/Epoxy Facesheets, Aluminum Honeycomb Core)	4-11
4-9 Blanket Housing Pallet Panel Assembly Structure (Graphite/Epoxy Facesheets, Aluminum Honeycomb Core)	4-12
4-10 Stowed Blanket Flexible Polyimide Foam Isolation Padding Assembly (Bonded to inner Surface of Lid and Pallet Structures)	4-13
4-11 Stowed Blanket Preload/Release Torque Tube Mechanism (Plan View)	4-14
4-12 Stowed Blanket Preload/Release Torque Tube Mechanism (Cross-Sectional View)	4-15
4-13 Negator Spring Blanket Tension Unit (Seven Required at 9N or 2 lbf per Unit)	4-17
4-14 Negator Spring Tensioned Guidewire Mechanism (2 Required at 5 N or 1 lbf per Unit)	4-18
4-15 Baseline Blanket Deployment Mast System	4-20
4-16 Mast System Details	4-21
4-17 Effects of Deployed Wing Strength on Mast System Weight (Canister Deployed Fiberglass Continuous Tri-Longeron ABLEMAST)	4-22
4-18 Mast Tip Fitting Connecting the Lid Structure to Outboard End of Mast	4-24
4-19 Thin Silicon Solar Cell Stack	4-26
4-20 In-Plane Single Loop Discrete Interconnector	4-27
4-21 Schematic of Three-Panel SPA Electrical Circuitry	4-28
4-22 Flexible Blanket Solar Panel Assembly (SPA) (First of Three Panels in SPA Shown)	4-29

ILLUSTRATIONS (Continued)

	Page
4-23 String Turnaround and Termination Details	4-31
4-24 Outboard Termination Segment of Electrical Harness	4-32
4-25 Solar Panel Assembly (SPA) Flexible Printed Copper Circuit Electrical Harness Segment	4-32
4-26 Inboard Termination Segment of Electrical Harness (Interface with Diode Box Shown)	4-33
4-27 Electrical Harness Segment Splice Pad Detail	4-34
4-28 Comparative Thickness of Electrical Harness to Solar Cell Stack	4-36
4-29 Electrical Harness Hinge Line and Splice Details	4-37
4-30 Details of Positive, Negative, and Panel Substrate Grounding Terminations for Electrical Harness	4-38
4-31 Location of Diode Box	4-39
4-32 Diode Box Assembly	4-40
4-33 Schematic Circuit Diagram of Diode Box (Left-Hand Harness Run Shown)	4-42
4-34 Diode Board Assembly Details	4-43
4-34 Diode Board Assembly Details	4-43
4-35 BOL and EOL Solar Array Electrical Performance (Two Wings), 10-Year Geosynchronous Mission	4-44
4-36 Solar Cell Stack Design Parameters	4-45
4-37 Baseline Wing Cantilevered Frequency and Mode Shape Characteristics	4-48
4-38 Stowed solar Array Wing, Shuttle Launch Interface Limit Loads	4-50
4-39 Wing Equilibrium Deflection Shape	4-51
4-40 Wing Deflected Shape Under Maximum Inertia Loading	4-52
4-41 Effect of Array Power level on BOL and EOL specific Power	4-57
4-42 Results of Parametric Study of GaAs Solar Cell Thickness and Efficiency	4-59
4-43 Results of Parametric Study of Thin Film Amorphous Silicon Cell Efficiency on Wing Performance	4-61

ILLUSTRATIONS (Continued)

	Page
4-44 State of the Art for Terrestrial Large Area Amorphous Modules in Terms of Conversion Efficiency Versus Module Size	4-62
4-45 Relative Effect of Interplanetary Distance on Solar Array Insolation	4-64
4-46 Solar Cell Stack Temperature Response of the APSA Array Due to Varying Solar Insolation	4-65
4-47 The Magnitude of LILT Effects on Cell Performance (Best and Worst Variations) Relative to a Cell Population that Normally Produces Equal Output	4-67
4-48 The Range of Possible Cell Efficiencies and Relative Power Output Under LILT Conditions for APSA	4-68
4-49 Kapton Mass Loss Weights	4-73
4-50 Changes in Environmental Conditions Over Orbit	4-73
4-51 Atomic Oxygen Density Profiles	4-74
4-52 Solar Activity Predictions	4-74
4-53 Projected Kapton Mass Loss per Year in Orbit Based on Velocity Effects, One-Side Erosion	4-75
5-1 Prototype Wing Configuration (Option A)	5-2
5-2 Solar Array Prototype Integration and Deployment Test Fixture	5-4
5-3 Blanket Manufacturing Flow Diagram	5-5
5-4 Semiautomated Solar Cell Stack Assembly and Panel Installation Line	5-7
5-5 Solar Cell Stack Assembly and Installation Flow Diagram	5-9
5-6 Cell Laydown Fixture (Concept Shown)	5-11
5-7 Wing Fabrication and Integration Flow Plan	5-12
5-8 Prototype Wing Development Schedule, Option A Wing Configuration, Phase II and Phase III Activities	5-15

TABLES

	Page
1-1 Performance Goals Advanced Photovoltaic Solar Array Design	1-4
1-2 Design Evaluation Criteria	1-6
2-1 Solar Array Wing Equipment List	2-10
2-2 BOL and EOL Design Factors Used for Sizing the Solar Array, 10-Year Geosynchronous Mission, Ceria-Doped Glass-Covered 10 -cm B-BSF/Al-BSR, 63 m Silicon Cell	2-13
2-3 Solar Array Performance Summary, 10-Year Geosynchronous Mission	2-14
3-1 Existing Experience for Blanket/Mast Arrangements	3-4
3-2 Blanket Substrate Material/Construction Options	3-13
3-3 Design Parameters for Housing Structure	3-19
3-4 Design Criteria for Housing Structure	3-19
3-5 Stowed Blanket Preload Mechanism Concepts	3-28
3-6 Candidate Blanket Deployment Mast Systems	3-35
3-7 Comparison of Mast System Performance	3-43
3-8 Potential Blanket/Mast Interference Under 0.02 g Quasi-Static Uniformly Distributed Loading Condition	3-60
3-9 Comparison of Solar Cell Module Trades	3-65
3-10 Solar Cell Options	3-67
3-11 Cover Glass Options	3-69
3-12 Cell Interconnection Options	3-71
3-13 Summary of Electrical Harness Design Trades	3-78
3-14 GEO Space Plasma Environments (Reference 5)	3-86
3-15 Wing Weight Summary, BOL/EOL Power of 4800/3500 Watts, $F_N = 0.15$ Hz, $N = 0.012$ g, 2.36 Wing Aspect Ratio	3-88
3-16 Wing Weight Summary, BOL/EOL Power of 4800/3500 Watts, $F_N = 0.12$ Hz, $N = 0.011$ g, 5.0 Wing Aspect Ratio	3-89
3-17 Wing Weight Summary, BOL/EOL Power of 4800/3500 Watts, $F_N = 0.11$ Hz, $N = 0.012$ g, 8.5 Wing Aspect Ratio	3-90

TABLES (Continued)

		Page
3-18	Specific Power Characteristics	3-92
3-19	EOL Power Density Performance Trends, Thin Silicon Solar Cell Stack Array	3-94
4-1	Comparison of Mast Design Options on Mast System Weight	4-23
4-2	BOL and EOL Design Factors Used for Sizing the Solar Array 10-Year Geosynchronous Mission	4-46
4-3	Baseline Solar Array Wing Weight Summary, BOL/EOL Power of 5200/3700 Watts, $F_n = 0.11$ Hz, $N = 0.015$ g	4-53
4-4	Solar Array Wing Equipment List	4-55
4-5	10-Year LEO APSA Solar Array Power Output Relative to GEO Performance	4-70
4-6	Susceptibility of Array Components to LEO Atomic Oxygen Erosion	4-72
4-7	Effect of Stowed Wing Configuration on Wing Performance	4-77

NOMENCLATURE AND TERMINOLOGY

To provide more clarity to the discussion in this Final Technical Report, the following illustration and lists of definitions and acronyms are provided. Figure i illustrates the generic flatpack, foldout, flexible blanket wing configuration.

DEFINITIONS

1. Solar array. All of the photovoltaic power generation wings on a spacecraft, including structural support elements, blanket tensioning devices, extension and retraction mechanisms, stowed blanket protection structure and mechanisms, blanket substrate, solar cell stacks, blanket electrical harness, circuit isolation diodes, electronic packages to activate/control deployment operations, and structural hardpoints. The wing orientation/power transfer mechanisms and transition harness from the wing orientation/power transfer mechanisms are not part of the solar array system. For most spacecraft applications, a solar array consists of two wings deployed from opposite sidewalls of the spacecraft. For geosynchronous spacecraft, the wings are typically attached and stowed on the north and south sidewalls of the spacecraft.
2. Wing. A solar cell blanket assembly with extension mast and associated mechanisms, containers, and housings.
3. Solar cell stack. A single solar cell with interconnectors attached (welded or soldered) and a solar cell cover glass bonded together. The stack assembly is also known as a cover integrated cell (CIC). This basic photovoltaic electrical generation unit is attached in series to other solar cell stacks in sufficient number to obtain a circuit module that produces the design bus voltage.
4. Solar panel. The part of the blanket assembly between adjacent fold lines, with interconnected solar cell stacks. The solar panel is the smallest unit of a solar panel assembly (SPA).
5. Solar panel assembly (SPA). A number of solar panels that are conducive to cost-effective fabrication and assembly of the total blanket assembly (BA). The SPA includes segments of the blanket harness.
6. Blanket assembly (BA). A group of SPAs and interconnected blanket harness, along with the appropriate number of leader panels that constitute the total electrical generation portion of the wing. In the case of a one-blanket wing, there is only one BA. In the case of a two-blanket wing, there are two BAs.
7. Blanket. A flexible structural accordion-folded membrane which serves as the substrate on which interconnected solar cell stacks and electrical harness runs are adhesively bonded.
8. Blanket harness. A grouping of conductors, typically located along the outer edges of the blanket assembly, for the purpose of transmitting the electrical power from the solar cell circuit modules on the solar panels to the isolation diodes at the base of the wing (located on the pallet structure).

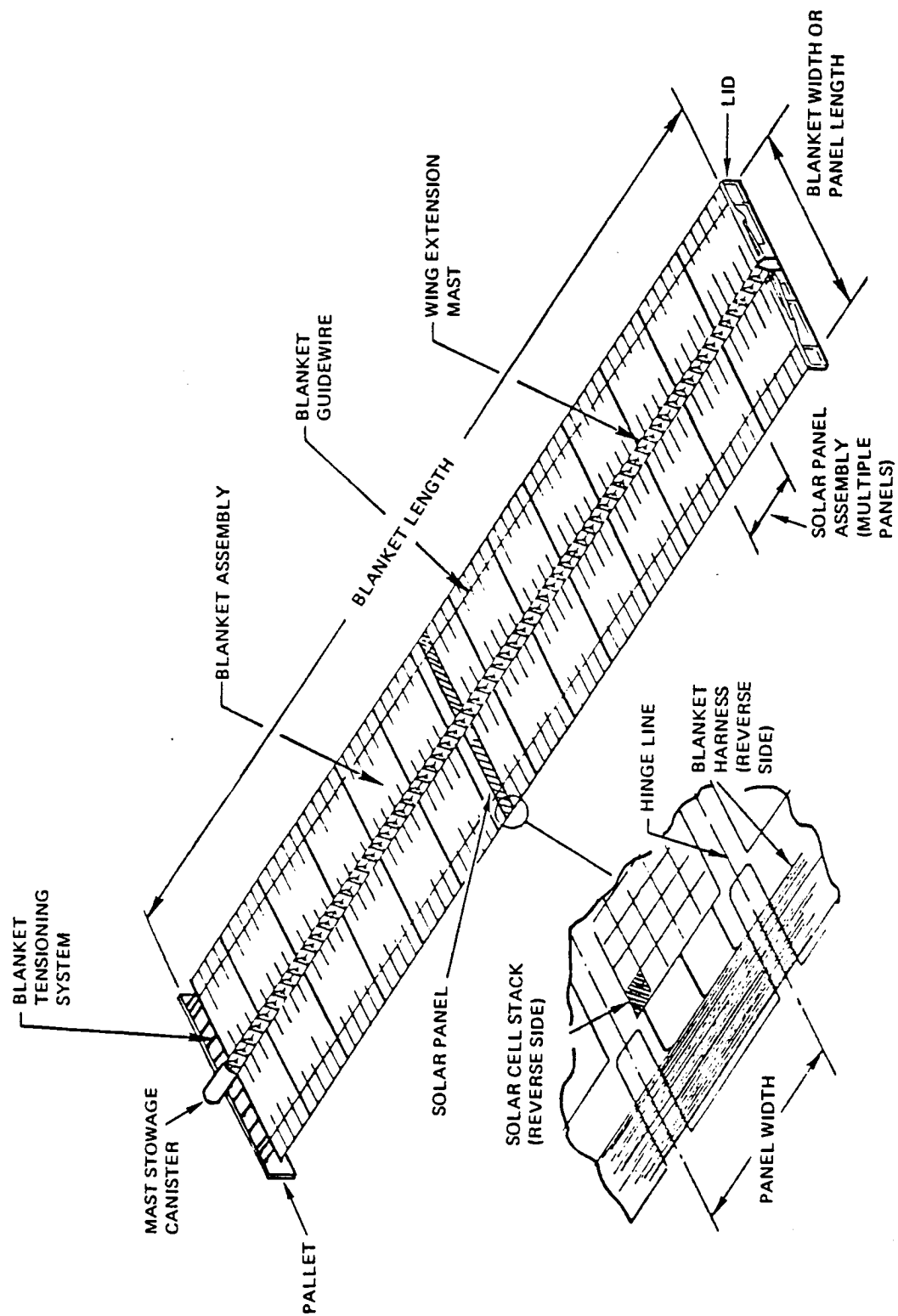


Figure i. Generic Wing Structure (Rear Side Shown)

9. Blanket housing assembly (BHA). Structural system consisting of a container (lid and pallet), lid latching/release mechanism, stowed blanket assembly preload mechanism, deployed blanket assembly tensioning mechanism, and deployed blanket guidewire mechanism. The primary purpose of the BHA is to protect the stored (folded) blanket assembly during the launch phase of the mission, help guide the blanket assembly during deployment (unfolding) or retraction (refolding) operations, and provide longitudinal tension on the fully deployed blanket assembly.
10. Blanket deployment mast assembly (BDMA). Structural system, consisting of an extendable element (boom or mast) whose primary function is to deploy the blanket assembly from its folded condition to its fully extended condition, a housing structure (canister) to contain the stowed extendable element, and any actuators and control electronics required to automatically operate the BDMA.

ACRONYMS LIST

ACS	attitude control system
ACT	advanced component technology
AMO	air mass zero
APSA	Advanced Photovoltaic Solar Array
AR	antireflective; aspect ratio
BA	blanket assembly
BDMA	blanket deployment mast assembly
BHA	blanket housing assembly
BOL	beginning of life
BSF	back surface field
BSR	back surface reflector
CIC	cover integrated cell
CTS	Canadian Technology Satellite
DMSP	Defense Meteorological Spacecraft Program
DoD	Department of Defense
DORA	double rollout array
E&TD	Engineering and Test Division (TRW)
EOL	end of life
ESD	electrostatic discharge
EVA	extravehicular activity
FDR	final design review
FEP	fluorinated ethylene propylene
FPC	flexible printed circuitry

FRUSA	flexible rollup solar array
FTR	final technical report
GEO	geosynchronous earth orbit
IR	infrared
IR&D	independent research and development
ITO	indium tin oxide
I	current
JPL	Jet Propulsion Laboratory (NASA)
LEO	low earth orbit
LMSC	Lockheed Missiles and Space Company
LSAT	large communications satellite (aka Olympus)
MANTECH	Manufacturing technology
NASA	National Aeronautics and Space Administration
OAST	Office of Aeronautics and Space Technology (NASA)
PEP	power extension package (shuttle power augmentation solar array)
PDR	preliminary design review
ROSA	rollout solar array
S&TG	Space & Technology Group (TRW)
SAFE	Solar Array Flight Experiment (on STS-41D)
SEPS	solar electric propulsion stage
SOLPRO	a solar flare proton model
SP	Space Platform (aka 25-kW Power Module)
SPA	solar panel assembly
ST	Space Telescope
STS	Space Transportation System
UV	ultraviolet
V	voltage
VDA	vacuum deposited aluminum

1. INTRODUCTION

1.1 BACKGROUND

Power requirements in the 5 to 25 kW range at beginning of life (BOL) are projected by NASA, DoD, and commercial spacecraft planners for future missions. In some instances, steady-state power requirements could grow to over 100 kW (BOL). These power requirements represent a significant increase in power over the 1 to 3 kW levels for current spacecraft missions. The primary method of obtaining that power will continue to be through the use of photovoltaic conversion planar solar arrays until such time as the feasibility/technology readiness is demonstrated for advanced techniques such as photovoltaic concentrator arrays, solar dynamic generators, or nuclear/radioisotope power sources.

High-power arrays can represent the largest (and sometimes the heaviest) element of all the spacecraft systems, so that array design (type and configuration) can have a significant influence on the spacecraft design. Since the array interacts extensively with the entire spacecraft, the design and technological trade-offs for the array system can extend to trade-offs for the entire spacecraft system.

For high-altitude earth orbits or interplanetary missions, the constraints on solar array mass, size, storage volume, and unattended long-term operation are dominant factors that govern the selection of the particular type of array. This is the result of the restricted booster capability to place heavy payloads into orbit. Even with the future availability of heavy-lift vehicles and space tugs (i.e., orbital maneuvering vehicles), payload mass and size will remain important factors because of the substantial increase in power demands. Another reason to reduce the mass and improve the photovoltaic performance of the array is so that more of the spacecraft mass fraction can be allocated to the orbital communications, observations, and other equipment packages on board the spacecraft.

These mass-critical, high-power missions favor the use of flexible blanket arrays because of their attendant high specific power (watts/kilogram), high packaging efficiency, and simple deployment systems. Present array technology using conventional silicon solar cells can provide array performance of 66 W/kg at 120 W/m² (BOL) for power levels above 25 kW. However, at lower power levels, the current designs lead to lower specific power performance because elements of the array system are not directly scalable with power level. This is especially true for the structure in which the packaged blanket is contained and the array deployment structure/mechanism.

Studies recently performed by NASA suggest that array systems having BOL specific power performance of over 130 W/kg in the 5 to 10 kW power range will be necessary for many future missions. An array with this capability could also provide a high-performance, cost-effective alternative to RTGs for interplanetary missions. The technology drive for these mission applications dictates continued improvement in the following areas:

1. Specific power (higher solar cell operating efficiency, reduction in solar array structure and solar cell module mass)

2. Power density (higher cell operating efficiency, increase in cell packing factor)
3. Stowage and deployment structure/mechanisms (high specific strength and stiffness, reduced mass).

However, these improvements can't be achieved at the expense of reduced system reliability or increased manufacturing/verification test complexity. The array design still must be able to ensure protection for the more fragile components (i.e., solar cell stacks) during launch and deployment operations. The tiedown/release/deployment mechanisms and structure must operate in reliable fashion to ensure extension of the array from its stowed configuration and provide adequate deployed strength and stiffness. The array system must be able to generate and transmit electrical power to the spacecraft bus after long-term (5 to 15 years) operation in space which is characterized by ultraviolet and charged particle environments, vacuum, deep temperature extremes, temperature cycling, debris/micrometeoroids, and spacecraft-induced vibro-acoustic loading environments. Finally, the array system must be producible and design-verifiable for a reasonable cost.

The Jet Propulsion Laboratory (JPL) of the California Institute of Technology has the responsibility for developing high-performance solar array technology to support the long-range objectives of the National Aeronautics and Space Administration (NASA). During the past 7 years, a broad base of technology, ranging from ultrathin silicon solar cells to new array structural concepts, has been funded through JPL programs sponsored by the NASA Office of Aeronautics and Space Technology (OAST). In addition to the NASA-sponsored work, there have been parallel and concurrent array technology developments sponsored by DoD and private industry, as well as Japan and the European space community. Based on the technology status of various array elements, it appears that the critical technology is available (or shortly will be available) to permit development and demonstration of an array that could exceed by a factor of two the specific power performance of the 66 W/kg flexible-blanket array that was developed (although not space qualified) by NASA-OAST during the 1970s and early 1980s.

The focus of the present JPL Advanced Photovoltaic Solar Array (APSA) program is to combine these separate advanced performance array element efforts and demonstrate a producible second-generation high-performance array system. JPL selected >130 W/kg (BOL) specific power and >135 W/m² power density as near-term performance goals (with long-term goals of >300 W/kg and >300 W/m² [BOL]). The second-generation APSA system could also be used as a testbed to evaluate advanced photovoltaic and structural elements as they become available to help attain the long-term performance goals. The objective of the current APSA program is to develop an array design such that a prototype system could be designed, fabricated, and ground-demonstrated by early 1988, with flight experiment demonstration by 1990 and/or transfer of the interim array system technology to an early 1990s space flight such as those planned under the Mariner Mark II program.

1.2 SCOPE

The objective of this study (which is considered to be Phase I of a multi-phase APSA program) was to define the design of an ultralightweight, high-performance, producible, advanced photovoltaic solar array that would be suitable

for all shuttle-launched, long-term, non-Space-Station missions for NASA and U.S. commercial space organizations. No hardware fabrication and component testing was required under Phase I.

A series of performance goals was established (see Section 1.3), against which the suitability and effectiveness of the design could be evaluated. While no specific mission or spacecraft was identified on which the solar array would be used, an arbitrary power level and orbital geometry were established for a point design (namely, 10 kW [BOL] two-wing array for a 10-year geosynchronous mission). The design goals selected implied that the array would represent a factor of 3 to 4 improvement in specific power performance over current operating arrays in the 5 to 10 kW power range.

Definition of the preferred array design included the development of suitable engineering drawings and layouts that would permit fabrication of a prototype wing, specification of a major parts list with source and space flight heritage, and development of an implementation plan for the fabrication of a prototype wing scheduled for Phase II of the program. The implementation plan included definition of the prototype wing configuration, fabrication flow plans, development schedules, and budgetary and planning cost estimates for Phase II. Definition and costing of design verification tests for Phase III were not considered part of the implementation plan, but instead would be developed under Phase II of the program.

1.3 ARRAY PERFORMANCE GOALS

Table 1-1 presents the solar array performance goals established by JPL at the start of the program, based on inputs from the two study contractors (TRW and LMSC). These goals were used to perform design trade studies during the preliminary design phase to establish a recommended final design concept and to better understand the sensitivity of key issues such as strength, stiffness, aspect ratio, and voltage level on the critical performance goals of specific power and power density. Based on the preliminary design data, it was decided to design the array for the high end of the strength/stiffness/voltage range studied (namely, 0.01 g ultimate deployed load, 0.10 Hz deployed cantilevered frequency, 200 volts open circuit voltage). This decision was influenced by a market survey performed as part of the study to assess the utility of the proposed advanced photovoltaic solar array being developed under this program (see Appendix for results of the survey).

While a point design was established to meet the above performance goals for a-10 kW (BOL) array for a 10-year geosynchronous mission, without any specific spacecraft in mind, it was also a study task to address broader aspects of the utility of the array design. Table 1-2 lists the key issues and factors of interest. These would be used to select the preferred design to carry into the prototype fabrication phase of the program. Array design performance was defined as the most important of the four criteria listed in Table 1-2, with the other three sharing equal but lesser importance. The factors under each criteria were neither weighted nor listed in any particular order of importance.

Table 1-1. Performance Goals Advanced Photovoltaic Solar Array Design

1. Array (two wings) power level of nominal 10 kW at beginning of life (BOL).
2. Primary purpose is to perform array design trades using 10-year geosynchronous earth orbit (GEO).
3. Compatible with standard shuttle launch environments.
4. BOL specific power at operating temperature in GEO of >130 W/kg at equinox conditions.
5. End-of-life (EOL) specific power at operating temperature after 10 years in GEO of >105 W/kg at equinox conditions.
6. EOL power density at operating temperature after ten 10 years in GEO of >110 W/m² at equinox conditions.
7. Design must be compatible with all aspects of the long-term design environment.
8. Technical maturity of the design to allow a fabrication contract for a prototype wing starting in September 1986.
9. Array design that is compatible with accommodating advanced technology components to improve performance beyond that for the prototype design.
11. Deployed stiffness and frequency are not specified; however, perform array design trades assessing impact of frequency on wing design and weight over the range 0.01 to 0.10 Hz (cantilevered).
12. On-orbit loads are not specified; however, perform array design trades using 0.002 g as a quasi-static ultimate load about any axis of the wing. Assess impact of load on wing design and weight over the range 0.001 to 0.01 g ultimate.
13. Partial extension, partial retraction, full retraction, and full restowage are not required.
14. For trade study, assume aspect ratio and wing length/width limitations are dictated by available array stowage volume in shuttle and deployed frequency/strength requirements.
15. Solar cell module circuitry as well as power harness, panel arrangement, and other wiring shall be such that current-induced magnetic fields and moments are minimized.

Table 1-1. Performance Goals Advanced Photovoltaic Solar Array Design
(Continued)

16. Array BOL and EOL voltage levels are not specified. For trade study assume voltage level is selected to be compatible with space environment and prudent electrical design practices, and conducive to reducing array weight. Voltage shall not exceed 200 volts at BOL open circuit, normal operating temperature.
17. There are no transfer orbit power generation requirements between shuttle orbit and GEO.
18. Functional wing operations include:
 - a. Releasing the wing from its stowed launch configuration.
 - b. Any secondary deployment to orient the wing normal to the spacecraft body.
 - c. Unfolding or extension of the wing to its fully deployed length.
 - d. The wing weight shall include allocations for array mechanical/electrical components to provide primary and secondary deployment, exclusive of any command packages and solar array drive assembly.
19. The deployed array is not subjected to any shadowing and is pointed normal to the sun.
20. The trapped radiation will be that described in JPL Publication 82-69, Solar Cell Radiation Handbook, 3rd edition, based on the AEI 7LO electron environment and the AP8 proton environment.
21. The solar flare proton model (spectrum and fluence) will be that described by Pruett in Aerospace Report ATM-74 (4624-01)-5.

Table 1-2. Design Evaluation Criteria

1. Array Design Performance

The degree to which the proposed design meets or exceeds the BOL and EOL specific power goals for a nominal 10 kW (10 \pm 2 kW) array power system. The factors to be considered are:

- a. Specific power at operating temperature of 105 W/kg after 10 years in a geosynchronous orbit
- b. Power density at operating temperature of 110 W/m² after 10 years in a geosynchronous orbit
- c. BOL specific power of 130 W/kg.

2. Array Design Maturity

The degree to which the proposed design can be fabricated into prototype hardware (within 15 months), ground tested, and space qualified. The factors to be considered are:

- a. Flight heritage of materials/components
- b. Shuttle environmental compatibility.

3. Array Design Utility

The degree to which the proposed design meets near-term (10 years) NASA, commercial, and defense requirements. The factors to be considered are:

- a. Degree of difficulty in making subsequent modifications to the design for other earth orbital or interplanetary mission applications
- b. Ability to accommodate advanced photovoltaic components.

4. Implementation Plan

The degree to which the implementation plan reflects the contractor's intention and ability to demonstrate and fabricate the proposed array design within 15 months and within the limits of the available funding (goal of \$500,000). The factors to be considered are:

- a. Availability of facilities and personnel
- b. Management structure.

1.4 TECHNICAL APPROACH

A review of the goals and intent of the proposed program indicated that the APSA must have the following characteristics.

- o High performance. Reduced overall array mass and high efficiency,² radiation-resistant solar cells to achieve high power density (W/m^2) and high specific power (W/kg).
- o Producibility. Array design must be practical and based on current or near-term component technology that can lead to prototype wing demonstration hardware in 1987.
- o Adaptability. Modular and scaleable in design concept to meet the needs of different scientific, commercial, and specific defense missions; operational in orbit environments ranging from near-earth to geosynchronous and interplanetary; compatible for accommodating advanced technology components as they are developed.

Based on the above characteristics and prior review of previously developed, lightweight, high-performance solar arrays and advanced photovoltaic components in the U.S., Europe, and Japan, the approach chosen was to develop an improved version of a flexible blanket solar array, using thin solar cell modules, rather than considering rigid panel arrays or high concentration ratio arrays. Since prior trade studies by NASA and other solar array suppliers in the U.S. and Europe showed that the rollout flexible blanket configuration was 5 to 15 percent heavier than the foldout version (and was also more complex), we concentrated on improving the design of flatpack, foldout solar array configurations. Based on design complexity, producibility, weight, and testability issues, the study focused on: (1) planar versions of a flexible blanket array rather than flexible blanket arrays that included thin film secondary reflector panels to achieve low concentration ratio (2:1) systems, and (2) single blanket wing designs rather than multiple blanket wing designs.

Figure 1-1 illustrates the general approach used to develop the preferred array design. The design trade studies were supported by multidisciplinary analyses in the fields of electrical systems, structures, mechanisms, dynamics, thermal, stress, materials engineering, environmental interaction effects, electromagnetic compatibility, mass properties, producibility, and cost to identify and select promising design options and to estimate first-order array performance characteristics. These multidisciplinary analyses were applied to all major components that comprised the solar array (including the solar cell stack, interconnects, electrical harness, blanket substrate, blanket housing structure, and blanket deployment system) for the purpose of defining materials and designs that would result in credible, low-weight, high photovoltaic conversion efficiency array system configurations, producible by existing or evolutionary extensions of state-of-the-art manufacturing processes.

As input to the multidisciplinary, iterative design definition process, the following were used:

1. Recent technology development work on the NASA-sponsored flexible blanket Solar Electric Propulsion Stage (SEPS) solar array and the Solar Array Flight Experiment (SAFE I) demonstrated on Shuttle 41-D

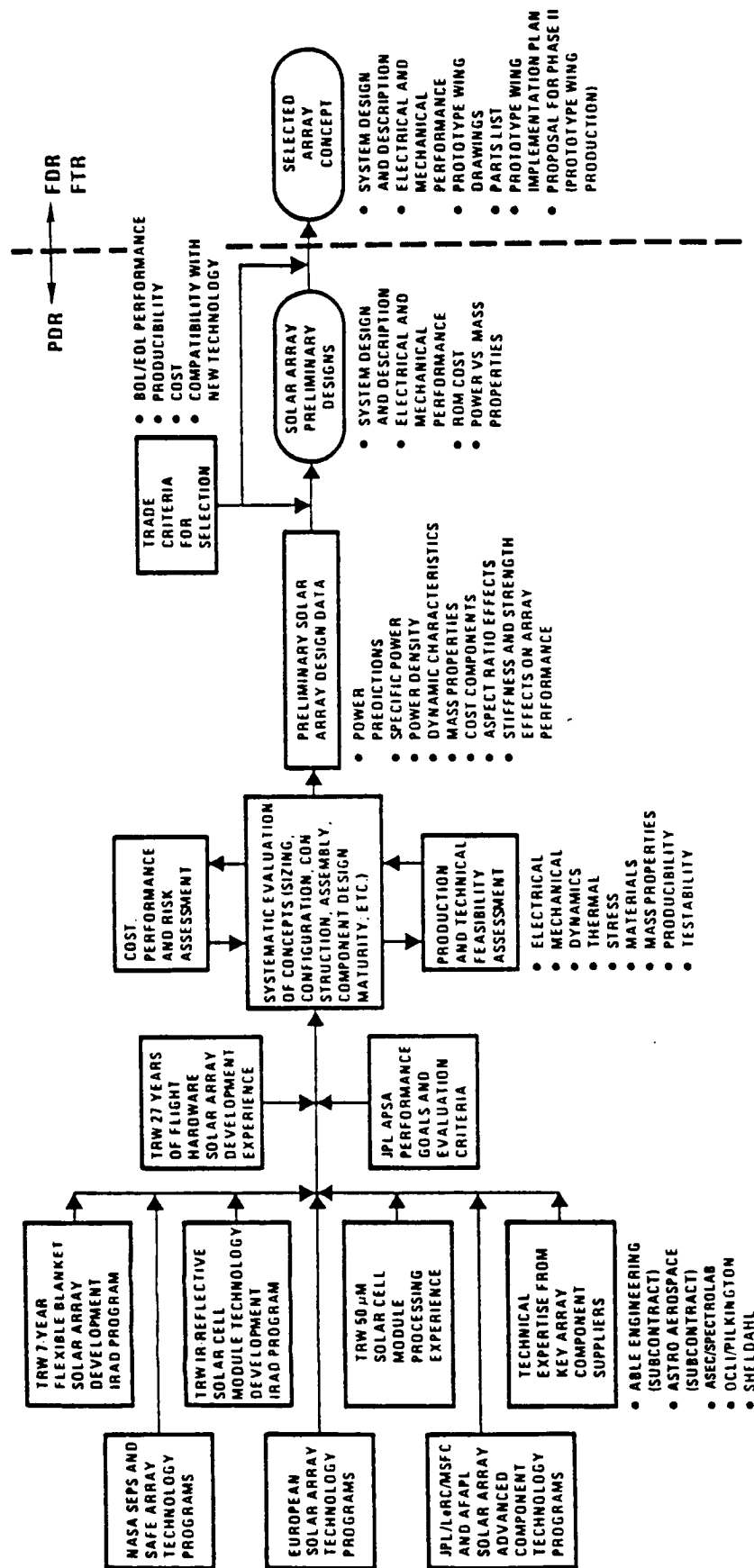


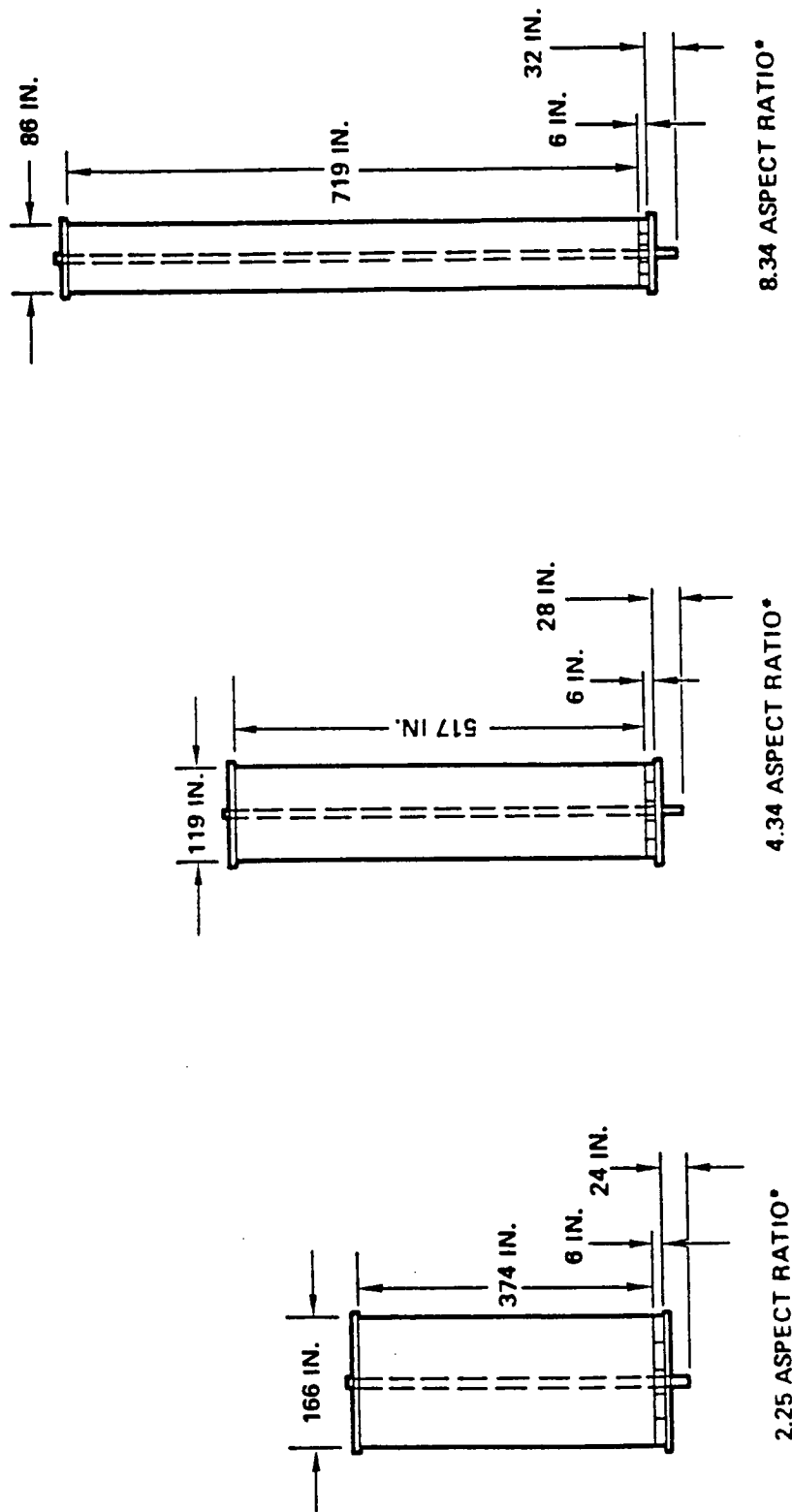
Figure 1-1. Advanced Photovoltaic Solar Array Design Development Flow Plan

2. Recent advances in European solar array system-level development work
3. NASA- and DoD-sponsored work in advanced solar cell module technology
4. TRW work under JPL Contract 956402 dealing with the automated assembly of gallium arsenide and 50- μ m-thick silicon solar cell modules (Ref 4 and 5)
5. TRW independent research and development (IR&D) programs that led to the fabrication and testing of prototype flexible blanket wing hardware and low-operating-temperature solar cell module technology (Ref 6.)
6. TRW work under NAS8-33428 and NAS9-15870 dealing with Phase B design definition studies for high-power, low-weight flexible blanket solar arrays for SEPS, Space Platform (25 kW Power Module) and the Power Extension Package for shuttle.
7. TRW's 27 years of flight hardware solar array development experience.

While TRW was responsible for the overall trade studies and design definition, technical expertise was obtained from key solar array component suppliers. This was particularly true for the selection of solar cells, cover glass, electrical harness, blanket material, and the wing deployment mechanism/structure. Because of the criticality of the wing deployment mechanism/structure to the overall success of achieving the specific power, deployed strength, and deployed stiffness goals, subcontracts were issued to two leading suppliers: Astro Aerospace Corporation and AEC-Able Engineering, Inc., both in California. Based on preliminary design requirements provided to them by TRW, they performed most trade studies in conjunction with the overall array design trades to develop preferred wing deployment system approaches and detail design concepts.

During the preliminary design phase, electrical and mechanical design trades were performed on three aspect ratio wings having a nominal power output of 5 kW (BOL) (see Figure 1-2). The sizing and mass properties for several of the components were based on early conceptual definitions and analyses. This approach permitted the evaluation of the key parameters of aspect ratio, deployed stiffness, and deployed strength on overall wing weight, specific power, power density, electrical circuit layout, and electrical harness design. Based on these trades, plus an examination of spacecraft integration issues (i.e., wing stowage volume and geometry, attachment/stowage location on typical spacecraft, etc.), a preferred wing aspect ratio and size was selected for more detailed design studies.

At the preliminary design review, held approximately half-way through the 11-month APSA study, the trade study results were presented and a preferred approach was recommended based on such critical criteria as BOL/EOL performance (specific power and power density), maturity of the design and proposed components, compatibility with new technology, accommodation of other functional requirements, adaptability to other orbital missions, and scalability to other power levels. The final design activity consisted of developing the preferred design approach in greater detail, defining a prototype wing configuration, producing engineering drawings and an equipment list for the purpose of prototype hardware fabrication, developing an implementation plan (cost and schedule estimates for the prototype wing), revising array performance characteristics



* NOTE: THE RESULTS FOR THESE ASPECT RATIO WINGS WERE EXTRAPOLATED TO SLIGHTLY DIFFERENT ASPECT RATIOS AFTER MORE DETAILED DEFINITION OF ELECTRICAL CIRCUIT AND BLANKET HARNESS WERE OBTAINED

Figure 1-2. Nominal 5 kW (BOL) Wing Sizes and Aspect Ratio Used in Trade Studies

(specific power, power density, strength, stiffness, dynamic characteristics, electrical characteristics), assessing implementation risk for the preferred design, and assessing the utility of the design to accommodate advanced technology components and to meet different mission and functional performance requirements.

2. SUMMARY

The objectives of the Advanced Photovoltaic Solar Array (APSA) program are realistic and achievable by early 1990. A 10-kW (BOL) flatpack, foldout, flexible blanket array design was defined under Phase I of the APSA program that can meet the performance goals established at the outset of the program. The design would have a BOL specific power of 136 W/kg and an EOL specific power of about 97 W/kg after a 10-year geosynchronous (GEO) mission, with deployed strength and stiffness characteristics of 0.01 g and 0.10 Hz, respectively. The EOL power density is about 95 W/m². The array design utilizes existing and near-term available components that will permit prototype wing demonstration (fabrication and testing) by late 1987. With a focused effort in support of a specific mission, a flight array could be developed for spacecraft integration about 2 years after completion of prototype wing demonstration.

While the present program was done for an array design at 10 kW (BOL), 7 kW (EOL), for a GEO mission, the preliminary data generated indicated that the design could be scaled for power levels ranging from 5 to 20 kW (BOL) and could meet a wide range of spacecraft integration constraints. It could be readily modified to handle other missions (e.g., near-earth orbits, interplanetary) and incorporate other functional/operational requirements (e.g., retraction, enhanced strength, and stiffness) without a significant impact on specific power and power density performance. As advanced photovoltaic components become available and are proven practical and cost effective, the array could accommodate these components, thereby resulting in further improvements in array performance.

2.1 ARRAY DESIGN

Figures 2-1 through 2-4 illustrate the deployed and stowed configuration of the 5.2 kW (BOL) APSA wing. The overall wing geometry is similar to the SAFE I and Olympus wing designs. The wing consists of a flatpack, foldout, one-blanket assembly, 15.2 m long by 2.7 m wide (600 by 108 inches), that is comprised of 39 cell-covered panels and three blank leader panels. The blanket assembly consists of 13 three-panel solar panel assemblies (SPAs) and two leader assemblies attached together via piano-hinge joints. Because of the need to ground the blanket substrate to prevent electrostatic charge buildup for the geosynchronous substorm environments, the substrate is made from 50 μ m (2 mil) thick carbon-loaded Kapton polyimide film.

When stowed, the folded blanket assembly is sandwiched between two graphite/epoxy facesheet aluminum honeycomb plate structures, with a polyimide foam layer on the inner surfaces to cushion the folded blanket during launch operations. The plate structures are nominally 2.8 m long by 0.43 m wide (110 by 17 inches), 13 mm (0.5 inch) thick with 0.25 mm (10 mil) facesheets. A torque tube, motor-actuated, multiple latch/release mechanism is integrated to the lid/pallet structure to provide a 6900 Pa (1 psi) average stowage pressure on the folded blanket by partial compression of the foam layers. There is no padding on the blanket assembly panels to prevent cell-to-cell contact from adjacent folded panels.

The blanket assembly is deployed by a motor-actuated, fiberglass, continuous tri-longeron lattice mast that uncoils from an aluminum canister attached to the pallet structure (Figure 2-5). To provide the necessary deployed strength and

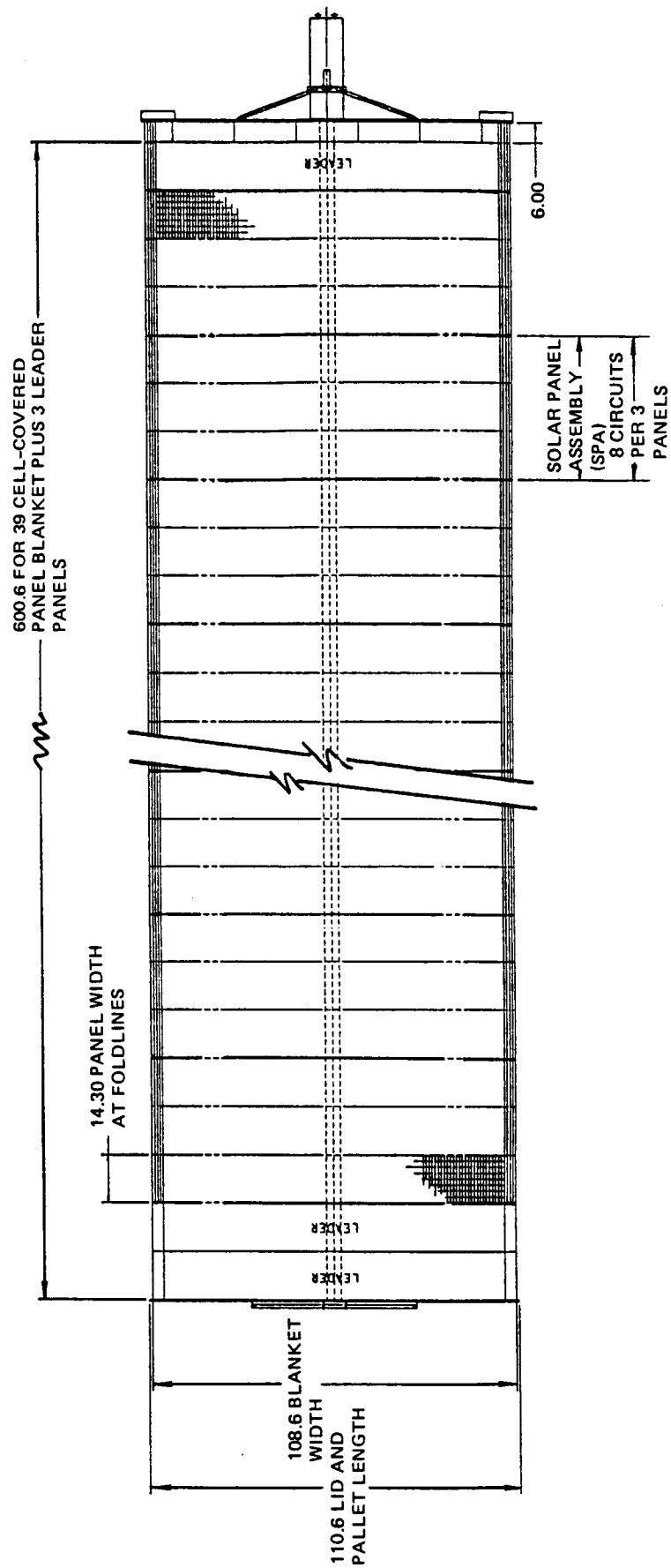


Figure 2-1. 5.2 kw (BOL) GEO Deployed Solar Array Wing Configuration (dimension in inches)

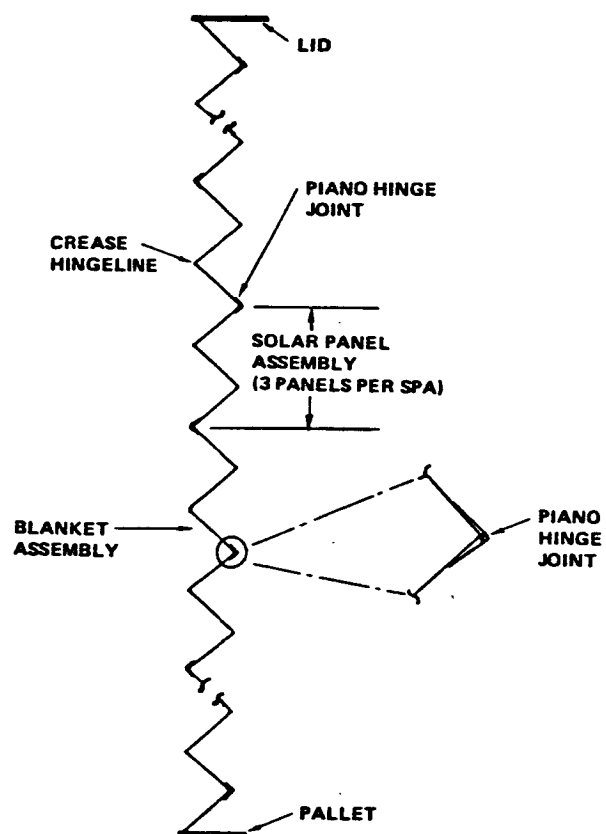


Figure 2-2. Detail of Accordion Folding and Definition of Solar Panel Assemblies

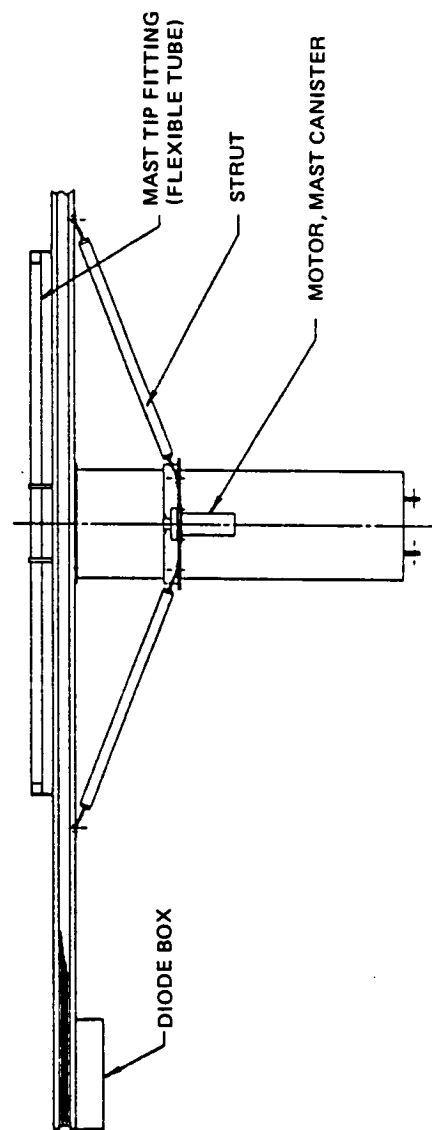
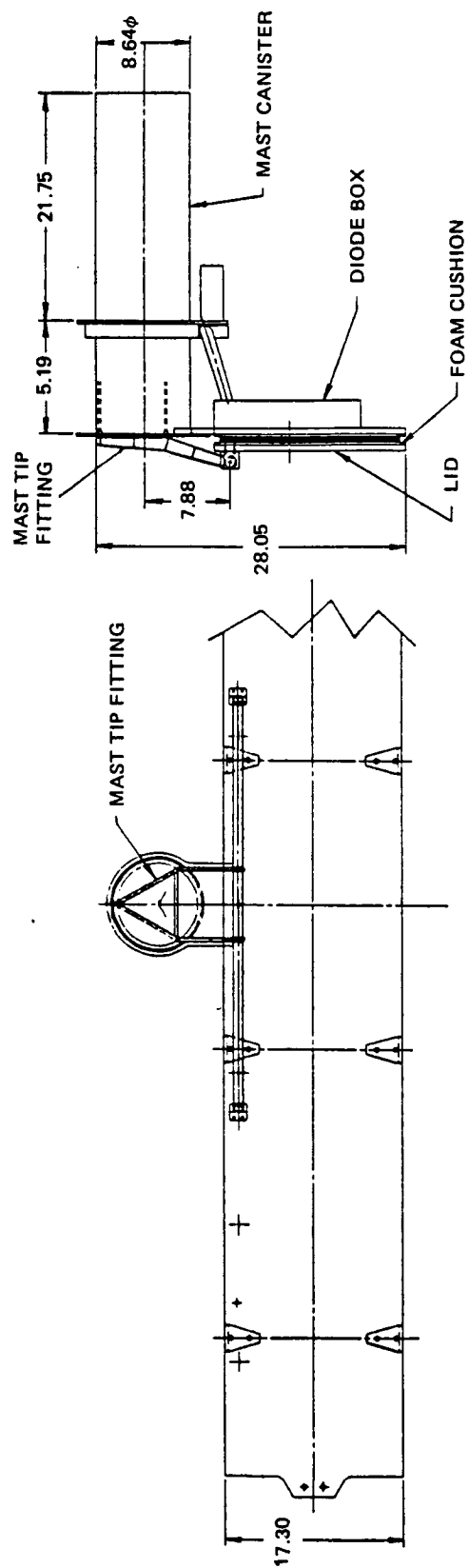


Figure 2-3. Stowed Configuration of 5.2 kW (BOL) GE0 Solar Array Wing (Viewed from Lid Structure) (dimensions in inches)

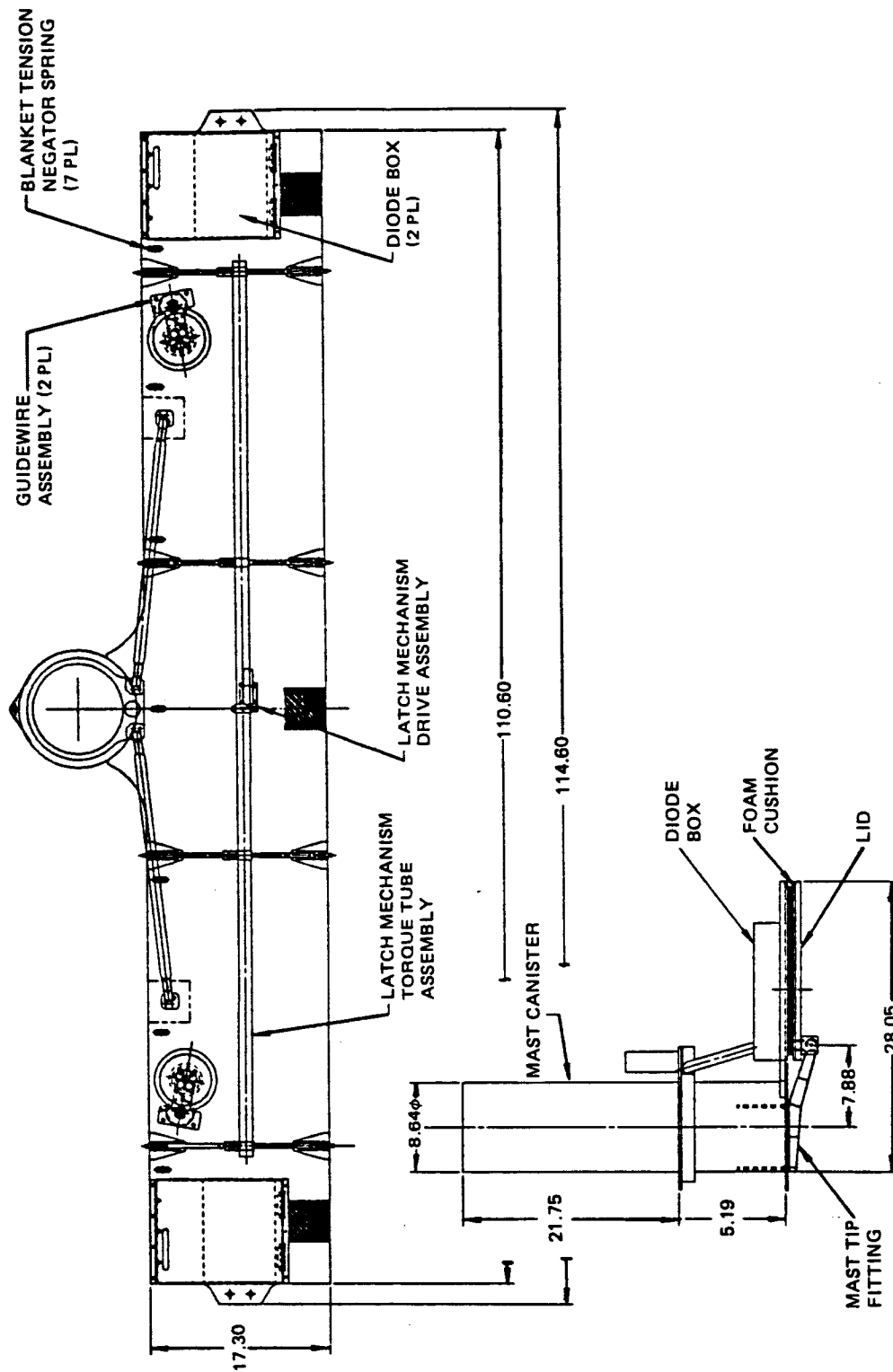


Figure 2-4 Stowed Configuration of 5.2 kW (BOL) GEO Solar Array Wing
(Viewed from Pallet with Latching/Release Mechanism)
(dimensions in inches)

- COILABLE, CONTINUOUS TRI-LONGERON FIBERGLASS LATTICE MAST DEPLOYED FROM ALUMINUM MOTORIZED CANISTER
- MOTOR-ACTUATED DEPLOYMENT AND RETRACTION CAPABILITY
- 8.2" DIAMETER MAST, 0.15" DIAMETER LONGERON
- SIZED TO PROVIDE 0.1 Hz AND 0.01 G DEPLOYED WING FREQUENCY AND STRENGTH CHARACTERISTICS, RESPECTIVELY

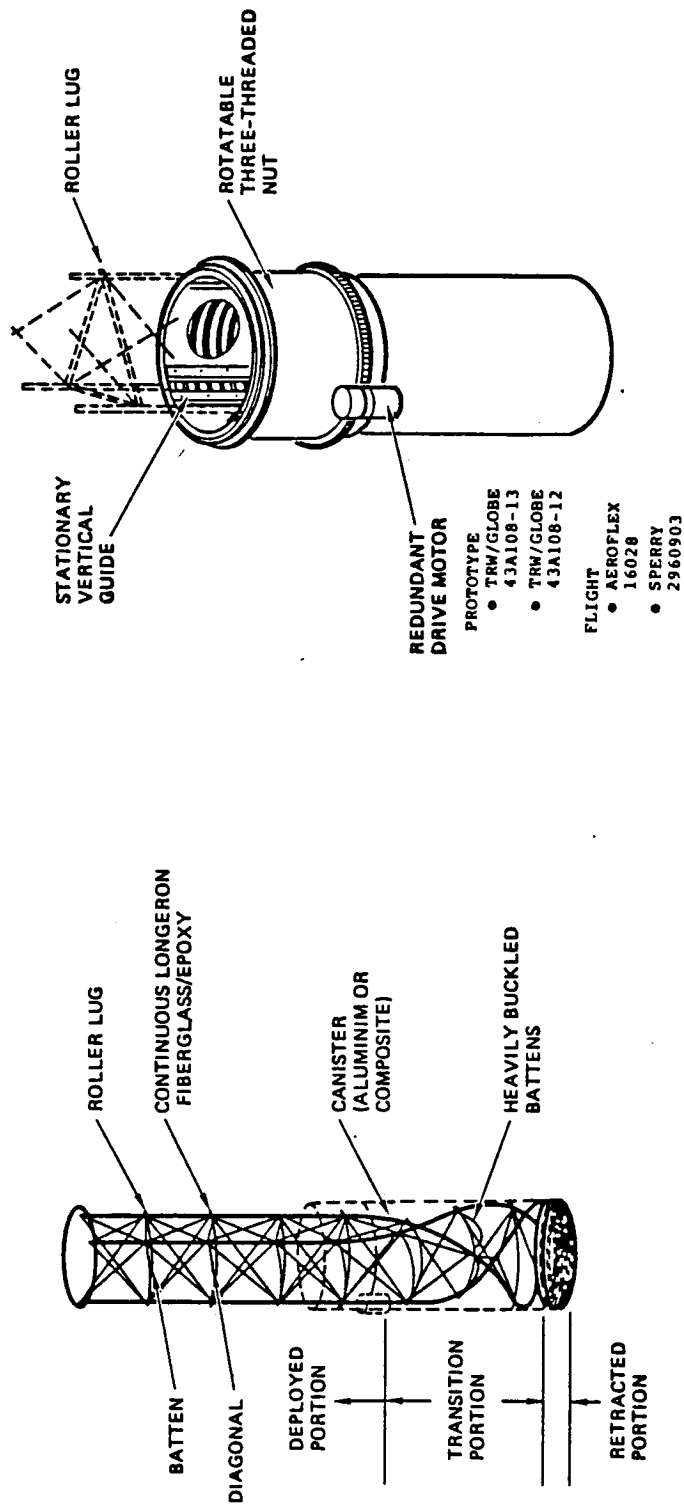


Figure 2-5. Blanket Deployment Mast System

stiffness, the mast is 0.2 m in diameter (8.2 inches), with 3.8 mm (0.15 inch) diameter longerons. The aluminum canister is nominally 0.7 m (27 inches) long by 0.28 m (11 inches) diameter (including allocation for ring stiffness and attachment hardware).

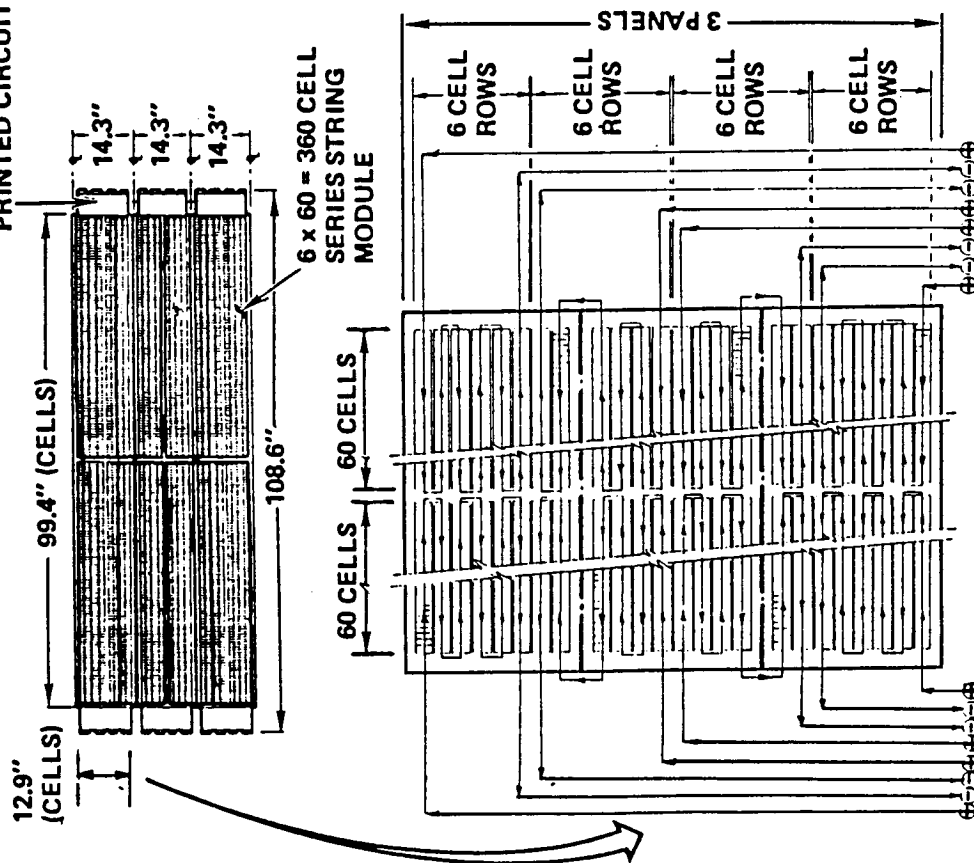
Each cell-covered panel contains 960 solar cell stacks, for a total of 37,440 cells per blanket assembly. Each solar cell stack consists of a 63 μm (2.5 mil) thick by 2x4 cm back surface field, back surface reflector polished silicon cell, with a photovoltaic conversion efficiency of 13.5 percent (at 28°C AMO conditions). The cover glass is 50 μm (2 mil) thick ceria-doped glass coated with an enhanced emittance filter and a UV-rejection filter. DC93500 silicone adhesive is used to bond the solar cell module to the blanket substrate as well as the cover glass to the solar cell.

Figures 2-6 and 2-7 illustrate the nature of the blanket circuitry. Each blanket assembly contains 104 soldered single-cell series circuit modules (360 cells per circuit) using two discrete inplane stress relief loop 25 μm (1 mil) thick Invar interconnectors for each cell-to-cell connection. The electrical circuits are arranged in a serpentine fashion on the blanket to create a mirror-imaged layout to minimize current-induced magnetic field effects. Electric power is collected via flexible printed circuit Kapton-insulated copper harness runs bonded along the outer edges of the blanket assembly. The harness traces consist of 2 oz (69 μm thick) copper, 0.63 mm (25 mils) wide, with 0.51 mm (20 mil) space between each trace, insulated by 38 to 50 μm (1.5 to 2 mils) of conventional Kapton polyimide film. The average width of each harness run is 0.11 m (4.5 inches). Each electrical harness run terminates at the inboard end of the wing in a blocking diode box located on the pallet structure.

During blanket unfolding and deployment, the blanket assembly is supported by two tensioned guidewire systems at 5 N or 1 pound tension force each) attached to the rear fold lines of the blanket. The guidewires provide out-of-plane constraint to the blanket to prevent any large out-of-plane excursions. When fully deployed, the blanket assembly is tensioned by a series of constant-force Negator springs at the inboard end of the blanket attached to the pallet structure. The total distributed tension force over the 2.7 m (108 inch) wide blanket assembly is nominally 63 N (14 pounds) and is required to eliminate undesirable low-frequency blanket dynamic modes and to control deflections of the blanket under inertia loading. The negator spring system also permits the blanket assembly to expand/contract under orbital temperature extremes without inducing additional loads in the blanket or allowing the blanket to become slack.

Table 2-1 presents a summary equipment list of key array components. All solar cell stack components (solar cells, cover glass, enhanced emittance filter coating, UV-filter coating, adhesives, interconnectors) are available from several sources. The fabrication, assembly, installation, and long-term thermal cycle testing of the proposed solar cell stack has been accomplished under NASA-sponsored and TRW IR&D-sponsored programs. The flexible printed circuit harness design can be implemented using standard fabrication processes. The blanket substrate design uses existing materials and is of a configuration similar to that used on other flight hardware programs. The blanket housing assembly structure is based on standard spacecraft construction using existing materials. The blanket preload, latching, and release mechanism is a unique design utilizing conventional components and materials. The lattice mast system represents a

ZONE FOR FLEXIBLE
PRINTED CIRCUIT HARNESS



DESIGN FEATURES	DESIGN RATIONALE
8 x 120 CELLS PER PANEL = 960 CELLS	<ul style="list-style-type: none"> • MAXIMIZE PACKING FACTOR • INTEGER NUMBER FOR CIRCUITS
2 x 4 CM, 2.5 MIL CELLS; 2 MIL COVERS	<ul style="list-style-type: none"> • MINIMIZE CELL STACK WT • MAX SIZE FOR THIN CELLS
360 CELLS IN SERIES	PROVIDE 176V (BOL) AND 147 V (EOL)
8 ELECTRICAL CIRCUIT MODULES FOR EVERY 3 PANELS	DRIVEN BY NUMBER OF CELLS PER CIRCUIT
104 ELECTRICAL CIRCUIT MODULES PER BLANKET	DRIVEN BY WING NOMINAL POWER REQUIREMENT
LAYOUT CANCELS CURRENT-INDUCED MAGNETIC FIELDS	MINIMIZE EFFECTS ON EXPERIMENT PACKAGES AND ATTITUDE CONTROL

Figure 2-6. Schematic of Solar Panel Assembly Circuitry
with Summary Design Features

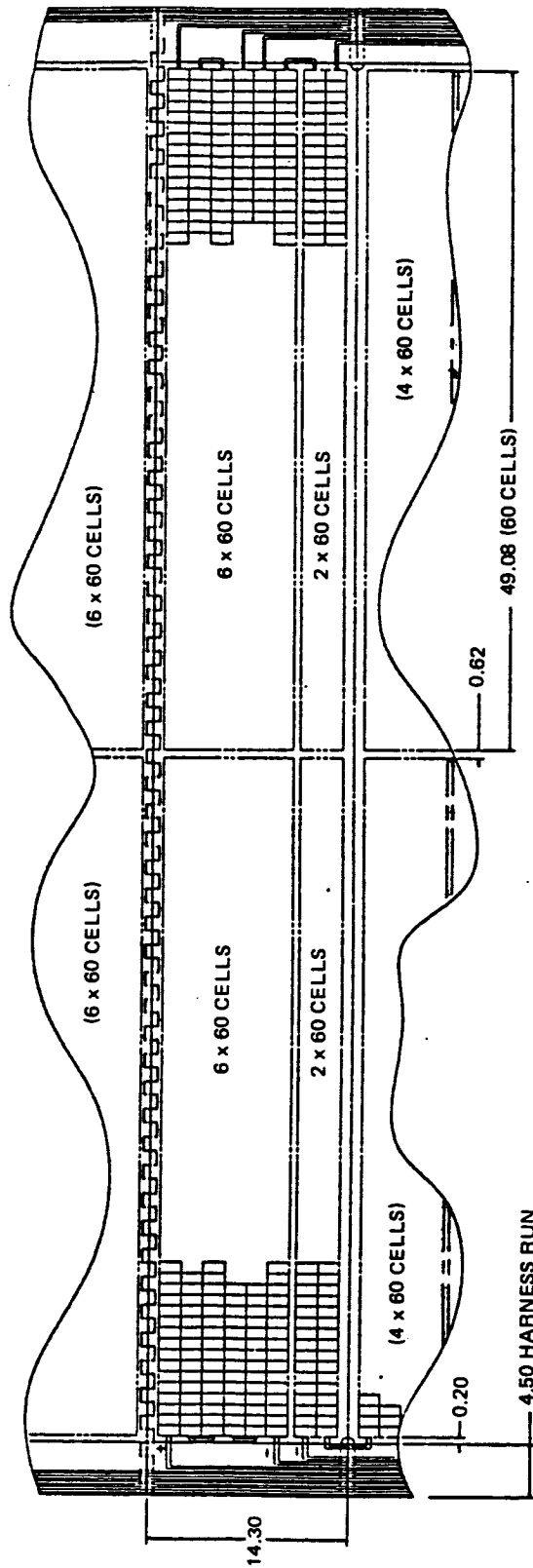


Figure 2-7. Typical Solar Panel Showing Layout of Solar Cell Modules and Electrical Harness (dimensions in inches)

Table 2-1. Solar Array Wing Equipment List

ITEM (DWG NO.)	DESCRIPTION	QTY PER WING	HERITAGE
SOLAR CELL (X700001)	10 Ω -CM B-BSF/AL-BSR SILICON; 2 x 4 cm x 65 μ m THK; $\eta_o = 13.5\%$ AT 28°C AMO	37440	AVAILABLE FROM 4 CELL VENDORS (ASEC, SL, SOLAREX, AEG); TRW HAS PROCESSED CELLS UNDER JPL CONTRACT
COVERGLASS (X700001)	2.015 x 4.015 cm x 50 μ m THK; CERIA-DOPED GLASS	37440	AVAILABLE FROM PILKINGTON; TRW HAS PROCESSED COVERS UNDER JPL CONTRACT
CELL STACK ADHESIVE	DC93500	—	STANDARD STOCK MATERIAL; AVAILABLE FROM DOW CORNING; USED ON TRW ARRAYS
INTERCONNECTOR	IN-PLANE STRESS RELIEF LOOP; 25 μ m THK Ag-PLATED INVVAR COATED WITH SOLDER	74880	STANDARD TRW STOCK ITEM; TRW HAS PROCESSED THESE INTERCONNECTORS ON CONTRACT/IRAD PROGRAMS USING WELDING OR SOLDERING
ELECTRICAL HARNESS (X700006, 7, 8)	KAPTON INSULATED (1 AND 2 MIL) FLEXIBLE PRINTED CIRCUITS (7 MIL THK); 4.5" WIDE x 45" LONG SEGMENTS WITH 91 TWO-OZ COPPER TRACES	2 RUNS OF 15 SEGMENTS EACH	FABRICATED USING STANDARD PROCESSES BY SHELD AHL
DIODES	SILICON, HIGH POWER, FAST RECOVERY, DOUBLE PLUG, SOLID MONOLITHIC; 6A; 150V	104	STANDARD TRW STOCK ITEM (1D013); (SIMILAR TO IN5811)
DIODE BOX ASSEMBLY (X700010, 13, 15)	10 x 12 x 1" ALUM BOX WITH PRINTED CIRCUIT BOARD FOR DIODE INSTALLATION	2 ASSEMBLIES	PROTOTYPE FABRICATED AND TESTED ON TRW IRAD PROGRAM
BLANKET ASSEMBLY (X142105, 119, 120) (X700000)	3-PANEL SPAs; 13 SPAs PLUS 3 BLANK LEADER PANELS FOR FULL SIZE BLANKET (109x600")	1 ASSEMBLY	CONFIGURATION SIMILAR TO THAT FLOWN ON CTS, SAFE I, OLYMPUS ARRAY; HOWEVER DIFFERENT MATERIAL
BLANKET MATERIAL	2 MIL THK CARBON LOADED POLYIMIDE KAPTON	453 FT ²	COMMERCIALY AVAILABLE FROM DUPONT (XC10 ¹⁰ OR XC10 ⁴ OR C601571-37)
BLANKET ADHESIVE	NITRYL PHENOLIC	—	USED IN TRW IRAD PROGRAM ON ULTRA- LIGHTWEIGHT FLEXIBLE BLANKET SOLAR ARRAYS
BLANKET HINGE PINS	50 MIL DIA PULTRUDED GRAPHITE/EPOXY RODS; 100" LONG	16	AVAILABLE FROM DIVERSIFIED FABRICA- TORS (1083-128)
BLANKET HOUSING ASSEMBLY (X142102, 103, 111)	2 - 0.5" THK HONEYCOMB PANEL SUBSTRATES WITH 0.5" THK POLYIMIDE FOAM ON INNER SURFACES	1 ASSEMBLY	STANDARD SPACECRAFT STRUCTURE CONSTRUCTION
COMPOSITE MATERIAL IN BLANKET HOUSING ASSEMBLY	[0/90] LAYUP; 10 MIL TOTAL THK PER FACESHEET; GY70	—	STANDARD SPACECRAFT COMPOSITE MATERIAL
BLANKET PRELOAD AND RELEASE MECHANISM (X142101, 106, 107, 108, 112-118)	TORQUE-TUBE ACTUATED CABLE/LATCH SYSTEM	1 ASSEMBLY OF 8 LATCHES	CONCEPT DESIGNED; KEY PARTS EASILY FABRICATED/ASSEMBLED USING STANDARD PROCESSES
BLANKET PRELOAD ACTUATOR	ELECTRICALLY REDUNDANT DC BRUSHLESS MOTOR	1	AEROFLEX 16028 OR SPERRY 2960903 OR EQUIVALENT, MODIFIED TO DUAL WINDING
MAST SYSTEM (X366-003, 004, 005)	ALUMINUM CANISTER DEPLOYED CONTINUOUS LONGERON LATTICE MAST; 8.2" DIA MAST; 0.16" DIA FIBERGLASS LONGERONS	1 ASSEMBLY	PROTOTYPE UNIT FLOWN ON SAFE I WING; UNIT FABRICATED TO FLY ON OLYMPUS ARRAY; REQUIRES LIGHTWEIGHT CANIS- TER DEVELOPMENT; AVAILABLE FROM ABLE ENGRG OR ASTRO AEROSPACE
MAST DEPLOYMENT ACTUATOR	ELECTRICALLY REDUNDANT DC BRUSHLESS	1	AEROFLEX 16028 OR SPERRY 2960903 OR EQUIVALENT MODIFIED TO DUAL WINDING
BLANKET TENSION MECHANISM (X142109)	NEGATOR SPRING UNIT; 2 LB FORCE EACH; HUNTER SPRING SH6F21	7	COMPONENTS AVAILABLE FROM AMETEK; PROTOTYPE UNITS ASSEMBLED/TESTED ON TRW IRAD PROGRAM
BLANKET GUIDEWIRE MECHANISM (X142110)	NEGATOR SPRING TENSIONED CABLE REEL; 0.020" DIA BRAIDED STEEL CABLE HUNTER 40008 SPRING	2	COMPONENTS AVAILABLE FROM AMETEK; PROTOTYPE UNITS ASSEMBLED/TESTED ON TRW IRAD PROGRAM

lightweight version of heavier existing hardware that has flight experience. The lightweight mast system will require additional development work.

2.2 ARRAY PERFORMANCE

Figure 2-8 shows the BOL and EOL electrical performance characteristics for the two-wing array. The electrical performance is based on design sizing factors listed in Table 2-2. The total 10-year GEO 1 MeV equivalent electron design 2 fluence level (including solar flare protons) was approximately 2×10^{15} e/cm².

Table 2-3 summarizes the APSA predicted performance. Without any contingency in weight and electrical performance, the array design essentially meets all the key performance goals of specific power, power density, deployed frequency, and deployed strength. With a 10 percent contingency, EOL performance is slightly below the study goals. Based on trade studies, the proposed 5.5 aspect ratio wing (blanket length divided by blanket width) results in a specific power performance 5 to 10 percent better than wings with wider (but shorter) or narrower (but longer) aspect ratios. The prototype wing can be fabricated in a time period 5 months shorter than the study goal.

2.3 DESIGN UTILITY

The baseline design has broad utility: (1) to accommodate advanced photovoltaic or structural components, (2) to fly other earth orbital or interplanetary missions, or (3) to accommodate other operational requirements without major redesign.

Figure 2-9 shows the impact of power level on specific power performance using the baseline thin silicon solar cell module. Power growth (or reduction) is achieved by adding (or removing) SPAs from the blanket assembly, with appropriate redesign of the electrical harness to account for the different number of electrical circuits. The blanket housing assembly (lid, pallet, latching/release mechanism, folded blanket cushioning provisions, guidewire and blanket tension mechanisms) would remain virtually unchanged. The blanket deployment mast system would be rescaled for length and diameter to provide deployed wing strength/stiffness characteristics similar to the baseline design.

Advanced photovoltaic solar cells, when available, could easily be substituted for the baseline thin silicon solar cell modules. Two options investigated included gallium arsenide solar cells and thin film amorphous silicon cells. Figures 2-10 and 2-11 illustrate the impact of these two advanced technologies on key array performance. Unless gallium arsenide (or other discrete cells such as indium phosphide) can be manufactured in 50 to 125 μm (2 to 5 mil) thicknesses (as opposed to 250 to 300 μm [10 to 12 mil] now available from the DoD MANTECH program), the specific power performance will be substantially below the APSA program goals, even though an improvement will be realized in power density (e.g., smaller array area). Thin film amorphous silicon cell modules are an emerging technology that has the potential for major increases in specific power, if it can be demonstrated that large area, high conversion efficiency modules (EOL $\eta > 10$ percent) can be manufactured and that the technology is compatible with long-term space operation. Specific power of 200 W/kg (EOL) may eventually be possible with a power density of 100 W/m² (EOL).

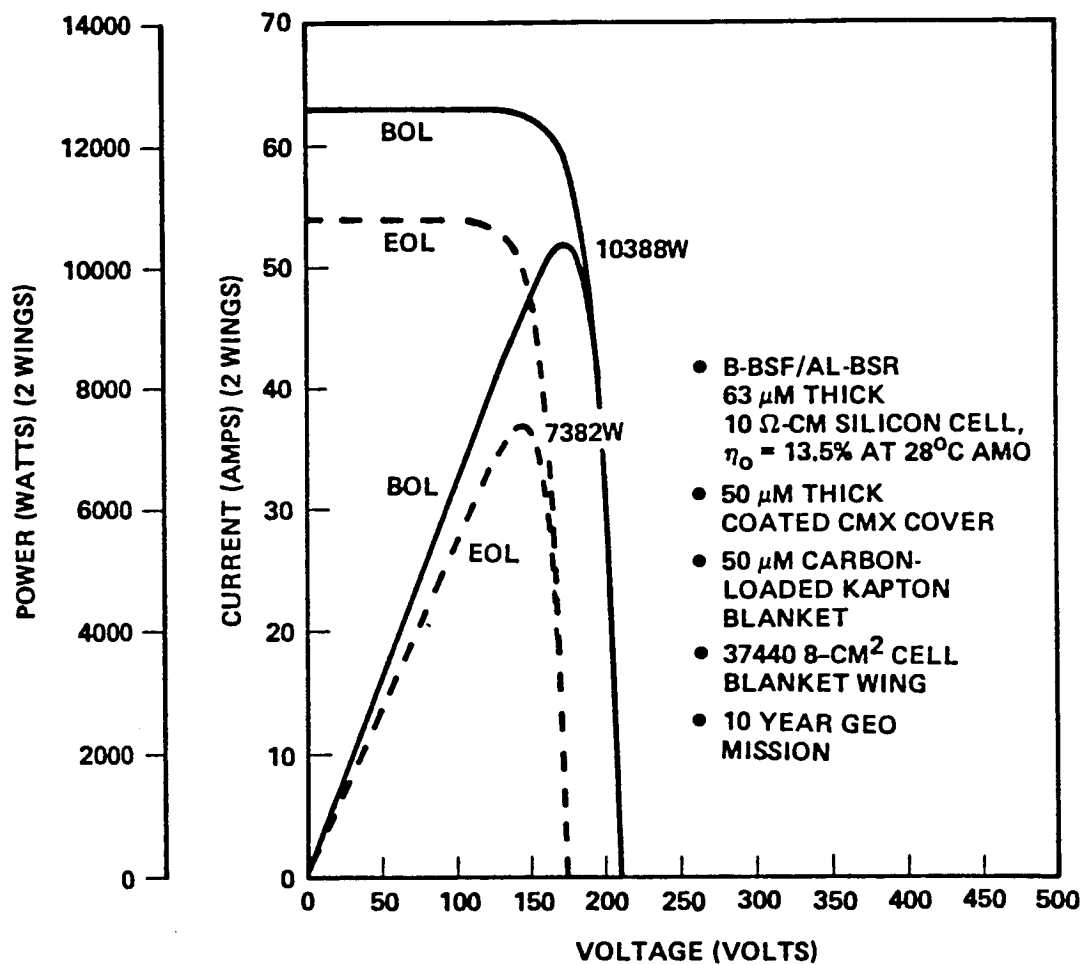


Figure 2-8. BOL and EOL Solar Array Electrical Performance (Two Wings), 10-Year Geosynchronous Mission

Table 2-2. BOL and EOL Design Factors Used for Sizing the Solar Array, 10-Year Geosynchronous Mission, Ceria-Doped Glass-Covered 10 Ω -cm B-BSF/Al-BSR, 63 μ m Silicon Cell

PARAMETER	BOL	EOL
INSTALLATION AND MISMATCH	0.985	0.985
ULTRAVIOLET	1.000	0.980
TEMPERATURE CYCLING	1.000	0.990
COVER DARKENING	1.000	1.000
ADHESIVE DARKENING	1.000	1.000
LOW ENERGY PROTONS	1.000	1.000
I _{SC} DEGRADATION	1.000	0.889
I _{MP} DEGRADATION	1.000	0.887
V _{MP} DEGRADATION	1.000	0.886
V _{OC} DEGRADATION	1.000	0.856
P _{MP} DEGRADATION	1.000	0.767
I _{SC} TEMP COEFF	0.048%/°C	0.048%/°C*
V _{OC} TEMP COEFF	-2.10 mV/°C	-2.10 mV/°C*
DIODE AND HARNESS LINE LOSS	0.975 (3.75V)	0.975 (3.75V)
OPERATING TEMP	26.5°C (1.007)	31.7°C (0.983)
• NET SIZING PARAMETER AT P _{MP}	0.967	0.702
<ul style="list-style-type: none"> • P_{MP} EOL/BOL = 0.72 • CELL PACKING FACTOR = 0.96 • PANEL PACKING FACTOR (W/O HARNESS) = 0.84 • PANEL PACKING FACTOR (WITH HARNESS) = 0.77 		

*CONSERVATIVELY ASSUMED THAT THE EOL VALUE WAS THE SAME AS BOL VALUE. IN REALITY THE I_{SC} COEFFICIENT INCREASES WITH RADIATION; WHEREAS THE V_{OC} COEFFICIENT REMAINS RELATIVELY CONSTANT. THE NET EFFECT ON EOL POWER IS SMALL SINCE THE OPERATING TEMPERATURE IS NEAR 28°C

Table 2-3. Solar Array Performance Summary, 10-Year
Geosynchronous Mission

PARAMETER	GOAL	PREDICTED PERFORMANCE
BOL POWER (GEO)	10 kW (2 WINGS)	10.4 kW (2 WINGS)
EOL POWER (10-YR GEO)	NOT SPECIFIED; 8 kW IMPLIED BY EOL SPECIFIC POWER GOAL	7.4 kW (2 WINGS)
BOL SPECIFIC POWER AT EQUINOX	> 130 W/kg	150 W/kg (W/O CONTINGENCY) 136 W/kg (10% CONTINGENCY)
EOL SPECIFIC POWER AT EQUINOX	> 105 W/kg	106 W/kg (W/O CONTINGENCY) 97 W/kg (10% CONTINGENCY)
EOL POWER DENSITY AT EQUINOX	> 110 W/m ² ; REFERENCE AREA NOT SPECIFIED	103 W/m ² (W/O HARNESS) 95 W/m ² (TOTAL PANEL AREA)
BOL O. C. VOLTAGE	< 200 VOLTS	210 VOLTS
DEPLOYED FREQUENCY	> 0.01 Hz; 0.1 Hz PREFERRED	0.10 Hz (CAN BE INCREASED)
DEPLOYED STRENGTH	> 0.001G; 0.01G PREFERRED	0.015G (CAN BE INCREASED)
CURRENT-INDUCED EFFECTS	MINIMIZED	MINIMIZED BY MIRROR-IMAGE CIRCUITRY LAYOUT
SHUTTLE COMPATIBILITY	TYPICAL LAUNCH ENVIRONMENTS	$N_X = 14.6G$; $N_Y = 11.2G$; $N_Z = 10.5G$ (ULT)
PARTIAL EXTENSION	NO	NO (CAN BE INCORPORATED)
RETRACTION (UNAIDED)	NO	NO (CAN BE INCORPORATED)
TRANSFER ORBIT POWER GENERATION	NO	NO (CAN BE INCORPORATED)
PROTOTYPE WING DEVELOPMENT PERIOD	< 15 MONTHS	10 MONTHS

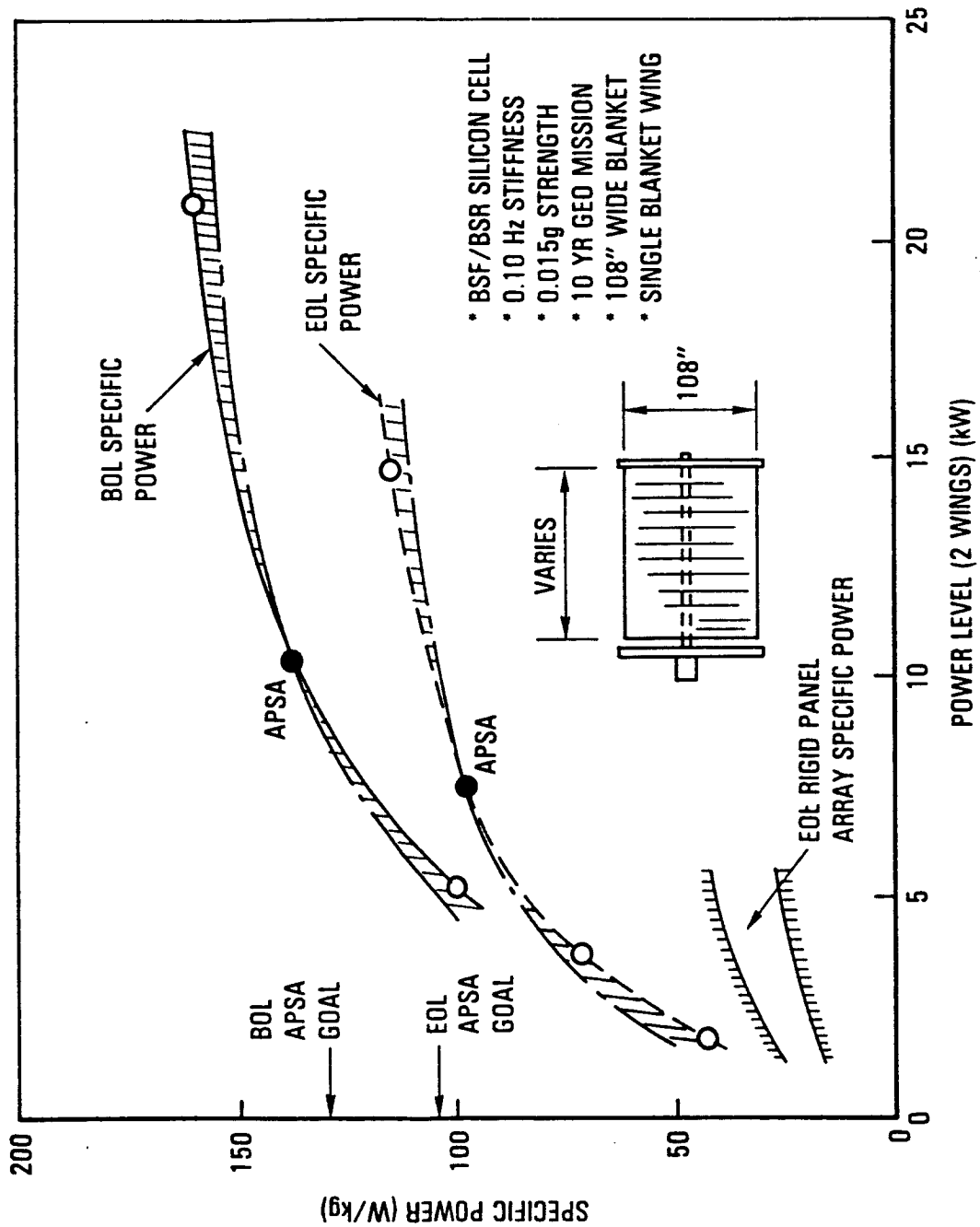
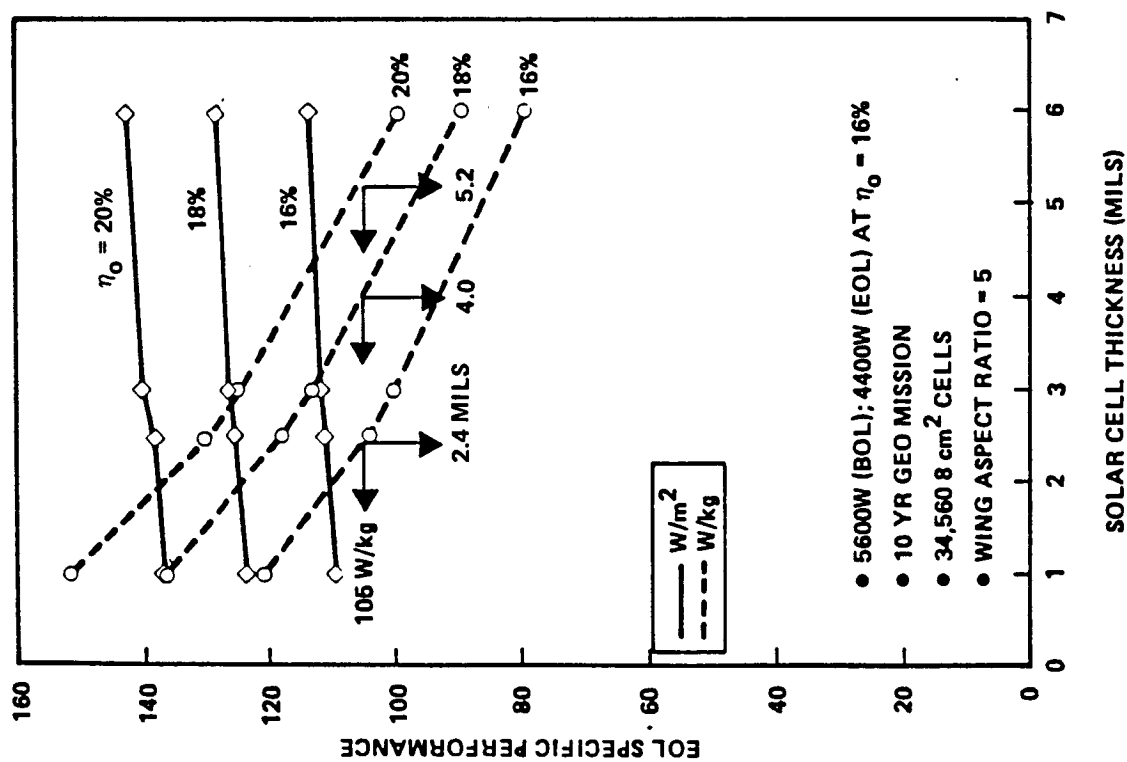


Figure 2-9. Effect of Array Power Level on BOL and EOL Specific Power



- CELL THICKNESS MUST BE SUBSTANTIALLY REDUCED TO BE EFFECTIVE IN TERMS OF ARRAY SPECIFIC POWER (W/KG) PERFORMANCE
- CELLS ARE BRITTLE AND DIFFICULT TO ASSEMBLE INTO MODULES
- HIGH CELL COST DUE TO LOW FABRICATION YIELDS

Figure 2-10. Impact of Gallium Arsenide Solar Cell Modules on EOL Wing Performance

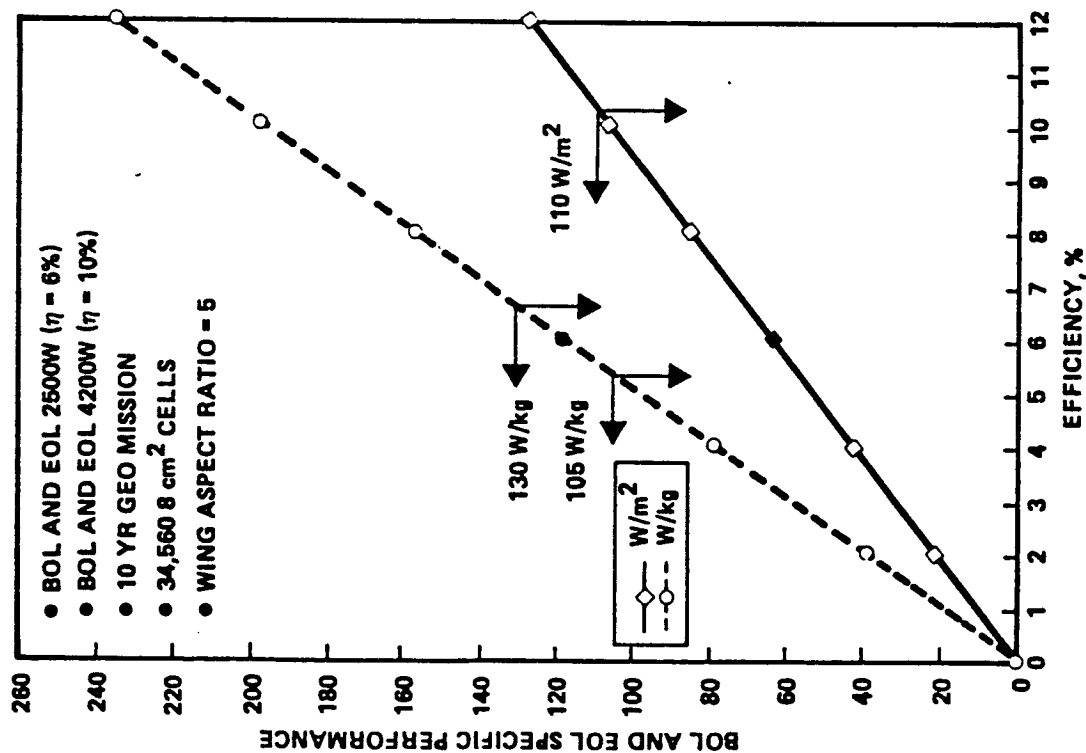


Figure 2-11. Impact on Thin Film Amorphous Silicon Solar Cell on BOL and EOL Wing Performance

- SPACE APPLICABILITY YET TO BE DEMONSTRATED; TEST PROGRAM REPRESENTS A SIGNIFICANT SCHEDULE AND COST IMPACT TO APSA PROGRAM
- PRESENT OPERATING EFFICIENCY OF 6% ACHIEVES 120 W/kg PERFORMANCE WITH AN ARRAY ABOUT TWICE AS LARGE AS BASELINE THIN SILICON CELL DESIGN
- FUTURE OPERATING EFFICIENCY OF 10% WILL RESULT IN PERFORMANCE IN EXCESS OF 200 W/kg WITH AN ARRAY SIZE EQUAL TO THAT FOR BASELINE THIN SILICON CELL DESIGN
- AMORPHOUS SILICON CELL TECHNOLOGY MERITS FURTHER EVALUATION/DEVELOPMENT
 - MAY BE KEY TECHNOLOGY TO ACHIEVING EXTREMELY HIGH PERFORMANCE ARRAYS

Analysis indicated that the baseline array design/materials could be used for interplanetary missions and sustain the temperature extremes associated with 0.5 to 5.0 AU solar distances. The issue for interplanetary missions is the reliable performance of the solar cell modules under low-intensity-low-temperature (LILT) conditions and high voltage conditions for solar distances >2.0 AU. The experimental data on present solar cell technology indicates that large deviations (± 10 to 20 percent) from nominal performance can occur for reasons that are yet to be fully understood.

For long-term, low earth orbit (LEO) missions, the baseline design could be used without significant modifications. The primary design issues for LEO operation were: (1) interconnector fatigue from the large number of temperature cycles (60,000 cycles over 10 years), and (2) atomic oxygen erosion effects at certain altitudes on the exposed materials (especially the Kapton blanket and silvered interconnectors). Recent TRW and NASA/LeRC experimental data (References 1 and 2) indicate that welded and soldered silicon cell modules on flexible blanket and rigid substrates could sustain 10-year LEO temperature cycle environments. Analysis, based on recent STS-derived erosion rate data, indicated that if the LEO altitudes are above 370 to 650 km (200 to 350 nmi) (depending on sunspot activity), the net erosion of the critical exposed array materials would be kept acceptably small, without requiring any protective coatings. However, there are interconnector material substitutions available and coating options being developed by NASA that could improve long-term atomic oxygen resistance, but with some impact on design and manufacturing complexity. The predicted performance of the baseline array for a 10-year 460 km (250 nmi), 0-degree inclined orbit mission would be as follows: 9 kW (BOL) power at 120 W/kg, 8.6 kW (EOL) power at 114 W/kg, 110 W/m² (EOL) power density. For a 32-degree inclined orbit, the above EOL performance would be reduced about 5 percent due to increased solar cell radiation degradation.

The baseline blanket deployment mast system is self-retractable; however, the present design of the blanket assembly does not permit refolding without substantial extravehicular activity (EVA) assistance because of the nature of the blanket substrate hinge lines. However, hinge line designs have been developed and tested that would permit array retraction. This was demonstrated on the NASA SAFE I solar array wing and on a TRW IR&D prototype wing. The overall array design would become more complex and increase in weight by about 10 percent. Array retraction is not recommended unless required to meet specific mission needs.

The array has utility for many military spacecraft missions because of the lightweight aspects of the design and because stiffness and strength characteristics can be readily changed. It can be designed to meet Joint Chiefs of Staff (JCS) nuclear hardness requirements; however, laser hardening for a deployed array would require major changes to the design and selection of materials. The implementation of retractability is one method to provide laser survivability capability, since the exposed surfaces of the blanket housing assembly and blanket deployment mast system canister can be protected more easily.

2.4 PROTOTYPE WING DESCRIPTION

Figure 2-12 illustrates the features of the proposed prototype wing (Option A) that would be fabricated and demonstrated under Phases II and III of the APSA

- FULL SIZE WING EXCEPT FOR TRUNCATED LENGTH
- 12-PANEL BLANKET COVERED WITH LIVE THIN CELL MODULES (10%) AND CELL MASS-SIMULATED ALUMINUM CHIPS WITH FLEXIBLE PRINTED CIRCUIT HARNESS RUNS
- FULL SIZE LIGHTWEIGHT VERSION OF MAST SYSTEM CANISTER WITH TRUNCATED LENGTH MAST (AT 15 FT)
- LIGHTWEIGHT VERSION OF BLANKET HOUSING ASSEMBLY

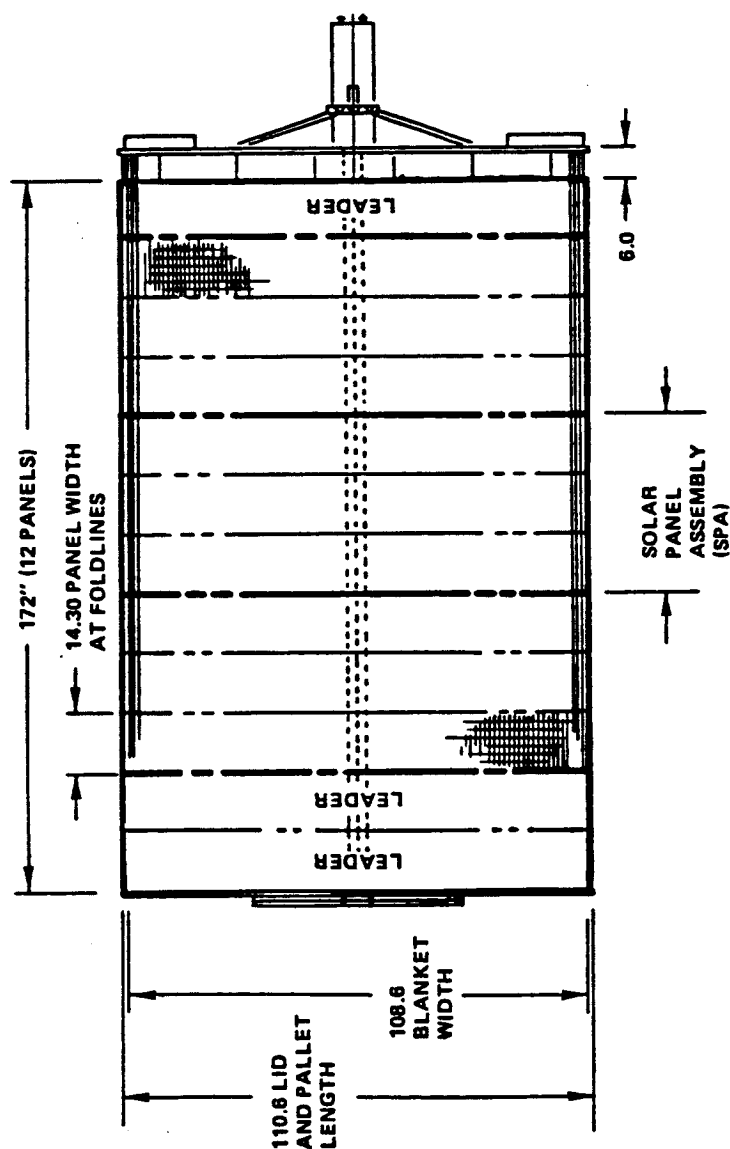


Figure 2-12. Prototype Wing for Phases II and III of APSA Program (Option A Shown)

program. The wing would be a high-fidelity representation of the baseline 5 kW wing, except for reduced length and the percentage of live interconnected solar cell modules.

The wing would include: (1) full-scale graphite/epoxy blanket housing assembly with a complete working stowed blanket preload/latching/release mechanism; (2) lightweight full-scale version of the blanket deployment mast system with a canister capable of storing over 15 m (50 feet) of mast, but with only 4.6 m (15 ft) of mast structure installed; (3) a full-width blanket assembly consisting of three of the 13 solar panel assemblies (SPA), along with the necessary leader panel assemblies. The SPAs would contain 1100 live thin silicon solar cell modules distributed into 120- to 360-series connected cell circuits, with mass-simulated aluminum chip cells covering the remaining SPA surface. The live solar cell circuits would be connected to representative flexible printed circuit harness runs installed along each edge of the shortened blanket assembly. One of the harness runs would terminate into a prototype diode box assembly on the pallet structure.

The prototype wing can be fabricated and assembled within 10 months and subjected to a series of design verification development tests over a subsequent 5-month period. The prototype wing would permit the evaluation of wing deployment characteristics; solar cell module protection features; structural integrity of the system under vibro-acoustic loads, quasi-static loads, and thermal environments. From the prototype hardware wing activities, issues related to producibility and operational/functional risk can be assessed. Also, the fidelity of the hardware permits a revised estimate of array flight hardware performance such as power density, specific power, weight, and size.

2.5 DESIGN IMPLEMENTATION RISK

Achieving a three- to four-fold improvement in specific power performance over current array systems is not without some developmental risk. Except for the development of a lightweight version of the blanket deployment mast system (primarily the canister assembly), all other materials and hardware components are available from suppliers and/or they can be developed by straightforward application of conventional/available design techniques and manufacturing processes.

The risk areas deal primarily with weight growth and not achieving acceptable structural and functional behavior as the result of launch environments and deployment operations. Handling and producibility of the blanket assembly needs to be demonstrated, although there is previous experience on other flexible blanket prototype and flight hardware programs to suggest that it can be done. Cell/circuit integrity during the vibro-acoustic launch phase and deployment phase must be demonstrated, although SEPS technology and SAFE I hardware experience suggest that the protection features incorporated in the design should be effective.

Depending on the nature and number of problems uncovered during Phases II and III of the program, the potential impact on specific power (i.e., weight growth) is estimated to be 5 to 15 percent; the impact on power density (i.e., increase in size) is estimated to be about 5 percent. The key risk areas cannot be assessed by analysis; they can only be resolved by fabricating and testing component-level and system-level hardware.

3. PRELIMINARY DESIGN RESULTS

3.1 ARRAY CONFIGURATION

Figure 3-1 illustrates several options for the stowed wing configuration. These would apply regardless of blanket stowage method (i.e., rollup or foldup). In the figure, the cylindrical element represents the deployment mast assembly (BDMA), and the rectangular element(s) represents the blanket box or blanket housing assembly (BHA). The prime factor that determines the use of one configuration over another is the size and shape of the stowage volume allotted to the solar array wing. This, in turn, is dictated by the spacecraft shape/size, the launch vehicle fairing envelope size/shape, and the interface of the array with other spacecraft appendages and systems (i.e., antennas, instrument platforms, attitude control thrusters, radiator panels, etc.). While there was no specific spacecraft size and geometry defined by JPL, stowage studies were conducted for Shuttle-launched spacecraft assuming a class of generic size spacecraft, in order to define dimensional limitations and configurational constraints for the solar array system.

Configuration A is the most straightforward option. It was used on SAFE I and the Canadian Technology Satellite (CTS) arrays, and is being used for the Olympus (or LSAT) array. The other configurations are more complex and/or heavier because of additional deployment mechanisms and because of the complications introduced into the assembly/integration and ground testing activities. Configurations E and F were proposed in one form or another for the SEPS spacecraft, Space Platform, and Space Station, and are particularly applicable for very high power arrays (>25 kW).

Figure 3-2 illustrates candidate blanket/mast arrangement options. Table 3-1 summarizes the previous history of blanket/mast options for flight, prototype, and conceptual design flexible blanket arrays. The two basic choices are one-mast or two-mast designs, with single or multiple blankets. In addition, for the split-blanket option, the blankets could be in the same plane or the blankets could be oriented in a V-configuration for the purpose of potentially improving deployed wing stiffness or stowed wing packaging efficiency.

Preliminary analyses showed that it was more weight-effective to use a single mast rather than two smaller masts in order to achieve the desired deployed wing strength and stiffness characteristics. Dynamic analysis (see Section 3.2.5) indicated that the V-configuration did not improve the dynamic characteristics to the degree necessary to warrant its consideration for stiffness reasons. A split-blanket design requires a longer blanket/mast than the single blanket design if the overall wing width is fixed. In addition, split blanket wings are more complicated to fabricate, assemble, and test. However, they are more conducive to efficient wing stowage. The single blanket wing (with offset mast) is less efficient for wing stowage (except in special cases) and there is the potential for blanket interference with the mast (e.g., blanket "slaps" the mast) when the deployed wing is subjected to inertia loads. This latter issue can be controlled by proper tensioning of the blanket and/or attaching the blanket to the mast at intermediate locations along the mast.

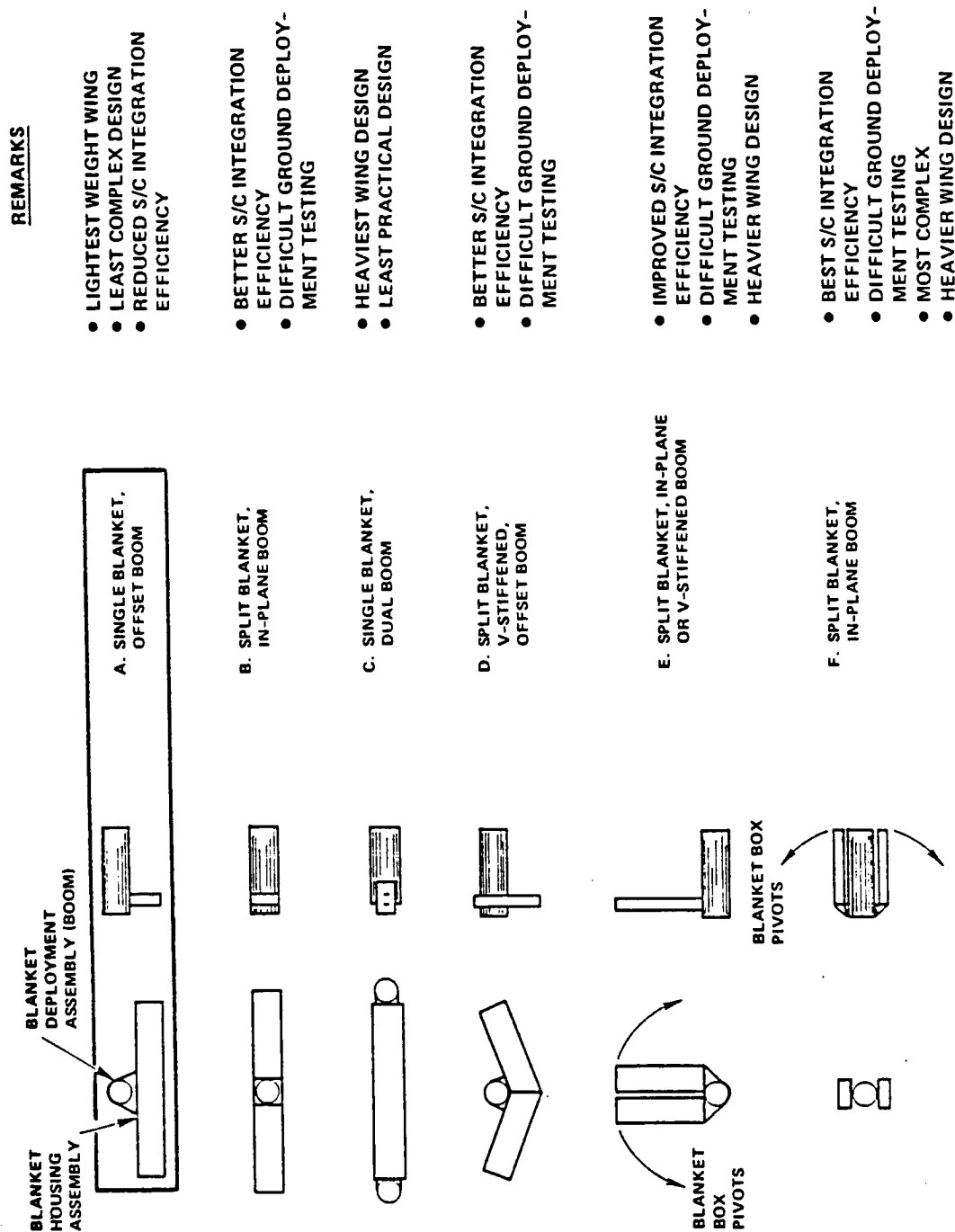


Figure 3-1. Stowed Wing Configuration Options

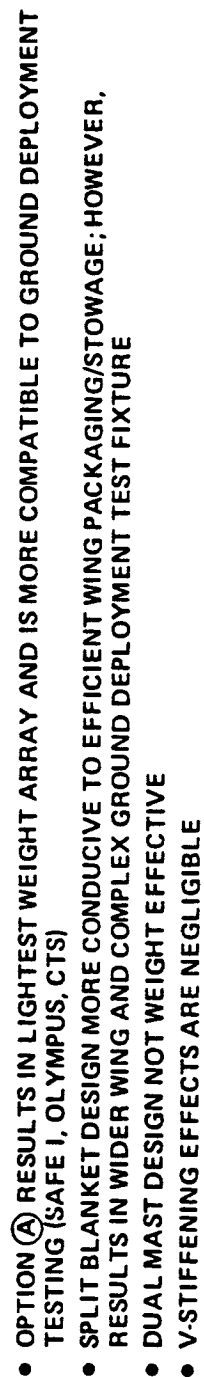


Figure 3-2. Wing Blanket/Mast Arrangement Options

Table 3-1. Existing Experience for Blanket/Mast Arrangements

PROGRAM	STATUS	BLANKET TYPE	BOOM TYPE (NO. PER WING)	BLANKET/BOOM ARRANGEMENT
CTS	FLIGHT	FOLDOUT	BISTEM (1)	SINGLE/OFFSET
FRUSA	FLIGHT	ROLLOUT	BISTEM (2)	SINGLE/IN-PLANE
X4	FLIGHT	FOLDOUT	TELESCOPING (1)	SPLIT/IN-PLANE
SAFE I	FLIGHT	FOLDOUT	COILABLE LATTICE MAST (1)	SINGLE/OFFSET
SPACE TELESCOPE	NEAR FLIGHT	ROLLOUT	BISTEM (2)*	SINGLE/IN-PLANE*
LSAT (OLYMPUS)	NEAR FLIGHT	FOLDOUT	COILABLE, LATTICE MAST (1)	SINGLE/OFFSET
SNIAS	PROTOTYPE	FOLDOUT	PANTOGRAPH (1)	SINGLE/OFFSET
DORA	PROTOTYPE	ROLLOUT	BISTEM (2)*	SINGLE/IN-PLANE*
ROSA	PROTOTYPE	ROLLOUT	BISTEM (2)	SINGLE/IN-PLANE
RAE	PROTOTYPE	FOLDOUT	TELESCOPING (1)	SPLIT/IN-PLANE
TRW ULWSA	PROTOTYPE	FOLDOUT	COILABLE, LATTICE MAST (1)	SINGLE/OFFSET
LMS/SPACE STATION	PROTOTYPE	FOLDOUT	ARTICULATED, LATTICE MAST (1)	SPLIT/IN-PLANE
PEP	STUDY	FOLDOUT	COILABLE, LATTICE MAST (1)	SINGLE/OFFSET
SEP	STUDY	FOLDOUT	COILABLE, LATTICE MAST (1)	SPLIT/IN-PLANE
SPACE PLATFORM	STUDY	FOLDOUT	COILABLE, LATTICE MAST (1)	SPLIT/IN-PLANE
JPL/GE	STUDY	FOLDOUT, ROLLOUT	COILABLE, LATTICE MAST (1)	SPLIT/V-STIFFENED

*HALF WING

Figures 3-3 through 3-7 illustrate the wing stowage arrangements and the resulting dimensional restrictions on the BHA (blanket box), thus on the total width of the blanket, using a shuttle-launched generic spacecraft. The critical spacecraft dimension of width was varied between 2.0 and 2.5 m (80 and 100 inches). The effect of horizontal mode spacecraft stowage (spacecraft longitudinal axis coincident with cargo bay longitudinal axis) and vertical mode spacecraft storage (spacecraft longitudinal axis perpendicular to cargo bay longitudinal axis) was examined. A diameter of 0.30 m (12 inches) was allocated to the size of the mast stowage canister. A blanket box width of 0.43 m (17 inches) was used based on layout studies to permit eight rows of 2x4 cm solar cells to fit on a blanket panel (see Section 3.3.3).

Figures 3-3 and 3-4 represent the most conventional stowage options and result in blanket box lengths (blanket widths) ranging from 1.8 to 3.3 m (72 to 129 inches), depending on the width of the spacecraft and location of the mast relative to the spacecraft sidewall. The results indicate that the split-blanket options shown in Figures 3-3 and 3-4 do not provide for an increase in overall wing width, when compared to widths obtained for the single blanket wing stowed like Section B-B in the figures. Figures 3-5 and 3-6 illustrate other stowage options, when the spacecraft is stowed horizontally in the shuttle cargo bay. For the most part, these options would be less likely to be possible relative to the more conventional options shown in Figures 3-3 and 3-4, or they require added complication to the wing design or spacecraft design. Nevertheless, if additional wing width is desired, then options such as these must be considered. Figure 3-7 shows the arrangement when the spacecraft is stowed vertically in the Shuttle cargo bay. For this case, the blanket box length would be limited by the length of the cargo bay allocated to the spacecraft.

In summary, the array configuration trades led to the selection of a single blanket, offset mast design because of the following reasons:

1. Least complex design, requiring fewer mechanisms, thus leads to the lightest weight array design
2. Less complex to fabricate, assemble, and ground test
3. Can be integrated to a typical size spacecraft and stowed in the shuttle cargo bay, and results in adequate blanket widths, ranging from 2.7 to 3.9 m (106 to 154 inches) depending on the size of the spacecraft and specific details of how it is integrated into the spacecraft.

3.2 MECHANICAL DESIGN TRADES

3.2.1 Blanket Assembly

The blanket assembly was considered to be the most critical and complex element of the flexible blanket array design. The blanket assembly had to meet several key requirements:

1. In conjunction with the blanket housing assembly, provide protection for the solar cell modules during the launch phase and wing deployment operations
2. Sustain long-term space radiation environments and cyclic temperature extremes without adverse degradation of mechanical or thermophysical properties

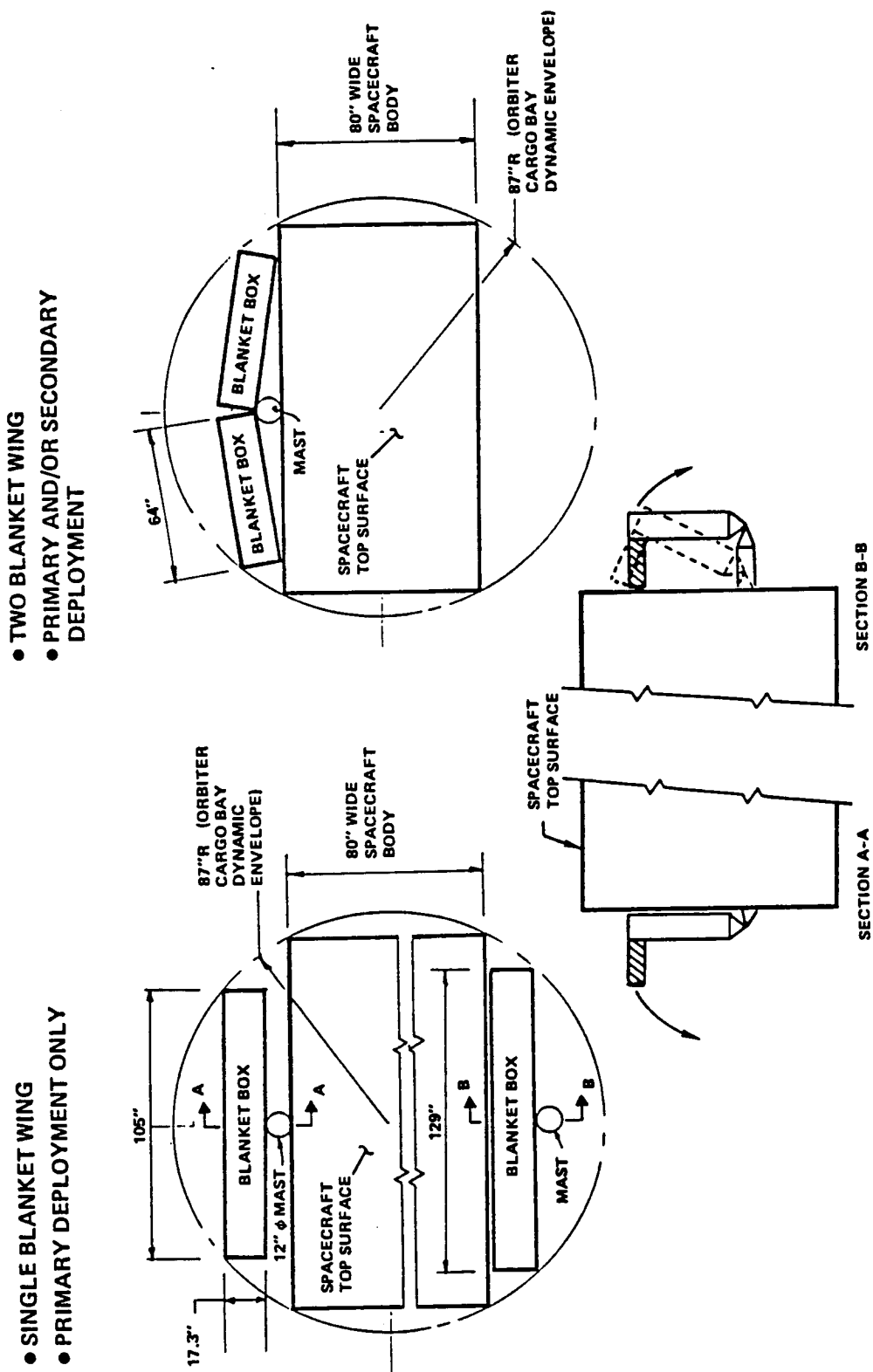


Figure 3-3. Spacecraft/Wing Integration Options, 2.0 m (80 Inches) Wide Spacecraft Body, Horizontal Shuttle Stowage Mode

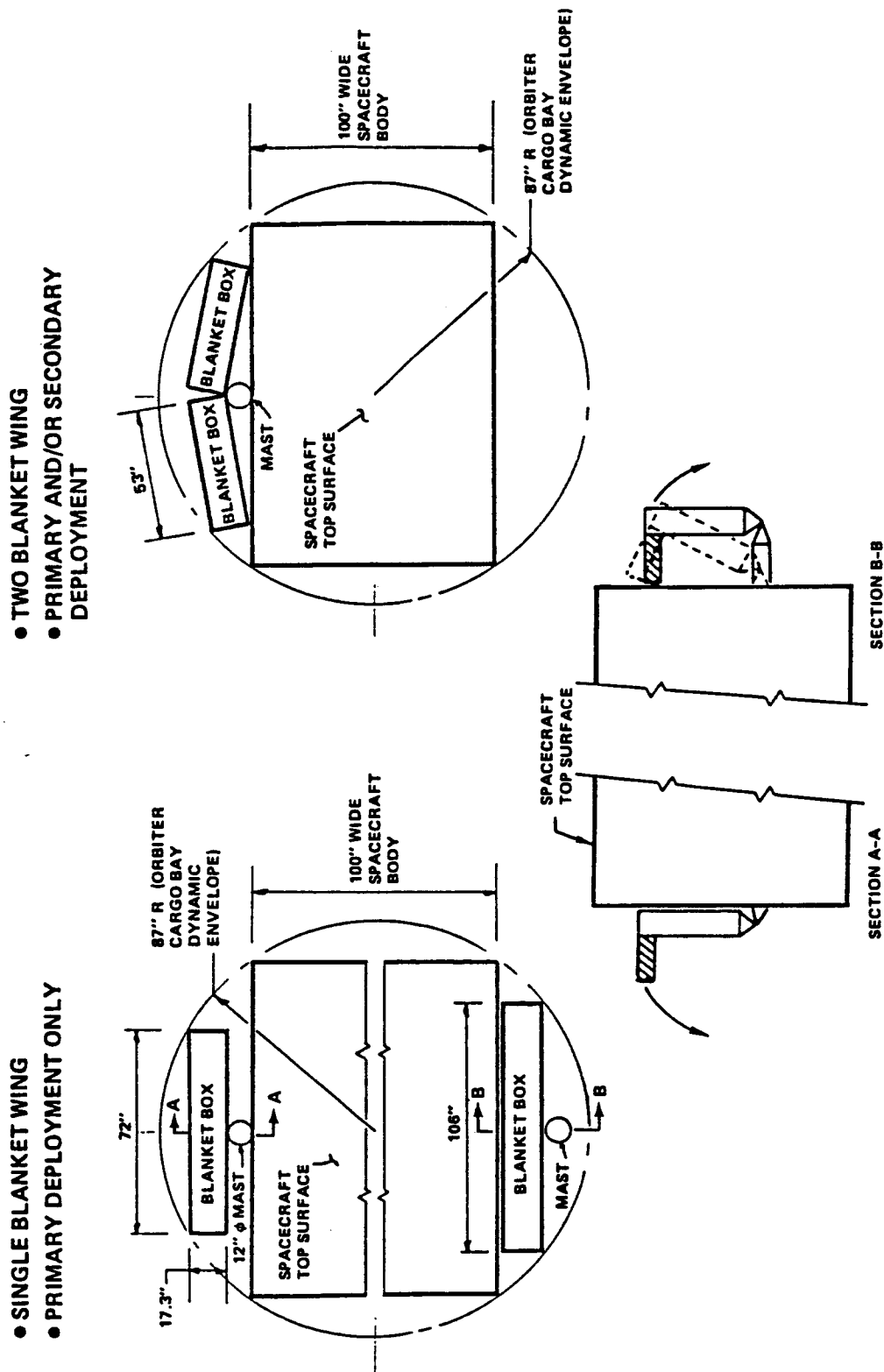


Figure 3-4, Spacecraft/Wing Integration Options, 2.5 m (100 Inches) Wide Spacecraft Body, Horizontal Shuttle Stowage Mode

- SINGLE BLANKET WING
- BLANKET BOX STOWED ON TOP OF SPACECRAFT WITH PRIMARY DEPLOYMENT ONLY; OR STOWED ON SIDE OF SPACECRAFT WITH SECONDARY DEPLOYMENT REQUIRED

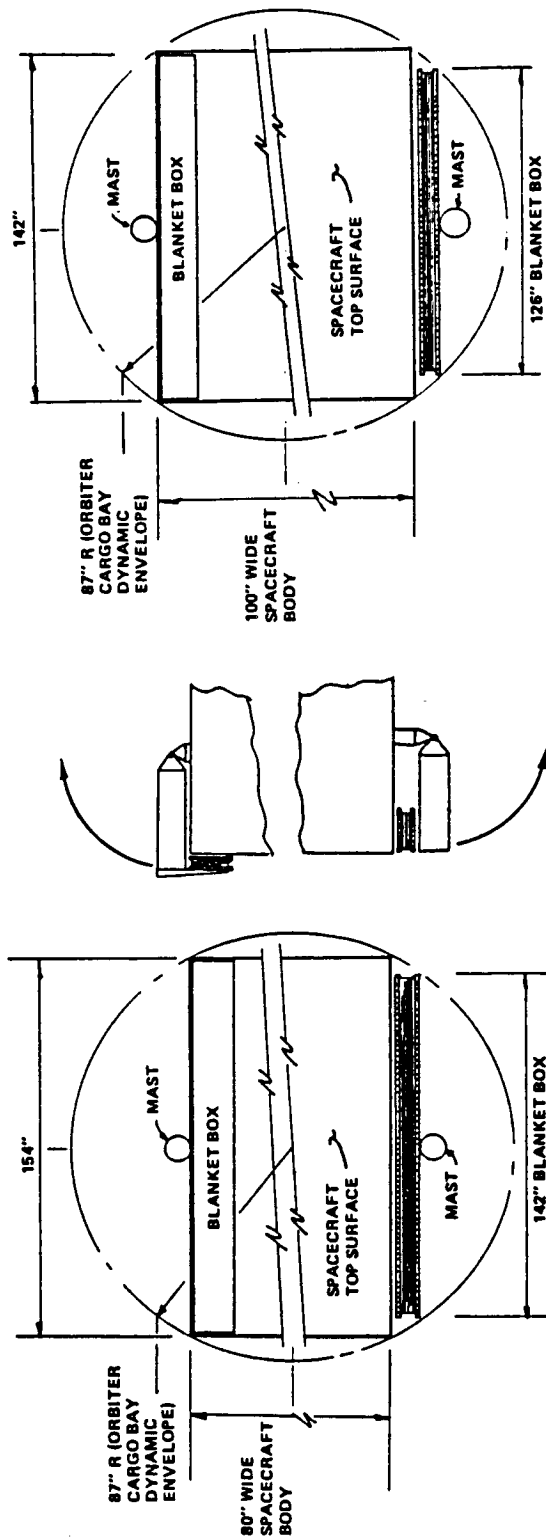
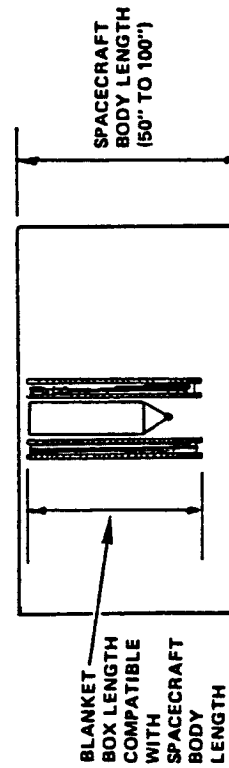
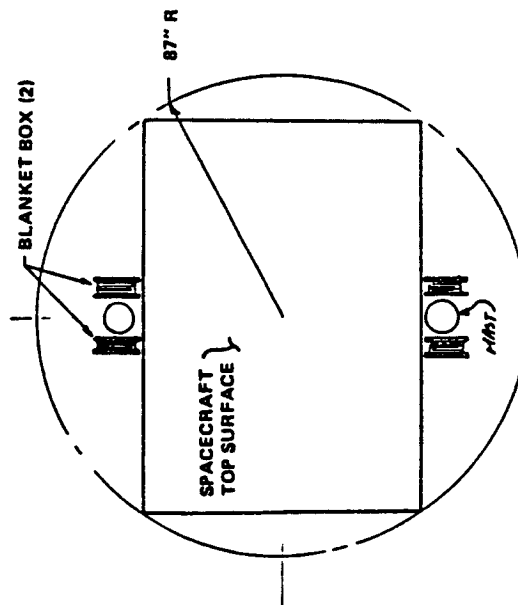


Figure 3-5. Other Spacecraft/Wing Integration Options, 2.0 to 2.5 m (80 and 100 Inches) Wide Spacecraft, Horizontal Shuttle Stowage Mode

- TWO BLANKET WING
- SECONDARY DEPLOYMENT REQUIRED



- SINGLE BLANKET WING
- MAY REQUIRE SECONDARY DEPLOYMENT TO PROVIDE SEPARATION DISTANCE BETWEEN SPACECRAFT SIDEWALL AND BLANKET BOX

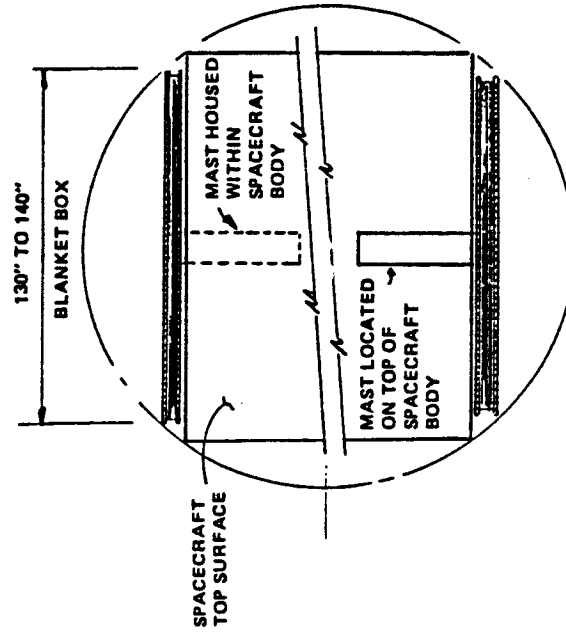


Figure 3-6. Other Spacecraft/Wing Integration Options, Horizontal Shuttle Stowage Mode

- SINGLE BLANKET WING
- PRIMARY DEPLOYMENT ONLY

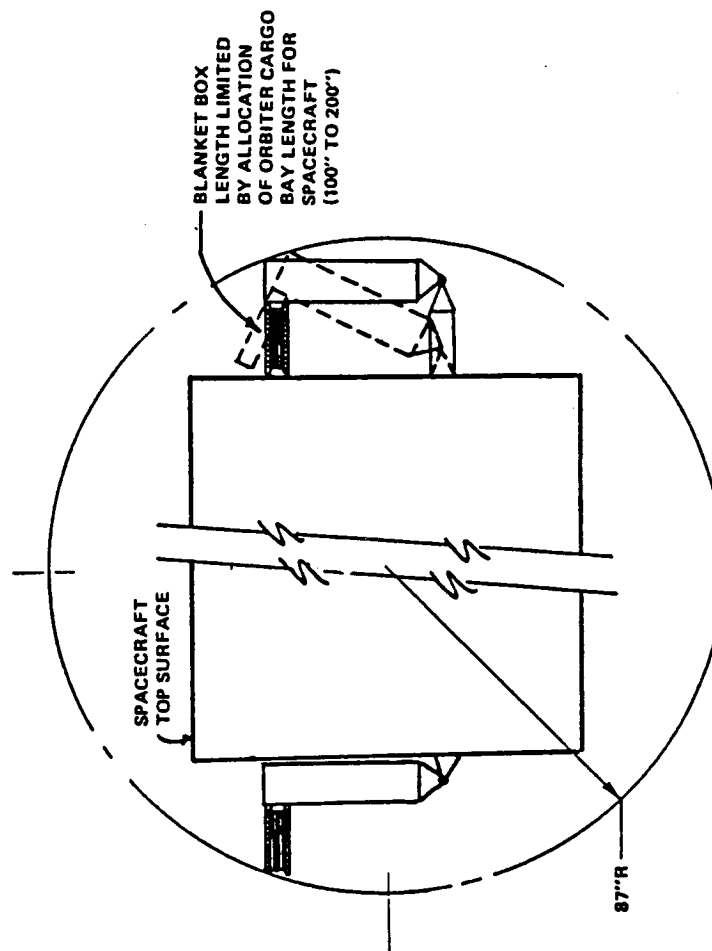


Figure 3-7. Spacecraft/Wing Integration Options, Vertical Shuttle Stowage Mode

3. Be resistant to electrostatic charge buildup from substorm environments
4. Retain high thermal emittance on the rear surface to help maintain low solar cell operating temperature
5. Be thermomechanically compatible with the interconnected solar cell modules to minimize thermal cycle fatigue damage to the circuits
6. Provide a degree of stiffness to enable blanket handling during ground operations and during wing deployment so as not to overstress the solar cell modules
7. Be compatible with cost-effective fabrication, assembly, and integration operations
8. Be compatible for simulated zero gravity deployment testing in a ground laboratory
9. Be of minimum weight consistent with low-risk production, packaging, launch, and in-orbit deployment and operation
10. Be conducive to prototype hardware fabrication within 15 months after completion of the design definition study
11. Be able to accommodate advanced photovoltaic components and be adaptable to operate in other earth orbital missions (non-geosynchronous) or interplanetary missions.

Some of the above requirements tend to lead to conflicting solutions that may compromise overall array performance. Thus, the design trades considered all aspects of ground, launch, and in-orbit environments to arrive at the best solution consistent with low-risk production and in-orbit operation.

3.2.1.1 Blanket Substrate

The total blanket assembly is accordion-folded into a series of discrete panels as illustrated in Figure 3-8. For proper folding, there must be an even number of panels. All panels are covered with solar cell modules except the first and last panels, which are termed "leaders." These leaders provide added protection between the blanket housing assembly structure and the adjacent cell-covered panels and also provide some separation distance between the blanket housing assembly structure (lid and pallet) and the adjacent cell-covered panels to eliminate chances of shadowing and to minimize thermal interactions.

Depending on the width of the blanket and the panel width, the number of panels can range from 20 to 100. Based on later wing aspect ratio trade studies and cell circuitry layout trade studies, the nominal panel width was about 0.38 m (15 inches) (distance between blanket foldlines) to accommodate eight rows of 2x4 cm cells (see Section 3.3.3). For a nominal 5 kW (BOL) power silicon cell wing, the number of cell-covered panels ranged from 24 to 48 when the blanket width ranged from 4.2 to 2.2 m (166 to 86 inches) (refer to Figure 1-2).

Table 3-2 lists several material/construction options considered for the blanket substrate. Many of the candidates are based on U.S./European flight

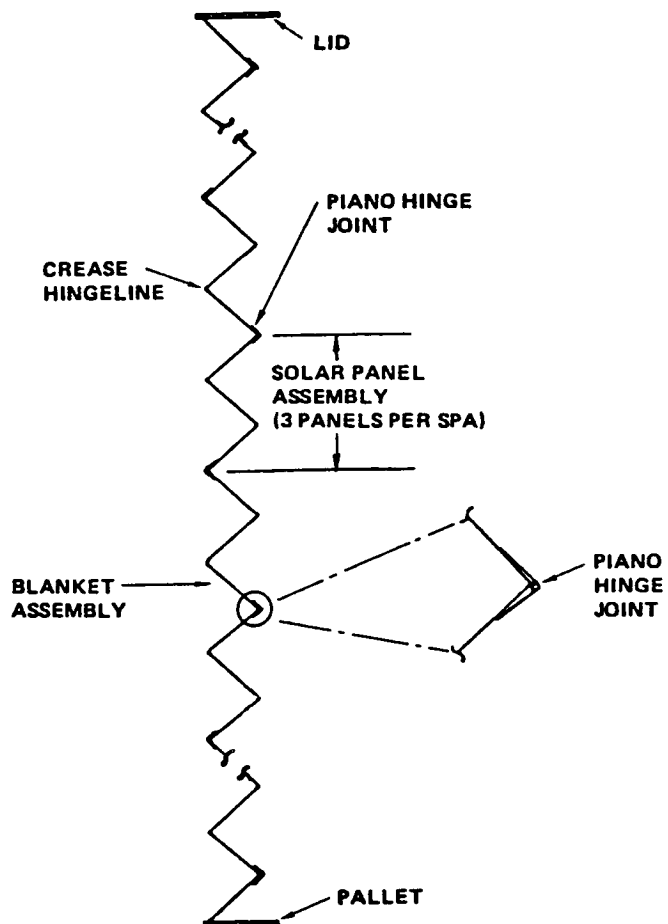


Figure 3-8. Accordion-Folded Blanket Assembly

Table 3-2. Blanket Substrate Material/Construction Options

CONSTRUCTION	AREAL WT (KG/M ²)	CTE IN/IN °C x 10 ⁻⁶	REMARKS
50 μM PLAIN KAPTON H	0.071	10	<ul style="list-style-type: none"> • MAY REQUIRE SECONDARY STIFFENING ELEMENTS • REQUIRES ATOMIC OXYGEN PROTECTION AT LEO • REQUIRES ANTI-CHARGE CONTROL AT HIGHER ORBITS
50 μM CARBON LOADED* (37%) KAPTON	0.074	10	<ul style="list-style-type: none"> • REQUIRES ATOMIC OXYGEN PROTECTION AT LEO • MAY REQUIRE SECONDARY STIFFENING ELEMENTS • CAN BE GROUNDED FOR ANTI-CHARGE CONTROL
25 μM KAPTON H/OPEN WEAVE FIBERGLASS CLOTH	0.087	9	<ul style="list-style-type: none"> • REQUIRES ATOMIC OXYGEN PROTECTION AT LEO • REQUIRES ANTI-CHARGE CONTROL AT HIGHER ORBITS • USED ON CTS, FRUSA, LSAT BLANKETS
25 μM KAPTON H/OPEN WEAVE GRAPHITE CLOTH	0.133 TO 0.150	4.5	<ul style="list-style-type: none"> • REQUIRES ATOMIC OXYGEN PROTECTION AT LEO • USED ON ULP (MBB) PANELS • CAN BE GROUNDED FOR ANTI-CHARGE CONTROL
13 μM KAPTON H/OPEN WEAVE FIBERGLASS CLOTH/ 25 μM KAPTON H	0.120	9	<ul style="list-style-type: none"> • REQUIRES ATOMIC OXYGEN PROTECTION AT LEO • REQUIRES ANTI-CHARGE CONTROL AT HIGHER ORBITS • USED ON SPACE TELESCOPE
RIBBED 25 μM KAPTON H/ RIBBED 25 μM KAPTON H	0.140	10	<ul style="list-style-type: none"> • REQUIRES ATOMIC OXYGEN PROTECTION AT LEO • REQUIRES ANTI-CHARGE CONTROL AT HIGHER ORBITS • DEVELOPED BY TRW FOR ITS PROTOTYPE WING MODEL
RIBBED 25 μM KAPTON H/76 μM KEVLAR CLOTH/RIBBED 25 μM KAPTON H	0.290	3.3	<ul style="list-style-type: none"> • REQUIRES ATOMIC OXYGEN PROTECTION AT LEO • REQUIRES ANTI-CHARGE PROTECTION AT HIGHER ORBITS • DEVELOPED BY TRW
RIBBED 25 μM KAPTON H/127 μM GRAPHITE CLOTH/RIBBED 25 μM KAPTON H	0.380	1.8	<ul style="list-style-type: none"> • REQUIRES ATOMIC OXYGEN PROTECTION AT LEO • REQUIRES ANTI-CHARGE PROTECTION AT HIGHER ORBITS • DEVELOPED BY TRW
76 μM KEVLAR CLOTH OR 76 μM FIBERGLASS CLOTH	0.120	≈ 3	<ul style="list-style-type: none"> • REQUIRES ATOMIC OXYGEN PROTECTION AT LEO • REQUIRES ANTI-CHARGE PROTECTION AT HIGHER ORBITS

*SELECTED AS BASELINE MATERIAL

hardware and technology development studies. In many instances, the prior flight programs failed to address all the key issues. The CTS array (using fiberglass-reinforced Kapton) for a geosynchronous mission did not include electrostatic charge control measures and, as a result, experienced electrostatic discharge-related anomalies. FRUSA and SAFE I were short-term low-earth orbit (LEO) flight experiments and didn't address atomic oxygen protection issues or electrostatic charge control issues. The Olympus (LSAT) array is using a CTS-type blanket except coated with a carbon-filled resin layer on the rear surface to handle the electrostatic charge control issues at its geosynchronous orbit. However, the blanket areal density is relatively high and the overall array design is quite weight inefficient (<30 W/kg specific power for a 7 kW [EOL] array). The Space Telescope (ST) blanket construction is known to be susceptible to atomic oxygen degradation at LEO and does not provide for electrostatic charge control. Thus, it was concluded that previous flight experience (or near-term flight hardware) did not provide obvious solutions to the requirements that must be met by the APSA design.

For the point design required by APSA (namely, a geosynchronous mission) atomic oxygen is not an issue; however, electrostatic charge control is a major issue. This point is further discussed in Section 3.3.6, where it is shown that for geosynchronous missions, grounding of the blanket substrate is a firm requirement. This implies some type of conductive (or semiconductive) surface on the rear side of the blanket to permit grounding of the blanket and bleed-off of the charge buildup from the substorm charged particle environments. Conductive paints, carbon soot impregnated resins, graphite fibers, carbon-loaded films, wire mesh, semiconductive coatings, and metallic coatings were all examined. Conductive paints, wire mesh, and other additives complicate the fabrication of the blanket and have a measurable weight impact. Metallic coatings result in unacceptably high cell operating temperatures because of their very low thermal emittance properties. The use of semiconductive indium-tin-oxide reduces the emittance such that the blanket size would have to be increased 5 to 10 percent to compensate for the slightly higher cell operating temperatures.

It was therefore concluded that the preferred material would be black conductive (carbon-loaded) Kapton. The carbon-loaded polyimide film is readily available from DuPont with resistivity sufficiently low to permit grounding of the substrate. Kapton has superior mechanical and space radiation resistant properties for a polymer film. The use of a 50 μm (2 mil) thick black Kapton substrate results in one of the lightest substrate options available.

Another key requirement for the substrate is to contribute to the protection of the solar cell modules during the launch environment. Three basic approaches were examined: (1) separate padding that is interleaved between the folded blanket panels, (2) discrete padding attached or integral to the substrate, and (3) foam padding only on the inner surfaces of the blanket housing assembly. CTS and Olympus were examples of the first approach, wherein thin open-cell polyurethane sheets are placed in the folded blanket stack to prevent direct cell-to-cell contact when the blanket is folded. When the blanket unfolds, the interleaves remain in the blanket housing assembly. Refolding of the blanket cannot be done automatically with this approach. The second approach had been developed in many forms. Options include rigid plastic protrusions or compliant ribs between the solar cell modules. These protrusions/ribs come into contact with each other (or come in direct contact with the cells) from the opposite facing

panel when the blanket is folded and pressure is exerted by a preload mechanism in the blanket housing assembly structure to immobilize the folded blanket assembly.

The third technique, and the one selected as the baseline, was to allow the solar cell modules to be in direct contact with one another from opposite facing folded panels and rely on the foam padding on the inner surfaces of the blanket housing assembly structure (lid and pallet) to apply a quasi-uniform compressive pressure to the folded blanket assembly. This preload pressure immobilizes the blanket panels from shifting around during the launch phase when vibro-acoustic forces could damage an unconfined/unrestrained folded blanket assembly. This technique was successfully demonstrated at the component level under the SEPS array technology development program and on prototype array flight hardware (SAFE I) for the protection of 6x6 cm conventional thickness solar cell modules and 2x2 cm thin cell modules. From the standpoint of design and manufacturing simplicity and weight considerations, this appears to be the best approach for solar cell protection.

3.2.1.2 Inter-Panel Hinge and Solar Panel Assemblies

The hinge between the blanket panels had to serve many functions:

1. Permit easy unfolding (and folding) of the blanket assembly
2. Have sufficient strength to withstand the static and dynamic blanket tension loads
3. Be compatible with all environmental considerations (space radiation, atomic oxygen, etc.)
4. Have a low thickness profile so as not to impede uniform packaging of the folded blanket
5. Provide a convenient method for replacement of blanket sections without major rework of the entire blanket assembly
6. If retractibility is a requirement (not for the baseline design), provide positive refolding torque and lateral stiffness at each hinge line.

Figure 3-9 illustrates several hinge configurations that were examined to create a flat-fold blanket assembly design. Some will perform all the functions listed above. However, without having a baseline requirement to perform in-orbit wing retraction, simple lightweight hinge designs can be used in place of the more complex designs that provide lateral stiffness and a positive refolding torque at the hinge line.

Based on the successful flight experience of the CTS array and the ground demonstration testing of the Olympus array, the two hinge designs that were selected include: (1) simple crease folds in the substrate and (2) at periodic locations, a piano hinge joint.

The blanket will be built up from a series of subunits termed "solar panel assemblies" (SPA), as was indicated in Figure 3-8. The use of SPAs is more

- FOR NON-RETRACTABILITY, THE SIMPLE CREASE AND PIANO HINGES ARE ACCEPTABLE (CTS, OLYMPUS)
- FOR RETRACTABLE WINGS, MORE COMPLICATED AND HEAVIER HINGE ASSEMBLIES WITH POSITIVE RESTOWING TORQUE CHARACTERISTICS ARE REQUIRED (SAFE I, TRW IRAD)

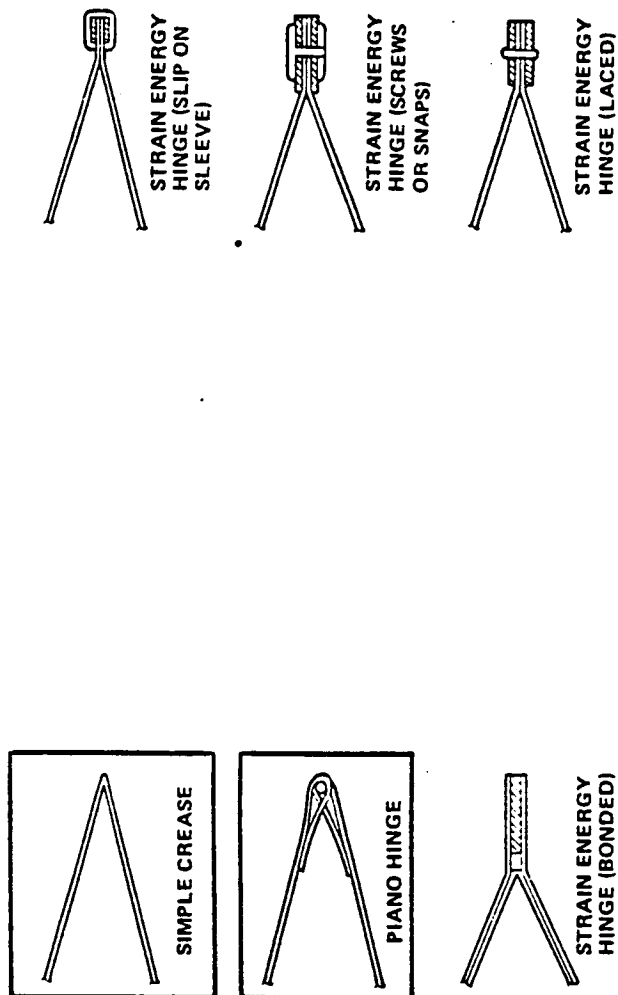


Figure 3-9. Candidate Blanket Assembly Hinge Designs

conductive to efficient blanket fabrication, handling, assembly, and integration (and workarounds) than one continuous, integral blanket assembly. Each SPA consists of an odd number of panels to minimize the buildup of thicker piano hinges on one side of the folded blanket assembly. The number of panels per SPA will be three because of the width limitations on the available carbon-loaded Kapton substrate material. If more panels are used for each SPA (i.e., five or seven), then the basic Kapton substrate must be lap-spliced in order to obtain an adequate size of material to form the SPA. The SPAs, in turn, are joined together by the piano hinge, which is formed as an integral part of the SPA substrate. A small diameter graphite or fiberglass rod is used as the hinge pin to connect together adjacent SPAs.

3.2.2 Blanket Housing Assembly

The purpose of the blanket housing assembly is to: (1) protect the folded blanket assembly during integration of the array to the spacecraft, (2) protect the folded blanket assembly during launch and transfer orbit vibro-acoustic environments, (3) assist in the guidance and control of the blanket during the deployment/retraction process, and (4) help support the blanket assembly when fully deployed.

It was recognized that the blanket housing assembly (along with the mast system) must be lightweight and be structurally/mechanically efficient if the performance goals for the array were to be met. The design approach taken was to pattern the blanket housing assembly after the flight proven CTS solar array design and our prototype flexible blanket wing.

3.2.2.1 Housing Structure

Figure 3-10 conceptually shows the housing structure. For weight reasons the primary structural elements consist of two rigid honeycomb sandwich plates, rather than a completely enclosing box-like structure. The "pallet" plate would be rigidly attached to the mast stowage canister and the "lid" plate would be rigidly attached to the outboard end of the mast. Both the lid and the pallet act as "spreader bars" to help provide a quasi-uniform tension force across the blanket width when the blanket is fully deployed. The plates must also react the launch vibro-acoustic loads; however, the primary loading condition that determined the structural sizing of the plates was the quasi-uniform pressure loading applied to the folded blanket assembly during launch operations. This pressure is used to immobilize the folded blanket assembly while being subjected to the launch vibro-acoustic environments. The pressure is developed through compression of a layer of foam padding that covers the inner surfaces of both the lid and pallet plates.

The plate design to achieve minimum blanket housing assembly weight involved a trade-off of plate stiffness, the number of latch points used to hold the lid to the pallet, and the uniformity and intensity of the stowage pressure loading. A preliminary structural analysis was performed on the plate structure for the purpose of determining the system weight sensitivity to various material and configuration parameters to facilitate the selection of a minimum weight, optimum stiffness design. Tables 3-3 and 3-4 summarize the various parameters evaluated and design criteria established. A NASTRAN finite element model of a generic sandwich structure was developed to represent the lid or pallet plate whereby the structure was idealized as a narrow rectangular plate on an elastic foundation

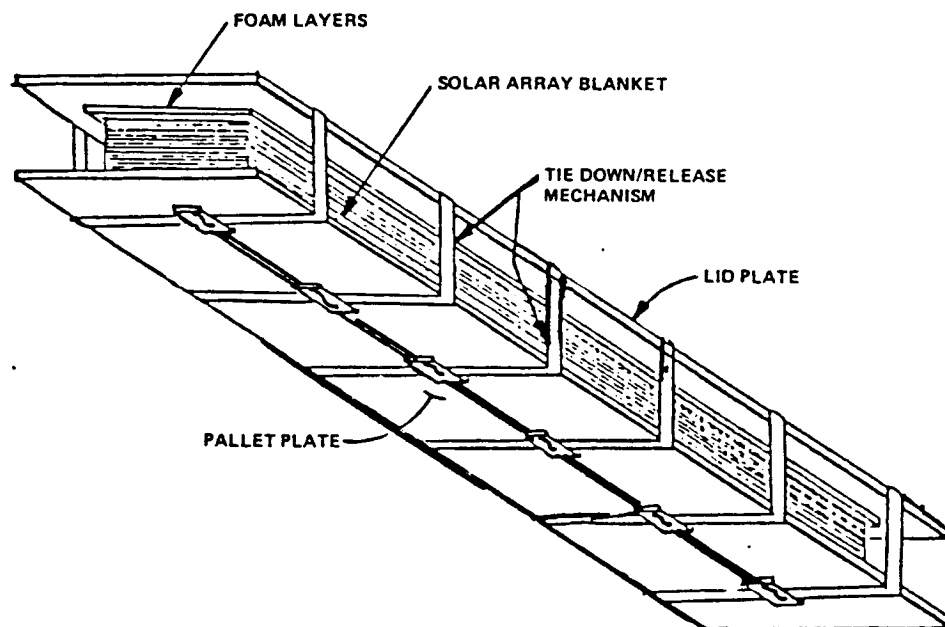


Figure 3-10. Conceptual Configuration of Housing Structure

Table 3-3. Design Parameters for Housing Structure

<u>Sandwich Construction</u>	<u>Foam Stiffness</u>
<ul style="list-style-type: none"> • Facesheet-stiffened • Rib-stiffened 	<ul style="list-style-type: none"> • 2 psi/inch • 10 psi/inch
<u>Facesheet Material</u>	<u>Tiedown Spacing</u>
<ul style="list-style-type: none"> • GY70 Graphite/Epoxy • Beryllium 	<ul style="list-style-type: none"> • 16 to 48 inches
<u>Facesheet Thickness</u>	<u>Tiedown Method</u>
<ul style="list-style-type: none"> • 10 mils 	<ul style="list-style-type: none"> • Straps • Clamps
<u>Sandwich Thickness</u>	<u>Plate Size</u>
<ul style="list-style-type: none"> • >0.25 inch 	<ul style="list-style-type: none"> • 16 inches wide x length
<u>Foam Pressure Range</u>	<u>Aspect Ratio</u>
<ul style="list-style-type: none"> • 1 psi average • >0.5 psi minimum • <2.0 psi peak 	<ul style="list-style-type: none"> • Wing aspect ratio of 2.5 to 10

Table 3-4. Design Criteria for Housing Structure

PROPERTY	FACE SHEET		CORE
	BERYLLIUM	GY-70 GRAPHITE	
E (msi)	42.0	22.0	—
G (msi)	20.0	0.71	0.022
ν	—	—	0.3
FTU (ksi)	40.0	35.0	—
FTY (ksi)	30.0	—	—
W (pci)	0.066	0.06	0.0018*

*3.1 LB/FT³ CORE (3/16-5052-0.001P)

DESIGN FACTORS — LIMIT LOAD = 1.4
YIELD STRESS = $1.1 \times 1.4 = 1.54$
ULT STRESS = $2.0 \times 1.4 = 2.80$

with discrete loading points representing the location of the latch points used to hold the lid to the pallet. The elastic foundation was idealized by a series of distributed linear springs with characteristics representative of the measured foam stiffness (load-deflection characteristics). A total of 72 conditions were evaluated representing different combinations of the various parameters identified.

Figure 3-11 illustrates typical results for the graphite/epoxy facesheet aluminum honeycomb core sandwich plate design and shows the relationship between tiedown spacing (i.e., the distance between latch points) and minimum required honeycomb core thickness for different design criteria (exceeding critical facesheet stress, exceeding maximum pressure of 13,800 Pa [2 psi], going below minimum acceptable pressure of 3500 Pa [0.5 psi]) for two values of foam stiffness (350 Pa/m [2 psi/in] and 1750 Pa/m [10 psi/in]). Similar curves were done for beryllium facesheet, aluminum honeycomb core panels. The results indicated that the facesheet stress criteria governed the determination of acceptable plate thickness for the soft foam 350 Pa/m (2 psi/in), but the pressure criteria governed the determination of acceptable plate thickness for the firm foam 1750 Pa/m (10 psi/in).

Figure 3-12 shows a summary of the earlier data and represents a "composite" envelope of the critical criteria for both foam stiffness levels and the two types of facesheet materials under consideration. Figure 3-13 plots the resulting lid and pallet areal weight versus tiedown spacing. The results indicated that the graphite/epoxy design would require a slightly thicker plate than the beryllium design; however, because of slight differences in material densities, the weight differences were negligible. Since beryllium structures are more costly and difficult to fabricate, graphite/epoxy was selected as the baseline facesheet material for the lid and pallet structure. In fact, except for fittings and mechanism components, graphite/epoxy material was used wherever possible in the blanket housing assembly structure to reduce weight.

Figure 3-14 shows the projected combined weight for the key structural components of the blanket housing assembly (lid, pallet, tiedown/release mechanism) versus the number of tiedown/release latch mechanism pairs (or the spacing between the latch points). The preliminary weight for the tiedown/release/latch mechanism was derived from other trade studies discussed in Section 3.2.2.4. The size of the blanket housing assembly shown (i.e., 0.42 x 2.8 m [16.5 x 112 inches]) would be that required for a mid aspect ratio wing. The results indicated that the system weight was relatively insensitive to the number of tiedown/release/latch mechanism pairs selected beyond four. For the preliminary design, six pairs were selected; however, for the final design, in order to reduce the number of piece parts and because the core thickness of at least 0.5 inch was preferred for installation of inserts and reaction of other concentrated loads, four latch mechanism pairs spaced about 0.76 m (30 inches) apart were selected.

3.2.2.2 Stowed Blanket Protection

Several approaches were reviewed for protection of the solar cell stacks and circuitry during the launch environment, in addition to placing the folding blanket assembly within a rigid structural container. The four primary approaches included: (1) separate padding that is interleaved between the folded blanket panels, (2) discrete padding attached or integral with the blanket panel substrate, (3) foam padding only on the inner surfaces of the structural container, and (4) some combination of the other three.

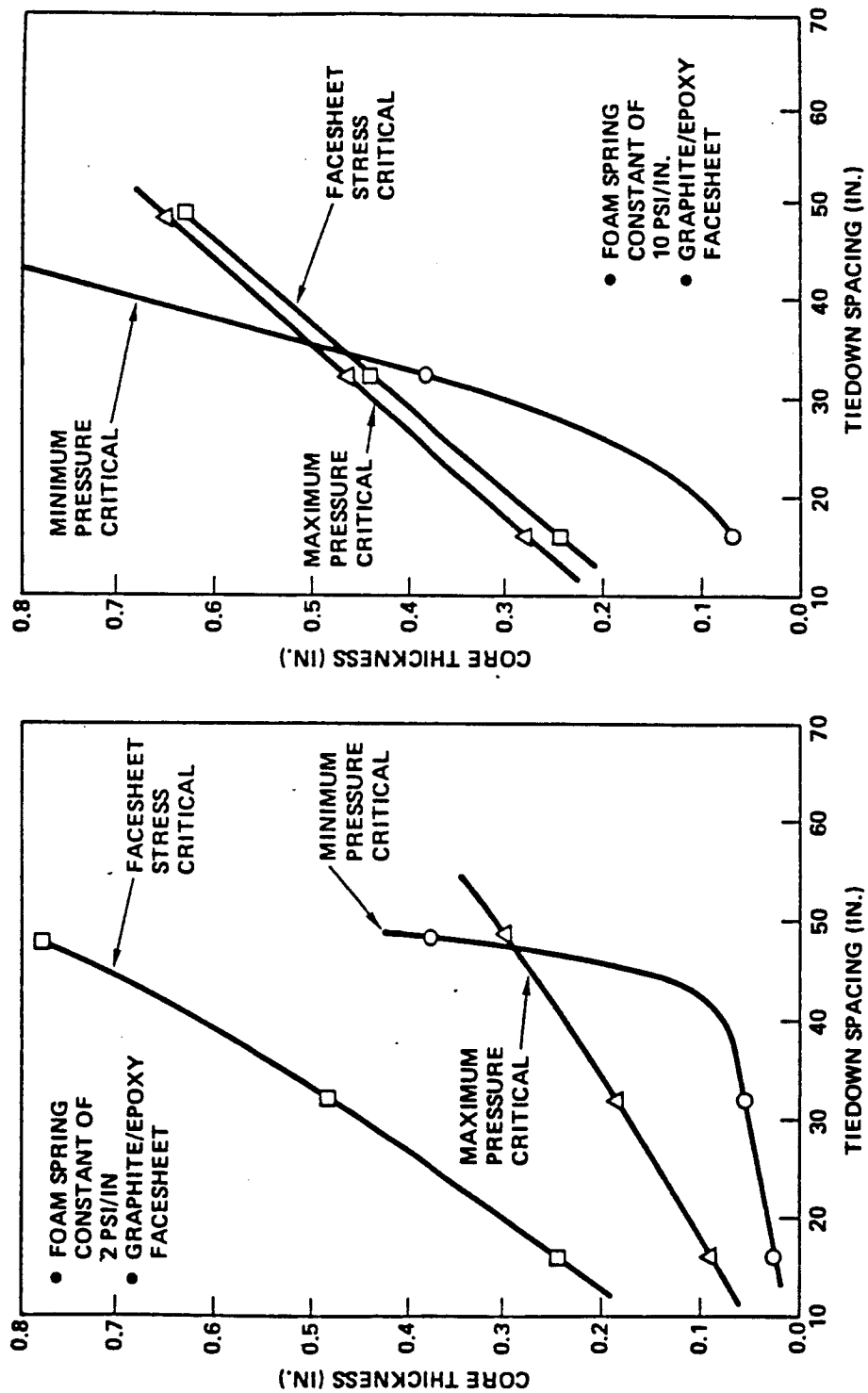


Figure 3-11. Required Sandwich Core Thickness for Lid and Pallet Structure of Tiedown Spacing and Design Criteria, 0.25 mm (10 mil) GY70 Graphite/Epoxy Facesheets

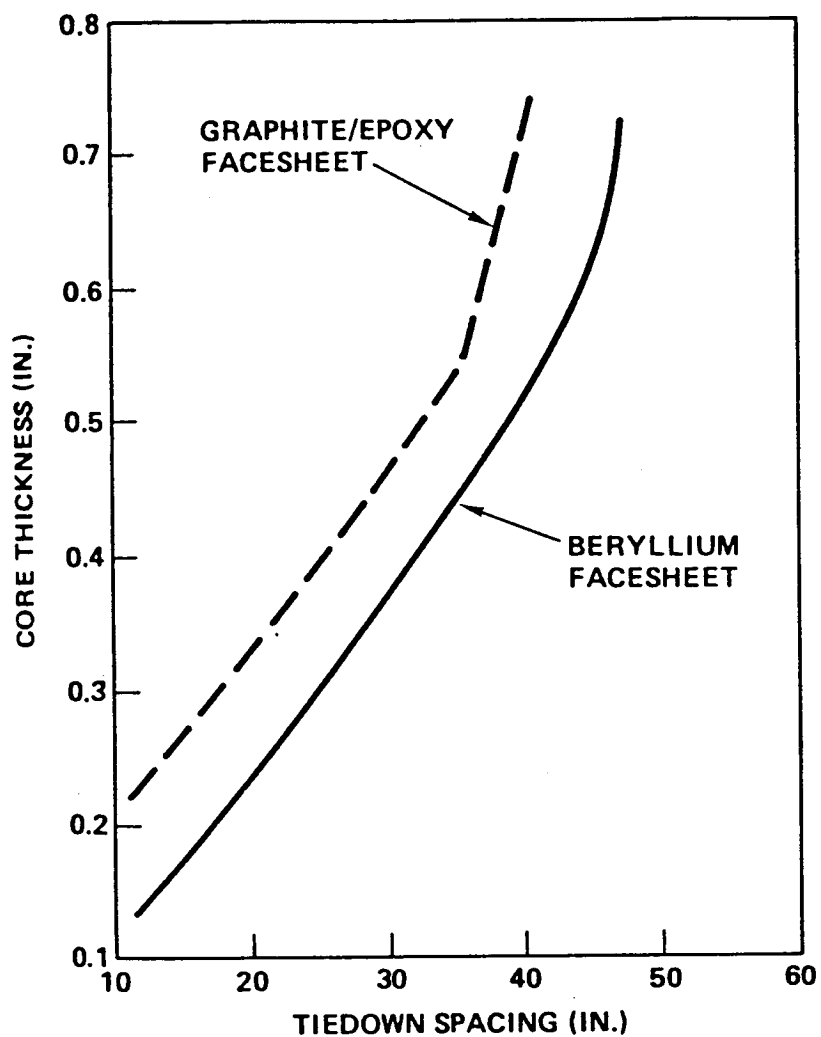


Figure 3-12. Required Sandwich Core Thickness for Lid and Pallet Structure as a Function of Tiedown Spacing, 0.25 mm (10 mil) Facesheet Thickness

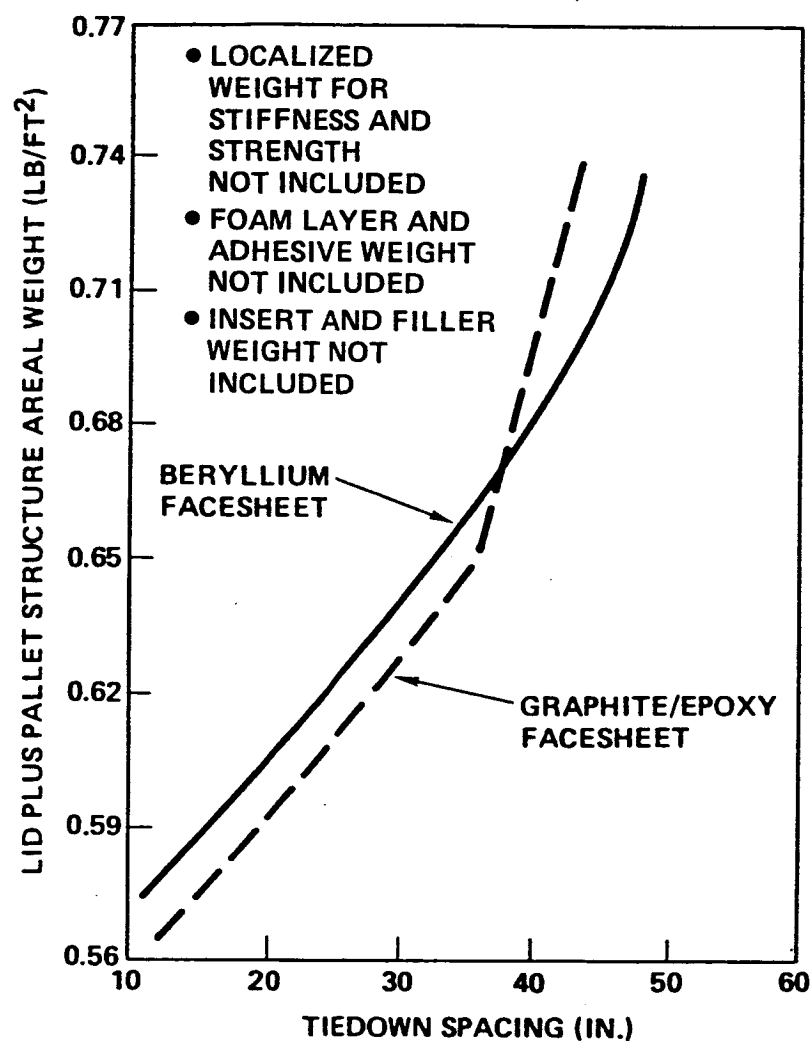


Figure 3-13. Areal Weight Trends for Lid and Pallet Structure as a Function of Tiedown Spacing, 0.25 mm (10 mil) Thick Facesheets, 50 kg/m³ (3.1 pcf) Aluminum Honeycomb Core

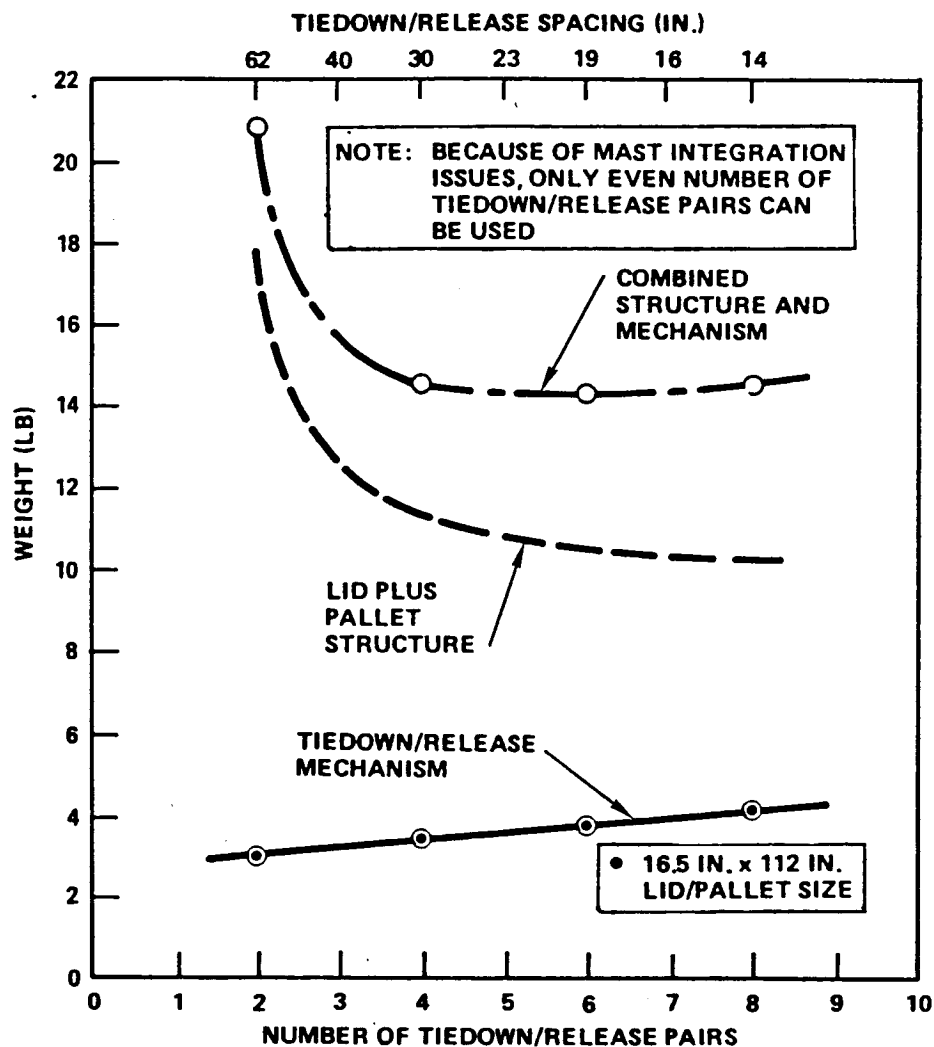


Figure 3-14. Weight Trends for Mid Aspect Ratio Wing Blanket Housing Assembly as a Function of Number of Tiedown Pairs, Graphite/Epoxy Facesheet Sandwich Housing Construction

CTS and Olympus solar arrays were examples of the first approach, wherein thin, open-cell polyurethane sheets were placed in the folded blanket stack to prevent direct cell-to-cell contact. Pressure is applied to the folded blanket to immobilize the blanket assembly. When the blanket deployed, the interleaves remained attached to the housing structure. Wing retraction was not possible with this approach. The rollout-type arrays like FRUSA and Space Telescope used corrugated Kapton interleaves that were retained on separate take-up rollers.

The second approach has been developed in many forms. Options include rigid RTV protrusions or compliant ribs between the solar cell stacks that stick above the height of the stacks. These protrusions/ribs come in contact with each other (or come in direct contact with the stacks) from the opposite facing blanket panel when the blanket is folded and pressure exerted by a preload mechanism attached to the housing structure. This approach is compatible with wing retraction; however, the design of the blanket substrate is more complicated and costly.

The third technique is to permit the solar cell stacks to be in direct contact with one another from opposite facing folded panels and to rely on foam padding on the inner surfaces of the housing structure to apply a quasi-uniform distributed compressive load to the folded blanket assembly via a preload mechanism in the housing structure. The preload pressure immobilizes the blanket panels from shifting around. This technique was successfully used on the SAFE I flexible blanket wing for the protection of 6 x 6 cm conventional thickness cells and 2 x 2 cm thin cells. Padding thickness was about 13 mm (0.5 inches) with pressure ranging from 3500 to 6900 Pa (0.5 to 1 psi). This approach is compatible with wing retraction and permits a simple membrane structure to be used for the blanket substrate.

From the standpoint of design and manufacturing simplicity and weight considerations, the use of foam padding on the inner surfaces of the housing structure was selected as the preferred approach for the baseline design. It was also recommended that during fabrication of the APSA prototype wing, that additional component tests be performed to better assess the acceptability of this approach.

As part of the preliminary design activity, a candidate flexible polyimide foam material was tested to measure its stiffness characteristics and long-term relaxation characteristics. The resulting load-deflection curve was non-linear, with stiffness values ranging from 350 to 1750 Pa/m (2 to 10 psi/in), with the lower values occurring during the initial stages of compression. Figure 3-15 shows the relaxation characteristics of the polyimide foam. The results indicate that the initial blanket preload pressure from the compressed foam will decrease slowly over time; but sufficient residual pressure will be retained after reasonable time periods (3 to 6 months) to serve the purpose for which it was intended.

3.2.2.3 Preload/Latch/Release Mechanism

Weight considerations of the lid and pallet structure dictated that multiple preload/release latches be used on the housing structure to secure the lid to the pallet and apply the proper pressure to the stowed blanket assembly. During the preliminary design phase, concepts were examined to varying degrees of detail in terms of feasibility, complexity and weight. It was decided that the mechanism must simultaneously actuate all the latches rather than having a sequential unlatching of the lid from the pallet. It was also decided that the mechanism

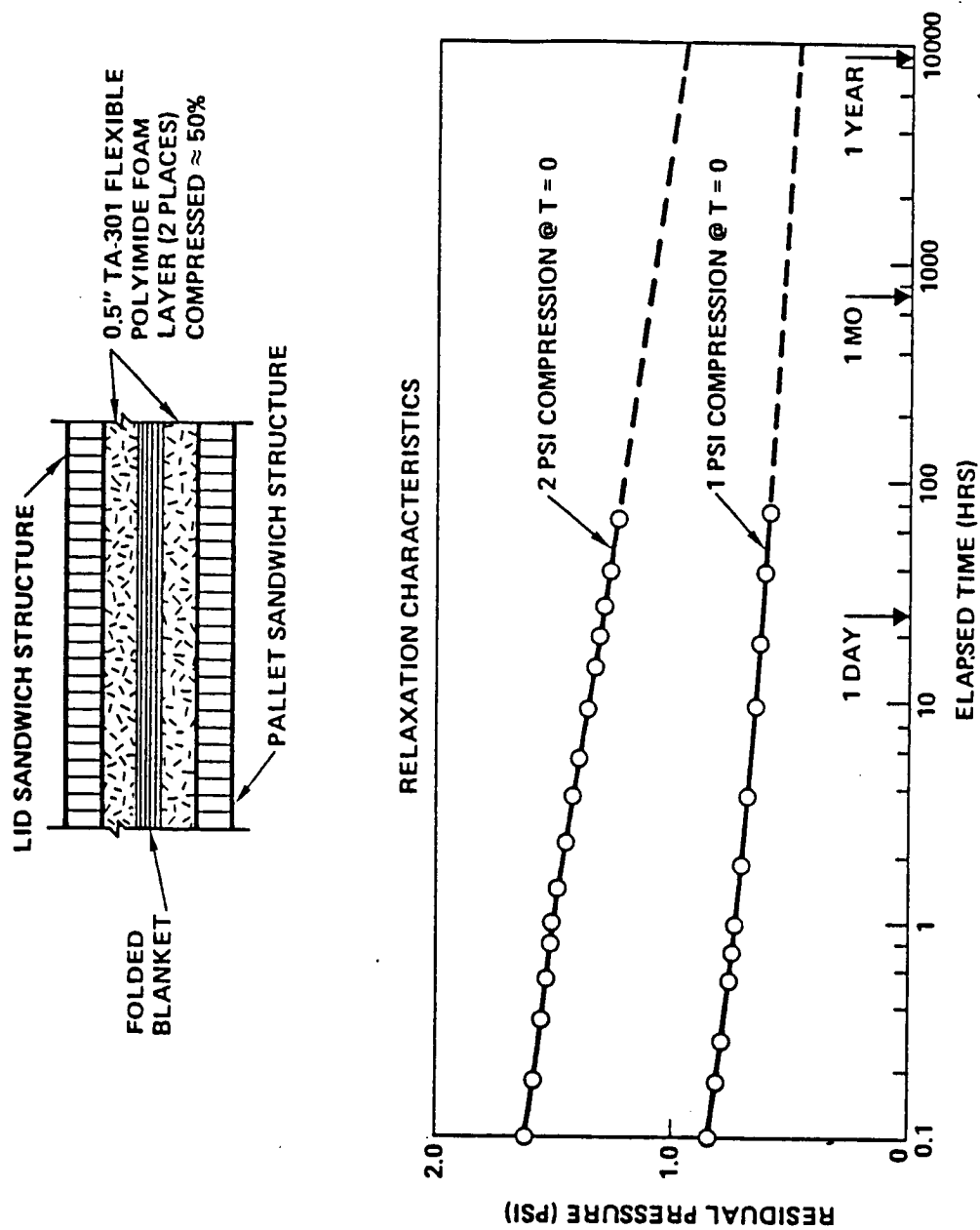


Figure 3-15. Stowed Pressure Relaxation Characteristics for Candidate Polyimide Foam Padding

must activate automatically in terms of release operations; however, automatic resecuring of the lid to the pallet was not required since wing retraction and restowage to the spacecraft sidewall in the launch configuration was not a requirement. Mechanisms that permit both automatic release and resecuring have been developed for the SAFE I wing and our prototype flexible blanket wing.

Table 3-5 lists the three concepts examined along with their qualitative advantages and disadvantages. Figures 3-16 and 3-17 illustrate the two primary concepts. In all cases, the mechanism is primarily located on the underside of the pallet structure so that only a small percentage of the mechanism weight would be deployed to the outboard end of the wing and to eliminate any complex electrical wiring that would have to go to any actuators located on the lid.

Figure 3-16 shows the "pushrod cable release mechanism." A long loop of braided steel cable attached to the lid wraps around to the pallet structure and is held by a pair of "hook" release latches. A motor-actuated pushrod attached to the pallet translates causing the "hook" latch mechanism to open up and release the cable. As the pushrod is being translated and the latches are opening, the lid is slowly being allowed to move away from the pallet as the pressure from the compressed foam layer is being released. A flexure built into the mast tip fitting that attaches the lid to the mast permits the lid to translate about 13 mm (0.5 inch) (without having to activate the mast motor) until there is no further pressure on the stowed blanket. Figure 3-17 shows an alternate to the pushrod mechanism. In this option the pushrod is replaced by a rotating torque tube and linkage mechanism which rotates "hook" latches located on the edge of the pallet. The last option defined eliminates all motors and mechanisms in favor of some type of pyro-release strap which wraps around the lid and pallet structure. A miniaturized heating unit, located in each strap, heats through a temperature-sensitive region of the strap (i.e., melts a lap-soldered zone, or melts a low melting temperature plastic, or burns through a Kevlar strap).

The pushrod and torque tube mechanisms had similar advantages and disadvantages. The pyro-release approach was potentially the lightest weight option; however, relatching would not be possible (a problem for ground testing) and it would require substantially more development to define the right combination of materials and controlled melting devices to make the concept practical. The choice between the pushrod and torque tube mechanism was somewhat arbitrary. The torque tube approach was eventually selected for the baseline design because it was of more traditional approach and relies on a more positive drive concept to release the latches. While the concept could be activated by the mast motor through a flex-drive system, thereby eliminating a separate motor just for the release operation, it was decided to use a separate motor to activate the release mechanism, thereby simplifying the overall design.

3.2.2.4 Blanket Tension Mechanism

The solar array blanket is extremely flexible in the deployed mode and acts like a membrane with negligible bending stiffness. In order to eliminate undesirable low-frequency blanket modes and to provide stiffness and control of the deployed blanket, a quasi-uniformly distributed tension load is applied in the longitudinal direction of the blanket. Sections 3.2.5 and 3.2.6 discuss the effect of blanket tension level on wing frequency characteristics and the displacement of the blanket relative to the mast when subjected to inertia loads.

Table 3-5. Stowed Blanket Preload Mechanism Concepts

CONCEPT	ADVANTAGES	DISADVANTAGES
PUSHROD CABLE RELEASE	<ul style="list-style-type: none"> • LOCKS OVER-CENTER • CAN BE MANUALLY RE-LATCHED • "LOW PROFILE" MECHANISM LIES FLAT AGAINST PALLET SURFACE • NOT AFFECTED BY LID/PALLET ALIGNMENT • LOW WEIGHT 	<ul style="list-style-type: none"> • 8" CABLE LOOPS DANGLE FROM LID
TORQUE TUBE CABLE RELEASE	<ul style="list-style-type: none"> • LOCKS OVER-CENTER • CAN BE MANUALLY RE-LATCHED • NOT AFFECTED BY LID/PALLET ALIGNMENT • $\approx 10\%$ HEAVIER WEIGHT MECHANISM • SHORTER CABLE LOOPS ($\approx 2"$) 	<ul style="list-style-type: none"> • HIGH CONCENTRATED LOADS ON INSERTS IN PALLET STRUCTURE • HIGHEST NO. OF PARTS ($\approx 10\%$ MORE THAN PUSHROD DESIGN)
PYRO-RELEASE STRAP	<ul style="list-style-type: none"> • POTENTIALLY LIGHTEST WEIGHT RELEASE MECHANISM ($\approx 10\%$) • SIMPLE – VERY FEW PARTS • NOT AFFECTED BY LID/PALLET ALIGNMENT 	<ul style="list-style-type: none"> • RE-LATCHING REQUIRES NEW STRAPS (CAN'T BE RE-LATCHED) • DIFFICULT TO CONTROL RELEASE RATE • REQUIRES MORE DEVELOPMENT – MATERIAL SELECTION IN RELEASE REGION OF STRAP

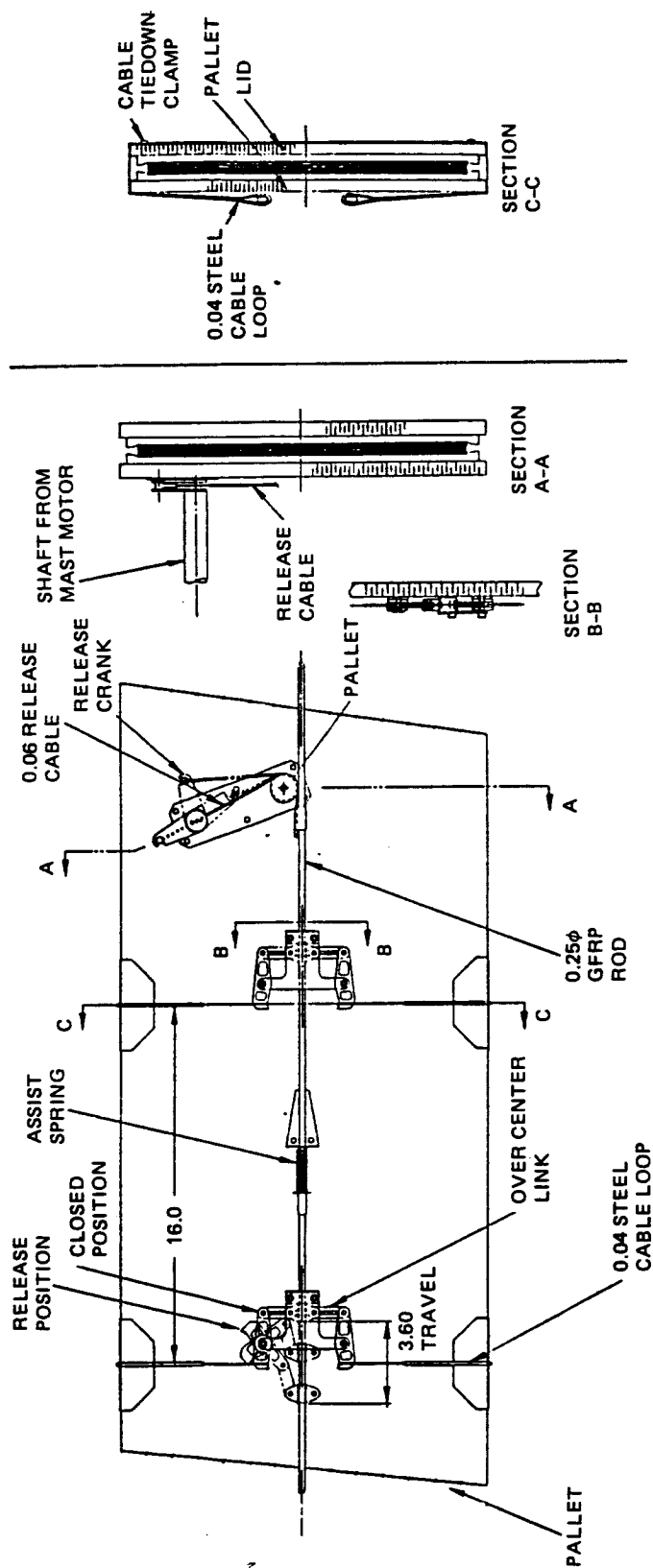


Figure 3-16. Pushrod Stowed Blanket Preload Mechanism Concept

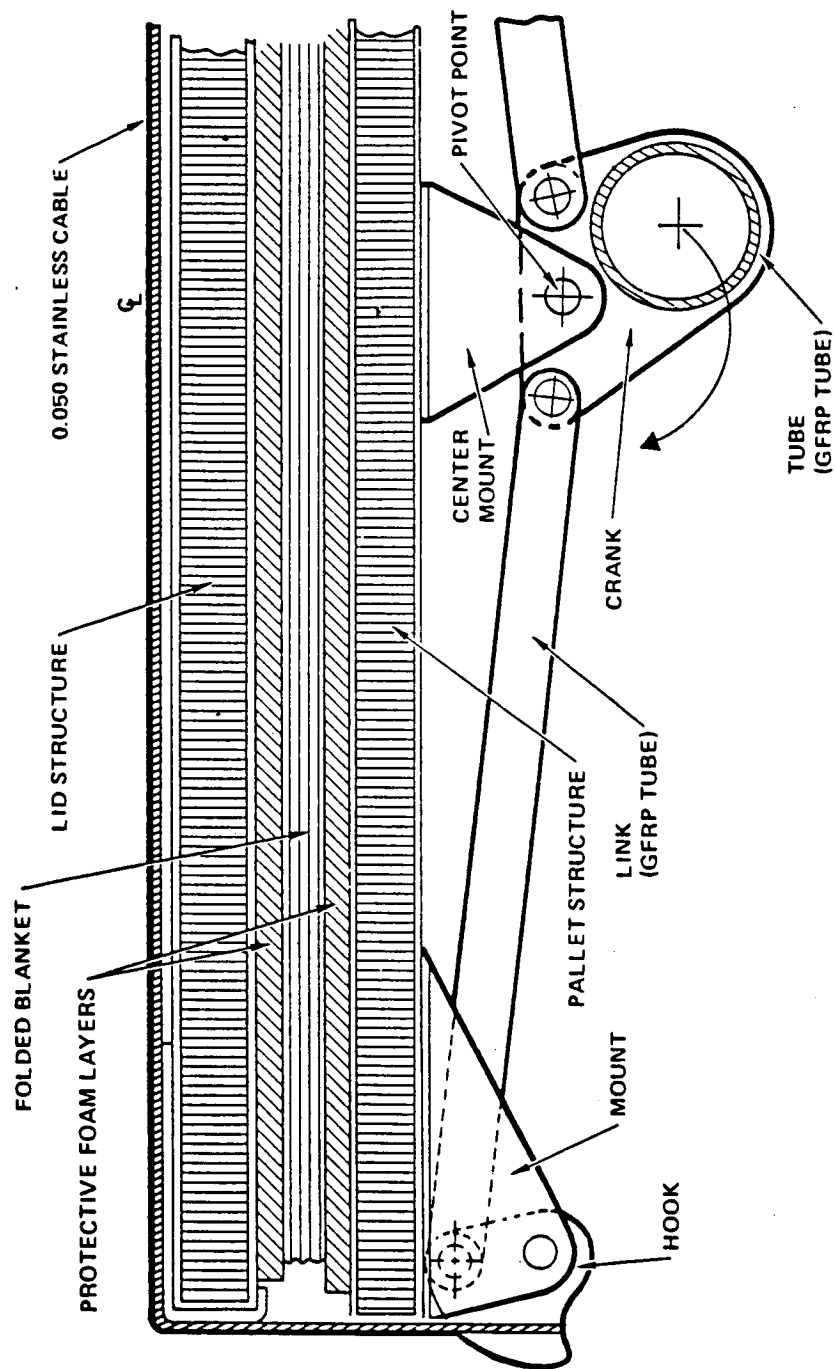


Figure 3-17. Torque Tube Stowed Blanket Preload Mechanism Concept

In addition to frequency and displacement considerations, a means must be provided to permit the blanket assembly to expand and contract under orbital temperature extremes (30 to -160°C in GEO, 60 to -85°C in LEO) without allowing the blanket to become slack or to increase its tension level to an unacceptably high value. Calculations indicate that changes in length could range from 25 to 50 mm (1 to 2 inches).

The design concept selected is shown in Figure 3-18 and is based on the successful approach used on a prototype flexible blanket wing developed by TRW in the early 1980s. It consists of a series of constant-force Negator coil springs attached to the inboard end of the leader panel at the base of the blanket assembly, with the other end of each spring attached to a small reel unit mounted on the underside of the pallet sandwich structure. The blanket becomes tensioned when fully unfolded during the last 0.15 m (6 inches) of mast extension, at which time the Negator springs become extended. The 0.15 m (6 inches) separation between the base of the blanket assembly and pallet structure provides ample distance for the thermal excursions of the blanket assembly. The negator springs have sufficient length capability (≈ 0.3 m [12 inches]) to permit the blanket to deflect under inertia loads without bottoming out the springs. In turn, the tension load induced by the springs keeps the blanket from deflecting to the extent that it could interfere with (slap) the mast under inertia loads.

Dynamic and deflection analyses (Sections 3.2.5 and 3.2.6) indicated that the total blanket tension load required was less than 70 N (15 pounds) over the wing aspect ratio range studied to control a 0.02 g quasi-static inertia load uniformly applied normal to the blanket plane. This meant that if four to eight Negator spring units were used, each spring would be required to develop a force of 9 to 18 N (2 to 4 pounds). Such springs are available from Hunter Spring Division of AMETEK.

3.2.2.5 Blanket Guidewire Mechanism

The guidewire system provides out-of-plane support to the blanket during unfolding and refolding operations, since the blanket tension Negator spring system is only effective when the blanket is fully deployed. The guidewires are there to prevent or restrict any large out-of-plane blanket excursion that might impede the wing deployment/retraction process.

Figure 3-19 illustrates the conceptual design approach for the guidewire system that was successfully developed for our prototype flexible blanket wing in the early 1980s and proven in a series of tests conducted on the ground and in NASA's KC-135 aircraft zero gravity facility. The design consists of a series of tensioned cables that pass through guides attached to the blanket rear hingelines on the backside of the blanket. The guidewires (two to four per blanket, depending on blanket width and the magnitude of expected inertia loads during deployment/retraction operations) run from the lid structure to Negator spring tensioned take-up reels located on the underside of the pallet structure.

At issue is whether guidewires are required for a solar array wing that does not have any requirement for on-orbit retraction. Extensive testing with our prototype wing and on the SEPS Technology and SAFE I wing programs clearly indicated the need for guidewires for retraction operations during zero gravity and partial gravity conditions. They would probably prove useful during deployment under "unplanned" partial gravity environments.

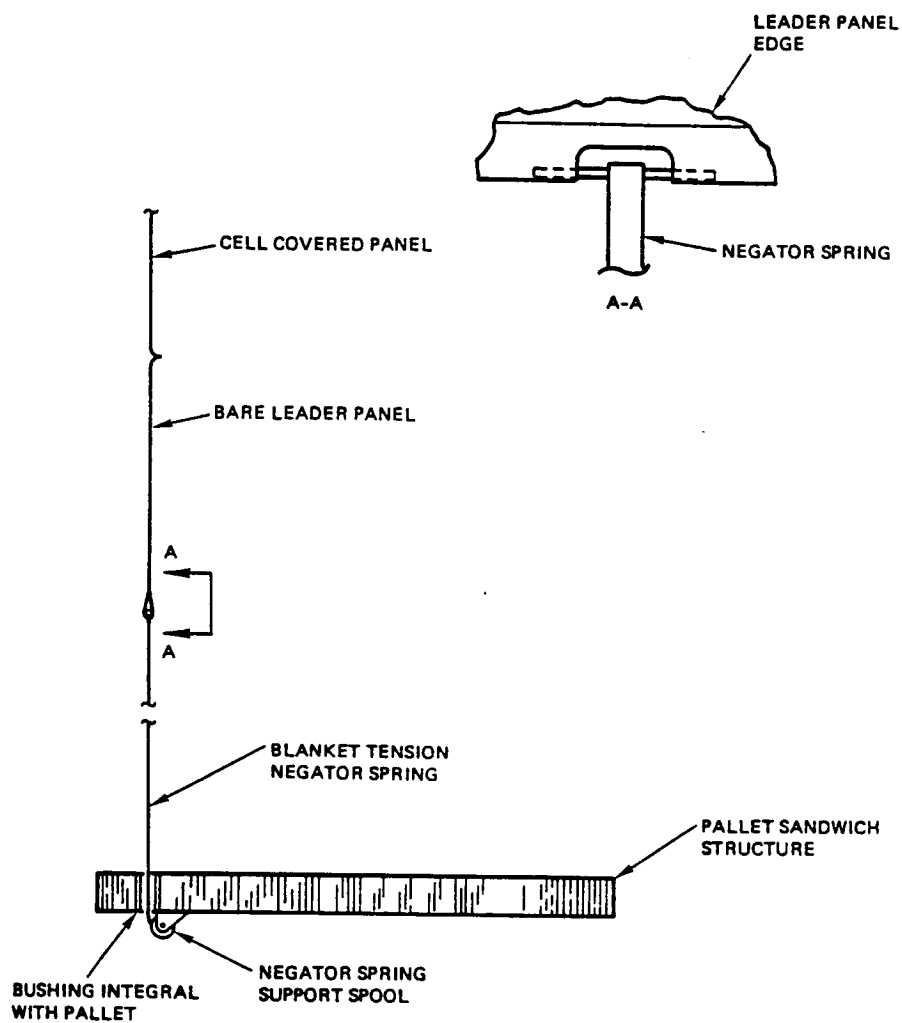


Figure 3-18. Blanket Tension System (Four to Eight Units per Blanket Assembly)

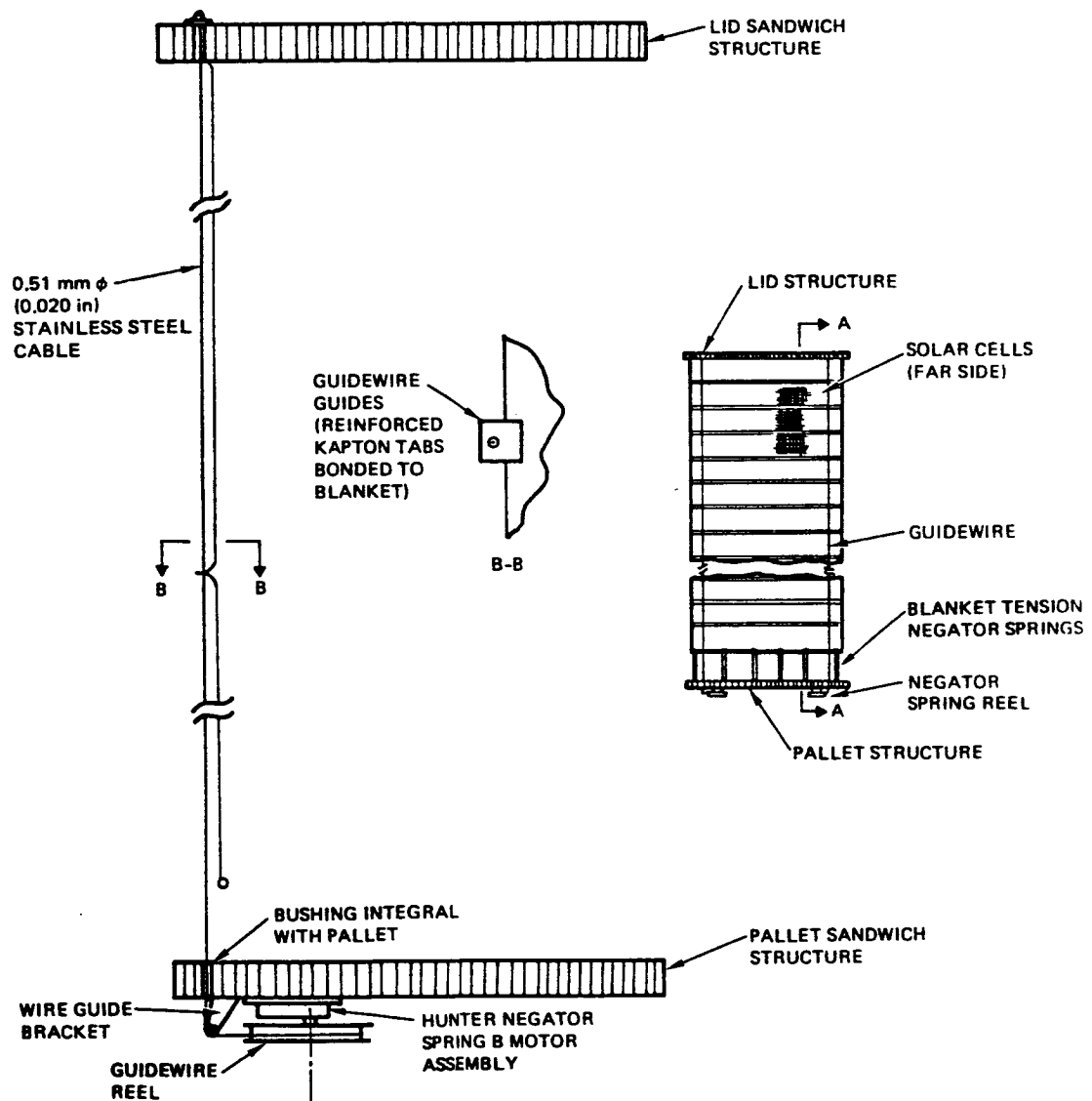


Figure 3-19. Blanket Guidewire Mechanism Concept
(Two to Four Units per Blanket Assembly)

Even though on-orbit retraction may not be a requirement for the present APSA, retraction on the ground will occur during normal development, qualification, and checkout operations on prototype and flight hardware wings. Therefore, the best justification for guidewires may be to simplify test fixturing and retraction during ground operations. They could even be removed after ground checkout operations if proven unnecessary for deployment operations.

Hence, guidewire mechanisms will be retained in the baseline design for preventative reasons at this time. A tension level of 5 to 10 N (1 to 2 pounds) per guidewire appears sufficient to provide out-of-plane support under near zero gravity conditions.

3.2.3 Blanket Deployment System

The blanket deployment mast system is the primary structural element in the solar array wing. It extends the folded flexible blanket assembly, provides strength and deployed stiffness to the wing, and reacts (through the lid structure) the distributed blanket tension load. Table 3-6 lists some of the types of mechanisms/linear elements that could be used. The desired features of any deployment system include: (1) high specific stiffness (stiffness divided by weight), (2) high specific strength (strength divided by weight), (3) high stowage efficiency (small stowage volume), and (4) low thermally induced deflections.

Two mast subcontractors (Astro Aerospace, Carpinteria, CA; and AEC-Able Engineering, Goleta, CA) performed preliminary trade studies on candidate blanket deployment mast system designs. The trades were performed on three aspect ratio wings (see Figure 1-2) against a set of preliminary requirements and performance goals:

1. Consider two blanket deployment sequences: (a) blanket deployment that is simultaneous with mast extension and (b) blanket deployment after full mast extension (i.e., a "flagpole" approach).
2. Deployment systems must be in a state of development that would permit delivery of prototype hardware by April/May 1987, with fabrication authorization-to-proceed in October 1986.
3. Primary emphasis on minimizing mast system weight, with a goal of less than 9 kg (20 pounds).
4. Mast to be sized to provide a wing deployed fundamental frequency ranging from 0.01 to 0.1 Hz.
5. Mast to be sized to provide a wing deployed ultimate strength ranging from 0.001 to 0.01 g (uniformly distributed load about any axis).
6. Mast must develop full stiffness and strength at any deployed length.
7. Automatic partial deployment, partial retraction and full retraction are desirable, but not required.

Based on prior experience, low weight and design maturity were considered more important than the other items.

Table 3-6. Candidate Blanket Deployment Mast Systems

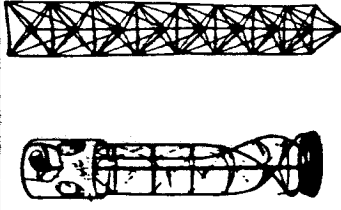
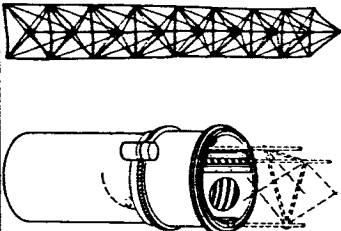
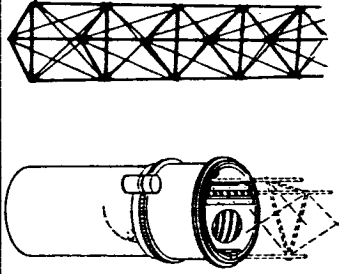

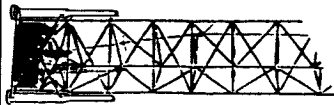
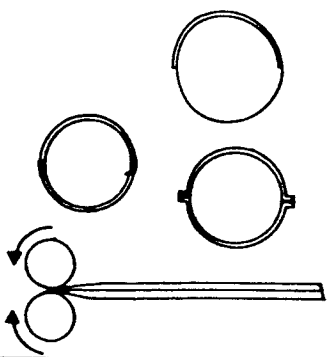
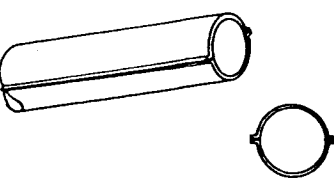
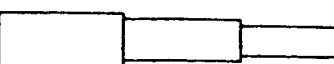
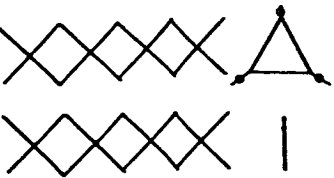
NAME	ILLUSTRATION	DESCRIPTION AND OPERATION	SOURCE	FLIGHT EXPERIENCE	REMARKS
CONTINUOUS LONGERON COILABLE LATTICE MAST (LANYARD DEPLOYED)		<ul style="list-style-type: none"> MAST STRUCTURE CONSISTS OF THREE CONTINUOUS LONGERONS, BATTENS AND THREE DIAGONALS PER BAY LONGERON AND BATTEN MATERIAL IS FIBERGLASS EPOXY • DIAGONAL MATERIAL IS STRANDED WIRE OR FIBERGLASS • MAST SELF-DEPLOYS DUE TO STRAIN ENERGY IN COILED LONGERONS AT A RATE CONTROLLED BY PAYOUT OF A MOTORIZED RESTRAINING LANYARD 	ASTRO AEROSPACE ABLE ENGINEERING	USED ON NUMEROUS SPACECRAFT FOR DEPLOYMENT OF SCIENTIFIC INSTRUMENTS	<ul style="list-style-type: none"> HIGH STIFFNESS-TO-WEIGHT RATIO • MAST IS AT FULL STRENGTH /STIFFNESS ONLY WHEN FULLY DEPLOYED • MAST CAN BE RETRACTED EXTENDED PORTION OF MAST ROTATES DURING DEPLOYMENT • LOW WEIGHT SYSTEM SINCE COMPLEX STOWAGE CANISTER NOT REQUIRED SYSTEM NOT AMENABLE TO ATTACHING BLANKET AT INTERMEDIATE POINTS ALONG THE MAST
CONTINUOUS LONGERON COILABLE LATTICE MAST (CANISTER DEPLOYED)		<ul style="list-style-type: none"> MAST STRUCTURE SIMILAR TO LANYARD DEPLOYED MAST • DEPLOYMENT IS ACTUATED BY LARGE MOTORIZED, THREE-THREADED, ROTATING NUT MECHANISM WITH STOWAGE CANISTER 	ASTRO AEROSPACE ABLE ENGINEERING	OAST SOLAR ARRAY FLIGHT EXPERIMENT ON STS-41 IN 1984	<ul style="list-style-type: none"> HIGH STIFFNESS-TO-WEIGHT RATIO • MAST IS AT FULL STRENGTH/ STIFFNESS AT ALL TIMES DURING DEPLOYMENT • MAST CAN BE RETRACTED SYSTEM WEIGHT HEAVIER THAN LANYARD DEPLOYED VERSION BECAUSE OF CANISTER/NUT MECHANISM • EXTENDED PORTION OF MAST DOES NOT ROTATE DURING DEPLOYMENT SYSTEM NOT AMENABLE TO ATTACHING BLANKET AT INTERMEDIATE POINTS ALONG THE MAST
LATCHING, ARTICULATED LATTICE MAST (CANISTER DEPLOYED)		<ul style="list-style-type: none"> MAST STRUCTURE CONSISTS OF THREE LONGERONS, BATTENS AND SIX DIAGONALS PER BAY THE LONGERONS ARE SEGMENTS OF METALLIC, FIBERGLASS OR GRAPHITE TUBES/RODS, WHICH ARE ARTICULATED AT THE BATTEN FRAMES WITH UNIVERSAL HINGE FITTINGS • DIAGONAL MEMBERS, TYPICALLY METALLIC CABLES • DEPLOYMENT REQUIRES LATCHING OF THREE DIAGONALS PER BAY • DEPLOYMENT IS ACTUATED BY LARGE MOTORIZED, THREE-THREADED ROTATING NUT MECHANISM WITH STOWAGE CANISTER 	ASTRO AEROSPACE ABLE ENGINEERING	PROTOTYPES DEVELOPED FOR VARIOUS GROUND APPLICATIONS AND HIGH POWER ARRAYS. NO FLIGHT EXPERIENCE	<ul style="list-style-type: none"> VERY HIGH STIFFNESS/STRENGTH ACHIEVABLE • MAST IS AT FULL STRENGTH/ STIFFNESS AT ALL TIMES DURING DEPLOYMENT • MAST CAN BE RETRACTED HEAVY SYSTEM WEIGHT • EXTENDED PORTION OF MAST DOES NOT ROTATE DURING DEPLOYMENT • SYSTEM NOT AMENABLE TO ATTACHING BLANKET AT INTERMEDIATE POINTS ALONG THE MAST
LATCHLESS, ARTICULATED LATTICE MAST (LANYARD DEPLOYED)		<ul style="list-style-type: none"> MAST STRUCTURE CONSISTS OF THREE LONGERONS, BATTENS AND SIX DIAGONALS PER BAY LONGERONS ARE SEGMENTS OF METALLIC, FIBERGLASS OR GRAPHITE TUBES/RODS, WHICH ARE ARTICULATED AT THE BATTEN FRAMES WITH SPECIAL HINGE JOINTS • DIAGONAL MEMBERS TYPICALLY METALLIC CABLES WITHOUT ANY LATCH MECHANISM BATTENS COILABLE FIBERGLASS • MAST SELF-DEPLOYS DUE TO STRAIN ENERGY IN COILED BATTENS AT A RATE CONTROLLED BY PAYOUT OF A MOTORIZED RESTRAINING LANYARD 	ABLE ENGINEERING	DEVELOPMENTAL (TO BE APPLIED FOR SPACE STATION TRUSS STRUCTURE)	<ul style="list-style-type: none"> VERY HIGH STIFFNESS/STRENGTH ACHIEVABLE • MAST IS AT FULL STIFFNESS/ STRENGTH ONLY WHEN FULLY DEPLOYED MAST CAN BE RETRACTED • EXTENDED PORTION OF MAST DOES NOT ROTATE DURING DEPLOYMENT • LOWER WEIGHT SYSTEM SINCE COMPLEX STOWAGE/ DEPLOYMENT MECHANISM NOT REQUIRED SYSTEM AMENABLE TO ATTACHING BLANKET AT INTERMEDIATE POINTS ALONG THE MAST

Table 3-6. Candidate Blanket Deployment Mast Systems (Continued)

NAME	ILLUSTRATION	DESCRIPTION AND OPERATION	SOURCE	FLIGHT EXPERIENCE	REMARKS
STACBEAM (STACKING TRIANGULAR ARTICULATED COMPACT BEAM)		<ul style="list-style-type: none"> MAST STRUCTURE CONSISTS OF THREE LONGERONS, BATTENS AND THREE DIAGONALS PER BAY ELEMENTS MADE FROM METAL, FIBERGLASS OR GRAPHITE EPOXY THE LONGERON AND DIAGONALS ARE SEGMENTS OF TUBES/RODS WHICH HAVE HINGES AT THEIR MIDPOINTS AND AT THE BATTEN FRAMES • HINGES HAVE TORQUE SPRINGS TO OBTAIN HINGE RESTRAINING MOMENT CAPABILITY 	ASTRO AEROSPACE	DEVELOPMENTAL	<ul style="list-style-type: none"> STIFFNESS/STRENGTH PROPERTIES SUBJECT TO STIFFNESS/STRENGTH OF HINGES MAST IS AT FULL STRENGTH/STIFFNESS AT ALL TIMES DURING DEPLOYMENT EXTENDED PORTION OF MAST DOES NOT ROTATE DURING DEPLOYMENT RETRACTION CAPABILITY NOT DEMONSTRATED AT THIS TIME WEIGHT COMPARABLE TO CANISTER-DEPLOYED LATTICE MASTS • MAST AMENABLE TO ATTACHING BLANKET AT INTERMEDIATE POINTS ALONG THE MAST • DEPLOYER MECHANISM IN CONCEPTUAL STAGE (MAST PROTOTYPE UNIT BUILT)
METALLIC STRIP BOOM, EXTENDABLE REEL STORED (STEM, BI-STEM, EDGELOCK)		<ul style="list-style-type: none"> TUBES FORMED BY ONE OR MORE METALLIC CYLINDRICAL, THIN STRIPS STRIPS ARE STOWED BY ELASTICALLY FLATTENING THE SECTION AND REELING THEM ON SPOOLS TUBE IS FORMED BY MOTORIZED ROTATION OF THE SPOOLS MATERIAL TYPICALLY STAINLESS STEEL OR BERYLLIUM COPPER • SOME VERSIONS PERMIT INTERLOCKING OF THE STRIP EDGES TO IMPROVE TORSIONAL STIFFNESS 	ASTRO AEROSPACE FAIRCHILD	IN ONE FORM OR ANOTHER, USED IN NUMEROUS FLIGHT PROGRAMS FOR ANTENNAS, GRAVITY GRADIENT BOOMS, ETC. USED ON CTS, FRUSA AND SPACE TELESCOPE SOLAR ARRAYS	<ul style="list-style-type: none"> PRIMARY CONSIDERATION WOULD BE FOR LOW POWER ARRAYS, WHERE MINIMUM SIZE LATTICE MAST SYSTEMS ARE TOO HEAVY • VERY COMPACT STOWAGE LOW TORSIONAL STIFFNESS • RETRACTION POSSIBLE NOT AMENABLE TO ATTACHING BLANKET AT INTERMEDIATE POINTS ALONG THE TUBULAR BOOM
METALLIC STRIP BOOM, LENTICULAR WELDED BEAM		<ul style="list-style-type: none"> TUBE FORMED BY TWO METALLIC OR GRAPHITE HALF-LENTICULAR, METALLIC STRIPS STRIPS ARE WELDED (BONDED) AT THEIR EDGES TO FORM LENTICULAR CROSS SECTION TUBE TUBE IS STOWED BY ELASTICALLY FLATTENING THE SECTION AND ROLLING IT UP ON A MOTORIZED REEL 	LMSC BOEING ASTRO AEROSPACE	USED ON MARS VIKING BIOLOGICAL EXPERIMENT PACKAGE	<ul style="list-style-type: none"> PRIMARY CONSIDERATION WOULD BE FOR LOWER POWER ARRAYS, WHERE MINIMUM SIZE LATTICE MAST SYSTEMS ARE TOO HEAVY • VERY COMPACT STOWAGE HIGH TORSIONAL STIFFNESS RELATIVE TO STEM, BI-STEM, EDGELOCK SYSTEMS NOT AMENABLE TO ATTACHING BLANKET AT INTERMEDIATE POINTS ALONG THE TUBULAR BOOM • RETRACTION POSSIBLE
TELESCOPING CYLINDERS		<ul style="list-style-type: none"> CONCENTRIC METALLIC OR GRAPHITE TUBES IN GRADUATED DIAMETERS • SECTIONS ARE EXTENDED AND LATCHED IN THE FULL EXTENDED POSITION USING GAS ACTUATION 	BRITISH AEROSPACE	SMALL VERSION FLOWN ON BRITISH X4 SATELLITE	<ul style="list-style-type: none"> 6 TO 16m LENGTH VERSIONS BEING DEVELOPED • NOT EASILY AMENABLE TO RETRACTION NOR TO ATTACHING THE BLANKET AT INTERMEDIATE POINTS ALONG THE TUBULAR BOOM INEFFICIENT STOWAGE EFFICIENCY FOR HIGH POWER ARRAYS HEAVY SYSTEM WEIGHT
1D AND 2D CROSS-SECTION PANTOGRAPH		<ul style="list-style-type: none"> FOLDED MULTI-LINK ARMS ATTACHED TOGETHER TO CREATE ONE-DIMENSIONAL OR TWO-DIMENSIONAL CROSS-SECTION TRUSS BEAM LINKS ARE METALLIC • ACTUATION BY SPRINGS AT THE HINGE POINTS 	COMSAT (SNIAS) LMSC TRW	NONE	<ul style="list-style-type: none"> LOW LATERAL AND TORSIONAL STIFFNESS • COMPACT STOWAGE • AMENABLE TO ATTACHING BLANKET AT INTERMEDIATE POINTS ALONG THE BEAM RETRACTION POSSIBLE

The nine mast system design options listed in Table 3-6 were considered to varying degrees of detail. Those given the most emphasis are shown in Figures 3-20 and 3-21, along with some brief comments about each option. These were selected for more detailed analysis because of a combination of factors: state-of-development, weight, risk, cost.

For the "flagpole" approach (Figure 3-21a) to work would require the lid structure of the blanket housing assembly to be attached to the mast structure by some type of roller or rail system so that it could be translated from the root of the mast to the top of the mast, then rigidly secured to the mast, after which the blanket assembly would be "hoisted" or deployed. Both subcontractors concluded that the "flagpole" approach to blanket deployment was too complicated and would be too heavy. Thus, the primary deployment sequence studied was the simultaneous deployment option, whereby the blanket is deployed at the same rate as the mast is being extended.

Concepts were evaluated where the blanket was attached at intermediate locations along the mast length to potentially improve the deployed dynamic characteristics and to better control potential blanket-to-mast slapping during inertia loading. The STACBEAM and FASTMast system would permit intermediate attachment of the blanket to the mast. Dynamic analyses (see Section 3.2.5) indicated that the improvement in frequency for the first two modes (out-of-plane bending and in-plane bending) were moderate (10 to 30 percent); however, the third mode (first torsional mode) was unaffected. When analyzing a total spacecraft with two deployed wings, it is the torsional mode in many cases which becomes the critical mode because of the rotational or tipping effects this mode has on the spacecraft body, which introduces pointing errors to the on-board sensor payloads. It was concluded that a mast concept that permitted intermediate attachment of the blanket created overly complicated designs that would not be weight-effective in improving overall wing performance. Therefore, the primary design configuration studied only had the blanket attached to the mast system at the inboard and outboard ends of the blanket (through the pallet and lid structures, respectively), with no intermediate attachments.

Analysis of the BISTEM-type boom, which was used on the low power CTS array, indicated that it would only be effective for low power, low aspect ratio wing designs. BISTEM booms larger than 34 mm (1.34 inches) diameter or for the aspect ratio wings other than 2.3 studied would not be weight-effective relative to the other leading candidate design options nor would it have adequate strength to resist the deployed inertia loads.

Both mast subcontractors concluded that the drum-nut driven canister deployed lattice mast design concepts (ASTROMAST, ABLEMAST, FASTMast) were the best choices for all wing aspect ratios studied. The generic concept had sufficient design maturity (based on prior developmental and flight hardware applications) to meet the 1987 time constraint for prototype wing application and had the potential for reduction in weight relative to existing hardware. The primary area where additional development would be required was weight reduction of the canister system, since weight-efficient mast element designs had already been developed.

Table 3-7 summarizes some of the key design trade results for the three aspect ratio wings analyzed. Figures 3-22 and 3-23 plot ABLE-generated mast system weight trends versus deployed strength and frequency for the two more

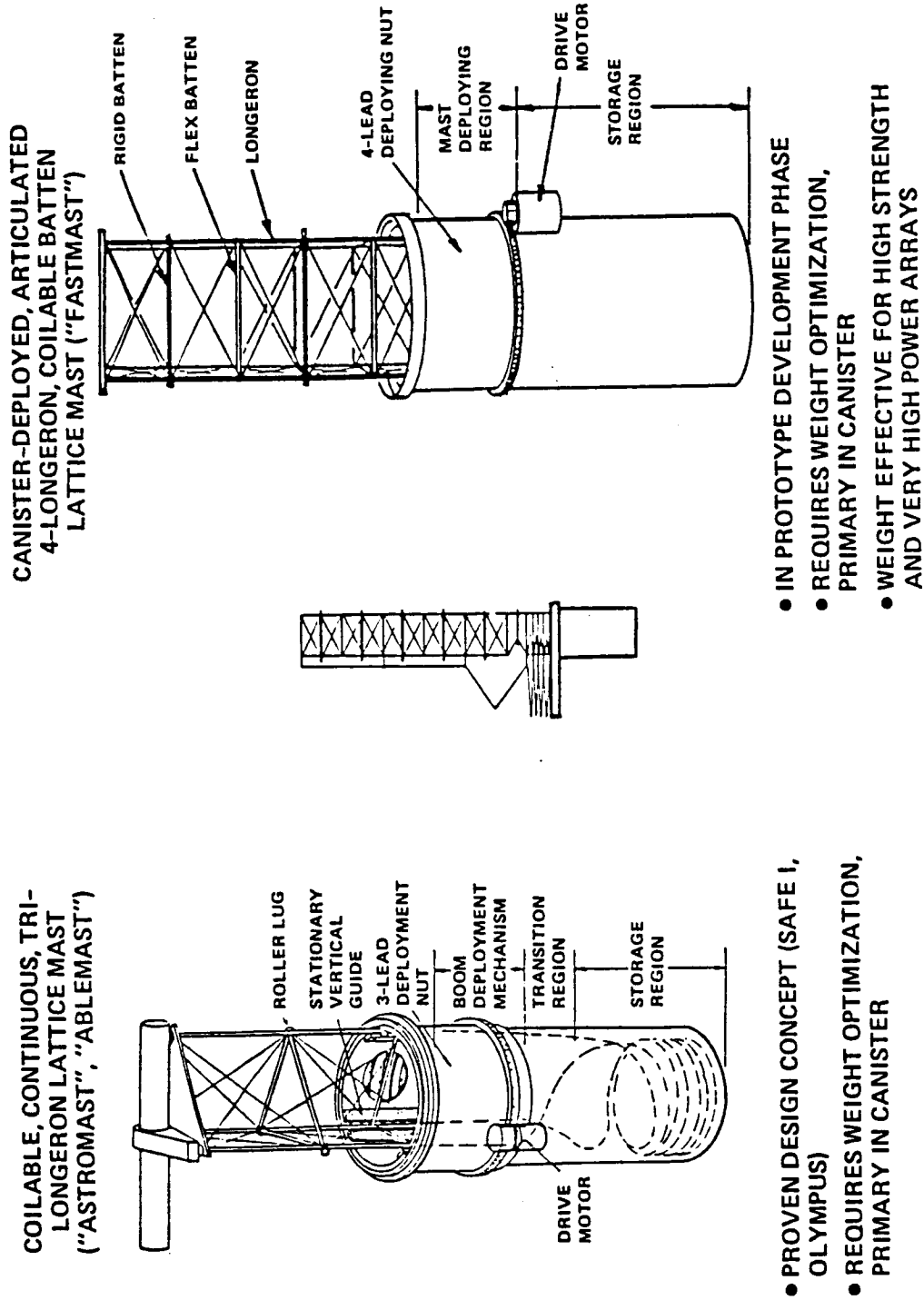
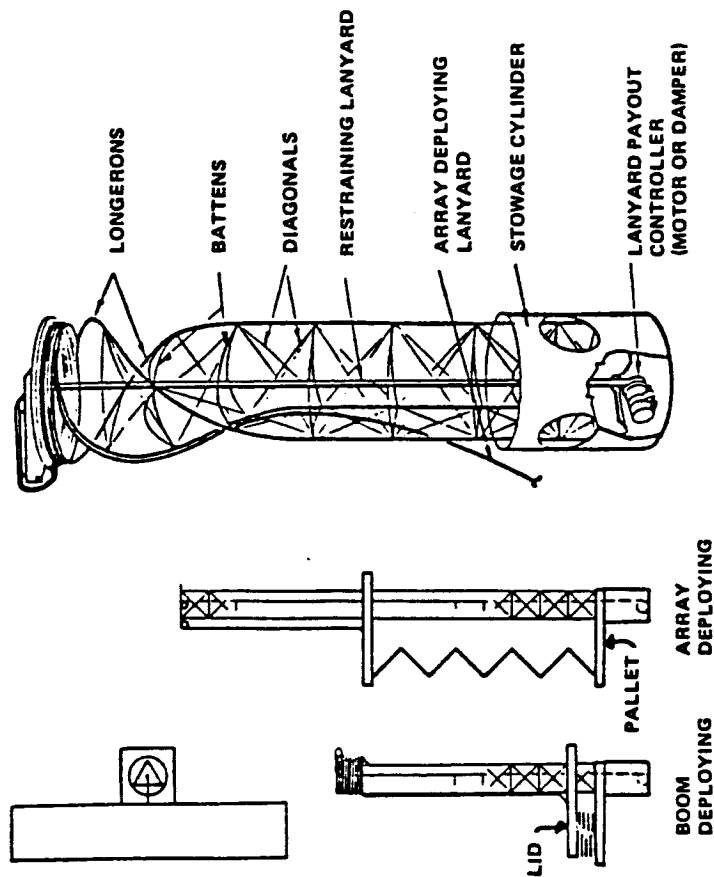


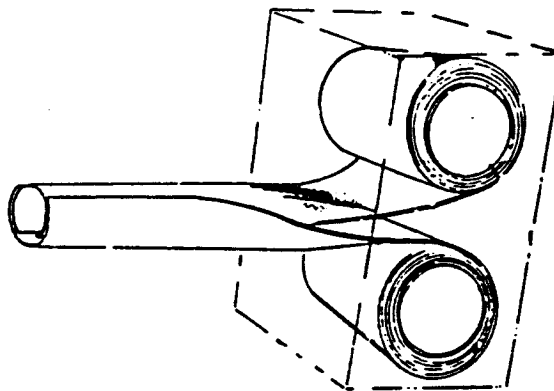
Figure 3-20. Principal Mast System Options

"FLAG POLE" OPTION USING LANYARD
DEPLOYED, CONTINUOUS, COILABLE
TRI-LONGERON LATTICE MAST



• LID TRACKING MECHANISM TOO COMPLEX
AND HEAVY FOR SERIOUS CONSIDERATION

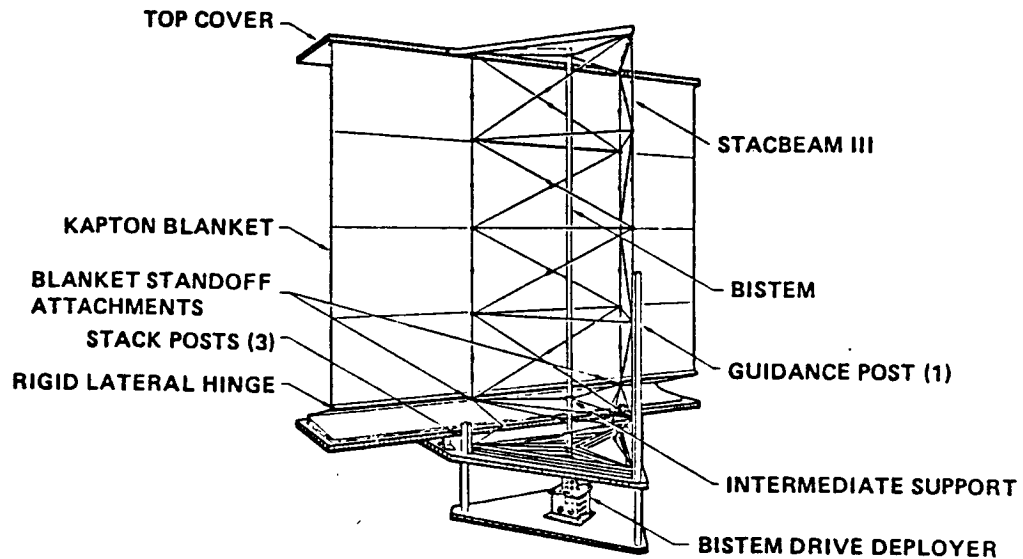
"BISTEM" EXTENDABLE REEL
STORED METALLIC STRIP
BOOM



• LIMITED TO SHORT, LOW POWER, LOW
STIFFNESS AND LOW STRENGTH WING
DESIGNS

Figure 3-21. Other Mast System Options

**STACKING TRIANGULAR ARTICULATED
LONGERON COMPACT BEAM
("STACBEAM")**



- STILL IN DEVELOPMENTAL STAGE
- PERMITS BLANKET-TO-MAST ATTACHMENT AT INTERMEDIATE LOCATIONS TO IMPROVE DEPLOYED FREQUENCY CHARACTERISTICS AND TO REDUCE BLANKET LATERAL DEFLECTIONS
- TOO HEAVY FOR ULTRALIGHTWEIGHT WING DESIGNS

Figure 3-21. Other Mast System Options (Continued)

Table 3-7. Comparison of Mast System Performance

WING ASPECT RATIO	MAST LENGTH (IN.)	DEPLOYED STATIC STRENGTH (GS)	DEPLOYED FREQUENCY (Hz)	MAST VENDOR	MAST TYPE	MAST DIAMETER (IN.)	MAST SYSTEM WEIGHT (LB)	EDL WING SPECIFIC POWER (W/KG)
2.25	380	0.017	0.12	ASTRO	ASTROMAST	7.0	12.6	89.9
		0.010	0.05	ASTRO	BISTEM	1.34	13.7	88.7
		0.012	0.15	ABLE	ABLEMAST	6.6	6.6	97.5
		0.010	0.12	ABLE	FASTMAST	12.8	7.2	96.7
		0.014	0.23	ABLE	FASTMAST	12.8	8.5	95.0
4.34	523	0.012	0.09	ASTRO	ASTROMAST	7.0	15.0	93.3
		0.029	0.11	ASTRO	ASTROMAST	9.0	16.3	91.7
		0.011	0.12	ABLE	ABLEMAST	7.2	9.4	100.9
		0.011	0.21	ABLE	FASTMAST	13.4	11.1	98.4
8.34	725	0.007	0.06	ASTRO	ASTROMAST	7.0	16.9	92.2
		0.021	0.08	ASTRO	ASTROMAST	9.0	18.7	90.1
		0.012	0.11	ABLE	ABLEMAST	8.4	15.7	93.7
		0.013	0.18	ABLE	FASTMAST	12.8	15.0	94.6

ASTROMAST, ABLEMAST - COILABLE, CONTINUOUS TRI-LONGERON LATTICE MAST, MOTORIZED CANISTER DEPLOYED

FASTMAST - ARTICULATED 4-LONGERON, COILABLE BATTEN, LATTICE MAST, MOTORIZED CANISTER DEPLOYED

BISTEM - EXTENDABLE, REEL-STORED, METALLIC STRIP BOOM

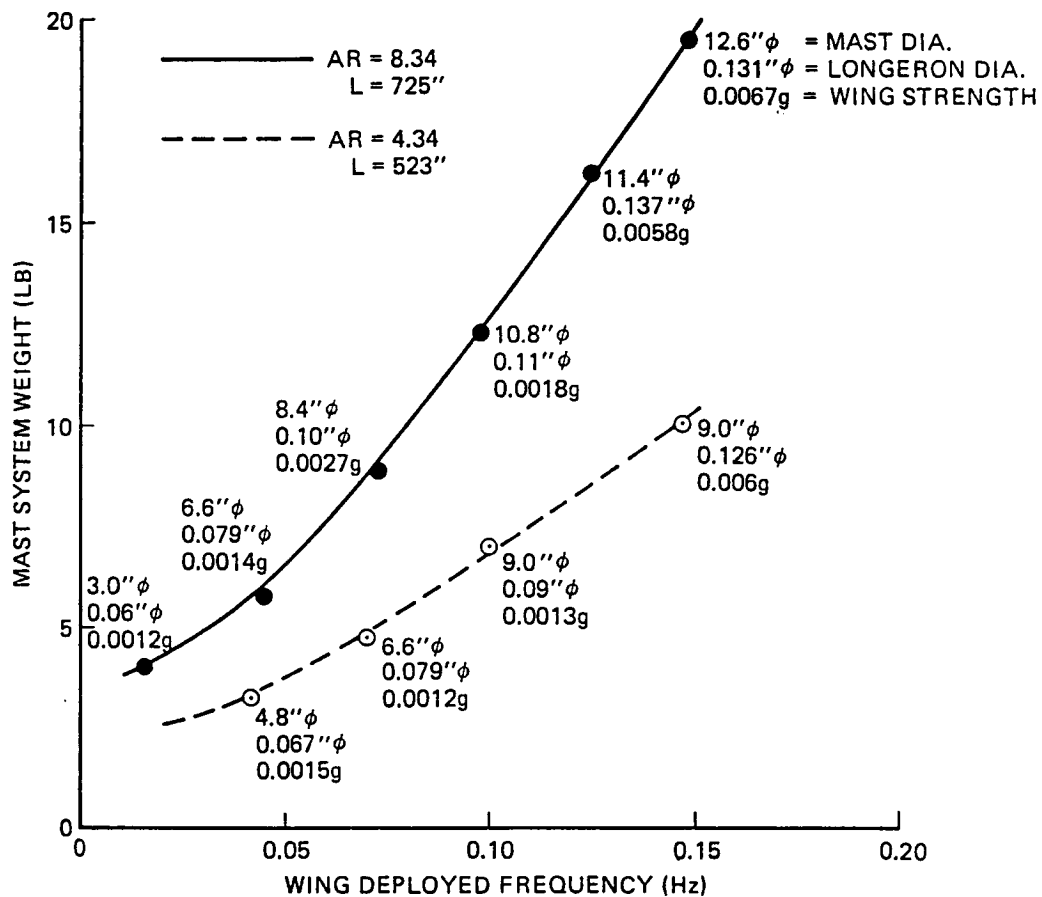


Figure 3-22. ABLEMAST System Weight versus Deployed Wing Fundamental Frequency, Preliminary Estimates (Fiberglass Mast, Graphite/Epoxy Canister)

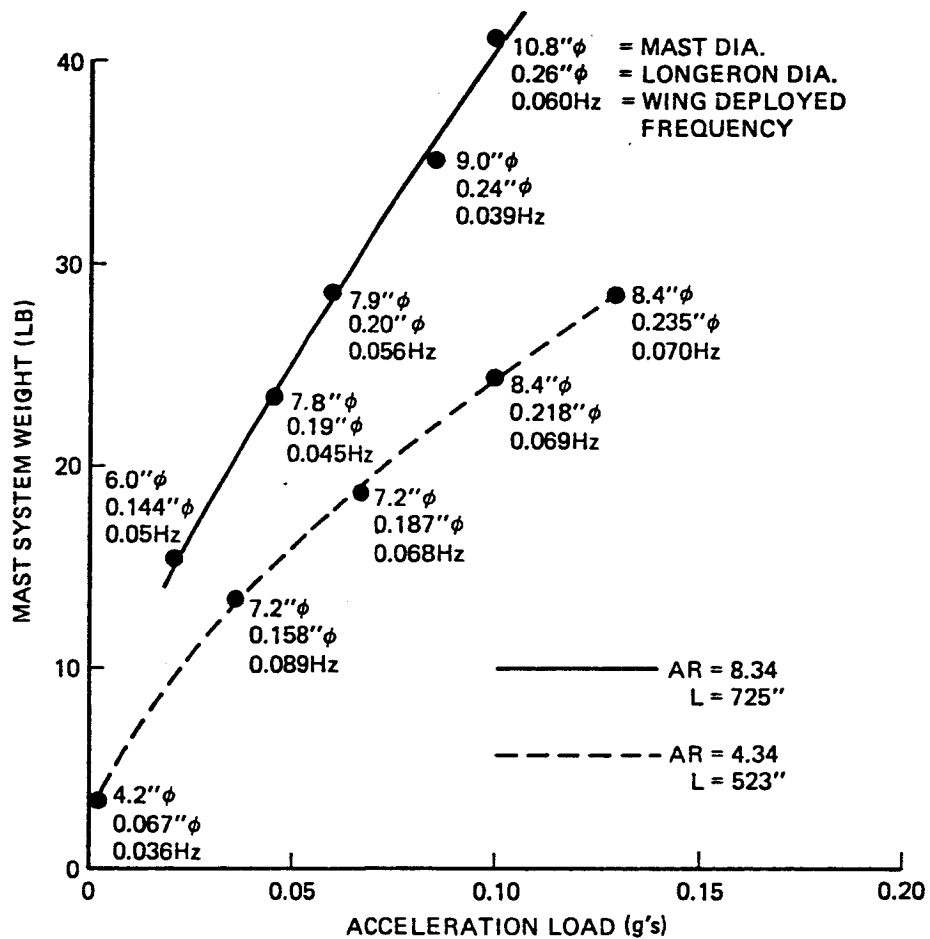


Figure 3-23. ABLEMAST System Weight versus Deployed Wing Strength, Preliminary Estimates (Fiberglass Mast, Graphite/Epoxy Canister)

promising wing aspect ratios. The key results from the mast trade studies were as follows:

1. The ABLEMAST and ASTROMAST continuous longeron drum-nut driven canister deployed lattice mast system provides the most weight-effective design options for the range of strength, stiffness, and length studied. The ABLEMAST design was lighter than the ASTROMAST design.
2. The material for the mast elements is fiberglass. The use of graphite/epoxy canister over an aluminum canister results in a mast system weight savings of 8 to 13 percent; however, the benefits of this potential weight savings (0.9 to 1.4 kg [2 to 3 pounds]) must be traded against the greater development time, cost, and risk associated with the graphite/epoxy approach ($\Delta\$ = \$150K$). For the prototype design, an aluminum canister appears to be the best selection.
3. Deployed wing strength is the primary design driver in sizing the mast elements (longeron diameter, mast diameter) and total mast system weight, especially at the higher end of the strength range requirement.
4. The BISTEM system was applicable only for the smallest aspect ratio (short length) wing configuration. Even then its weight is greater than the estimated weights for the lattice mast options.
5. The FASTMAST articulated longeron design has potential application at strength, stiffness, and array power levels greater than those studied (namely >10 kW array, >0.05 g, >0.1 Hz).

3.2.4 Wing Integration Hardware

Other than integrating the blanket assembly to the lid and pallet structures, the primary assemblies that must be attached to one another are the blanket housing assembly and the blanket deployment mast system. Figure 3-24 shows how that would be accomplished. The pallet structure will be attached to the top of the mast canister through an interface ring on the mast canister above the rotating drum-nut. The pallet will be stabilized by two graphite/epoxy tubular struts going from the pallet structure to an interface ring on the mast canister just below the rotating drum-nut. This will create a rigid interface between the pallet structure and mast canister.

The lid will be secured to the top of the tri-longeron mast through a tip fitting as shown in Figure 3-25. The aluminum triangular-shaped tip fitting is mechanically attached via threaded fasteners to lugs integral with the mast upper batten frame corner fittings. The tip fitting is, in turn, attached to the lid through a graphite/epoxy tubular flexure bar which is stiff in torsion. The flexure bar permits the lid to separate away from the pallet about 13 mm (0.5 inch), without activation of the mast motor, as the latch release mechanism is slowly releasing the latches. When the latching mechanism motor is turned off, there is no residual preload on the stowed blanket, and the mast motor can be activated to begin extension of the mast and deployment of the folded blanket assembly. The flexure bar is in the plane of the blanket assembly and guidewires so that the lid will deploy with the mast without tipping.

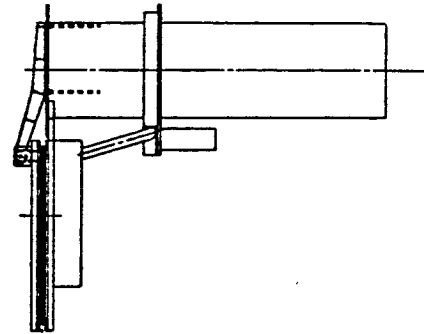
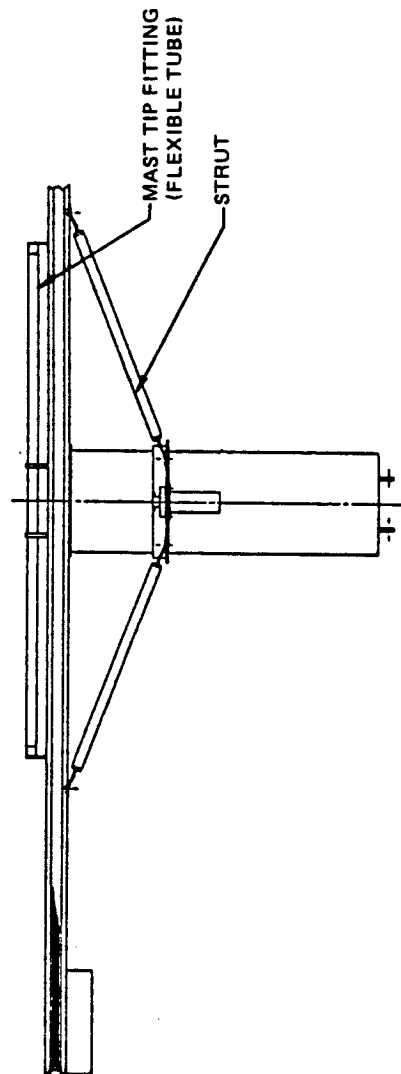
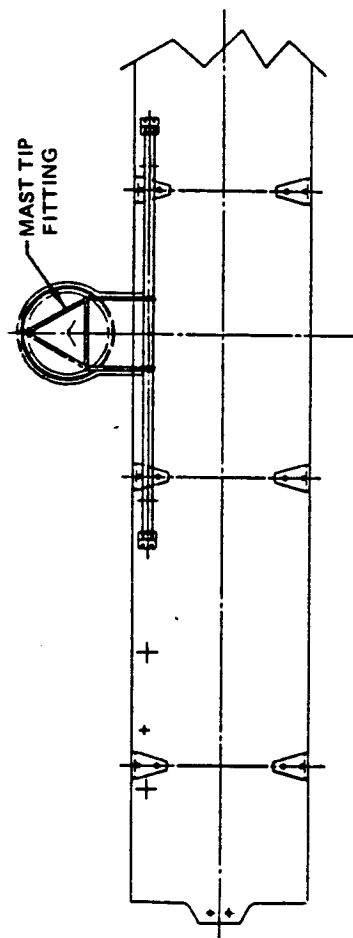


Figure 3-24. Attachment of Blanket Housing Assembly to Mast System

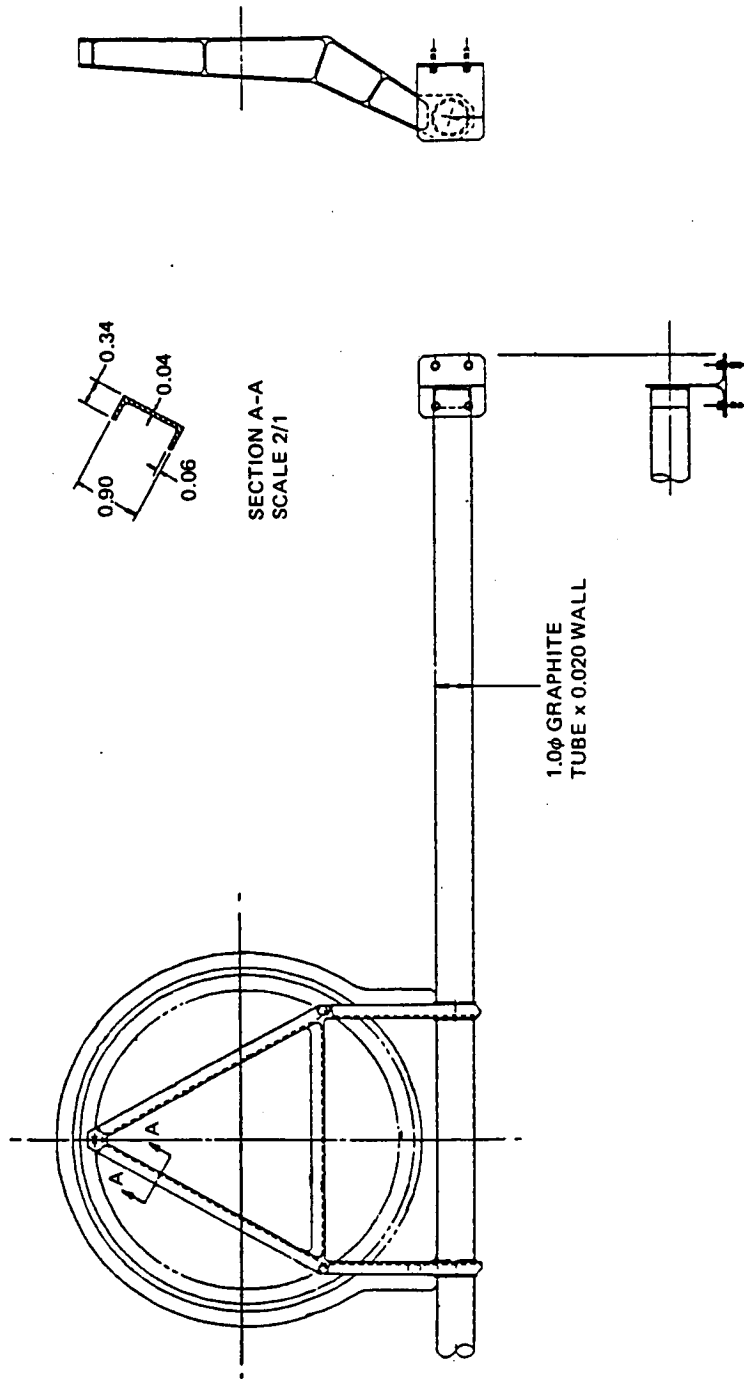


Figure 3-25. Mast Tip Fitting Connecting Lid Structure to Outboard End of Mast
(dimensions in inches)

3.2.5 Wing Dynamic Characteristics

NASTRAN finite element analysis was implemented in a series of parametric studies on a deployed cantilevered flexible blanket wing in order to determine the interplay of key parameters on the dynamic characteristics of the wing and how those parameters affected the design of key structural components and wing weight. The parameters investigated were: wing aspect ratio, mast stiffness, blanket tension, blanket tensioning spring constant, separation distance between the mast centerline and the blanket plane, single versus multiple blanket wing, planar wing (Figure 3-26a), wing with canted blankets instead of planar blankets (Figure 3-26b). The wing aspect ratios analyzed were those shown in Figure 1-2. The fundamental mode frequency range of interest was 0.01 to 0.10 Hz. The results of these studies were provided to the mast subcontractors to help guide them in their mast definition studies.

3.2.5.1 Model Description

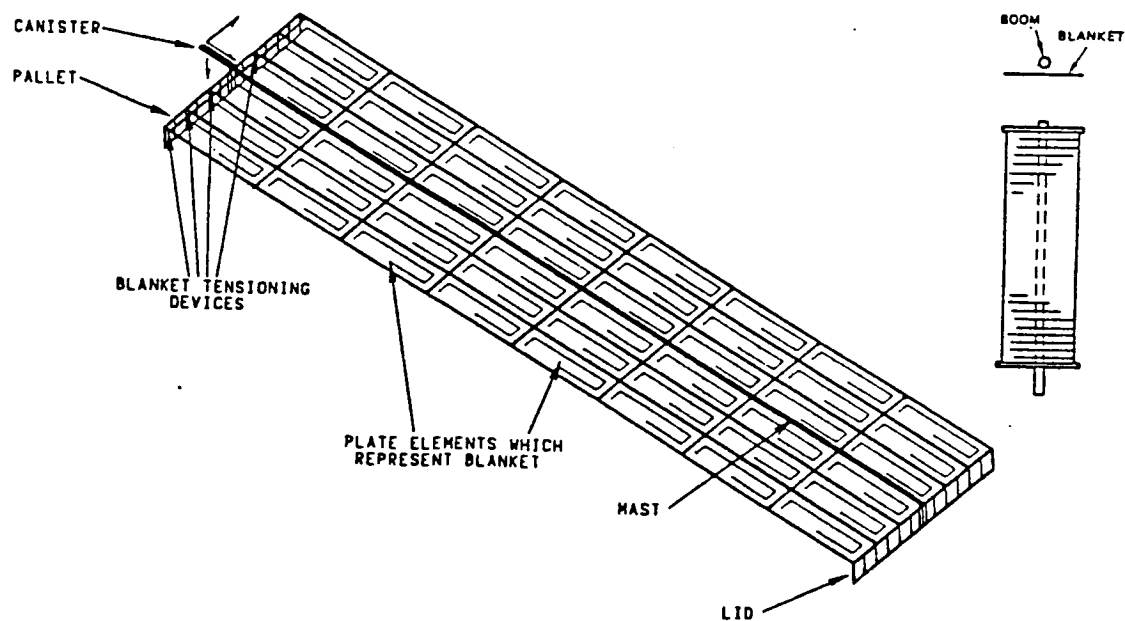
The models representing the wing consisted of a single mast which held two rigid cross members, the lid and pallet, between which the blanket assembly(s) was held with a specified tension in the longitudinal direction. The outboard end of the blanket was rigidly attached to the lid structure; the inboard end was connected to the pallet structure through a series of constant-force or linear springs which provided the blanket tension load. In most cases the blanket was only attached to the lid and pallet structure; however, a few analyses were done where the blanket was also attached to the mast at intermediate locations between the lid and pallet.

The mast in these models were represented by individual bar elements connected in series. The stiffness properties of the bar elements were representative of those for a coilable continuous tri-longeron lattice mast (ABLEMAST or ASTROMAST) or for a BI-STEM-type mast. The stiffness properties were based on formulae provided by the mast subcontractors. The pallet and lid structures were modelled of quadrilateral plate elements. Plate elements were also used to represent the blanket assembly with their properties chosen such that the effective stiffness of the blanket was almost entirely due to the tension in the blanket. The modelling of the split/canted blanket wing was identical to that for the uncanted single blanket wing with the following exceptions: two canted blankets were used instead of one uncanted blanket; and linear springs were used to provide blanket tension instead of constant-force Negator springs.

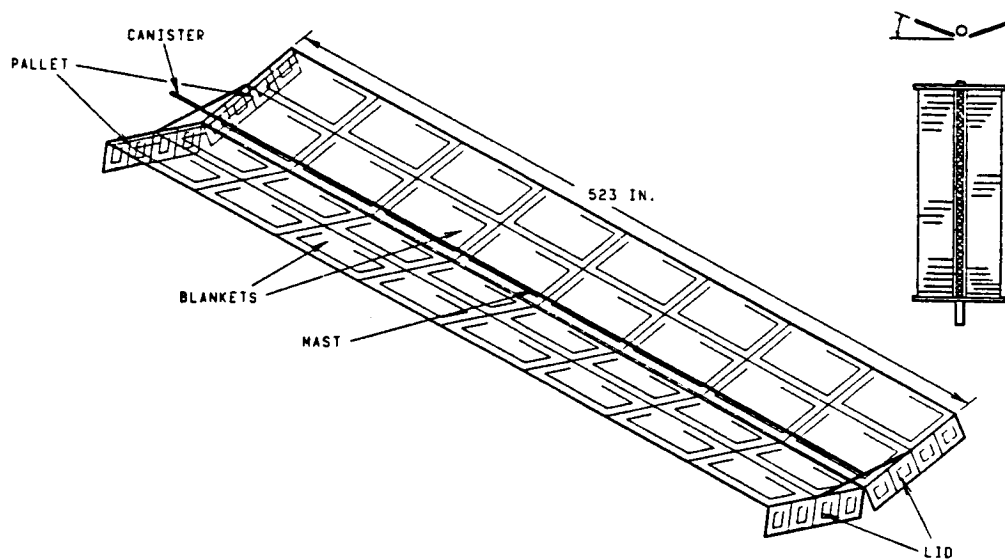
3.2.5.2 Dynamic Analysis Results

An example of the results is shown in Figures 3-27a through 3-27c for the mid aspect ratio uncanted wing. Similar results were generated for the other aspect ratio wings but are not included because of the extensive amount of available data. The results are generally the same for all aspect ratios, except for the mast stiffness and blanket tension level required to produce a given frequency response. From these analyses, the following conclusions were drawn:

1. At very low blanket tension loads (<5 N [1 pound]), the dynamic characteristics of the wing are dominated by the blanket dynamics. At higher tension levels, the mast stiffness (EI, GJ) characteristics play the dominant role. Over a wide range of tension, wing frequency for a given mast stiffness is insensitive to blanket tension level (first and second modes especially).

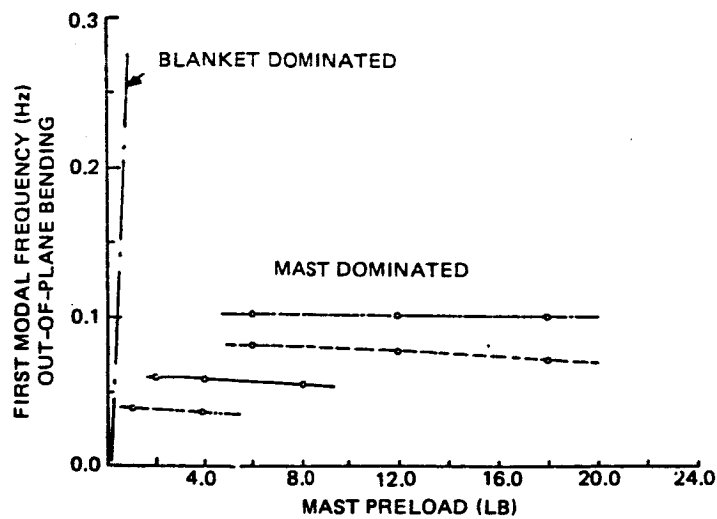


a. Single Blanket Uncanted Wing

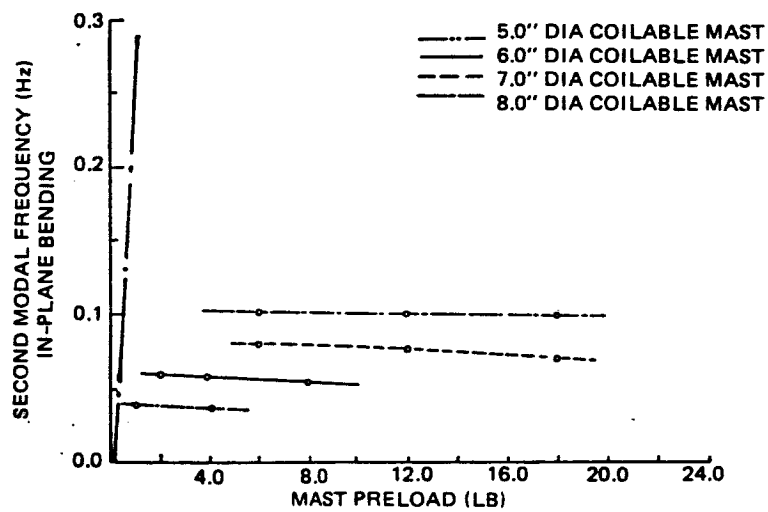


b. Split Blanket Cantled Wing

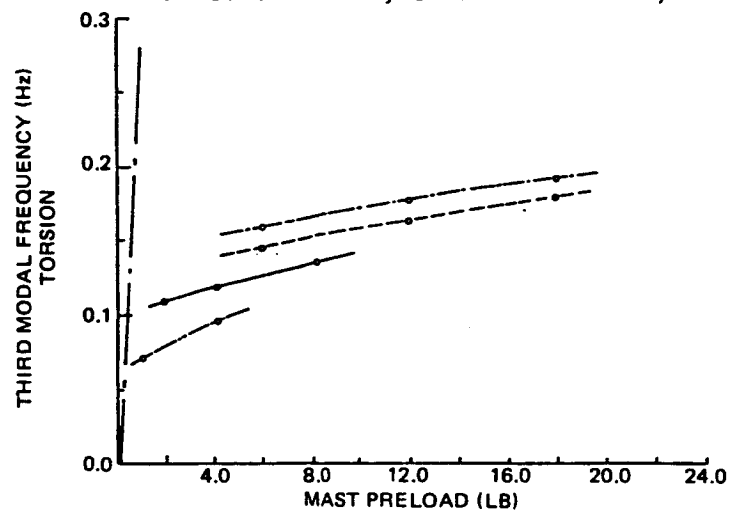
Figure 3-26. NASTRAN Finite Element Models Used for Dynamic and Deflection Analyses



a. First Mode, Out-of-Plane Bending



b. Second Mode, In-Plane Bending



c. Third Mode, Torsion

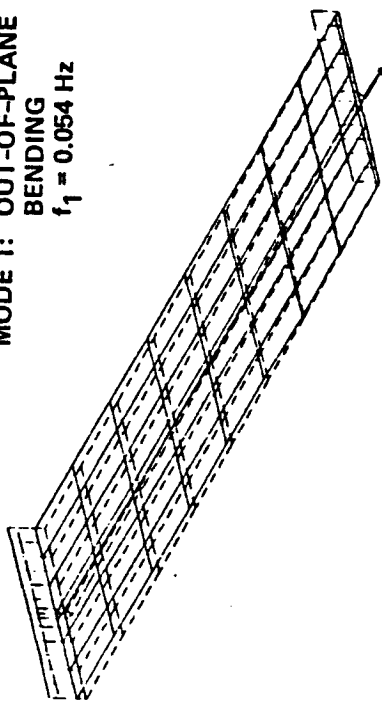
Figure 3-27. Effect of Blanket Tension and Mast Stiffness on Deployed Wing Frequency, 4.34 Aspect Ratio Wing

2. As the blanket tension level increases, the resulting compression level in the mast reduces the effective bending stiffness of the mast and the wing first and second modal frequencies begin to decrease. At the load level where mast Euler column buckling occurs, the frequency becomes zero. Hence frequency increase due to blanket tensioning is limited by mast buckling restrictions. A rule of thumb is not to let blanket tension be greater than 30 percent of the mast buckling load to provide a margin for on-orbit external loading conditions.
3. Except at very low blanket tension levels, the fundamental mode is out-of-plane bending of the wing. Mode 2 is in-plane bending. Mode 3 is torsion of the wing, and Mode 4 is blanket flapping, as illustrated in Figure 3-28.
4. As mast stiffness increases, the frequency increases (Figure 3-29). This occurs at the expense of increasing mast system weight. Beyond a reasonable mast size, the use of a stiffer mast system is inefficient.
5. Wing aspect ratio will impact wing frequency. For the same mast stiffness, a "long-narrow" wing configuration relative to a "short-wide" wing configuration will decrease frequency. Or conversely, for a given frequency level, the mast size and stiffness decreases with decreasing aspect ratio. However, as the wing width is increased, the blanket housing assembly becomes longer and its weight increases.
6. The separation distance between the mast centerline and the blanket plane had negligible impact on the modal results. The separation distance plays a more important role when determining relative blanket/mast deflections due to inertia loading and the possibility of blanket-mast interference.

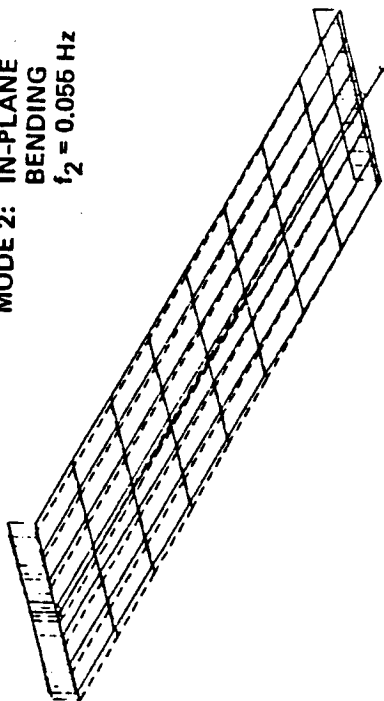
Figure 3-30 presents results from an earlier study on a flexible blanket wing where the blanket is connected to the mast at intermediate locations. The wing in this study was about twice as long as the mid aspect ratio wing analyzed under the present study. However, the results are indicative of the impact of intermediate blanket attachments. Both the first and second modal frequencies are moderately increased by the additional support points. However, the third mode (wing torsion) is unaffected. Further examination concluded that the design techniques to accomplish intermediate attachment of the blanket were complex and considered not weight-effective relative to the issue of reducing mast system weight to obtain a given frequency.

It was anticipated that the presence of a canted split blanket and the use of linear springs rather than constant-force springs to provide blanket tension might increase the effective bending stiffness of the wing system, thereby resulting in a corresponding increase in the frequency of the first two modes. This increase in modal frequency, hopefully, would be sufficiently large to offset the added system weight and complexity of a split blanket design such that the overall wing weight would be less for a given frequency requirement relative to the uncanted design. The key results for the mid aspect ratio wing are shown

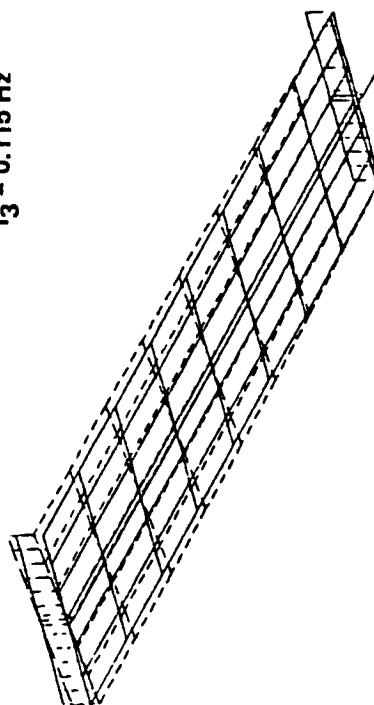
MODE 1: OUT-OF-PLANE
BENDING
 $f_1 = 0.054 \text{ Hz}$



MODE 2: IN-PLANE
BENDING
 $f_2 = 0.055 \text{ Hz}$



MODE 3: TORSION
 $f_3 = 0.115 \text{ Hz}$



MODE 4: BLANKET
FLAPPING
 $f_4 = 0.180 \text{ Hz}$

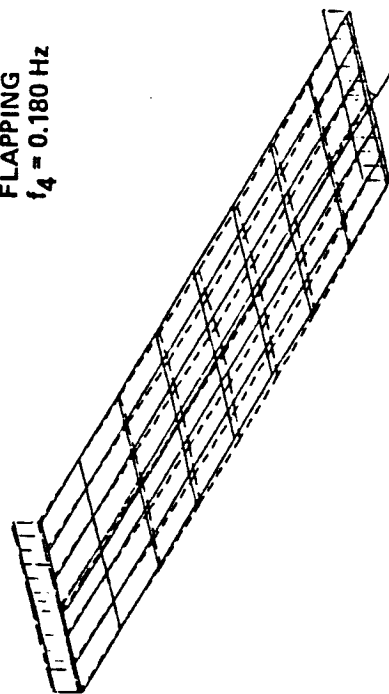


Figure 3-28. Cantilevered Deployed Mode Shapes for 4.34
Aspect Ratio Wing (Blanket Tension = 18 N [4 pounds]);
 $EI_M = 1.18 \times 10^3 \text{ N-m}^2$ [$0.64 \times 10^6 \text{ lb-in}^2$]; $GJ_m = 86 \text{ N-m}^2$
[$3 \times 10^4 \text{ lb-in}^2$.]

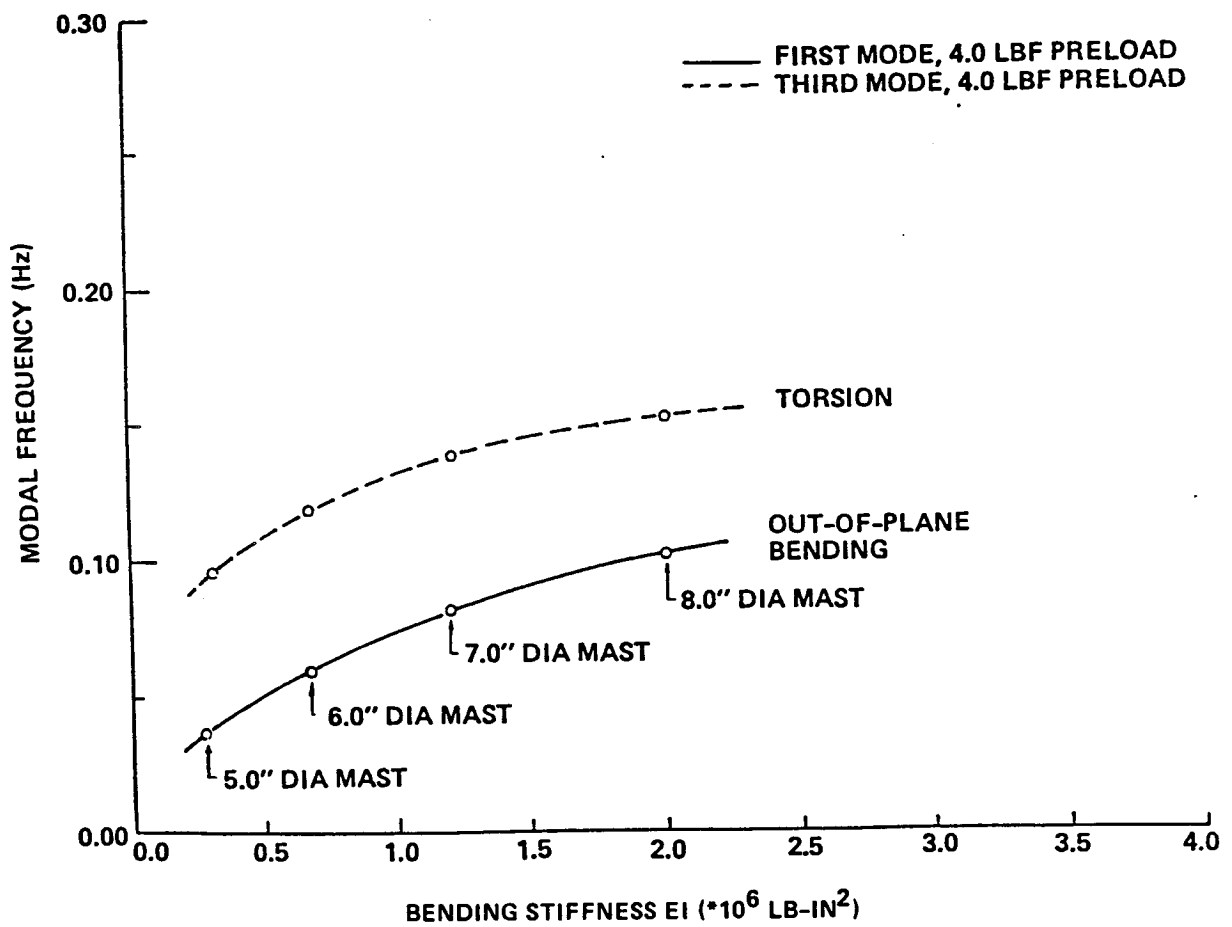


Figure 3-29. Effect of Mast Stiffness on Deployed Wing Frequency (4.34 Aspect Ratio Wing)

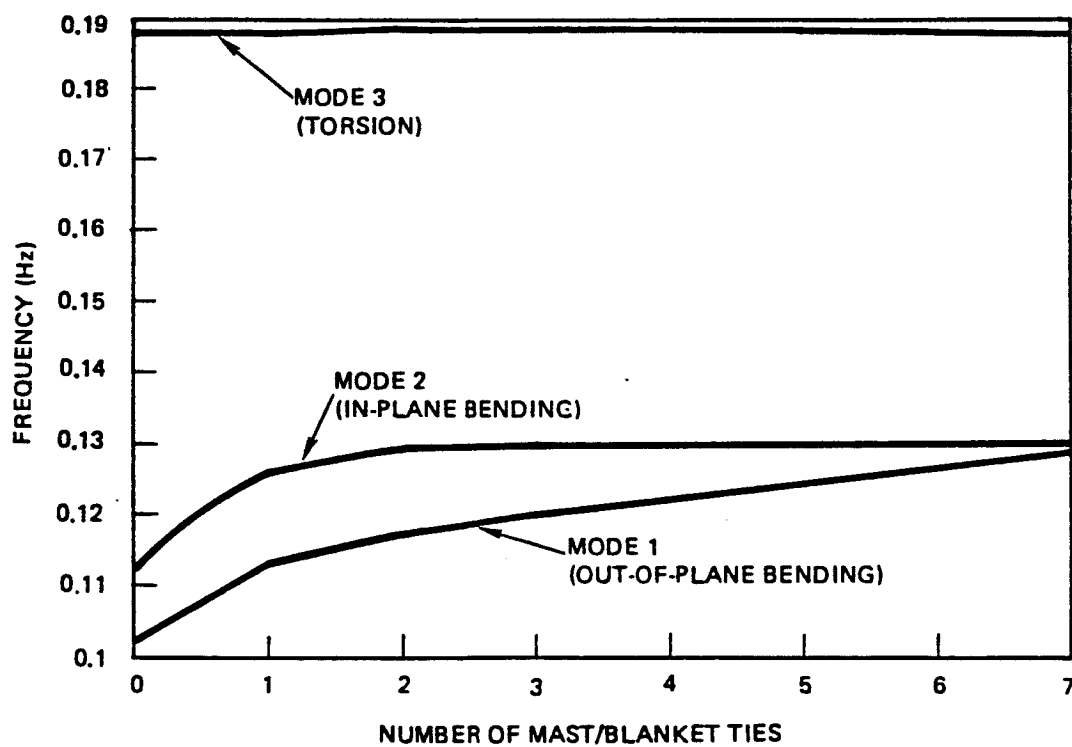


Figure 3-30. Effect of Number of Blanket/Mast Intermediate Attachments on Wing Frequency; 10 kW (BOL) Wing; AR - 7:1, 0.36 m (14 inches) Diameter Mast; 90 N (20 pounds) Blanket Tension. (Note: Only Full Integer Conditions Apply.)

in Figures 3-31 and 3-32. From these and other analyses the following was concluded:

1. Fundamental frequency of the split blanket design is relatively insensitive to blanket cant angle for angles less than 15 degrees, regardless of the tensioning device spring rates.
2. Fundamental frequency is relatively insensitive to tensioning device spring rates less than 1760 N/m (10 lb/in).
3. Blanket cant angles greater than 15 degrees were considered undesirable due to the reduction in power output from insolation cosine losses and because of wing stowage issues.
4. Due to the added weight and complexity of the canted split blanket design, with only a small increase in fundamental frequency, the design was dropped from further consideration in favor of the uncanted single blanket configuration.

3.2.6 Wing Deflection Characteristics

The deflected response of a single blanket cantilevered wing design to specified inertia loadings was analyzed. The magnitude of the inertia loading ranged from 0.001 to 0.01 g uniformly distributed normal to the blanket plane. For the preliminary design analysis, it was assumed that the inertia loads were impulsively applied, thereby resulting in deflections corresponding to a quasi-static loading of twice the inertia loading (namely 0.01 g inertia impulse load = 0.02 g quasi-static load). For the final design analyses (discussed in Section 4.4.2.4), this was revised to reflect the assumption that the 0.001 to 0.01 g reflected ultimate quasi-static loads per the requirements summarized in Section 1.3.

The equilibrium deflected shape of the mid aspect ratio wing under a 45 N (10 pound) blanket tension load plus 9 N (2 pounds) loading from the two guidewires is shown in Figure 3-33. The maximum deflection is about 0.15 m (6 inches) and is due to the offset loading condition imposed on the mast by the blanket and guidewires. Figure 3-34 shows the maximum positive and negative deflections for the wing under a 0.01 g impulsive load (0.02 g quasi-static load) applied normal to the blanket plane. As can be seen for the negative loading condition, it is possible for the blanket to impact the mast in the center when the load level exceeds a certain value. The potential interference is dependent upon the mast stiffness, blanket tension level and blanket-mast standoff distance. The problem of blanket-mast interference is a function of mast tip deflection, blanket sag with respect to its ends, and blanket-mast standoff distance. Figure 3-35 illustrates the effect of mast bending stiffness (EI) on mast tip deflection for the three aspect ratio wings for a quasi-static 0.02 g load. Figure 3-36 illustrates blanket maximum deflection as a function of blanket tension level. Table 3-8 indicates that by adjusting (increasing) the blanket-mast standoff distance for a given blanket tension level, the blanket-mast interference can be eliminated.

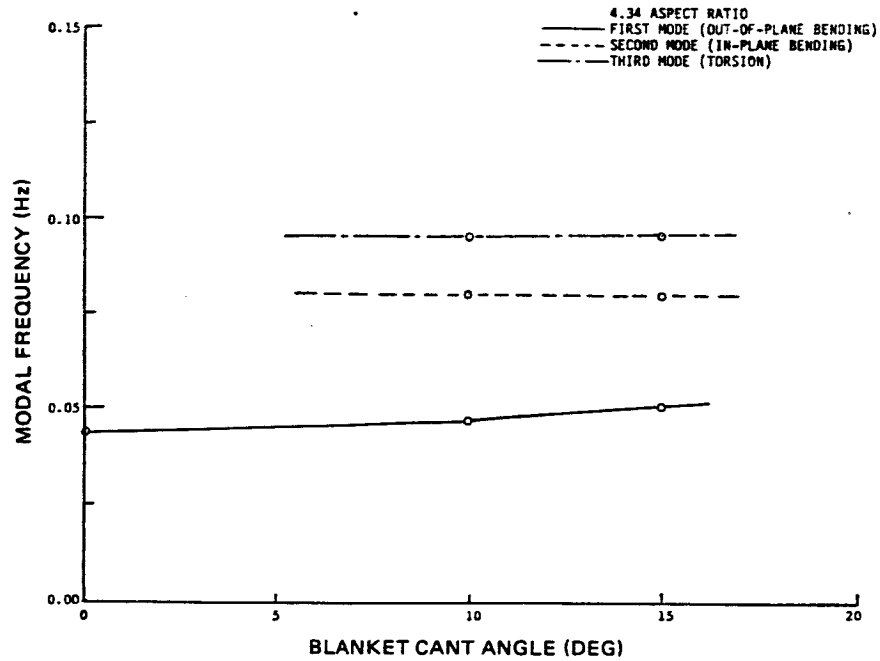


Figure 3-31. Deployed Wing Modal Frequency vs. Blanket Cant Angle (Blanket Tension = 18.0 N [4 pounds], $EI_m = 1.8 \times 10^3 \text{ N-m}^2$ [$0.64 \times 10^6 \text{ lb-in}^2$], $GJ_m = 86 \text{ N-m}^2$ [$3 \times 10^4 \text{ lb-in}^2$] Blanket Tensioning Device Spring Constant = 1760 N/m [10 lb/in])

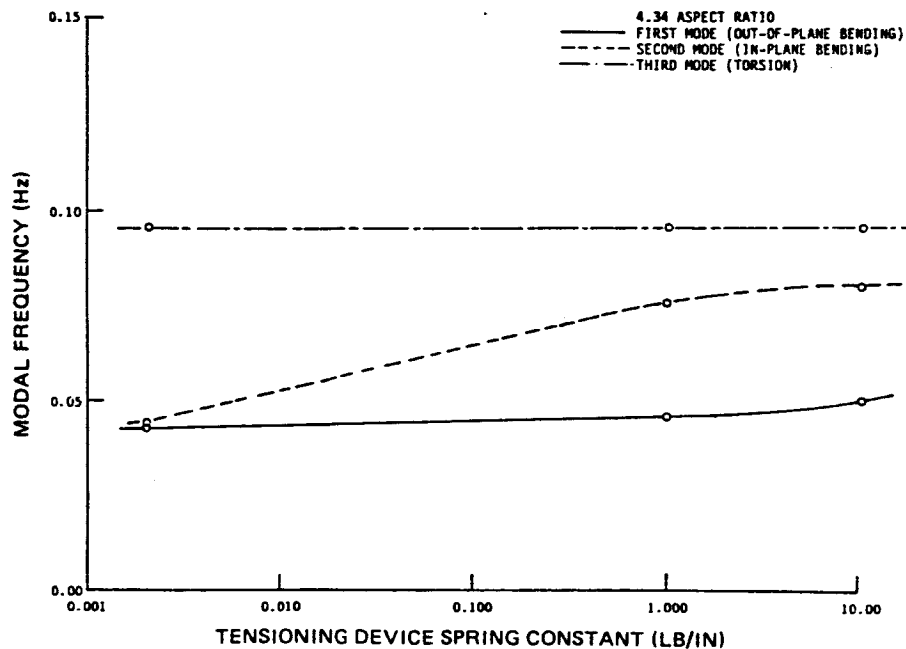


Figure 3-32. Deployed Wing Modal Frequency vs. Tensioning Device Spring Constant (Blanket Tension = 18.0 N [4 pounds], $EI_m = 1.8 \times 10^3 \text{ N-m}^2$ [$0.64 \times 10^6 \text{ lb-in}^2$], $GJ_m = 86 \text{ N-m}^2$ [$3 \times 10^4 \text{ lb-in}^2$], 15-degree Cant Angle)

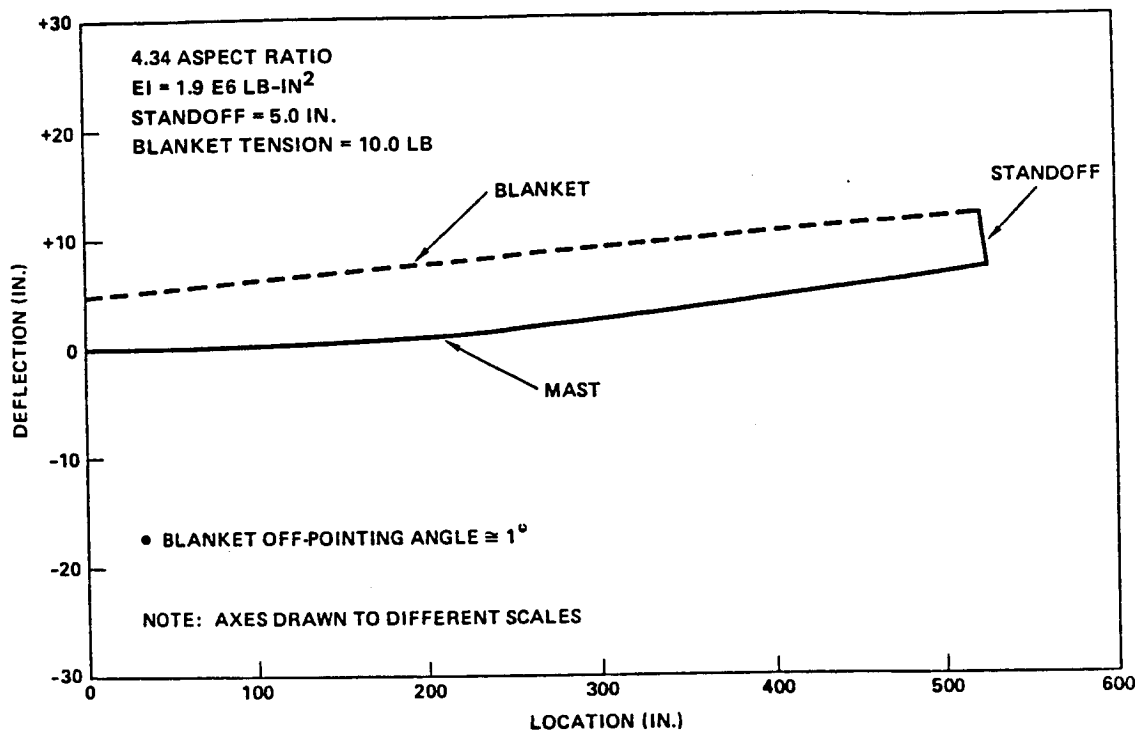


Figure 3-33. Cantilevered Equilibrium Shape of Wing

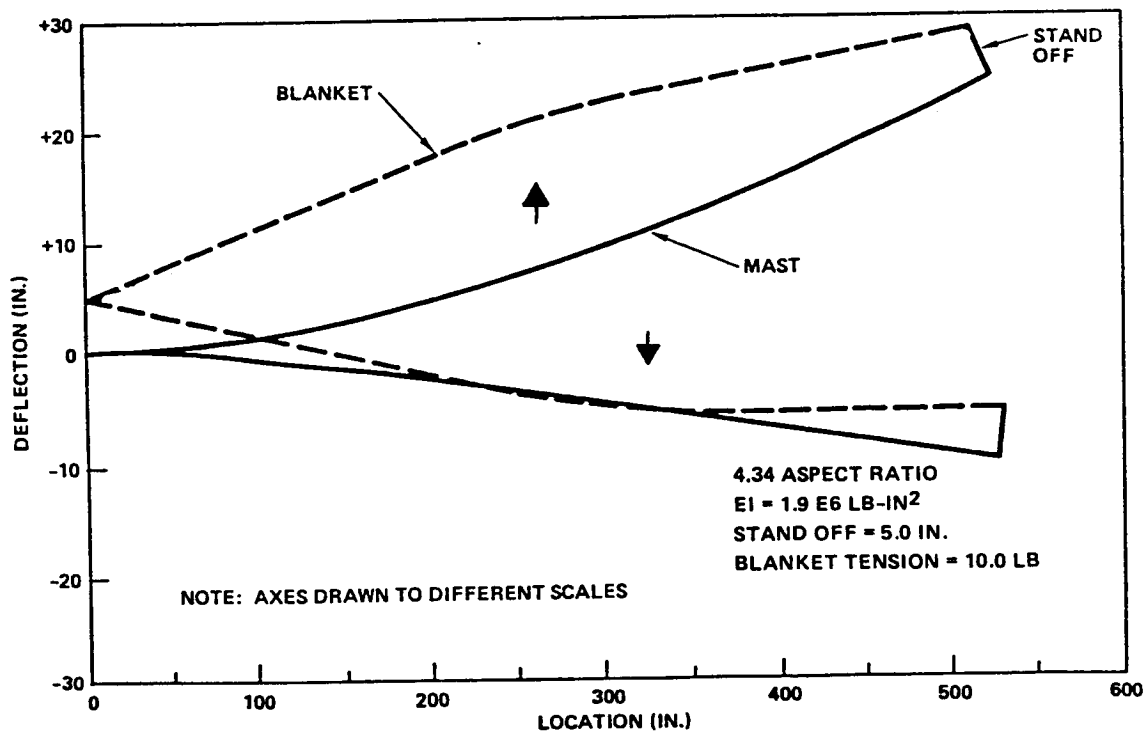


Figure 3-34. Cantilevered Deflected Shape of Wing (0.02 g Quasi-Static Uniformly Distributed Load Normal to Blanket Plane)

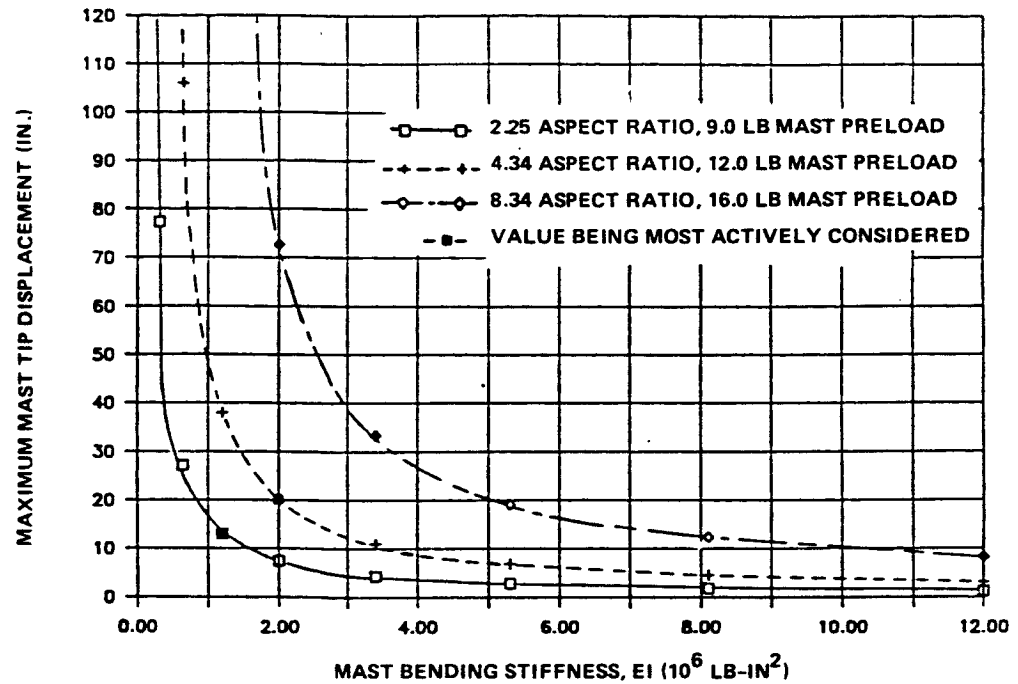


Figure 3-35. Cantilevered Mast Tip Deflection Versus Mast Bending Stiffness (0.02 g Quasi-Static Uniformly Distributed Load Normal to Blanket Plane)

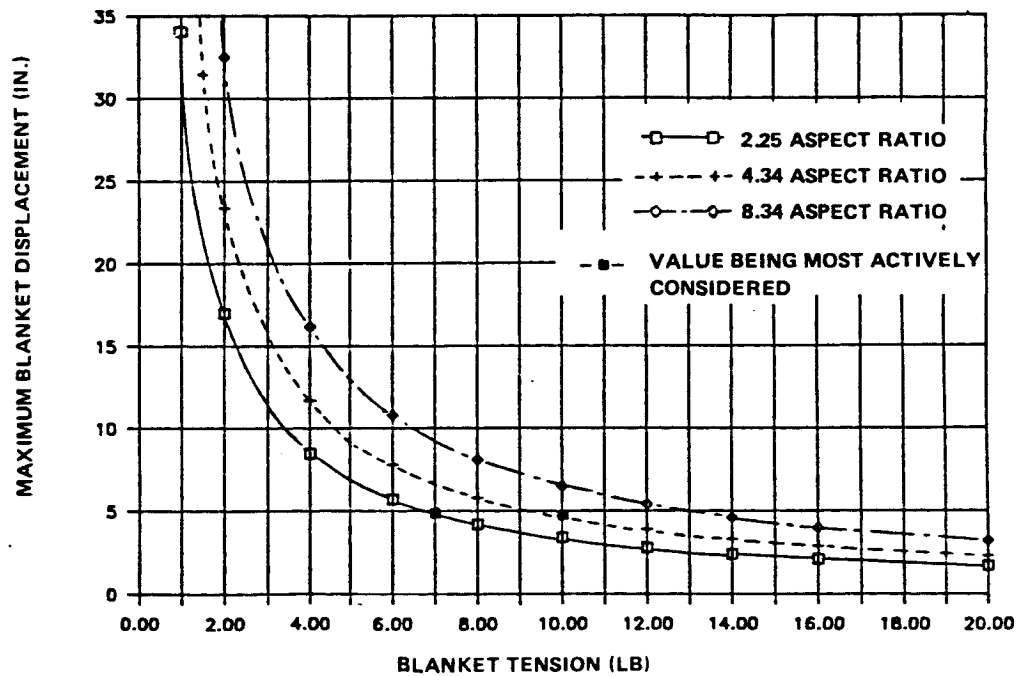
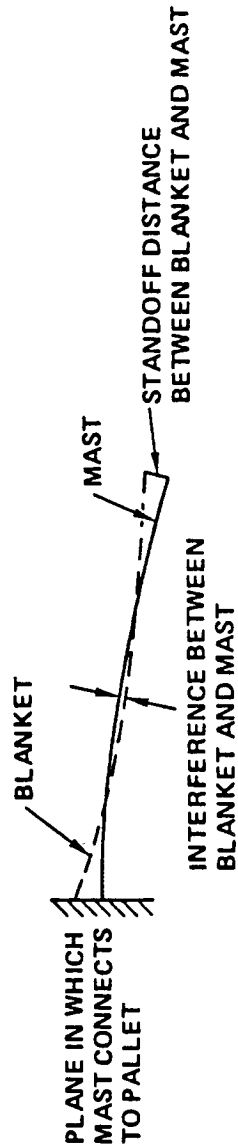


Figure 3-36. Deflection of Center Region of Blanket Relative to Its Ends Versus Blanket Tension (0.02 g Quasi-Static Uniformly Distributed Load Normal to Blanket Plane)

Table 3-8. Potential Blanket/Mast Interference Under 0.02 g Quasi-Static Uniformly Distributed Loading Condition



ASPECT RATIO	BLANKET TENSION (LB)	MAST PRELOAD (LB)	MAST EI (LB-IN ²)	MAST DIAMETER (IN)	BLANKET/MAST STANDOFF (IN)	FUNDAMENTAL FREQUENCY (Hz)	MAXIMUM BLANKET/MAST INTERFERENCE (IN)	APPROX IMPACT VELOCITY (IN/SEC)
2.25	7.0	9.0	1.4E6	6.6	5.0	0.123	0.22	1.2
2.25	7.0	9.0	1.4E6	6.6	5.3	0.123	NONE	NONE
4.34	10.0	12.0	1.9E6	7.2	5.0	0.097	0.44	1.3
4.34	10.0	12.0	1.9E6	7.2	5.5	0.097	NONE	NONE
8.34	14.0	16.0	3.6E6	8.2	5.0	0.085	0.86	1.5
8.34	14.0	16.0	3.6E6	8.2	5.8	0.085	NONE	NONE

The preliminary deployed wing deflection analyses led to the following conclusions:

1. The off-pointing of the wing due to the maximum inertia load under consideration (0.01 g impulsive or 0.02 g static) was small (less than 3 degrees).
2. Since deployed frequency response is insensitive to blanket tension level above a nominal value of tension (see Section 3.2.5), the blanket tension level, in combination with blanket-mast standoff distance, is selected to eliminate blanket-mast interference (slapping) under inertia loading. For the mid aspect ratio range, a blanket tension level of about 70 N (15 pounds) with standoff distance of about 0.15 m (6 inches) between the blanket plane and the face of the mast structure will provide substantial margin to preclude blanket-mast slapping under a 0.01 g loading.
3. By the simple design technique of increasing blanket tension level and blanket-mast standoff distance, in combination with greater strength mast systems, the wing can be designed to withstand inertia loadings greater than 0.01 g with only a small increase in weight (see Section 4.4.2.2.).

3.3 ELECTRICAL DESIGN TRADES

3.3.1 Power Element Definition

Figures 3-37 and 3-38 define the basic building blocks of the electrical portion of the APSA. The components of the electrical design include: the solar cell stack (cell, coverglass, and interconnects), the adhesives used to bond the stack to the substrate, the termination of the circuit, the electrical harness that transfers power to the base of the array, the termination of the harness at the spacecraft interface, and components required to protect the circuitry.

The individual solar cell stacks are interconnected to form a multi-cell circuit module that generates the proper voltage. A group of circuit modules are installed on a multi-panel segment of the total blanket assembly. This multi-panel segment is termed a solar panel assembly (SPA). The circuits on the SPA are grouped and series strung to form righthand and lefthand circuits to minimize current-generated magnetic fields/torques. Identical SPAs are integrated electrically in parallel (mechanically hinged together in series) to achieve the proper power output for each wing of the array. Electrical harnesses running along the sides of the wing carry the power to diode box assemblies on the wing pallet structure. The diode box assemblies provide blocking diode protection of the circuits and act as the electrical interface between the solar array and the spacecraft.

3.3.2 Solar Cell Stack

The selection of many of the component attributes were performed by stack-level trades. Evaluating the performance of stacks allowed the selection of components based on their ability to be integrated into the wing system. Table 3-9 summarizes the module-level trades. All of the design options were integrated onto identically sized wings with a BOL performance of approximately 5000 watts, when referenced to a conventional thickness silicon solar cell.

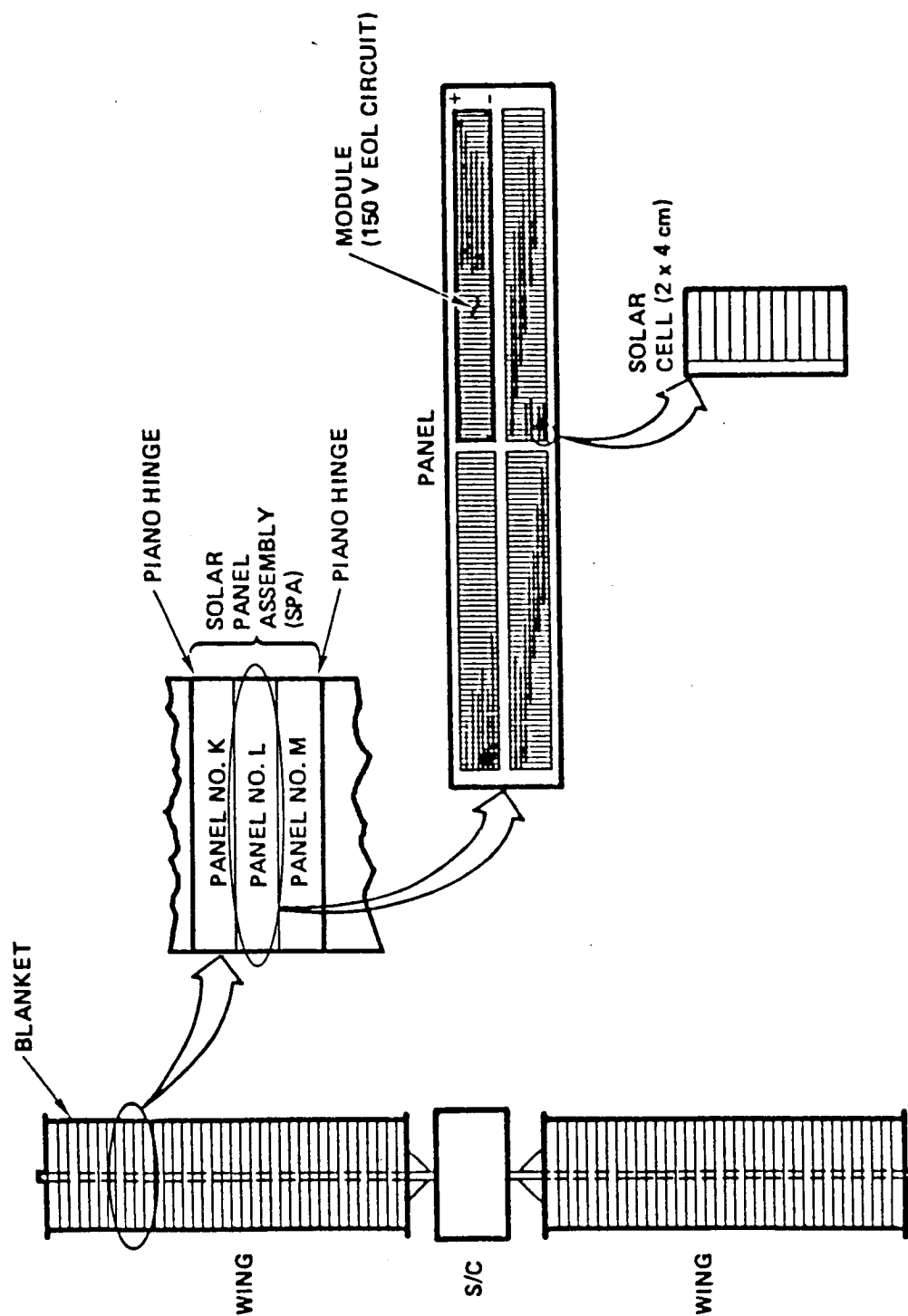


Figure 3-37. Primary Electrical Power Elements

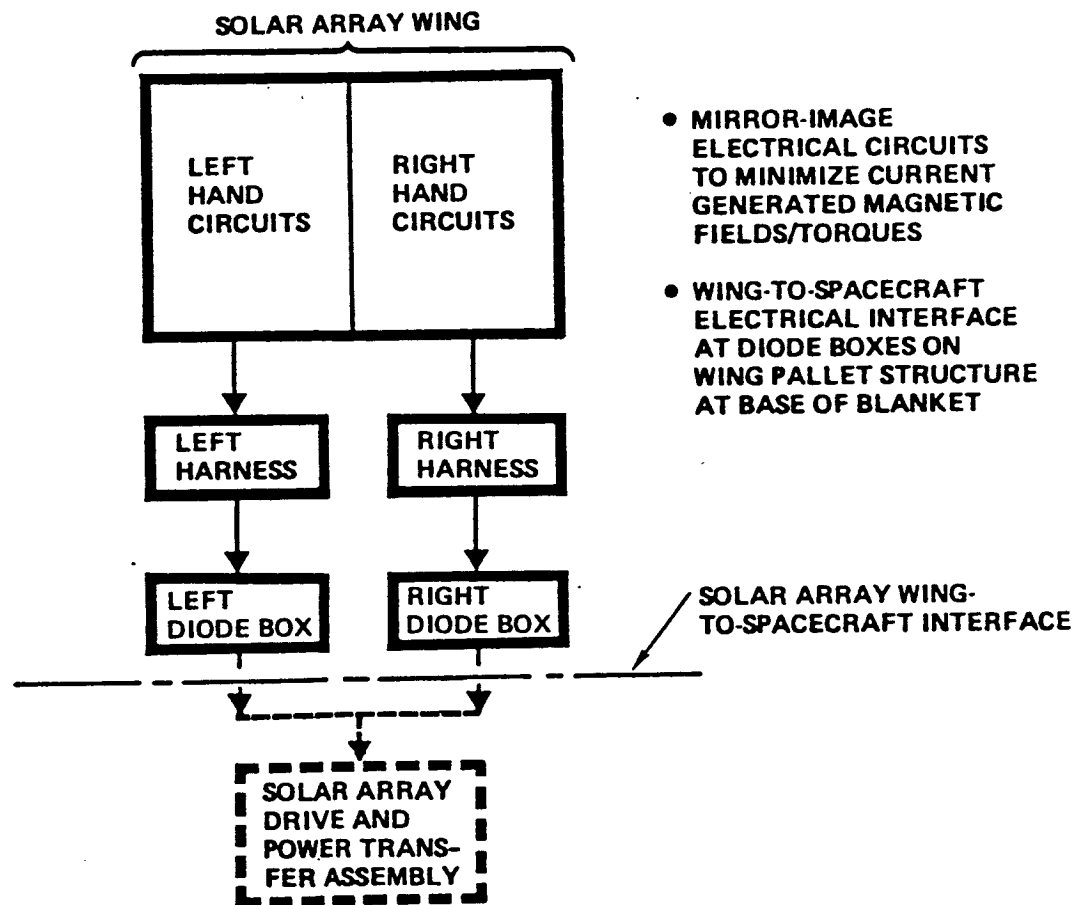


Figure 3-38. Primary Electrical Power Flow

Thus, the structural (or non-electrical) weight of each wing design was about the same except for slight differences in the deployment mast system weight to account for equal deployed strength/stiffness wing designs. The electrical performance of each solar cell stack option was calculated, its contribution to the total wing weight estimated, and the resulting specific power (W/kg) and power density (W/m²) characteristics derived.

Six basic solar cell stack design options were considered. They included: (1) a conventional thickness 200 μ m (8 mil) silicon cell, (2) three variations of a thin 63 μ m (2.5 mil) silicon cell, (3) gallium arsenide, and (4) thin film amorphous silicon. The thin gallium arsenide cell stack and the thin film amorphous silicon options were considered technology that would require significant additional development. The infrared-reflective and infrared-transparent cell stack options using a thin silicon cell were considered technology that would require some additional development.

3.3.2.1 Solar Cell

Initial trades indicated that the thinnest practical solar cell would be required to gain the greatest W/kg advantage, and that at the present thinness limit of about 63 μ m (2.5 mils) average, the penalty in W/m² was not significant. This is illustrated in Figure 3-39. This was confirmed in the module-level trades where a conventional thickness cell (200 μ m [8 mils]) was studied in comparison to the thin cell options. The conventional thickness silicon cell option was found to perform at 60 percent of W/kg (EOL) and at 90 percent of W/m² (EOL) available from the thinner cell options. Table 3-10 lists other aspects of the cell characteristics that were evaluated before selecting a baseline solar cell.

Three thin silicon solar cell design options were studied to investigate methods of providing efficient thermal control of the cell module, thereby minimizing temperature-induced reduction effects on power output. The first of the thin silicon cell options used a conventional approach. The cell was a polished cell with boron back surface field (B-BSF) and an aluminum back surface reflector (Al-BSR), with a thin full metallized back surface. The solar absorptance of the cell is aided by the BSR which rejects the long wave infrared (IR) back to space like a second surface mirror. Both ASEC and Spectrolab solar cell suppliers indicated that 13.5 percent efficiency (at 28°C AMO) was a reasonable production average for this cell. When IR-reflective technology is incorporated into the cell module through coating on the coverglass, the IR never reaches the solar cell and a texturing of the cell front surface can be considered without impacting the solar absorptance characteristics of the cell. Such an approach can result in a 14.4 percent average efficiency (at 28°C AMO); however, the presence of the IR-reflective coating creates up to a 6.5 percent transmission loss in the coverglass. When IR-transparent technology is incorporated into the cell module, the IR passes through the cell and out of the back of the blanket substrate. To accommodate this type of "optical" path, the cell must be polished and the backside metallization must be designed using grid-line contacts (just like the front side). The loss of backside full metallization lowers cell average efficiency to 13.3 percent (at 28°C AMO). In addition, the substrate material must also be infrared transparent. Kapton is not an efficient IR-transparent material. Thus, the substrate material would have to be changed to another material like Tedlar (polyvinylfluoride polymer film from duPont).

Table 3-9. Comparison of Solar Cell Module Trades

COMPONENT/PARAMETER	CONVENTIONAL THICKNESS SILICON CELL MODULE	THIN GALLIUM ARSENIDE CELL MODULE	THIN SILICON CELL MODULE	IR-REFLECTIVE CELL MODULE	IR-TRANSPARENT CELL MODULE	AMORPHOUS SILICON THIN-FILM SHEET MODULE
SOLAR CELL (2 x 4 CM) TYPE	AL-BSF/AL-BSR	-	B-BSF/AL-BSR	AL-BSF	B-BSF	-
THICKNESS (μ M)	200	63	63	63	63	0
SURFACE TEXTURE	POLISHED	POLISHED	POLISHED	TEXTURED	POLISHED	-
REAR STRUCTURE	FULL METALIZATION	FULL METALIZATION	FULL METALIZATION	FULL METALIZATION	GRIDDED METALIZATION	-
BOL EFFICIENCY (%)	14.3	16.0	13.5	14.4	13.3	6 (10)**
EOL EFFICIENCY (%)	9.6	13.3	9.8	10.5	9.7	6 (10)**
DESIGN MATURITY	MATURE	NOT AVAILABLE	AVAILABLE FROM VENDORS	DEVELOP- MENTAL COATING ISSUE	DEVELOP- MENTAL SUBSTRATE ISSUE	DEVELOP- MENTAL EFFICIENCY; RADIATION
TECHNOLOGY ISSUE						
COVER GLASS (2.04 x 4.04 CM)						
MATERIAL THICKNESS	CMX 100	CMX 50	CMX 50	CMX 50	CMX 50	-
FRONT COATING	UV REFL	HIGH EMIT UV REFL	HIGH EMIT UV REFL	HIGH EMIT UV REFL	HIGH EMIT UV REFL	-
REAR COATING	NONE	NONE	NONE	IR REFL	NONE	-
COATING TRANS LOSS (%)	0	0	0	6.5	0	-
ADHESIVE	DC93500	DC93500	DC93500	DC93500	DC93500	-
SUBSTRATE (50 μ M THICK)	CARBON-LOADED KAPTON	CL KAPTON	CL KAPTON	CL KAPTON	TEDLAR	CL KAPTON
SOLAR ABSORPTANCE	0.82	0.82	0.72	0.88	0.87	-
HEMISPHERICAL EMITTANCE	0.82	0.86	0.86	0.86	0.86	-
BOL/EOL TEMPERATURES ($^{\circ}$ C)	42.0/47.4	36.3/39.4	27.1/31.8	22.0/27.1	20.8/25.6	-
CELL STACK UNIT WEIGHT (MG)	864	519	366	366	327	NEGLIGIBLE
BOL/EOL WING POWER (WATTS)	4777/3191	5602/4400	4783/3487	4860/3535	4821/3493	2500 (4156)**
CELL STACK AND BLANKET WT FOR 34560 CELLS (36 PANELS)(KG)	32.2	21.5	16.2	16.2	14.9	4.0
OTHER STRUCTURAL SYSTEM WEIGHT (KG)	18.0	16.2	15.2	15.2	15.2	15.2
TOTAL WING WEIGHT WITH 10% CONTINGENCY (KG)	55.2	41.5	34.6	34.6	33.1	21.1
TOTAL BLANKET AREA (HARNES AND LEADERS)(M ²)	39.05	39.05	39.05	39.05	39.05	39.05
EOL SPECIFIC POWER (W/KG)	57.8	105.9	100.8	102.2	105.5	118.7 (197.4)**
EOL POWER DENSITY (W/M ²)	81.7	112.7	89.3	90.5	89.4	64.0 (106.0)**

*CONVERSION EFFICIENCY IS INSENSITIVE TO TEMPERATURE

**BOL ASSUMED EQUAL TO EOL; FIRST FIGURE FOR 6% η , SECOND FIGURE FOR 10% η

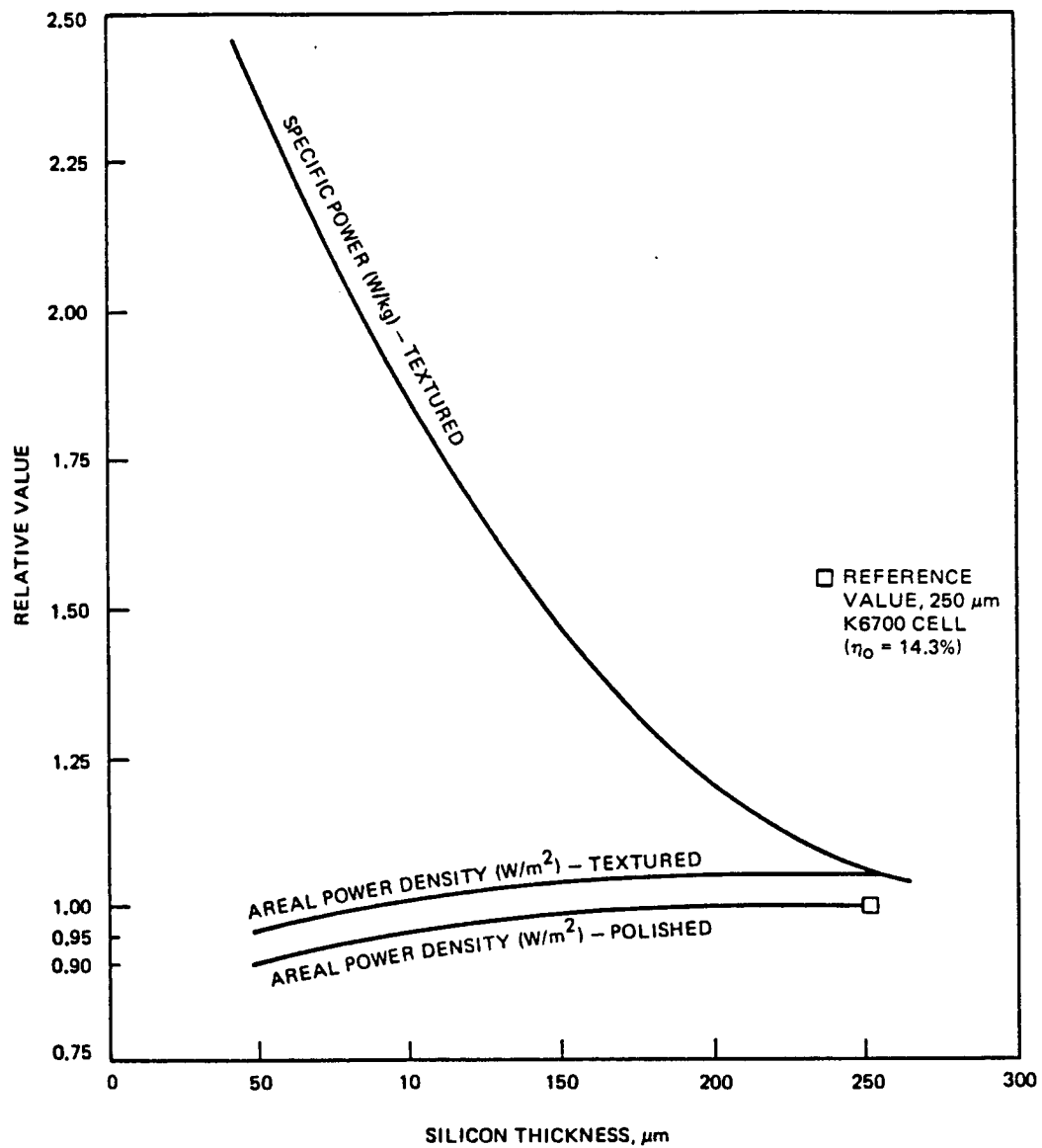


Figure 3-39. The Effect of Silicon Cell Thickness on Specific Power and Power Density Characteristics

Table 3-10. Solar Cell Options

PARAMETER	OPTION	SELECTED DESIGN	RATIONALE
THICKNESS	<ul style="list-style-type: none"> • 50 μm • 75 μm TO 200 μm 	50 μm NOMINAL (63 μm ACTUAL)	<ul style="list-style-type: none"> • THINEST PRACTICAL CELL AVAILABLE • LOW WEIGHT • ARRAY PRODUCTIBILITY
SIZE	<ul style="list-style-type: none"> • 2 x 4 cm • LARGE AREA (> 2 x 4 cm) 	2 x 4 cm (NOMINAL)	<ul style="list-style-type: none"> • AVAILABILITY • ARRAY PRODUCTIBILITY • COST
TYPE	<ul style="list-style-type: none"> • CONVENTIONAL SILICON, POLISHED • IR-REFLECTIVE SILICON, TEXTURED • IR-TRANSPARENT SILICON, POLISHED • GALLIUM ARSENIDE, POLISHED • THIN FILM AMORPHOUS SILICON 	<ul style="list-style-type: none"> • SILICON • B-BSF • AL-BSR • POLISHED • FULL COVERAGE METALLIZATION 	<ul style="list-style-type: none"> • AVAILABILITY (DESIGN MATURITY) • AREAL DENSITY (kg/m^2) • SPECIFIC POWER (w/kg) • POWER DENSITY (w/m^2) • COST • ARRAY PRODUCTIBILITY • SUBSTRATE DESIGN COMPLEXITY
METALLIZATION	<ul style="list-style-type: none"> • SOLDER-COVERED • SOLDERLESS • Ti-Ag • Ti-Pd-Ag • Au-Cr-Ag 	<ul style="list-style-type: none"> • SOLDERLESS • Ti-Pd-Ag 	<ul style="list-style-type: none"> • HUMIDITY RESISTANCE • COST • RISK • LOW WEIGHT
CONTACT CONFIGURATION	<ul style="list-style-type: none"> • FRONT/BACK • WRAPAROUND • WRAPTHROUGH 	FRONT/BACK	<ul style="list-style-type: none"> • HIGHER W/m^2 • AVAILABILITY • COST • COMPATIBILITY WITH EXISTING TRW AUTOMATED CELL INSTALLATION LINE

After reviewing the difference in module-level performance and current development status of the three thin silicon cell options, the thin polished B-BSF/Al-BSR fully metallized cell was selected as the baseline. The cell is available from several sources. The cell, when integrated into the wing assembly achieves about 95 percent of the specific power and about 100 percent of the power density characteristics potentially available from the emerging, but not yet fully demonstrated IR-reflective and IR-transparent technologies.

The possibility of using gallium arsenide and amorphous silicon cell technologies for the baseline array was given brief consideration. Further discussion of these technologies is covered in Section 4.6.2. Gallium arsenide was dropped because in order to achieve the specific power goals, a thin (50 to 100 μm [2 to 4 mil]) cell would be required, depending on the average cell efficiency selected (i.e., 16 to 20 percent). Since gallium arsenide cells are only available in 280 to 305 μm (11 to 12 mil) thicknesses, the resulting specific power performance would only be about half of that desired, even though the resulting power density characteristics would be about 10 percent above the 110 W/m^2 (EOL) goal. Amorphous silicon shows potential only if: (1) it can withstand long-term space radiation environments, and (2) the operating efficiency of amorphous silicon can be doubled from its present 5 to 6 percent level and be produced in large quantities. The present 6 percent efficiency (holding aside the concern about space stability) leads to acceptable array specific power characteristics; however, the power density would only be about half that desired.

The selection of cell size for the 63 μm (2.5 mil) thick BSF/BSR silicon cell (i.e., 2 x 4 cm or larger) was based on cost, availability, and array producibility and reliability. The thin cell is available up to 2.2 x 6.2 cm; however, the production yield is very low, thus cost is very high. Furthermore, chances of breakage when installed on the flexible blanket are greater. Assuming that the conversion efficiency is the same for a 2 x 4 cm and a 2 x 6 cm cell, the use of a larger cell would improve power density only slightly. That small improvement is not warranted in exchange for the added cost and risk. Thus, 2 x 4 cm was selected as the baseline cell size.

3.3.2.2 Cover Glass

Table 3-11 summarizes the cover glass options considered and the rationale for selection of the 50 μm (2 mils) ceria-doped glass (CMX) as the baseline material. The thickness was derived from trades of shielding versus mass, which showed the 50 μm (2 mils) material to provide the best specific power characteristics, without undue compromise in power density characteristics. The material is the thinnest and lowest cost polished material which does not significantly darken in GEO radiation environments. Polished fused silica is more space stable; however, it is not cost-effective below 150 μm (6 mils) thickness. The use of frosted (or non-polished) fused silica allows the thickness to be reduced to 100 μm (4 mils); however, it is more difficult to detect cell defects through frosted fused silica. Microsheet is less space stable than CMX.

Coatings for the cover glass were another subset of the cover glass trades that were performed. The coating options included improved versions of generic ultraviolet rejection and emittance enhancement designs, as well as the IR-reflective technology. The IR-reflective coating is on the inside (back) surface of the cover glass to reflect the IR energy over the wavelength range 1.1 to 4.0 μm before entering the solar cell, thus allowing a textured but higher

Table 3-11. Cover Glass Options

PARAMETER	OPTION	SELECTED DESIGN	RATIONALE
THICKNESS	<ul style="list-style-type: none"> • 25 μm • 50 μm • 100 μm • 150 μm 	50 μm (2 mil)	<ul style="list-style-type: none"> • LOW WEIGHT • ACCEPTABLE FRONT SIDE CELL RADIATION SHIELDING • AVAILABILITY • ARRAY PRODUCTIVITY • COST FOR THIN COVERS • ARRAY PRODUCTIVITY • ACCEPTABLE SPACE RADIATION COMPATIBILITY • SUBSTORM CHARGING COMPATIBILITY
MATERIAL	<ul style="list-style-type: none"> • POLISHED FUSED SILICA • FROSTED FUSED SILICA • CERIA-DOPED GLASS • MICROSHEET 	CERIA-DOPED GLASS (CMX)	<ul style="list-style-type: none"> • REDUCE REFLECTION LOSSES • REDUCE CELL OPERATING TEMPERATURE • REDUCE TRANSMISSION LOSSES
COATING	<ul style="list-style-type: none"> • AR • UV • ENHANCED EMITTANCE • NONE 	UV + ENHANCED EMITTANCE WHICH ALSO PROVIDES FOR ANTI-REFLECTION	<ul style="list-style-type: none"> • COMPATIBLE WITH AVAILABLE ULTRA-THIN (63 μm) SOLAR CELLS
SIZE	<ul style="list-style-type: none"> • 2 x 4 cm • LARGE AREA (> 2 x 4 cm) 	2 x 4 cm (NOMINAL)	

solar absorptance cell to be considered. The coating has yet to be fully developed and a transmission loss of 6.5 percent in the cell response region of 0.35 to 1.1 μm partially offsets the benefits of the increased efficiency from use of the textured solar cell.

The improvements in the generic UV-rejection coating and emittance enhancement coating can be used with all solar cell types; the improved coatings are available. For the CMX cover glass, both coatings would be combined into a single outside (front surface) coating. The UV coating would reflect the $\lambda < 0.35 \mu\text{m}$ energy before it is absorbed in the CMX bulk. The result is a lower solar absorptance by 0.03 which equates to an improvement in module performance of 1.5 percent. The emittance coating would suppress reflection of the bulk material in the far IR ($\lambda > 4.0 \mu\text{m}$), which would increase the hemispherical emittance by 0.04 (0.82 to 0.86) and result in an additional improvement of 1.5 percent in module performance.

3.3.2.3 Cell Stack Adhesives

Bonding of thin cover glasses to thin solar cells has been accomplished at TRW with success. This includes bonding of thin covers to bowed cells and bonding of thin frosted fused silica covers (JPL contracts 955139 and 956042). Cover glasses will be bonded to the cells with DC93-500 adhesive, which has been a standard procedure at TRW for many years. Adhesive bondline thicknesses of 38 to 50 μm (1.5 to 2 mils) have been achieved.

The most effective assembly method is by means of automation for which slightly bowed cells and covers, (having a bow radius greater than 20 cm), will still be acceptable.

Solar cell stacks will be bonded to the substrate using DC93-500 adhesive and 92-023 primer. The adhesive has been successfully tested for this application on several test programs. Thin adhesive bondline thicknesses ranging from 50 to 100 μm (2 to 4 mils) have been achieved.

3.3.2.4 Solar Cell Interconnector

Acceptable interconnector/solar cell joint fatigue life must be achieved to enable successful solar array design. Joint fatigue is primarily the result of thermally induced stresses in the joint as the solar array undergoes thermal cycles. The stresses come from two sources:

1. The actual differential expansion or contraction of the joint materials themselves
2. The forces applied to the joint by the interconnector.

The interconnector-applied force is the product of the interconnector stiffness and the intercell thermal displacement. The interconnector design problem is to select materials and configurations which: (a) minimize joint material differential expansion or contraction-induced stress; and (b) minimize interconnector stiffness.

Table 3-12 summarizes the interconnector options considered and rationale for selection of the silver-plated 25 μm (1 mil) thick rounded box loop, in-plane stress relief interconnector design for the thin solar cell stacks. The

Table 3-12. Cell Interconnection Options

PARAMETER	OPTION	SELECTED DESIGN	RATIONALE
MATERIAL	<ul style="list-style-type: none"> • COPPER • MOLYBDENUM • INVAR • OTHERS 	INVAR	<ul style="list-style-type: none"> • PROVEN FLIGHT EXPERIENCE • LONGEST FATIGUE LIFE • MAGNETICALLY SOFT-ACCEPTABLE • BEST LOW TEMPERATURE SOAK CAPABILITY
PLATING	<ul style="list-style-type: none"> • SILVER • OTHER 	SILVER	<ul style="list-style-type: none"> • LOW ELECTRICAL RESISTANCE ($< 0.1\%$ POWER LOSS FOR ARRAY) • EASILY SOLDERED OR WELDED
TYPE	<ul style="list-style-type: none"> • DISCRETE • PRINTED CIRCUIT 	DISCRETE	<ul style="list-style-type: none"> • SILVER-PLATED INVAR IS NOT COMPATIBLE WITH PRINTED CIRCUIT APPROACH
CONFIGURATION	<ul style="list-style-type: none"> • OUT-OF-PLANE U-SHAPED LOOP • IN-PLANE LOOP • STRAIGHT BUS BAR 	IN-PLANE LOOP	<ul style="list-style-type: none"> • LOW PROFILE COMPATIBLE WITH THIN CELL STACK HEIGHT • REDUCES THERMAL EXPANSION STRESS • LOW MASS
REDUNDANCY	<ul style="list-style-type: none"> • ANY 	<ul style="list-style-type: none"> • 1 JOINT PER CONTACT • 4 JOINTS PER CELL • 2 CURRENT PATHS PER CELL 	<ul style="list-style-type: none"> • LOW ELECTRICAL LOSS • FRACTURED CELL PIECES PICKED UP IN MOST CASES • HIGH RELIABILITY PER T/V TESTING
JOINING METHOD	<ul style="list-style-type: none"> • SOLDERING • WELDING • OTHER 	<ul style="list-style-type: none"> • SOLDERING • WELDING OPTIONAL (DESIGN IS FULLY COMPATIBLE WITH WELDING) 	<ul style="list-style-type: none"> • LOW RISK • ACCEPTANCE CRITERIA HAVE BEEN ESTABLISHED • PROVEN FLIGHT EXPERIENCE

interconnector selection process was greatly aided by work accomplished by TRW under JPL contract 956042, which dealt with the development and processing of thin silicon cell modules on rigid panel and flexible blanket substrates. Based on a review of that work, the rounded box loop interconnector shown in Figure 3-40 was selected. Based on subsequent long-term thermal cycle tests, in which several types of welded and soldered interconnectors were evaluated (connected to different size and thickness cells bonded to Kapton substrate), the selected interconnector design outperformed all other interconnectors. Furthermore, soldered interconnectors performed equally well as welded interconnectors for up to 40 equivalent years of GEO thermal cycling and over 10 equivalent years of LEO thermal cycling.

In a typical 2 x 4 cm cell module, two interconnectors are soldered to the negative contacts of each cell; thereafter, they are soldered to the positive contact of the next cell in series. This provides for redundant cell-to-cell connections.

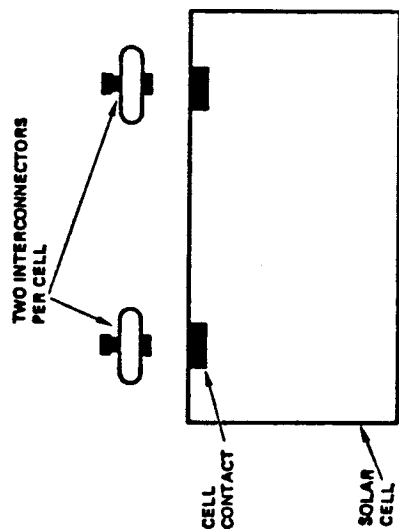
3.3.3 Circuitry Layout

In order to assess the importance of cell layout efficiency on the array design, three separate layouts were examined corresponding to three different aspect ratio wings. These layouts are illustrated in Figures 3-41 to 3-43. Each wing was sized to carry the same 96 single cell parallel circuits to 360 cells in series. The 360 cells in series provided about 150 volts of EOL bus voltage. The cell size (2 x 4 cm) and cell spacing were maintained as a constant. Three additional ground rules were used in establishing each design:

1. The circuits were allowed to extend only half-way across each panel to stay within illumination uniformity of existing Xenon pulsed simulator equipment and to create left-hand and right-hand mirror-image circuits to aid in minimizing current-induced magnetic fields/torques.
2. An even number of substrings were used to further aid in magnetic cancellation and to allow all circuit terminations to occur at the outer edge of the panel where the electrical harness is located, thereby reducing the complexity of panel wiring.
3. About 19 mm (0.75 inch) of space was not covered by solar cell stacks in the vicinity of the hinge lines.

The two extreme aspect ratio blankets (2.4 and 8.5) resulted in efficient layouts whereby four or two 360-cell circuits fit on each panel. Thus, the solar panel assembly (SPA) could be any number of odd number of panels (odd number to keep the piano hinges from all stacking up on one side of the folded blanket). The intermediate aspect ratio blanket required a slightly more complex layout in which eight 360-cell circuits fit on three panels, with jumpers in the electrical harness being required to continue a 360-cell circuit across a hinge line. This layout constrained the SPA to three panels, if only one SPA configuration was desired. Also, the substrate material only was available in 1.5 m (60 inches) wide rolls, thereby limiting a "seamless" SPA substrate to three panels, with each panel about 0.38 m (15 inches) wide.

When the three-wing layout designs were compared, it was found that the differences in layout efficiency among the options were small and outweighed by



- 25 μM THICK SILVER PLATED INVAR (TOTAL THICKNESS OF $\approx 45 \mu\text{M}$)
- COMPLIANT EXPANSION LOOPS
- FRONT CONTACT JOINT SANDWICHED BETWEEN CELL AND COVER GLASS
- COMPATIBLE WITH BOTH SOLDERING AND WELDING
- EXTENSIVE THERMAL CYCLE TESTING UNDER THW IRAD AND JPL CONTRACT

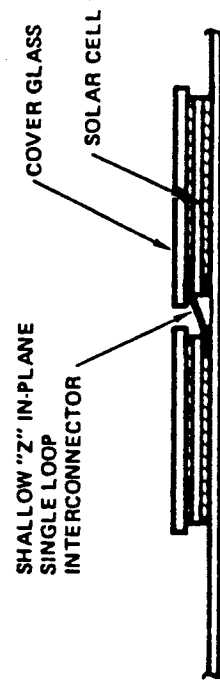
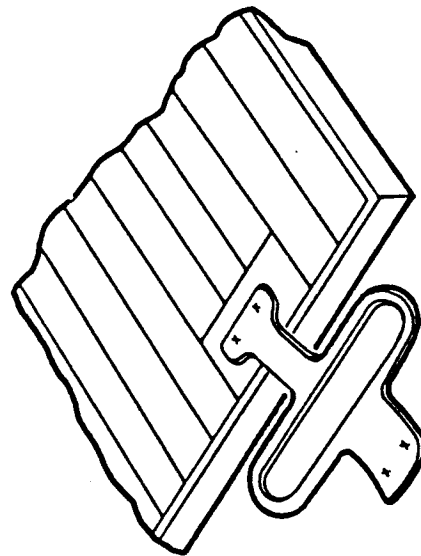
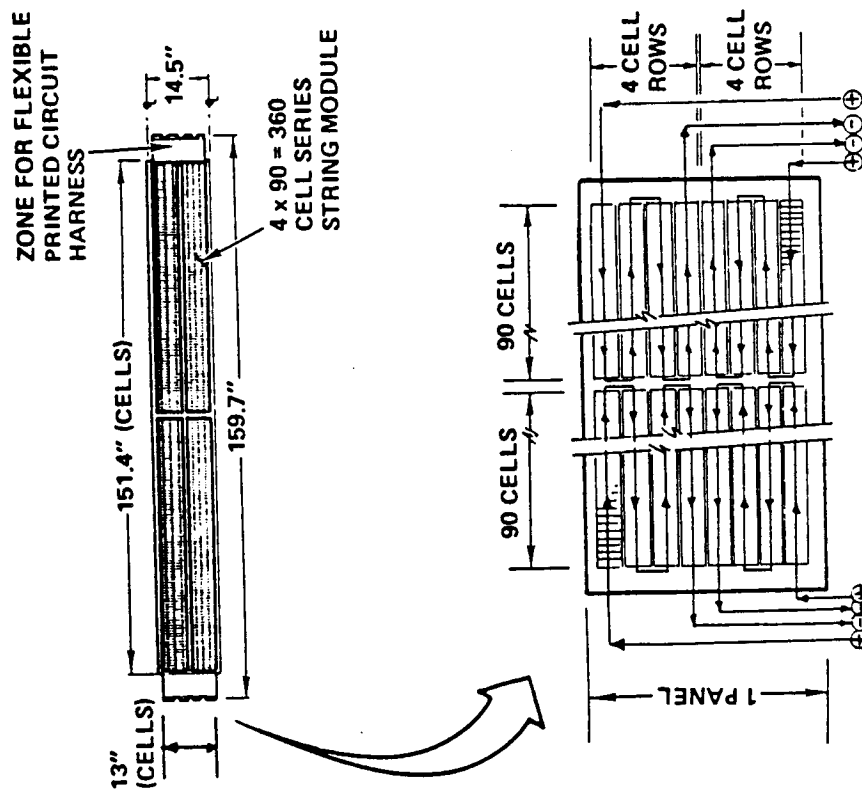


Figure 3-40. In-Plane Single Loop Discrete Interconnector



DESIGN FEATURES	DESIGN RATIONALE
8 x 180 CELLS PER PANEL = 1440 CELLS	<ul style="list-style-type: none"> • MAXIMIZE PACKING FACTOR • INTEGER NUMBER FOR CIRCUITS
2 x 4 CM 2 MIL THIN CELLS	<ul style="list-style-type: none"> • MINIMIZE CELL STACK WT • MAX SIZE FOR THIN CELLS
360 CELLS IN SERIES	PROVIDE 176 V (BOL) AND 150 V (EOL)
4 ELECTRICAL CIRCUIT MODULES PER PANEL	DRIVEN BY NUMBER OF CELLS PER CIRCUIT
96 ELECTRICAL CIRCUIT MODULES PER BLANKET	DRIVEN BY WING NOMINAL POWER REQUIREMENT
LAYOUT CANCELS CURRENT-INDUCED MAGNETIC FIELDS	MINIMIZE EFFECTS ON EXPERIMENT PACKAGES AND ATTITUDE CONTROL

Figure 3-41. Blanket Circuit Configuration, Wing Aspect Ratio = 2.40 (BOL/EOL Wing Power = 4800/3500 Watts for 24-Cell-Covered Panel Wing)

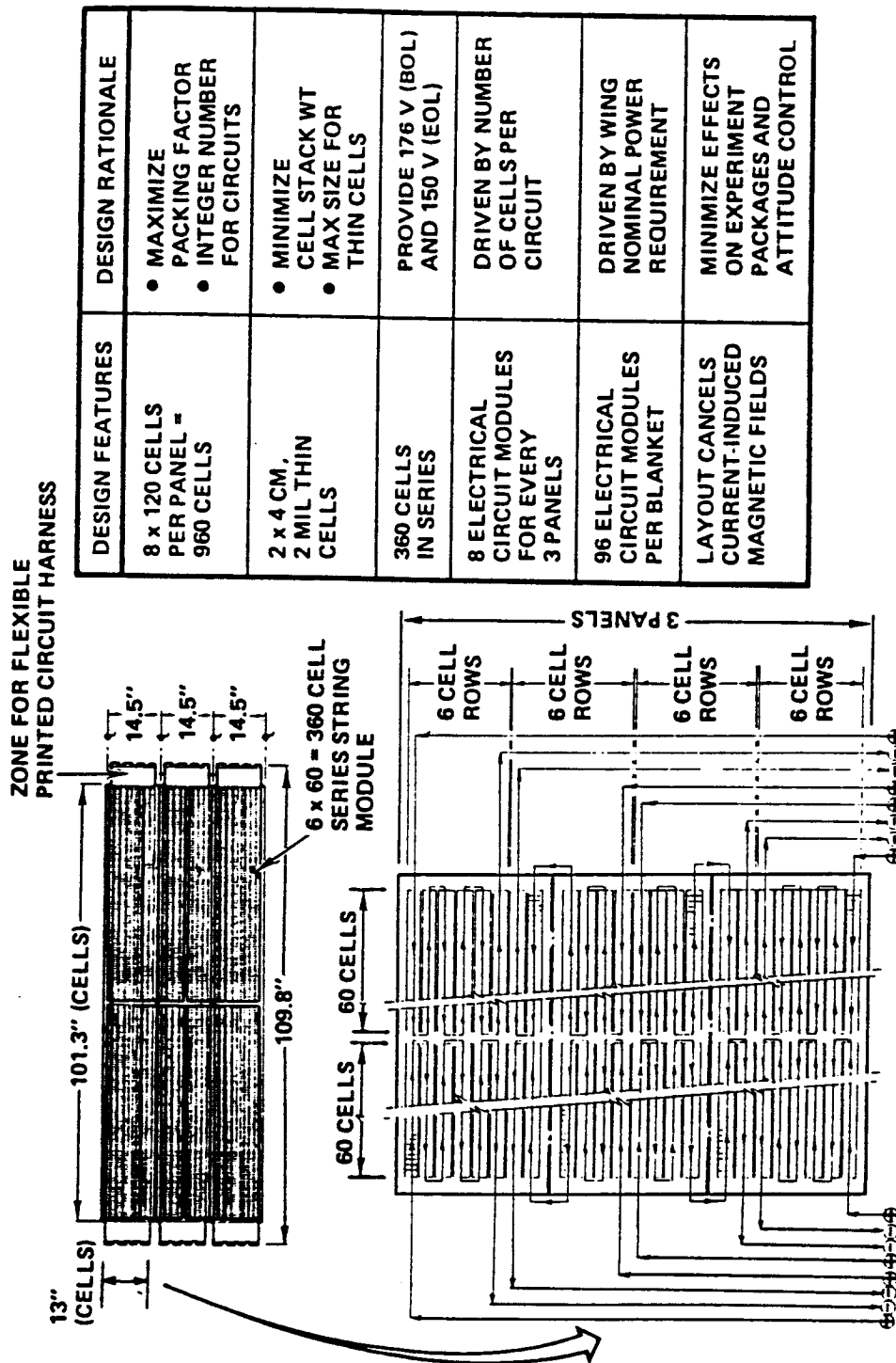


Figure 3-42. Blanket Circuit Configuration, Wing Aspect Ratio = 5.0 (BOL/EOL
Wing Power = 4800/3500 Watts for 36-Cell-Covered Panel Wing)

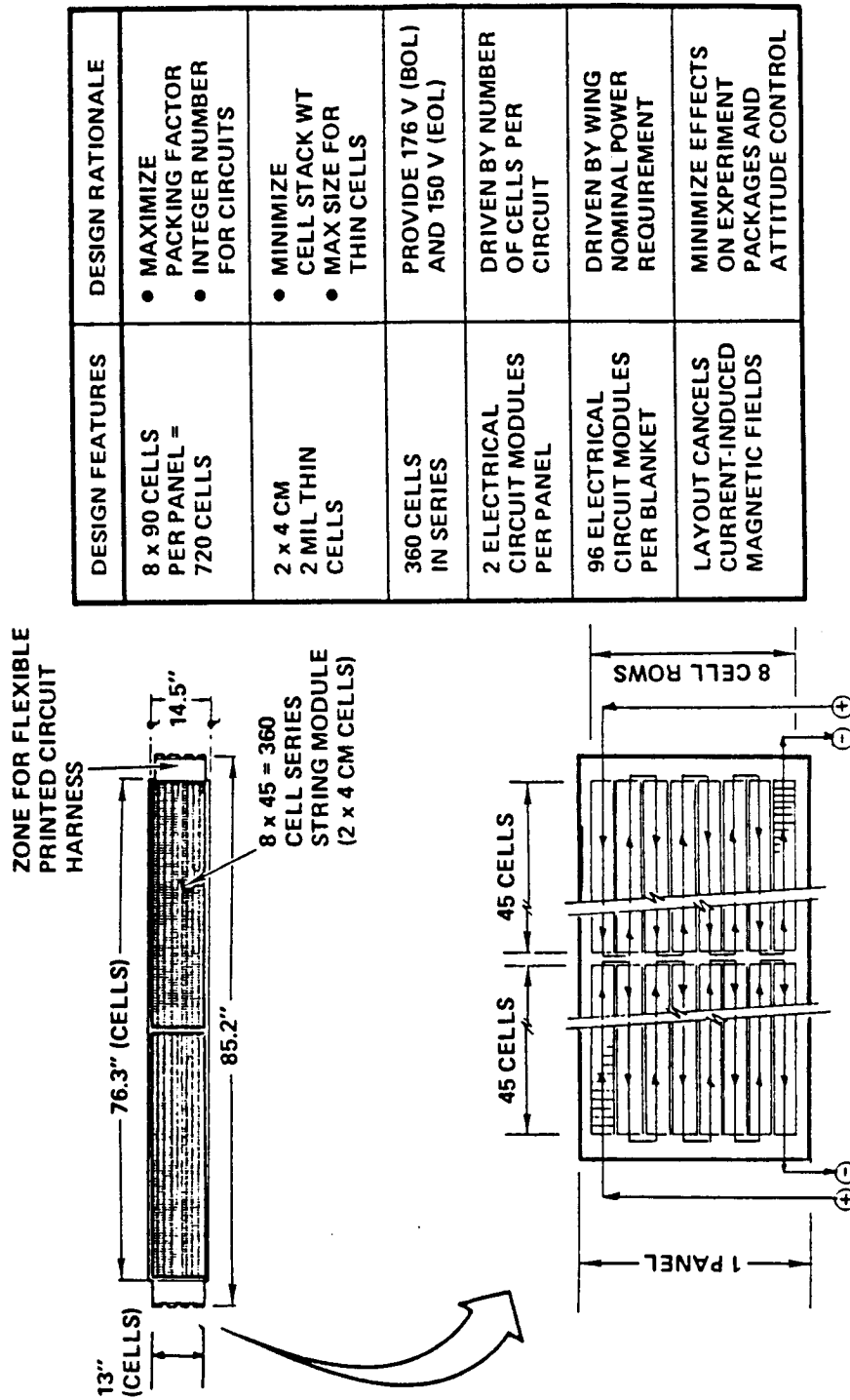


Figure 3-43. Blanket Circuit Configuration, Wing Aspect Ratio = 8.5 (BOL/EOL Wing Power = 4800/3500 Watts for 48-Cell-Covered Panel Wing)

the need to balance other factors such as the structural weight of the mast and blanket housing assembly. Therefore, the intermediate aspect ratio wing was selected, with its slightly more complicated circuitry because the weight of the intermediate aspect ratio wing was less than the other extreme aspect ratio wings, and the specific power performance was correspondingly greater.

3.3.4 Blanket Electrical Harness

The electrical harness had to meet certain requirements. These were: (a) producible by standard manufacturing processes; (b) can be integrated to the blanket assembly without complex fixturing; (c) conducive to low weight and minimization of blanket area required for its installation; (d) compatible with the folding, protection, and deployment of the blanket assembly; and (e) compatible with the long-term space environment.

Several trades were performed to develop a viable approach for the harness design. All trades were done with reference to the three aspect ratio wings illustrated in Figure 1-2. The trades dealt with the following issues and options:

1. Construction type (flexible printed circuit versus laminated flat ribbon conductors)
2. Conductor material (copper versus aluminum)
3. Voltage drop (percentage range consistent with minimum gage conductors, power density and weight)
4. Location (located along the blanket edges or distributed over the blanket substrate)
5. Fabrication (single ply versus multiple plies; one continuous run or segmented into shorter runs and spliced together)

Based on past experience and the design characteristics of other array components, certain aspects of the harness design were quickly resolved. Kapton was assumed to be the insulation material, based on its combination of excellent mechanical/electrical properties and space radiation-resistant qualities. Since the stack height of the solar cell module (exclusive of the adhesive to bond it to the blanket substrate) was about 165 μm (6.5 mils) and the thickness range of the harness conductor material and insulation material ranged from 38 to 76 μm (1.5 to 3 mils), it became apparent that only a one-ply harness would be compatible with the stowage of the blanket assembly. Since the blanket assembly was going to be composed of several three-panel SPA units that would subsequently be integrated together to form the total blanket, the harness would be made in segments and spliced together rather than made in one continuous run. The decision to use spliced harness segments was also more conducive to fabricating the harness as well as installing it afterwards on the blanket. Finally, distributing the harness across the blanket width was dropped in favor of locating the harness along the blanket edges because the harness width in a single ply was not that excessive (about 50 to 100 mm [2 to 4 inches]) and termination with the solar cell circuits would be easier.

Table 3-13 summarizes the results of the key trades. Data is presented that indicates the effect of construction type, wing aspect ratio, voltage drop, and

Table 3-13. Summary of Electrical Harness Design Trades

CONSTRUCTION METHOD	WING ASPECT RATIO	VOLTAGE DROP (%)	CONDUCTOR MATERIAL	HARNESS RUN WIDTH (PER RUN) (IN.)	WING HARNESS WEIGHT (2 RUNS) (LB)	ADHESIVE WEIGHT (2 RUNS) (LB)	TOTAL WING HARNESS WT (LB)	BOL WING SPECIFIC* POWER (W/KG)
LAMINATED (6.5 MIL THK)	2.36	2.5	ALUMINUM 35 MIL THK NOS. 28 TO 30 AWG	3.8	0.85	0.35	1.20	134.4
	5.00	2.5		3.9	1.10	0.50	1.60	139.0
	8.50	2.5		4.1	1.55	0.75	2.30	129.9
	2.36	4.0		3.8	0.85	0.35	1.20	131.0
	5.00	4.0		3.9	1.05	0.50	1.55	135.7
	8.50	4.0		4.1	1.30	0.75	2.05	127.1
	2.36	2.5	COPPER 35 MIL THK NOS. 28 TO 30 AWG	3.8	1.85	0.35	2.20	131.4
	5.00	2.5		3.8	2.20	0.50	2.70	137.0
	8.50	2.5		3.8	2.75	0.70	3.45	128.1
	2.36	4.0		3.8	1.85	0.35	2.20	128.1
	5.00	4.0		3.8	2.20	0.50	2.70	133.6
	8.50	4.0		3.8	2.75	0.70	3.45	124.9
PRINTED CIRCUIT (5.7 MIL THK)	2.36	2.5	COPPER 2.7 MIL THK NOS. 30 TO 36 AWG	2.3	1.20	0.20	1.40	133.7
	5.00	2.5		3.2	1.80	0.40	2.20	138.4
	8.50	2.5		3.6	2.70	0.60	3.30	128.5
	2.36	4.0		1.9	0.95	0.20	1.15	131.1
	5.00	4.0		2.4	1.40	0.30	1.70	136.4
	8.50	4.0		2.5	1.90	0.40	2.30	127.7

*INCLUDES EFFECTS ON LID, BLANKET AND PALLET WEIGHT DUE TO HARNESS WIDTH DIFFERENCES

conductor material on the critical harness characteristics of weight and width and the corresponding impact on wing specific power. The major observation was that the harness weight and width were surprisingly small; thus there were no design options that would result in significant improvement in specific power or power density. The key results from the trades were as follows:

1. The printed copper circuit design was narrower than the laminated designs because of the ability to more tightly control the laydown of the conductors by use of the photoresist process for making the printed circuit design. This results in better power density performance. The copper printed circuit design also weighed less than the equivalent design in laminated copper and almost the same as the aluminum conductor laminated design. Thus, the flexible printed circuit harness was preferred.
2. The use of aluminum over copper only makes sense if a laminated harness is used. Since aluminum can't be used in the printed circuit approach, and the printed circuit approach leads to better power density and specific power performance, copper was selected as the baseline conductor material in the printed circuit format.
3. The low aspect ratio wing resulted in the lighter harness weight; however, other aspects of the wing design resulted in the better specific power performance for an aspect ratio near 5.0.
4. The difference in harness weight (for a given aspect ratio and construction method) between 2.5 and 4 percent voltage drop was small; in some cases minimum gage issues for the conductors resulted in the same harness weight for the two voltage drop conditions considered. Minimum gage issues for the conductors precluded consideration of any higher voltage drop values.
5. A 2.5 percent voltage drop led to a slightly heavier harness; however, the 2.5 percent design resulted in better wing specific power performance because the relative wing power output (in comparison to the 4 percent design) was greater for the 2.5 percent design, thus offsetting the weight increase. The added harness width for the 2.5 percent design resulted in only a small impact on power density performance. Thus, because of specific power performance, the 2.5 percent voltage drop was selected as the conductor baseline sizing parameter.

The main concern with the decision to use a flexible printed copper circuit harness was the length of harness producible using conventional processes. Discussion with harness suppliers led to the conclusion that flexible printed copper circuit harnesses could be obtained in lengths up to about 1.2 to 1.5 m (48 to 60 inches). This was compatible with the requirements for the three-panel SPA and inboard termination segment of the harness.

The use of a single ply harness using 1-ounce (35 μm [1.4 mil] thick) copper conductors results in a harness thickness of about 150 μm (6 mils) when the adhesive and Kapton insulation is included. The use of 2-ounce (69 μm [2.7 mil] thick) copper conductors results in a harness that is slightly thicker than the

solar cell module (see Figure 3-44). The 2-ounce copper conductor was selected as the preferred thickness because of greater structural integrity characteristics at the joints.

The use of "cusp" folds in the harness run at the blanket assembly hinge-lines was selected to ensure adequate flexibility and differential growth between the blanket and harness (see Figure 3-45). Prior experience had shown that a flexible printed copper circuit harness could be crease-folded to create the "cusp" without delamination or fracture of the copper conductors.

3.3.5 Circuit Protection

The most familiar form of electrical circuit protection is the use of isolation diodes. These devices are usually silicon power rectifiers. The isolation diodes prevent forward bias damage of the cells in a string when and if their junctions are so biased by the main bus. These devices afford protection against two solar cell circuit failure modes. They are necessary to implement a shunt voltage limiter, and serve to protect the cells and the shunting device. They also prevent the solar array from loading the main spacecraft bus when it is not illuminated. The trade-off is between the level of redundancy and the performance penalty associated with the design approach. Series and parallel redundancy is more reliable, but causes more power loss and increased weight.

The approach adopted was to use single, non-redundant isolation diodes between each string and the common bus. The diodes are used in a highly derated manner to provide high reliability. This fact, combined with the quantity of individual circuits (≈ 100 circuits per 5 kW wing), provide array-level reliability.

The diodes are colocated in a small box (or boxes) which is attached to the pallet structure at the inboard end of each blanket electrical harness run. The box is thermally efficient and serves as the transition point between the flexible printed blanket harness and the stranded round wire harness leading to the spacecraft. This is conceptually shown in Figure 3-46.

The thermal design of the box relies on heat conduction through the diode leads, to the flat conductors through the insulators, the wall thickness of the box and into the facesheet of the pallet panel. This facesheet acts as a radiator for the heat. Also, the heat is conducted and radiated to the cover of the box and radiated out its front face. The design incorporates as few layers of insulation between the diodes and the radiators as are necessary to ensure electrical isolation. The box wall thickness is selected by trading off the lateral conductivity to reduce temperature gradients and the mass of the resultant container. The diode packing density (box footprint/size) and the resultant heat flux is traded off against the conductivity (wall thickness) to determine the optimum box size.

The use of bypass diodes was not evaluated in this study since: (1) a design ground rule was that there were no shadows on the solar cell side of the blanket assembly; and (2) the selection of single cell parallel circuits alleviated the need to protect the circuits against "hot spot" failure propagation when a single cell module fails. In a circuit with parallel cells, a failure in one of the cell modules drives the cells in parallel into reverse in order to pass the total circuit current and causes them to dissipate power (and generate

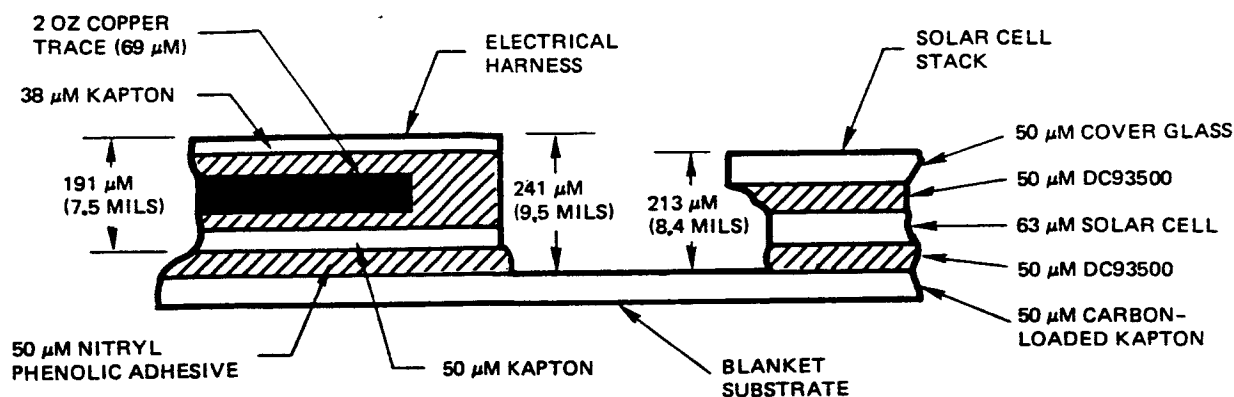


Figure 3-44. Comparative Thickness of Solar Cell Module and Flexible Printed Circuit Electrical Harness Using 1-Ounce Copper

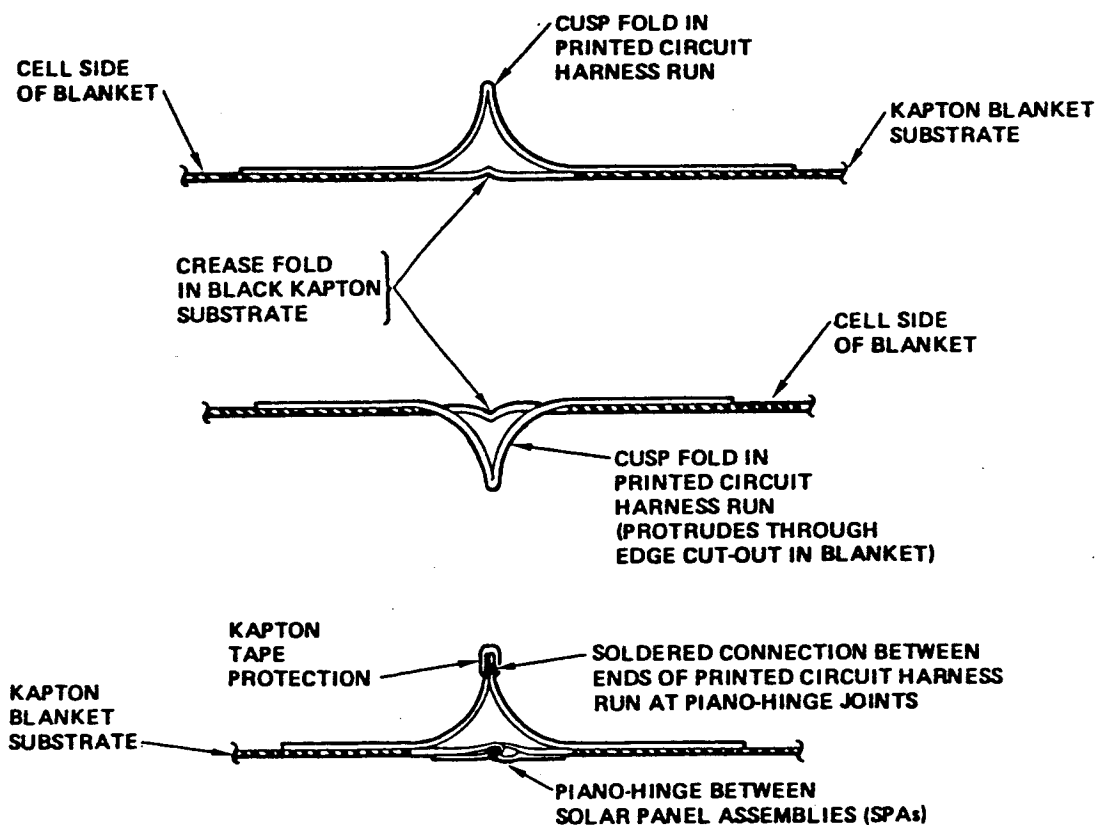
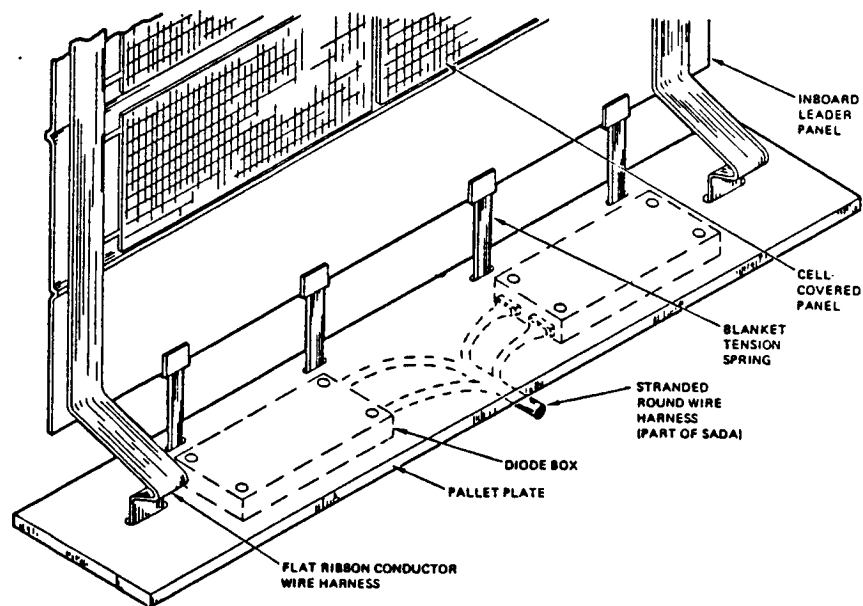
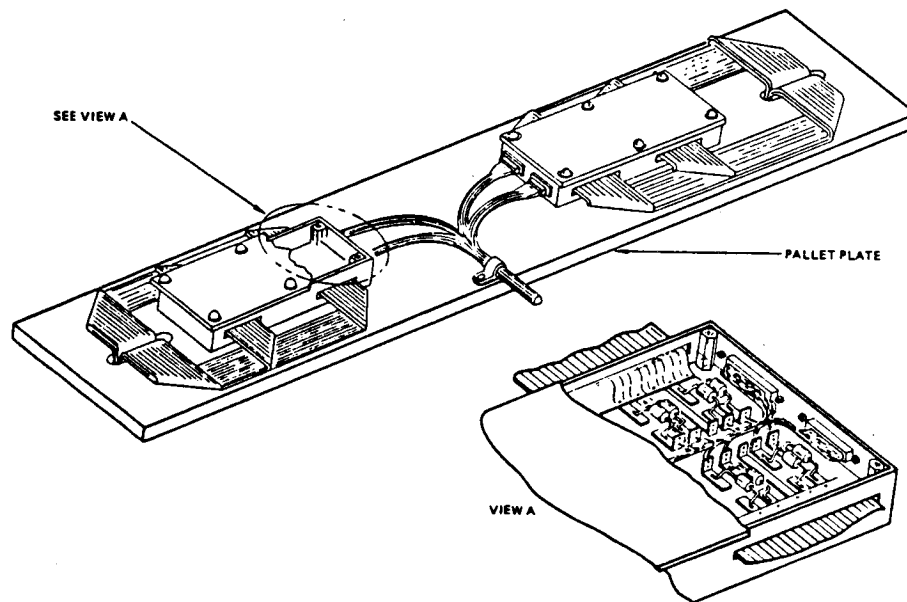


Figure 3-45. Harness Hinge and Splice Details



a. Top View of Pallet



b. Bottom View of Pallet

Figure 3-46. Conceptual Arrangement of Diode Box/
Blanket Harness/SADA Harness Interface

hotspots). These overstressed cells then begin to fail, and each failure will increase the over-stress on the remaining cells, which in turn accelerates the individual failures until the entire multiple parallel circuit fails.

Should the need arise to design for shadowing, the impact of implementing bypass diodes can be minimized by employing flat packaged diodes on the panels in the 19 mm (0.75 inch) wide zone adjacent to the hingelines near their intended circuit bypass location. Such an implementation would increase weight slightly, add complexity to the wiring layout, potentially impact reliability, reduce circuit granularity (i.e., the total number of circuits would be decreased), possibly lower panel packing factor, and reduce power density.

Since the implementation of bypass diodes would eliminate hotspot failure propagation in parallel cells, the number of bypass diodes could be reduced by using multiple parallel cells (or cross-strapping individual circuits at 10 to 15 cell intervals) to create small series/parallel modules, each protected by a single diode. An example of this paralleling would be to change the layout of a single panel (for the wing aspect ratio of 5 case) to four rows of cells in parallel running side-by-side with cross-straps across each 10 cells in series to create a module. The four-row circuit would turn around at the centerline of the panel and return to the same panel edge for a total of 4p x 120s. Connecting three panels in series would create a SPA with two circuits per three panels with each circuit having 4p x 360s cells. Thus, in a 12-SPA blanket, the number of 4p x 360s circuits would be 24 rather than 96 for the baseline single cell parallel circuit (1p x 360s, eight circuits per three-panel SPA). Thus, the circuit granularity would be reduced significantly. Now if one of the 4p x 360s circuits completely failed, about 4 percent of the power would be lost as opposed to about 1 percent of the power if one of the 1p x 360s circuits were completely failed. To implement this four-row parallel circuit example, a series of ribbon bus bars with stress relief loops would run along one side of each four-row group in the 19 mm (0.75 inch) space adjacent to the hingeline. The flat pack diode would be integrated to the ribbon to bypass each module as shown in Figure 3-47. The impact on overall panel packing factor is probably very small as would be the increase in weight due to the diodes, parallel interconnector ribbons, and bypass ribbon bus bars.

3.3.6 Environmental Interactions

The natural space environment consists of geomagnetically trapped energetic particles, solar flare and wind energetic particles, galactic cosmic rays, direct solar electromagnetic radiation (gamma rays, ultraviolet, infrared, microwave), reflected solar radiation (albedo) from the earth, emitted radiation (infrared) from the earth, vacuum, and atomic oxygen (at LEO missions only). For the baseline design at geosynchronous (GEO) orbits, the earth-related components of the environment are not a concern. The degradation of materials and reduction in power output due to the trapped and solar energetic particles, ultraviolet, and infrared radiation were considered straightforward issues that could be accommodated with proven techniques from past GEO spacecraft experience. The main issue addressed during the preliminary design phase was associated with electrostatic charging and the need (and associated design requirements) to mitigate the discharging from such a phenomenon.

A charging analysis was done using NASCAP (NASA Charging Analyzer Program) to determine the extent of this charging in a moderate and severe substorm

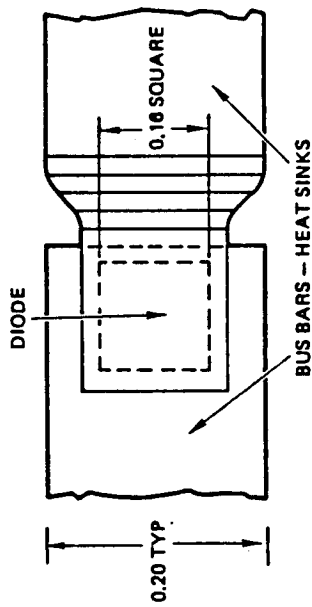
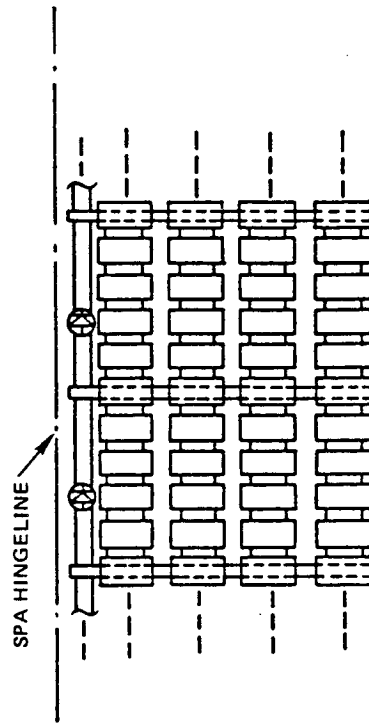
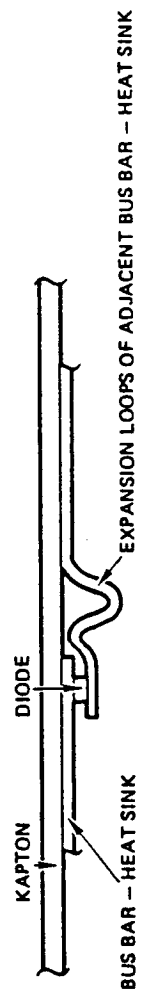


Figure 3-47. Conceptual Implementation of Flatpack Bypass Diodes for Shadow Protection on Panel Layout

environment (Table 3-14). Figure 3-48 shows the NASCAP model of the APSA wing. We anticipated grounding the blanket substrate to electrical ground so the maximum potential difference across the substrate would be the operating voltage of the wing. The problem can occur in substorm environments where each surface will collect a charge at a different rate and when a threshold voltage is exceeded, an arc will occur causing a transient into the power system.

In order to prevent arcing, conductive surface materials must be used and proper grounding techniques incorporated. Every effort was made in this program to use sufficiently conductive materials ($<10^{-9}$ Ω/\square surface resistivity) and to use proper grounding techniques.

Figures 3-49 and 3-50 show the output of the NASCAP analysis. Figure 3-49 is the response for a moderate substorm and Figure 3-50 is the response for a severe substorm. The results for the moderate substorm case indicate that charging is negligible; thus no charging problems are anticipated. The severe substorm condition lasts 5 to 6 minutes. As can be seen in Figure 3-50, the solar cell coverglass and laminated flexible printed circuit harness will charge positive with respect to the carbon-loaded Kapton blanket substrate. This could generate low-level arcs which is common in current solar arrays and does not appear to significantly impact the power system performance. No serious effect is anticipated from this differential charging for the APSA design.

For the severe substorm condition, the cover glass does not need to be grounded; however, the blanket substrate (including the rear surface of the electrical harness), deployment mast, and blanket housing structure surface must be grounded. To ground the carbon-load Kapton blanket substrate, provisions have been incorporated in the electrical harness to include grounding tabs that are part of the negative copper traces. There will be a total of two grounding tabs (one from each harness run) for each blanket panel. The tab is connected to the substrate with flexible conductive adhesive. For the mast elements either metallic wires will be embedded into the fiberglass longerons/ battens or the elements will be coated with a semiconductive dielectric. The surfaces of the lid, pallet and other exposed graphite/epoxy structure are partially conductive and will be grounded by directly bonding grounding circuits to these surfaces and/or a semiconductive dielectric coating will be used to improve the conductive quality of the surfaces. The mast canister is constructed from aluminum. Its grounding is considered straightforward. If a thermal insulation blanket is used to cover the outer exposed surfaces of the lid, pallet and mast canister structure, then provisions will be made to ground the thermal insulation blanket as is now done on current spacecraft.

3.4 WEIGHT TRENDS

Tables 3-15 through 3-17 present the wing weight breakdown for the three aspect ratio wings analyzed. The designs use similar thin silicon solar cell modules. The blanket deployment mast assembly was sized to provide about 0.01 g deployed strength and 0.1 Hz deployed frequency characteristics. The weights for the blanket substrate, hinges, electrical harness, and blanket housing assembly were derived from preliminary sizing and known material densities, based on structural, dynamic, and electrical analyses. The weights for the blanket deployment mast system were obtained from the mast subcontractors based on their

Table 3-14. GEO Space Plasma Environments (Reference 7)

	<u>MODERATE</u>	<u>SEVERE</u>
ELECTRON DENSITY (M^{-3})	4.16×10^5	1.30×10^6
ELECTRON TEMPERATURE (KEV)	9.25	22.0
ION DENSITY (M^{-3})	1.25×10^6	1.27×10^6
ION TEMPERATURE (KEV)	19.0	42.0
DURATION (MINUTES)	15	6

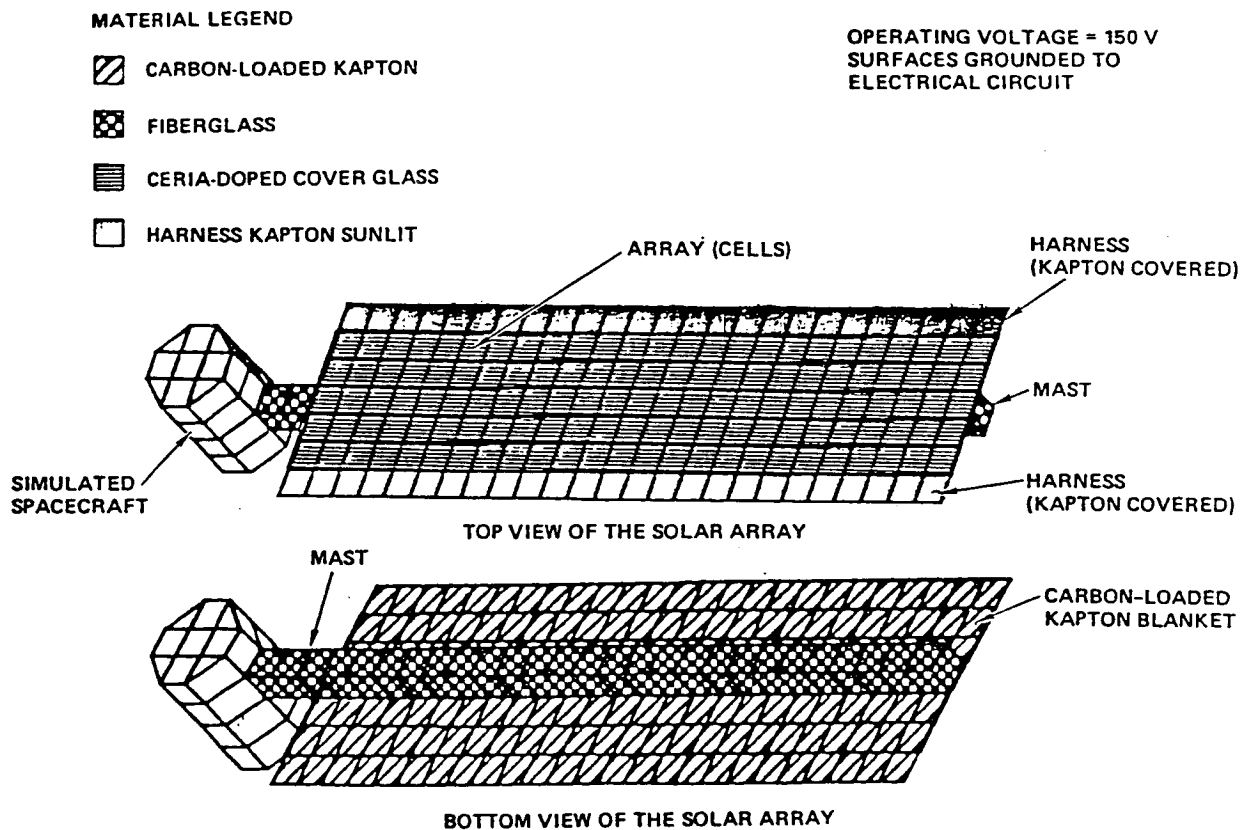


Figure 3-48. NASCAP Array Charging Analysis Model

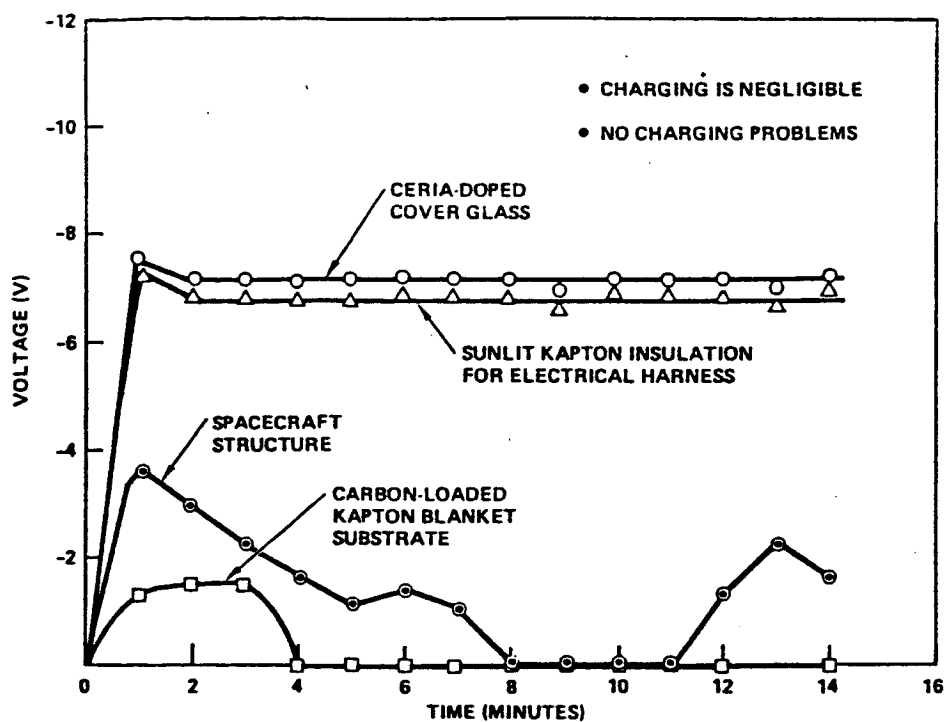


Figure 3-49. Negative Voltages Computed Under Moderate GEO Substorm Environment (Sunlight Charging)

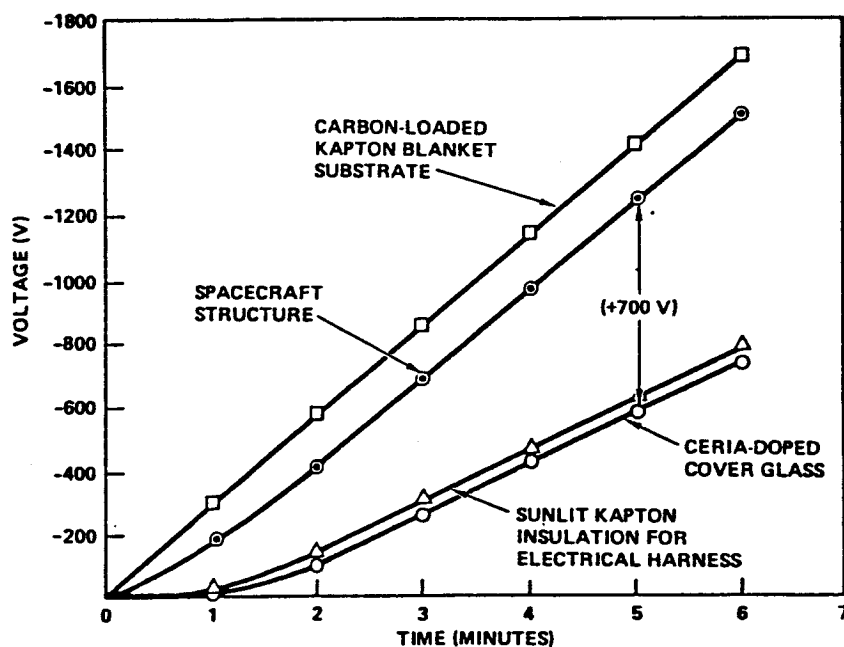


Figure 3-50. Negative Voltages Computed Under Severe GEO Substorm Environment (Sunlight Charging)

Table 3-15. Wing Weight Summary, BOL/EOL Power of 4800/3500 Watts,
 $F_N = 0.15$ Hz, $N = 0.012$ g, 2.36 Wing Aspect Ratio

● BLANKET ASSEMBLY (24 CELL-COVERED AND 2 LEADER PANELS; 1 BLANKET)	35.1 LB
SUBSTRATE (2 MIL CARBON-LOADED KAPTON, 200XA-C37)	5.3
HINGE ASSEMBLIES (5 PIANO HINGES)	0.2
HINGE REINFORCEMENTS (NYLON RIPSTOP)	0.3
SOLAR CELL (2.5 MIL; 2 X 4 CM, B-BSF/AL-BSR, POLISHED, AT 162 MG/CELL)	12.4
CELL-TO-SUBSTRATE ADHESIVE (2 MIL DC 93500)	3.3
COVER GLASS (2 MIL CMX, COATED AT 106 MG/COVER)	8.1
COVER GLASS ADHESIVE (2 MIL DC 93500)	3.3
INTERCONNECTORS (1 MIL AG-PLATED INVAR)	0.8
ELECTRICAL HARNESS (2 OZ CU, PRINTED CIRCUIT)	1.2
HARNESS ADHESIVE (2 MIL RTV 142)	0.2
● BLANKET HOUSING ASSEMBLY (1 PER WING)	30.0 LB
LID STRUCTURE (0.5 INCHES SANDWICH, 10 MIL G/E F/S)	7.4
PALLET STRUCTURE (0.5 INCHES SANDWICH, 10 MIL G/E F/S)	7.4
PROTECTIVE FOAM (2 LAYERS, 0.5 INCHES EACH, TA-301 POLYIMIDE)	0.8
BLANKET PRELOAD MECHANISM (8 LATCH SYSTEMS)	4.6
BLANKET TENSION SYSTEM (7 NEGATORS AT 1 POUND TENSION EACH)	0.7
BLANKET GUIDEWIRE SYSTEM (2 WIRES AT 1 POUND TENSION EACH)	2.1
LID/PALLET-TO-MAST ATTACHMENT	2.2
WING TIEDOWN FITTINGS	2.2
DIODE BOXES	2.6
● BLANKET DEPLOYMENT ASSEMBLY (COILABLE F/G LATTICE MAST)	6.6 LB
MAST (F/G; 6.6"φ, EI = 1.4 X 10 ⁶ LB-IN ²)	4.0
MAST CANISTER (G/E, 19.3"H X 7.0"φ)	2.3
MOTOR ACTUATOR	0.3
	WITHOUT CONTINGENCY
	10% CONTINGENCY
	TOTAL WING WEIGHT
	71.7 LB (32.5 KG)
	7.2 LB
	78.9 LB (35.8 KG)

BOL SPECIFIC POWER = 133.7 W/KG
 EOL SPECIFIC POWER = 97.5 W/KG

Table 3-16. Wing Weight Summary, BOL/EOL Power of 4800/3500 Watts,
 $F_N = 0.12$ Hz, $N = 0.011$ g, 5.0 Wing Aspect Ratio

• BLANKET ASSEMBLY (36 CELL-COVERED AND 2 LEADER PANELS; 1 BLANKET)	35.9 LB
SUBSTRATE (2 MIL CARBON-LOADED KAPTON, 200XA-C37)	5.3
HINGE ASSEMBLIES (7 PIANO HINGES)	0.2
HINGE REINFORCEMENTS (NYLON RIPSTOP)	0.3
SOLAR CELL (2.5 MIL; 2 X 4 CM, B-BSE/AL-BSR, POLISHED, AT 162 MG/CELL)	12.4
CELL-TO-SUBSTRATE ADHESIVE (2 MIL DC 93500)	3.3
COVER GLASS (2 MIL CMX, COATED, AT 106 MG/COVER)	8.1
COVER GLASS ADHESIVE (2 MIL DC 93500)	3.3
INTERCONNECTORS (1 MIL AG-PLATED INVAR)	0.8
ELECTRICAL HARNESS (2 OZ CU, PRINTED CIRCUIT)	1.8
HARNESS ADHESIVE (2 MIL RTV 142)	0.4
• BLANKET HOUSING ASSEMBLY (1 PER WING)	24.0 LB
LID STRUCTURE (0.5 INCH SANDWICH, 10 MIL G/E F/S)	5.1
PALLET STRUCTURE (0.5 INCH SANDWICH, 10 MIL G/E F/S)	5.1
PROTECTIVE FOAM (2 LAYERS, 0.5 INCH EACH, TA-301 POLYIMIDE)	0.6
BLANKET PRELOAD MECHANISM (6 LATCH SYSTEMS)	3.8
BLANKET TENSION SYSTEM (10 NEGATORS AT 1 POUND TENSION EACH)	1.0
BLANKET GUIDEWIRE SYSTEM (2 WIRES AT 1 POUND TENSION EACH)	2.2
LID/PALLET-TO-MAST ATTACHMENT	2.0
WING TIEDOWN FITTINGS	1.6
DIODE BOXES	2.6
• BLANKET DEPLOYMENT ASSEMBLY (COILABLE F/G LATTICE MAST)	9.4 LB
MAST (F/G; 72" ϕ , EI = 1.9×10^6 LB-IN ²)	6.4
MAST CANISTER (G/E, 23.6" H X 7.6" ϕ)	2.7
MOTOR ACTUATOR	0.3
WITHOUT CONTINGENCY	59.3 LB (31.4 KG)
10% CONTINGENCY	6.9 LB
TOTAL WING WEIGHT	76.2 LB (34.6 KG)

BOL SPECIFIC POWER = 138.4 W/KG
 EOL SPECIFIC POWER = 100.9 W/KG

Table 3-17. Wing Weight Summary, B0L/E0L Power of 4800/3500 Watts,
 $F_N = 0.11$ Hz, $N = 0.012$ g, Wing Aspect Ratio of 8.5

<ul style="list-style-type: none"> ● BLANKET ASSEMBLY (48 CELL-COVERED AND 2 LEADER PANELS; 1 BLANKET) 		37.1 LB
<ul style="list-style-type: none"> <ul style="list-style-type: none"> SUBSTRATE (2 MIL CARBON-LOADED KAPTON, 200XA-C37) HINGE ASSEMBLIES (9 PIANO HINGES) HINGE REINFORCEMENTS (NYLON RIPSTOP) SOLAR CELL (2.5 MIL; 2 X 4 CM, B-BSF/AL-BSR, POLISHED, AT 162 MG/CELL) CELL-TO-SUBSTRATE ADHESIVE (2 MIL DC 93500) COVER GLASS (2 MIL CMX, COATED, AT 106 MG/COVER) COVER GLASS ADHESIVE (2 MIL DC 93500) INTERCONNECTORS (1 MIL AG-PLATED INVAR) ELECTRICAL HARNESS (2 OZ CU, PRINTED CIRCUIT) HARNESS ADHESIVE (2 MIL RTV 142) ● BLANKET HOUSING ASSEMBLY (1 PER WING) 	5.3 0.3 0.3 12.4 3.3 8.1 3.3 0.8 2.7 0.6 4.0 4.0 0.4 3.0 1.4 3.2 1.8 1.4 2.6	21.8 LB
<ul style="list-style-type: none"> ● BLANKET DEPLOYMENT ASSEMBLY (COILABLE F/G LATTICE MAST) 		15.7 LB
<ul style="list-style-type: none"> <ul style="list-style-type: none"> MAST (F/G; 8.4"φ, EI = 3.6 X 10⁶ LB-IN²) MAST CANISTER (G/E, 30"H X 9.0"φ) MOTOR ACTUATOR 	11.4 4.0 0.3	15.7 LB
<div style="border: 1px solid black; padding: 5px; display: inline-block;"> B0L SPECIFIC POWER = 128.5 W/KG E0L SPECIFIC POWER = 93.7 W/KG </div>		
WITHOUT CONTINGENCY		74.6 LB (33.8 KG)
10% CONTINGENCY		7.5 LB
TOTAL WING WEIGHT		82.1 LB (37.2 KG)

preliminary designs to meet the deployed strength and frequency requirements. Solar cell module weights were based on measurements of representative hardware components.

The blanket assembly weight accounts for about 50 percent of the total wing weight and is approximately independent of wing aspect ratio. The electrical components weight (solar cell module, electrical harness, diode boxes) represents approximately 45 percent of the total wing weight and is approximately independent of wing aspect ratio. The two major assemblies that are affected by wing aspect ratio are the blanket housing assembly and the blanket deployment mast assembly.

The data for the wing aspect ratio range investigated suggest that aspect ratio does not have a significant effect on wing weight. The results also show that the weight associated with the non-electrical elements of the wing is critical to the success of achieving significant improvements in specific power, since minimum gages/weights have been selected for most of the electrical components (i.e., thin cell modules, thin gauge blanket substrate, thin gauge electrical harness).

3.5 ARRAY PERFORMANCE TRENDS

3.5.1 Specific Power

Table 3-18 and Figure 3-51 present the preliminary results of BOL and EOL specific power performance as a function of key design parameters: aspect ratio, deployed frequency, deployed strength. The solid-line curves in Figure 3-51 represent the results for essentially a constant area (or constant power) blanket, whose geometry is altered in terms of length and width to obtain the range of aspect ratios. The dashed-line curves in Figure 3-51 represent results for larger area blankets (by adding additional SPAs), thereby containing more solar cell circuit modules and providing more power than the other blanket geometry represented by the solid-line curves.

Key results are as follows:

1. BOL specific power characteristics will be above the 130 W/kg goal. EOL specific power characteristics will be close to the goal of 105 W/kg for a 10-year GEO mission.
2. For a given blanket area (or number of solar cell modules and power output) and given stiffness/strength requirements, aspect ratio does not have a significant effect on array specific power (less than 10 percent difference in specific power over the aspect ratio range studied).
3. Based on Item 2, the wing width selected should be as wide as possible consistent with stowage limitations on the spacecraft or interference issues relative to other deployed appendages or sensor fields of view on the spacecraft.
4. For the design wing power level of 5 kW (BOL), an aspect ratio of 5 to 6 provides the highest specific power characteristics. The corresponding wing width of 2.8 to 3.0 m (110 to 120 inches) is compatible for stowage on typical sized spacecraft launch from the shuttle cargo bay (refer to Section 3.1, Figures 3-3 to 3-7).

Table 3-18. Specific Power Characteristics

	WING ASPECT RATIO	BOL WING POWER (WATTS)	EOL WING POWER (WATTS)	TOTAL BLANKET LENGTH (IN.)	TOTAL BLANKET WIDTH (IN.)	MAST** DIAMETER (IN)	DEPLOYED FREQUENCY (Hz)	DEPLOYED STRENGTH (GS)	WING WT WITH 10% CONTINGENCY (KG)	SPECIFIC POWER (W/KG)	
										BOL	EOL
CURVE ②	2.36	4783	3487	377	159.7	4.2	0.054	0.0010	33.8	142.0	103.5
	2.54*	5182	3778	406	159.7	~4.5	~0.05	~0.001	35.4	146.1	106.5
	5.00	4783	3487	551	109.8	6.0	0.065	0.0011	32.0	148.9	108.5
	5.33*	5182	3778	609	109.8	~6.4	~0.06	~0.001	34.0	151.9	110.7
CURVES ④ AND ⑤	8.50	4783	3487	725	85.2	7.2	0.058	0.0011	33.0	143.5	104.6
	9.19*	5182	3778	783	85.2	~7.7	~0.05	~0.001	35.0	146.1	106.5
	2.36	4783	3487	377	159.7	6.6	0.148	0.012	35.7	133.7	97.5
	2.54*	5182	3778	406	159.7	~7.1	~0.15	~0.01	37.7	137.2	100.0
CURVES ④ AND ⑤	5.00	4783	3487	551	109.8	7.2	0.123	0.011	34.5	138.4	100.9
	5.33*	5182	3778	609	109.8	~7.7	~0.12	~0.01	36.7	140.9	102.7
	8.50	4783	3487	725	85.2	8.4	0.108	0.012	37.0	128.5	93.7
	9.19*	5182	3778	783	85.2	9.0	~0.10	~0.01	39.5	130.3	95.0

*DATA IN THESE OPTIONS WERE EXTRAPOLATED FROM CORRESPONDING 4783-WATT WING DATA

**COILABLE, CONTINUOUS, TRI-LONGERON LATTICE MAST, CANISTER DEPLOYED

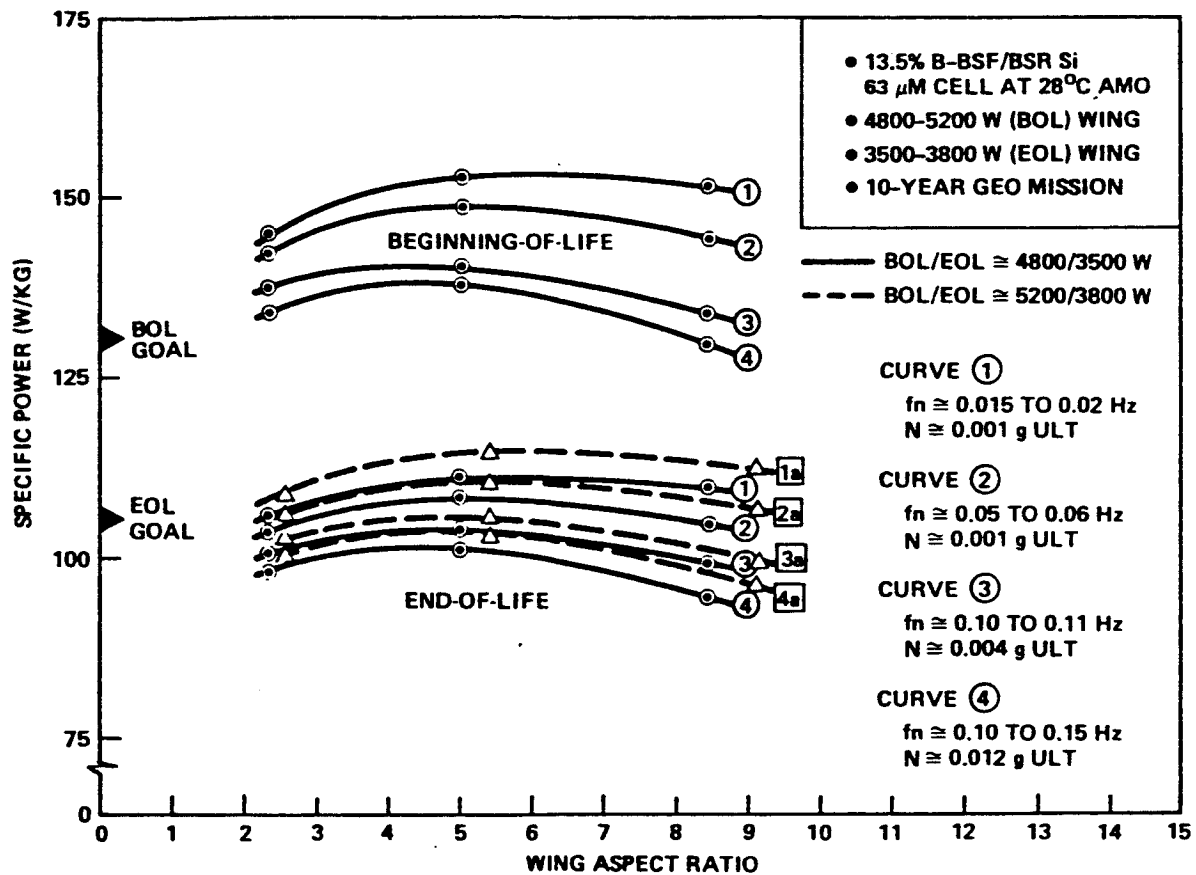


Figure 3-51. Effect of Key Array Design Parameters on Specific Power Performance

5. When adding more length to a blanket for a given width, the weight of the blanket housing assembly will not be affected; thus, the specific power will increase as array power increases.
6. The effect of increasing the strength/stiffness characteristics by an order-of-magnitude (i.e., from 0.001 g/0.01 Hz to 0.01 g/0.10 Hz) does not have a significant impact on specific power (10 to 15 percent variation).

3.5.2 Power Density

Table 3-19 presents the EOL power density characteristics for the wing configuration having an aspect ratio of about 5. The values range from about 90 to 115 W/m², depending on the referenced area used for the calculation. The lowest value is based on the total blanket area including the area of the electrical harness and the blank leader panels. The highest value is based on the area covered by a 360-cell group. The most reasonable reference area is that associated with a typical cell-covered panel, which includes all the area between the blanket edges and between adjacent panel hingelines. Therefore, a representative value for EOL power density is about 95 W/m², using the 10 Ω -cm, B-BSF/Al-BSR thin silicon solar cell module.

This value of 95 W/m² did not meet the program goal of 110 W/m² (EOL). The preliminary results were based on the best available solar cell type (consistent with meeting specific power goals) and a very high cell packing efficiency. Therefore, the ability to meet the power density EOL goal will depend upon development of an advanced, thin, low density solar cell module that has higher EOL conversion efficiency characteristics and operates at a lower temperature than the baseline solar cell module.

Table 3-19. EOL Power Density Performance Trends,
Thin Silicon Solar Cell Stack Array

BOL WING POWER (WATTS)	EOL WING POWER (WATTS)	NO. OF CELL COVERED PANELS PER WING	NO. OF BLANK LEADER PANELS PER WING	EOL POWER DENSITY (W/M ²)			
				BASED ON CELLED AREA IN PANEL	BASED ON PANEL AREA W/O HARNESS	BASED ON TOTAL PANEL AREA	BASED ON TOTAL BLANKET AREA
4783	3487	36	2	114.0	102.2	94.3	89.3
5182	3778	39	3	114.0	102.2	94.3	87.5

4. BASELINE DESIGN DEFINITION

Based on the results and trends obtained from the conceptual and preliminary design trades discussed in Section 3, a preferred array concept was selected and additional design details were developed for the various elements that comprised the array. Based on the details of the revised design, updated power, weight, strength, deployed frequency, specific power, and power density characteristics were calculated.

4.1 ARRAY CONFIGURATION

Figures 4-1 through 4-3 illustrate the deployed and stowed configuration of the 5.2 kW (BOL) wing. Overall deployed wing dimensions are 16.3 m (640 inches) long (from the inboard end of the mast canister at the solar array drive interface) by 2.8 m (110 inches) wide, with a blanket size of 15.4 by 2.7 m (606 by 108 inches). Two wings of this configuration integrated to opposite sides of a spacecraft body provide 10.4 kW (BOL) power at GEO and 7.4 kW of power at EOL after 10 years in orbit. Each wing consists of a one-blanket flatpack, foldout carbon-loaded Kapton polyimide blanket assembly. The blanket assembly consists of 39 cell-covered panels and three blank leader panels.

When stowed, the folded blanket assembly is sandwiched between two graphite/epoxy facesheet aluminum honeycomb plate structures, with a polyimide foam layer on the inner surfaces to cushion the folded blanket during launch operations. A torque tube, motor-actuated, multiple latch/release mechanism is integrated to the lid/pallet structure to provide a 6900 Pa (1 psi) average stowage pressure on the folded blanket by partial compression of the foam layers. There is no padding on the blanket panels to prevent cell-to-cell contact from adjacent folded panels. The blanket housing assembly is rigidly attached to the blanket deployment mast system through a series of struts and interface fittings, with no secondary articulation between the blanket housing assembly and the mast system.

The blanket assembly is deployed (unfolded) by extension of a motor-actuated, fiberglass continuous tri-longeron lattice mast, that uncoils from an aluminum cylindrical canister structure that is attached to the pallet structure. The lid plate is attached to the outboard end of the mast and acts as a spreader bar for the blanket assembly. To provide the necessary deployed strength and stiffness (0.01 g/0.10 Hz), the mast is 0.21 m (8.2 inches) in diameter, with 3.8 mm (0.15 inch) diameter fiberglass longerons. Canister dimensions are 0.28 m (11 inches) diameter by 0.69 m (27 inches) long.

During blanket unfolding and deployment, the blanket assembly is supported by two tensioned (5 N or 1 pound) guidewire systems attached to the rear fold lines of the blanket. The guidewires provide out-of-plane constraint to the blanket to prevent any large out-of-plane excursions. When fully deployed, the blanket assembly is tensioned in the longitudinal direction by a series of constant-force Negator springs at the inboard end of the blanket attached to the pallet structure. The total distributed tension force of 63 N (14 pounds), in conjunction with the stiffness of the mast and the 0.15 m (6 inches) clearance between the mast surface and the blanket plane, ensures acceptable wing dynamic characteristics and prevents the blanket from hitting the mast structure when subjected to the design ultimate 0.01 g inertia load.

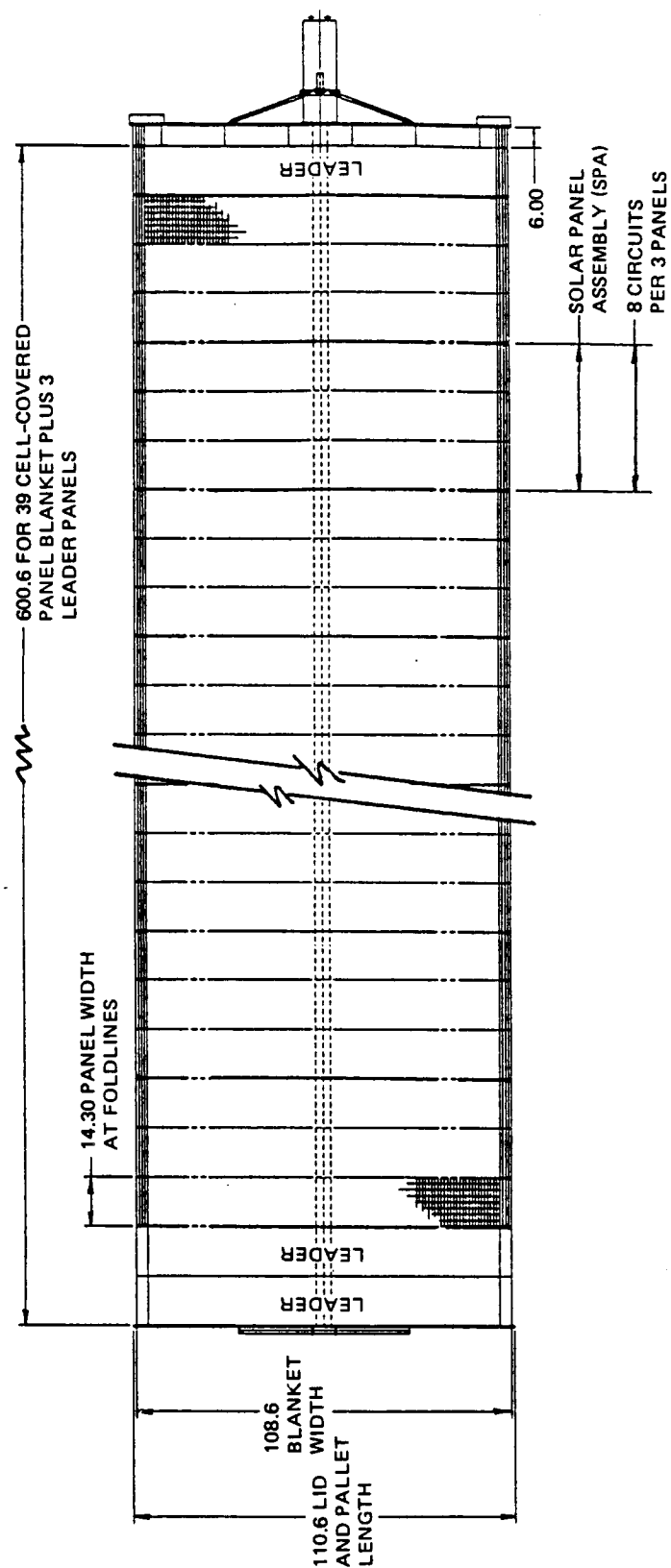


Figure 4-1. 5.2 kW (BOL) GE0 Deployed Solar Array Wing Configuration
(dimensions in inches)

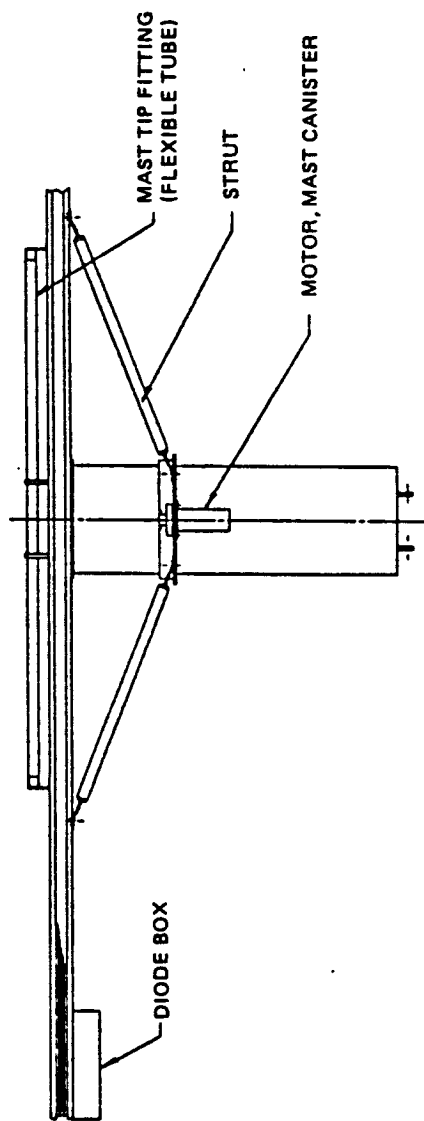
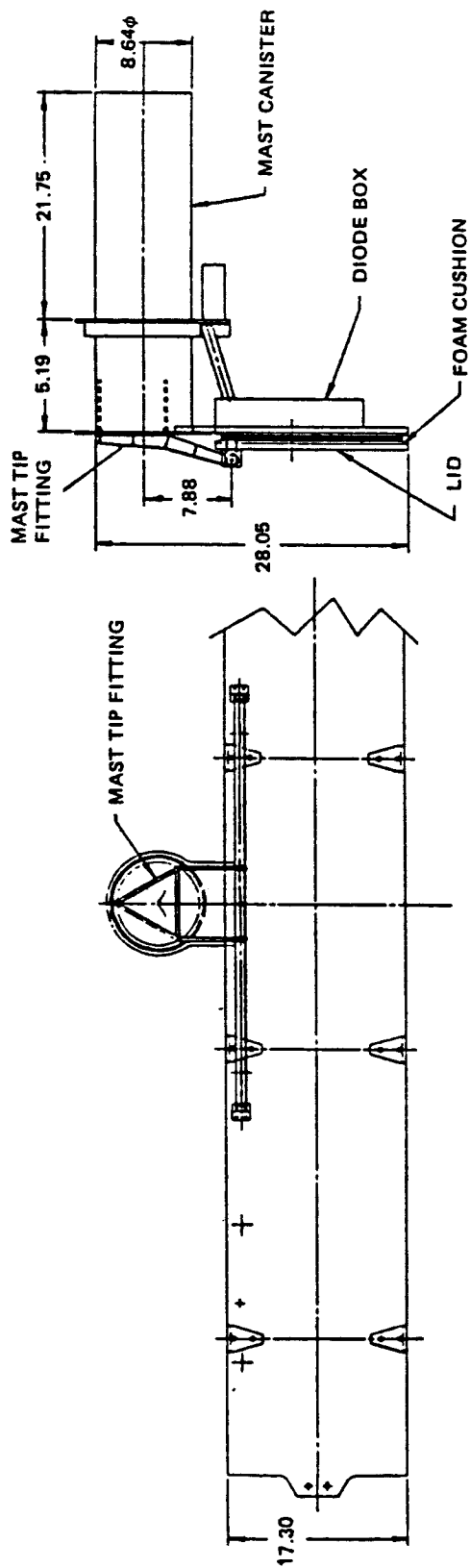


Figure 4-2. Stowed Configuration of 5.2 kW (ROL) GEO Solar Array Wing (Viewed from lid Structure) (dimensions in inches)

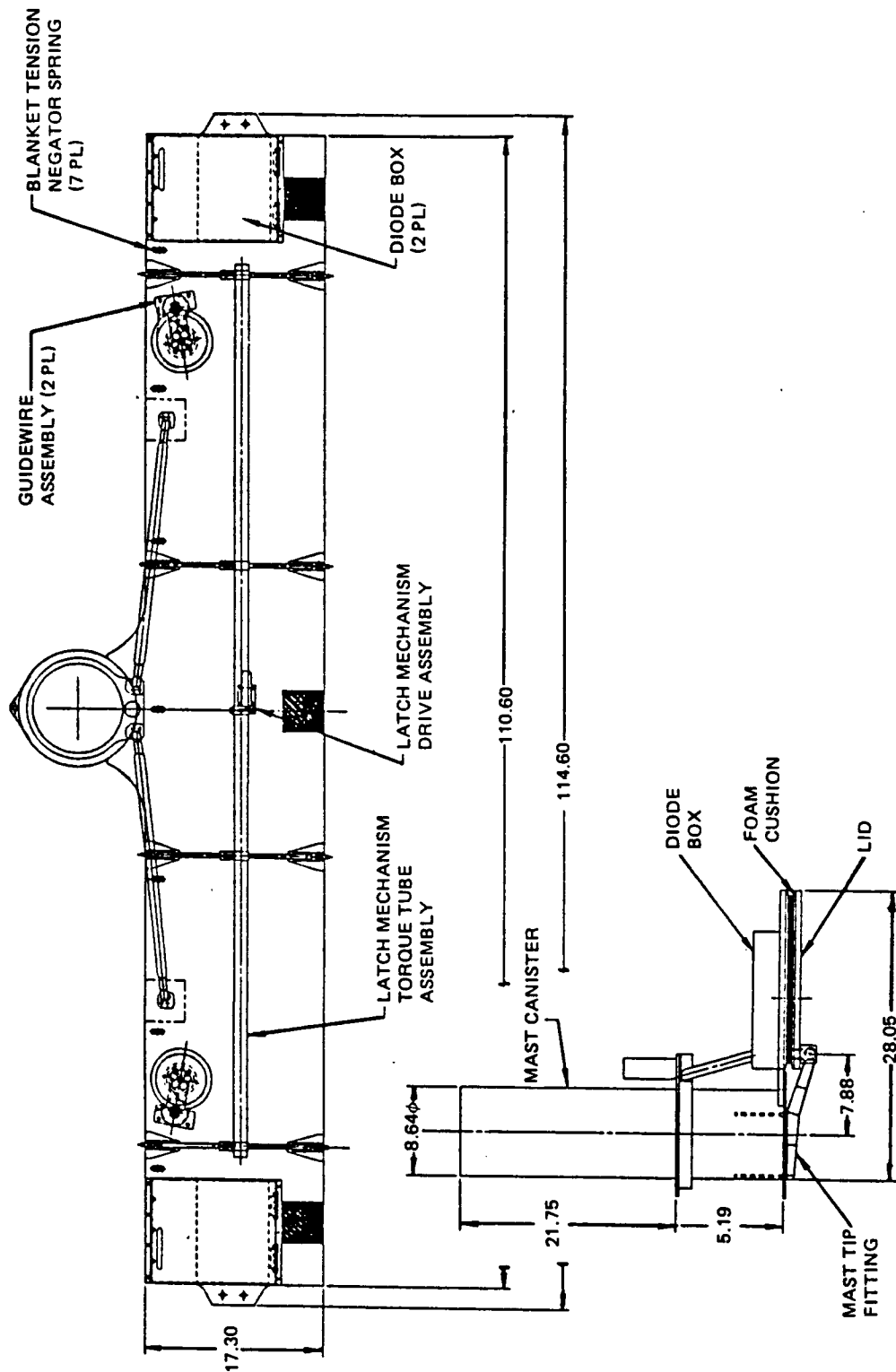


Figure 4-3. Stowed Configuration of 5.2 kW (R0L) GEO Solar Array Wing
(Viewed from Pallet Structure with Latching/Release Mechanism)
(dimensions in inches)

As envisioned, the T-shaped wing could be stowed (canted or parallel) to the sidewall of a spacecraft as shown in Figure 4-4. The bottom of the mast canister is connected to the solar array drive assembly (SADA) system through a hinge fitting. Three attachment fittings on the spacecraft sidewall pick up companion lug fittings attached to the front edge of the pallet structure. By actuation of a release device at each of the three attachment fittings, the wing is free to pivot approximately 90 degrees until the mast canister is normal to the spacecraft sidewall. Pivoting at the mast/SADA fitting is controlled by a motor system or a torque spring system. Final wing deployment is achieved by simultaneous release of the lid/pallet latches through motor-activation of the torque-tube mechanism on the pallet, followed by motor-activation of the mast canister rotating drum-nut mechanism. As the drum-nut rotates, the mast uncoils and extends from the canister, pulling the lid and unfolding the blanket assembly. This operation continues until the blanket assembly is fully unfolded and tensioned, at which time the mast drive motor shuts down.

4.2 MECHANICAL DESIGN

4.2.1 Blanket Assembly

As was initially discussed in Section 4.1, the blanket assembly substrate is approximately 15.4 by 2.7 m (606 x 108 inches). The basic material is 50 μ m (2 mil) thick carbon-loaded Kapton polyimide film from DuPont (commercially available under the name XC10¹⁶ or XC10⁴, which refers to the surface resistivity of the material). The resistivity of the material is sufficiently low to permit grounding of the blanket substrate to prevent electrostatic charge buildup from the GEO substorm environments, but sufficiently high to prevent shorting of the solar cell strings.

The blanket is accordion-folded into 42 panels, 39 of which are covered with solar cell modules. The blanket is assembled from 13 three-panel solar panel assemblies (SPAs) and two blank leader assemblies (one leader consists of one panel, the other has two panels). Figures 4-5 and 4-6 illustrate details of the SPA. Nominal panel size is 2.5 by 0.36 m (99 x 14 inches), exclusive of 0.12 m (5 inches) wide extensions bonded along each edge where the electrical harness runs are attached. The inter-SPA hingelines are unreinforced heat-set crease folds in the Kapton material. Each SPA is linked to the next SPA through a piano hinge constructed along each long edge of the SPA. The hinge pin is a 1.3 mm (50 mil) diameter pultruded graphite/epoxy rod.

The leader assemblies are shown in Figure 4-7. They are constructed in a similar fashion as the cell-covered three-panel SPAs. A piano-hinge type detail is incorporated at the interface with the Negator springs at the inboard end and with the lid structure at the outboard end.

The adhesive system used in the blanket construction (bonding the harness tabs to the blanket, bonding the piano-hinge construction together) is nitril phenolic. This adhesive system was successfully used in the construction of a prototype flexible blanket wing by TRW.

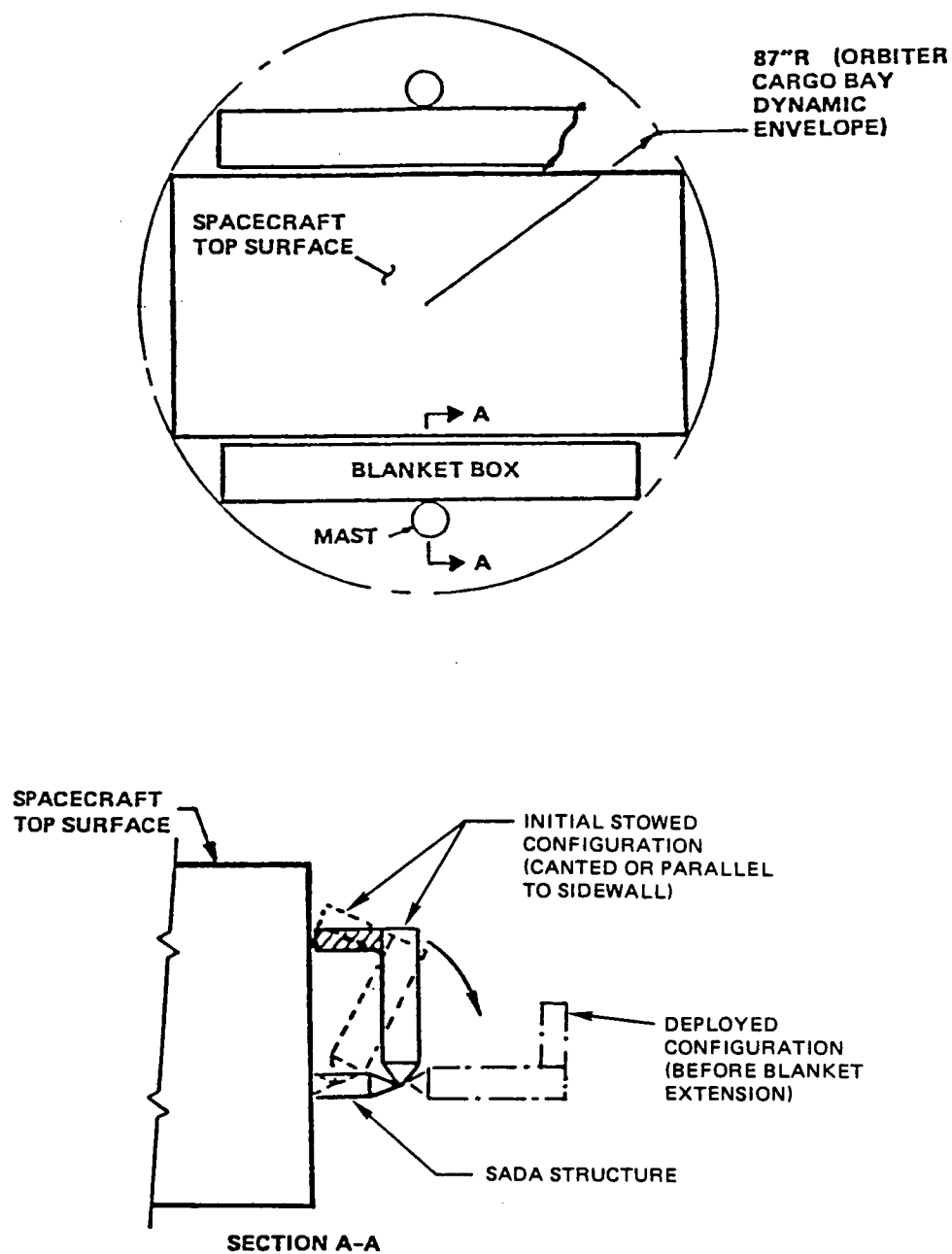


Figure 4-4. Installation of Solar Array on Spacecraft

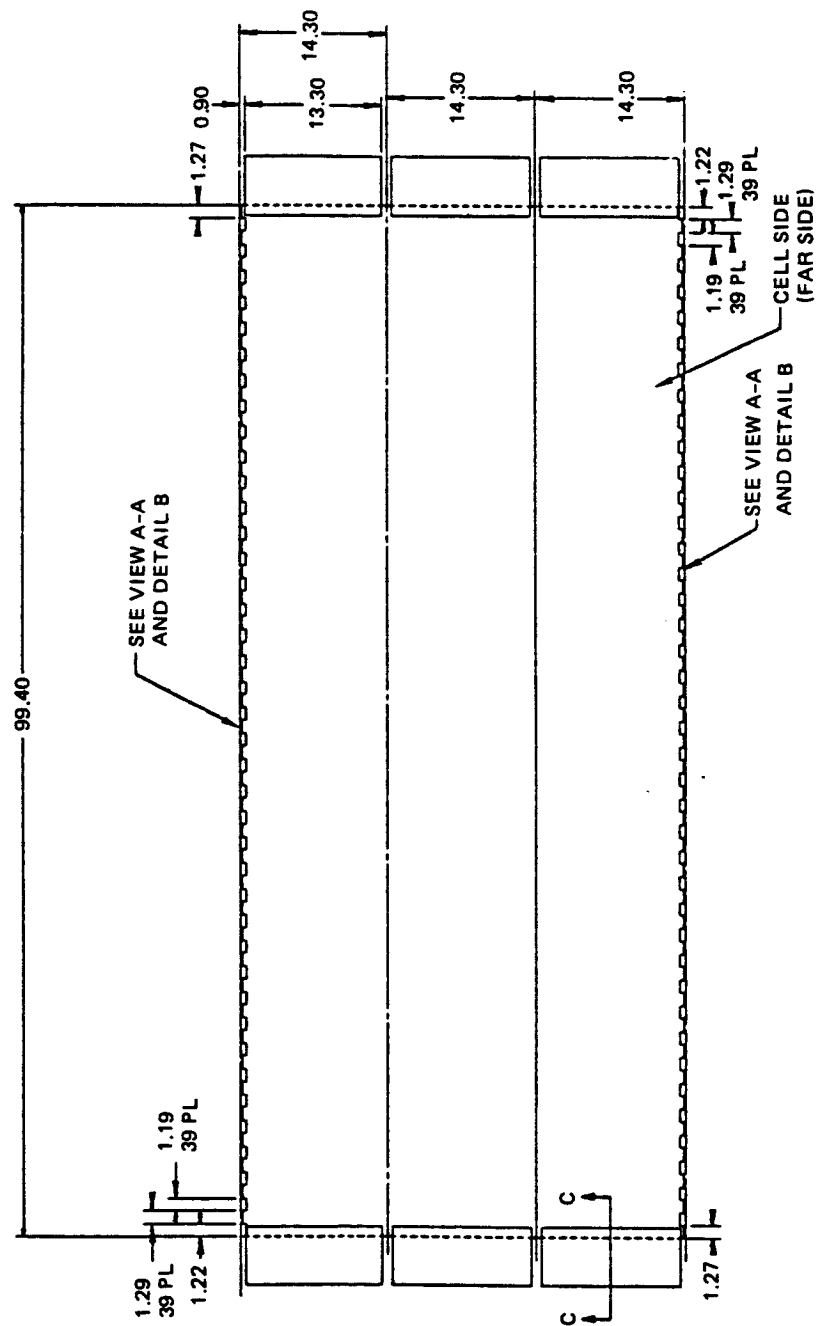


Figure 4-5. Flexible Blanket Solar Panel Assembly (SPA) Substrate
(dimensions in inches)

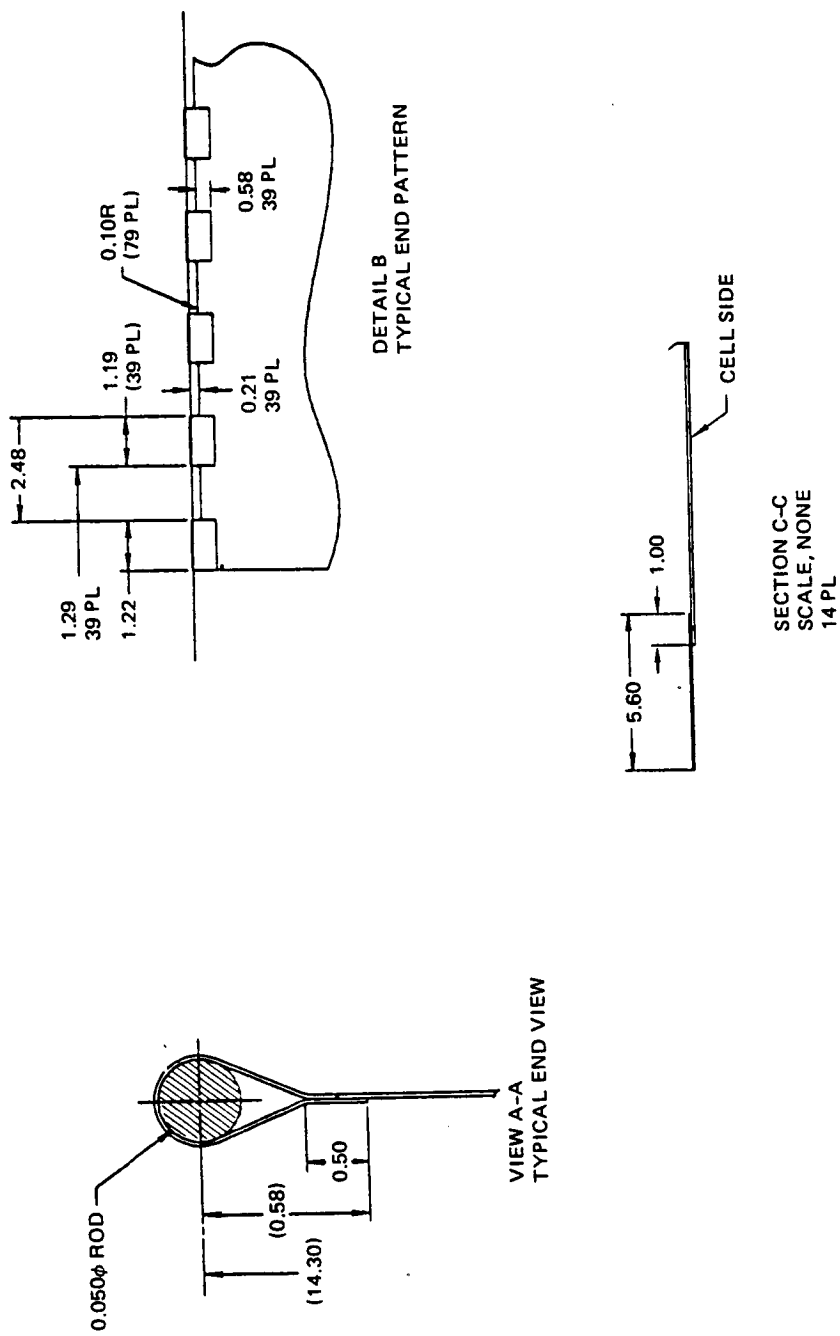


Figure 4-6. SPA Substrate Details (dimensions in inches)

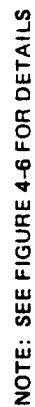


Figure 4-7. Flexible Blanket Leader Panel Assemblies
(dimensions in inches)

4.2.2 Blanket Housing Assembly

4.2.2.1 Housing Structure

Figures 4-8 and 4-9 show the blanket housing lid and pallet structures. Except for localized details they are identical in size and construction. Nominal panel size is 0.44 by 2.8 m (17.3 x 110.4 inches). On the ends of each panel are 0.05 by 0.10 m (2 x 4 inches) extensions which house conical fittings that permit the lid and pallet to seat against one another. Both panels are constructed from 0.25 mm (10 mil) high modulus (GY70 or P75) graphite/epoxy facesheets bonded to a 13 mm (0.50 inch) thick aluminum honeycomb core. The facesheet ply orientation is 0/90, with each ply approximately 0.13 mm (5 mils) thick. The aluminum honeycomb is 3/16-5052-0.001 with a density of 4.8 kg/m³ (3.1 pcf).

In four areas along each edge are reinforced zones where localized loads from the preload/release/latch fittings are located. Reinforcement includes a 0.5 mm (20 mil) sheet metal plate and core fill with 64 kg/m³ (40 pcf) syntactic foam. In two locations on the lid and two locations on the pallet are 0.1 by 0.1 m (4 x 4 inch) core fill areas to react concentrated loads from the mast tip fitting and diagonal struts from the mast canister, respectively. In three locations on the pallet along its front edge are 0.1 by 0.1 m (4 x 4 inch) core fill areas to react concentrated loads from spacecraft attachment fittings. In the center of the back edge of the pallet is a concave protrusion with six bolt holes. This is where the pallet attaches to the upper ring flange of the mast canister. The pallet also has slotted holes (two) and circular holes (nine) to provide access for the electrical harness going to the diode assembly boxes and for the blanket tension springs and guidewires to interface with the blanket assembly from small units mounted to the underside of the pallet.

NASTRAN finite element structural analyses were performed on the stowed wing structure to determine the internal loadings and stresses from shuttle lift-off and abort conditions. The worst-case limit loads were $N_x = 10.4$ g's, $N_y = 8.4$ g's, $N_z = 7.5$ g's. Structure was sized to provide positive margins of safety with a load factor of 1.4 on the design limit loads. In addition, the lid and pallet were designed to be able to apply a nominal 6900 Pa (1 psi) average stowage pressure load on the folded blanket assembly. Localized deflections of the panels were controlled such that the stowage pressure range was within the following limits: $3450 < p < 13,800$ Pa ($0.5 < p < 2.0$ psi).

Figure 4-10 shows the stowed blanket foam isolation padding assembly that is bonded to the inside surfaces of the lid and pallet structure. The material is 13 mm (0.5 inch) thick TA-301 flexible polyimide foam wrapped in a 12 μ m (0.5 mil) thick Tedlar polyvinylfluoride film. Figure 3-15 from Section 3.2.2.2 shows the load relaxation characteristics for the foam layer.

4.2.2.2 Preload/Latch/Release Mechanism

Figures 4-11 and 4-12 illustrate the motor-actuated torque tube mechanism used to simultaneously release the latches that secure the lid to the pallet structure. The lid is clamped to the pallet structure with 1.3 mm (50 mil) diameter braided steel cable at four locations along the length of the housing structure spaced about 0.7 m (28 inches) apart. The cable is attached to the lid structure and has small loops on each end which engage eight hook latches located on the

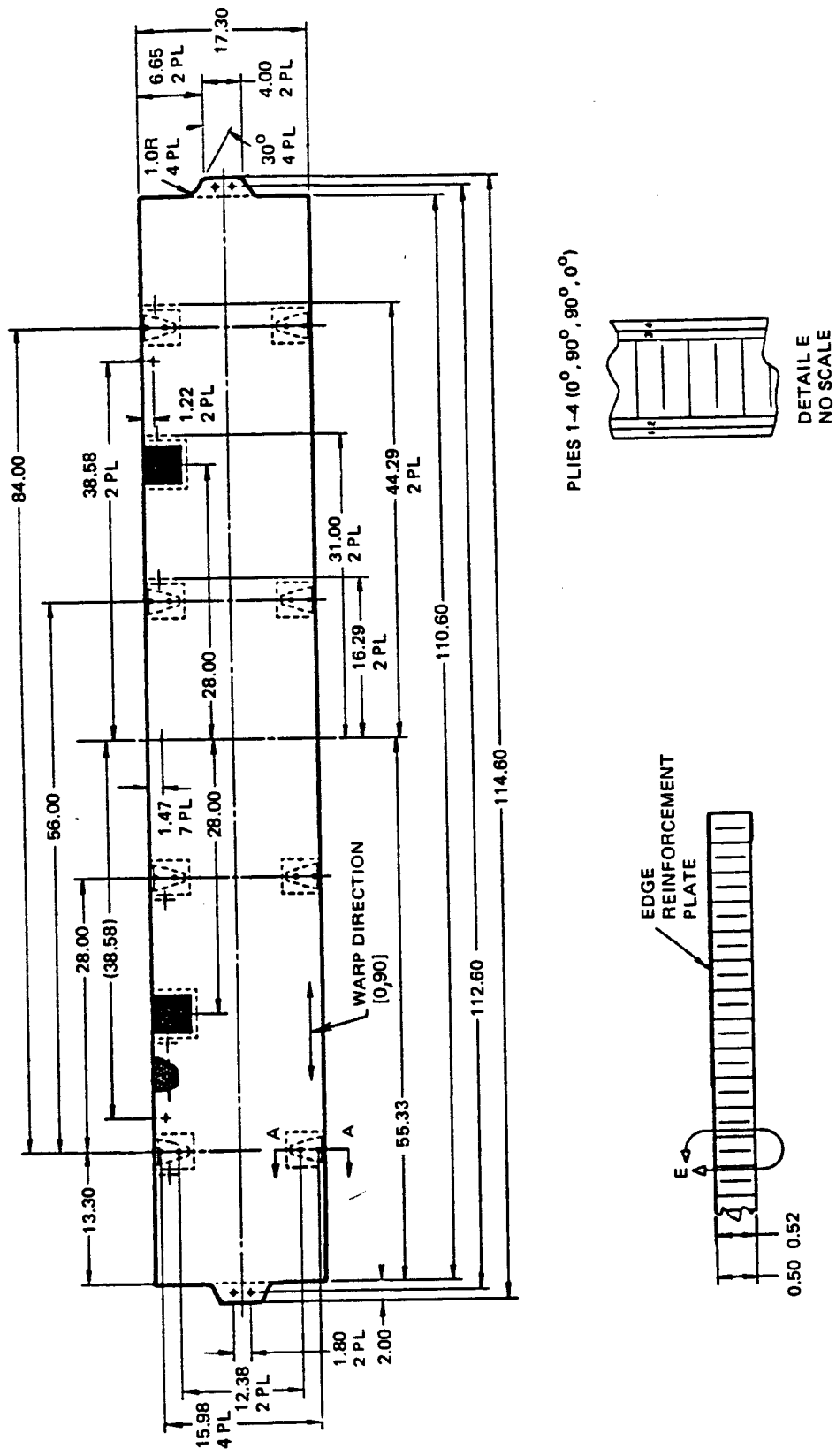


Figure 4-8. Blanket Housing Lid Panel Assembly Structure GY70
(Graphite/Epoxy Facesheets, Aluminum Honeycomb Core)
(dimensions in inches)

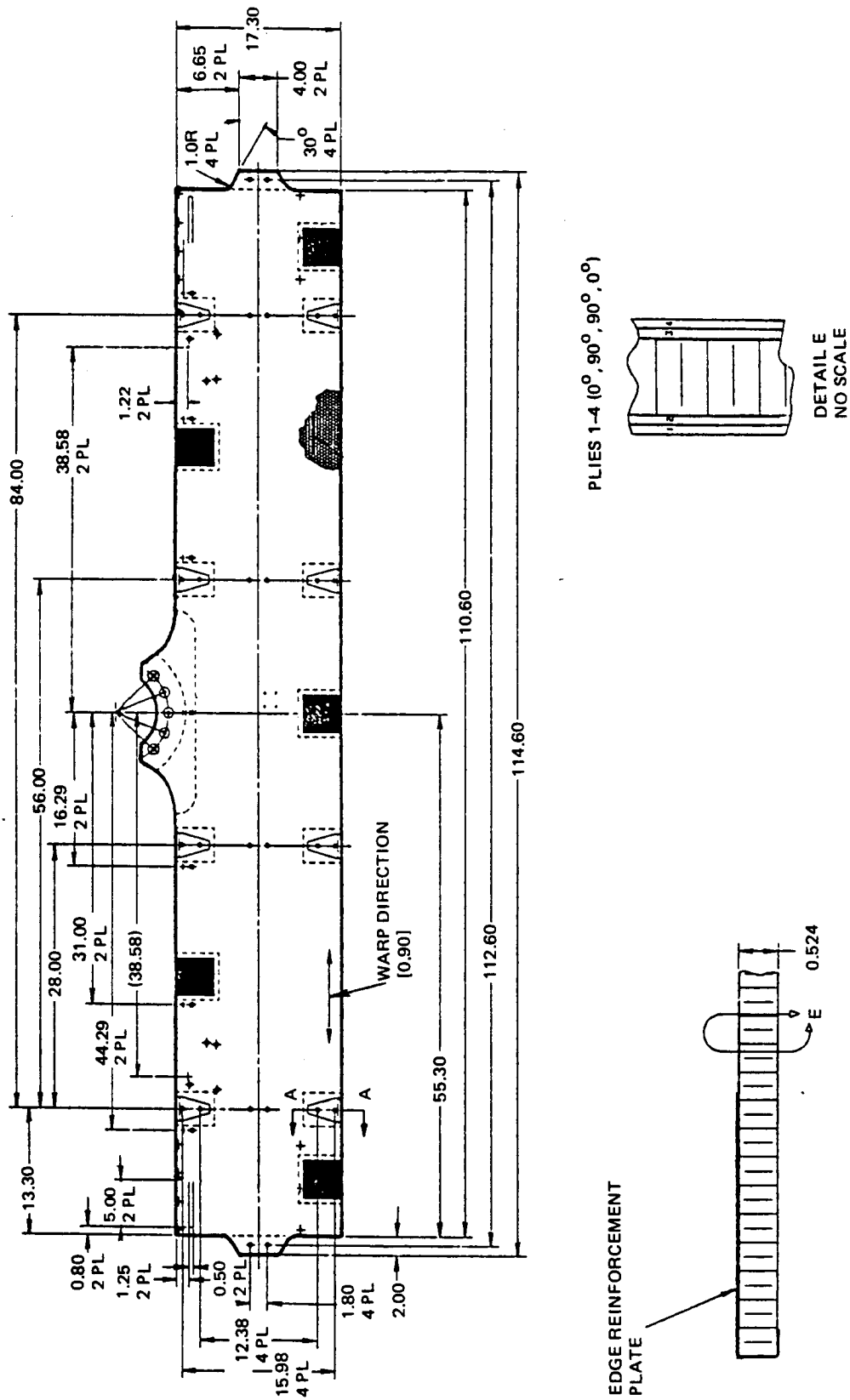


Figure 4-9. Blanket Housing Pallet Panel Assembly Structure
(Graphite/Epoxy Facesheets, Aluminum Honeycomb Core)
(dimensions in inches)

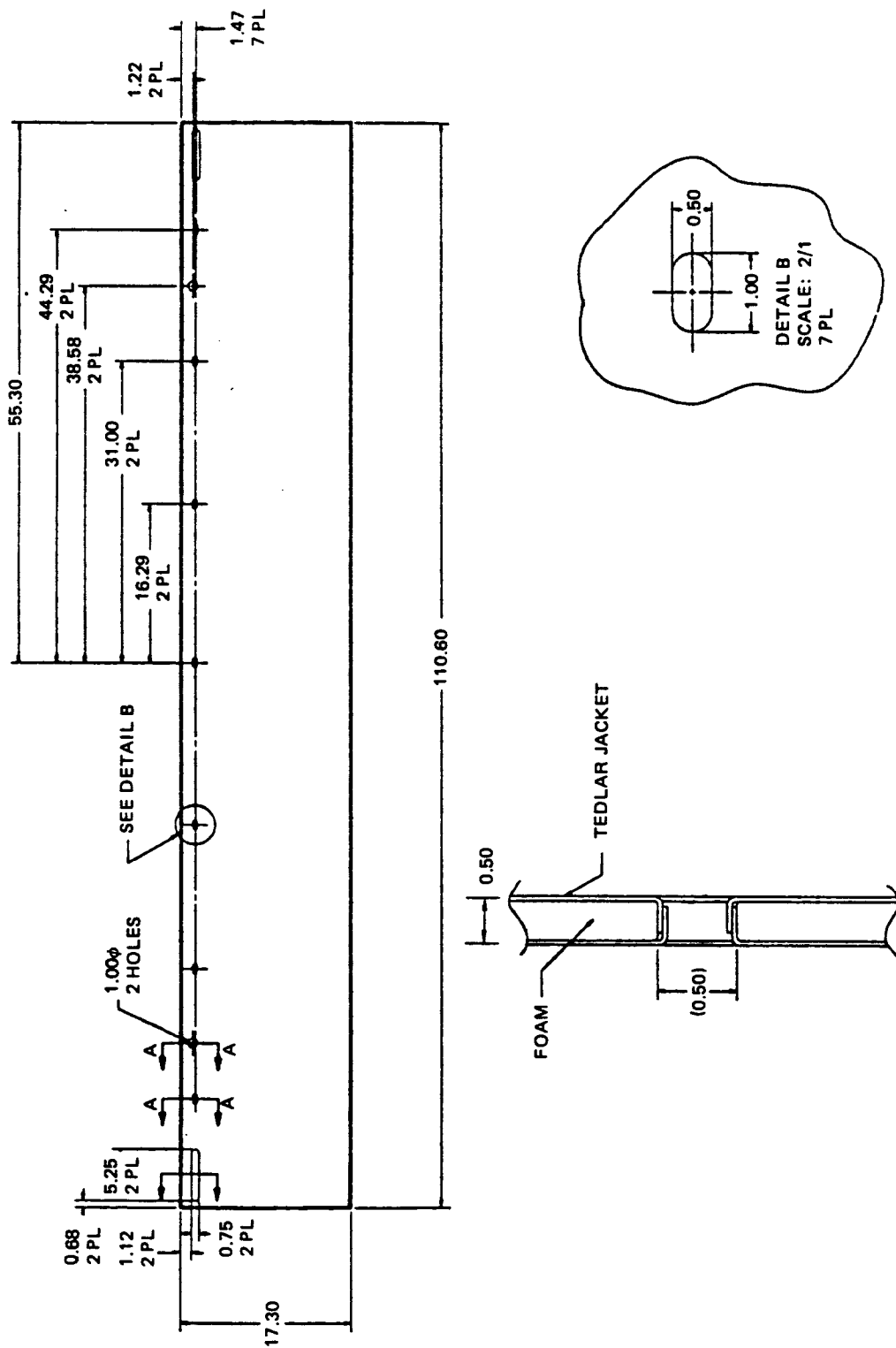


Figure 4-10. Stowed Blanket Flexible Polyimide Foam Isolation Padding Assembly
(Bonded to Inner Surface of Lid and Pallet Structures)
(dimensions in inches)

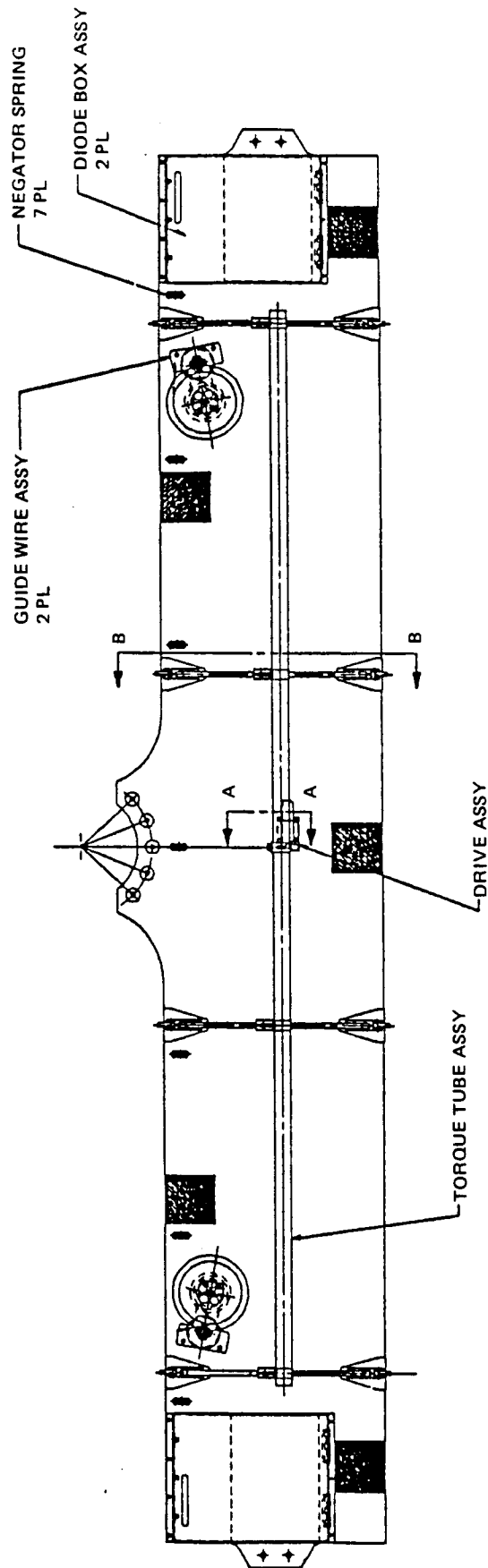


Figure 4-11. Stowed Blanket Preload/Release Torque Tube Mechanism (Plan View)

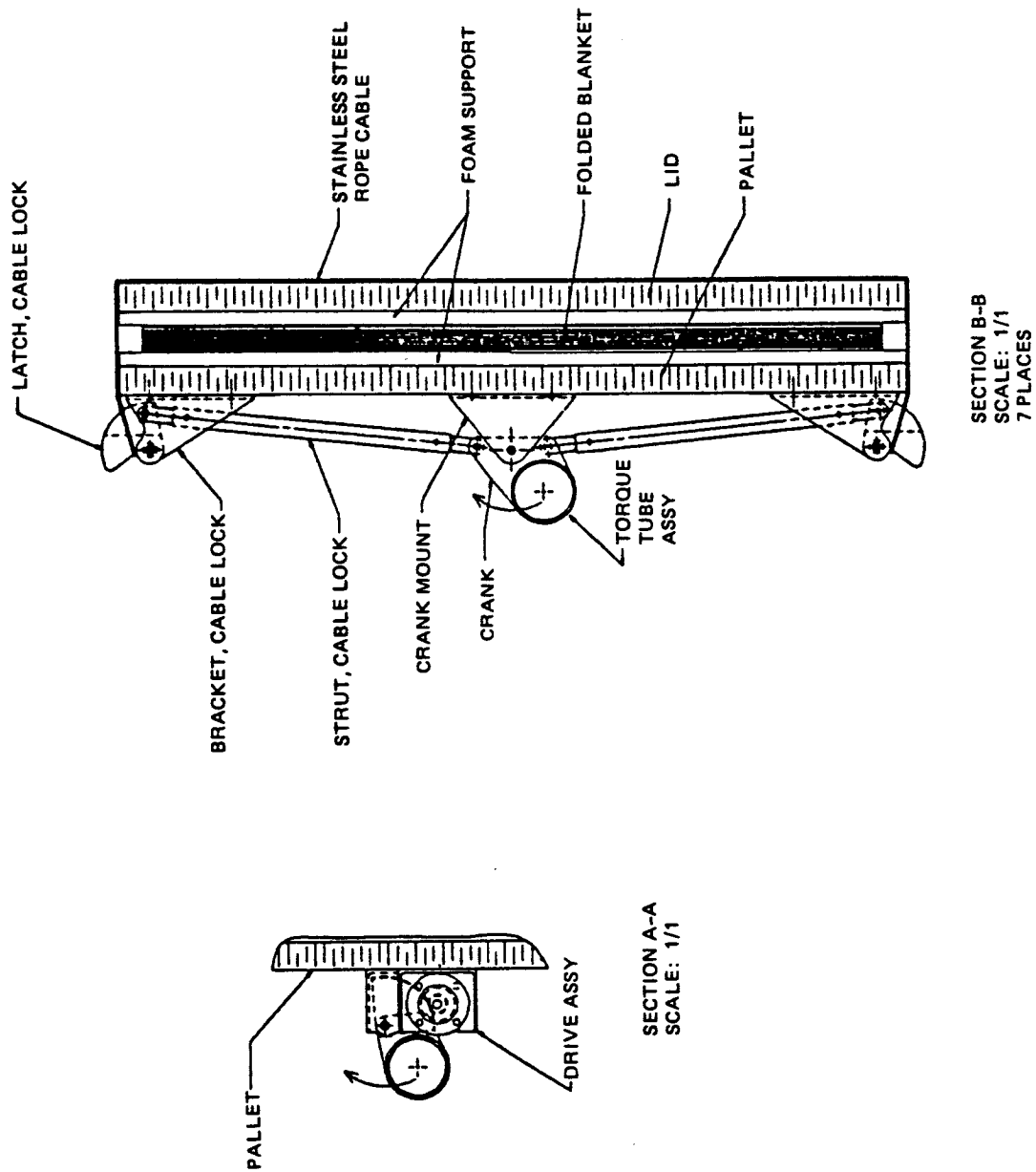


Figure 4-12. Stowed Blanket Preload/Release Torque Tube Mechanism
(Cross-Sectional View)

back edges of the pallet structure. The hooks are locked in place by small pushrod struts that are connected to an over-center crank on a central torque tube. The torque tube mechanism is attached to the underside of the pallet structure. The torque tube and struts are made of graphite/epoxy; the latches and all fittings/bracketry are made of aluminum.

The mechanism is actuated by a small, direct current, electrically redundant version of an Aeroflex 16028 or Sperry 2690903 direct-drive motor. The motor drives a gear plate attached to the torque tube.

4.2.2.3 Blanket Tension Mechanism

The design for the baseline wing was based on the conceptual approach discussed in Section 3.2.2.4. Figure 4-13 shows a typical constant-force Negator spring unit that is used to tension the blanket when the wing is fully deployed. Seven units are located on the underside of the pallet structure spaced approximately 15 inches apart. Each unit provides 9 N (2 pounds) of tension force to the blanket during the last 0.15 m (6 inches) of mast extension.

The spring goes through a hole in the pallet structure panel and attaches to a 1.3 mm (50 mil) diameter hinge pin rod located in a loop fabricated into the inboard edge of the leader panel at the base of the blanket assembly. The spring is stored on a plastic spool which, in turn, is mounted to a fixed axle aluminum bracket. Nominal extension of the spring is 0.15 m (6 inches) when the blanket is fully deployed; however, there is an additional 0.15 m (6 inches) of travel available from the spring to allow for thermal expansion/contraction of the blanket or motion of the blanket under inertial loads.

4.2.2.4 Blanket Guidewire Mechanism

The design for the baseline wing was based on the conceptual approach discussed in Section 3.2.2.5. Figure 4-14 shows a typical Negator spring tension guidewire mechanism. Two of these units are attached to the underside of the pallet structure and spaced about +0.96 m (+38 inches) from the longitudinal centerline of the blanket assembly (refer back to Figure 4-9).

The cable is 0.5 mm (20 mil) diameter braided steel and is stored on a plastic takeup reel which sits atop Negator spring reels. The cable reel and Negator spring reels are attached to an aluminum mounting bracket with vertical axle pins on which the reels rotate. The cable is threaded through a small tubular guide and through a hole in the pallet structure panel. The cable then passes through reinforced Kapton tabs that are bonded to each rear hinge line of the blanket assembly. The outboard end of the cable is secured to the lid structure. Thus, as the mast is deploying, resulting in movement of the lid away from the pallet, the blanket is being unfolded and supported by the tensioned guidewires that are simultaneously being payed out. The Negator spring was sized to provide about a 5 N (1-pound) tension load on the guidewire cable.

4.2.3 Blanket Deployment System

The PDR trades considered various types of deployment systems and schemes, and was concerned with understanding the impact of deployed frequency and strength on specific power over the ranges 0.01 to 0.10 Hz and 0.001 to 0.01 g, respectively. As a result of the PDR data, it was decided to select 0.10 Hz and

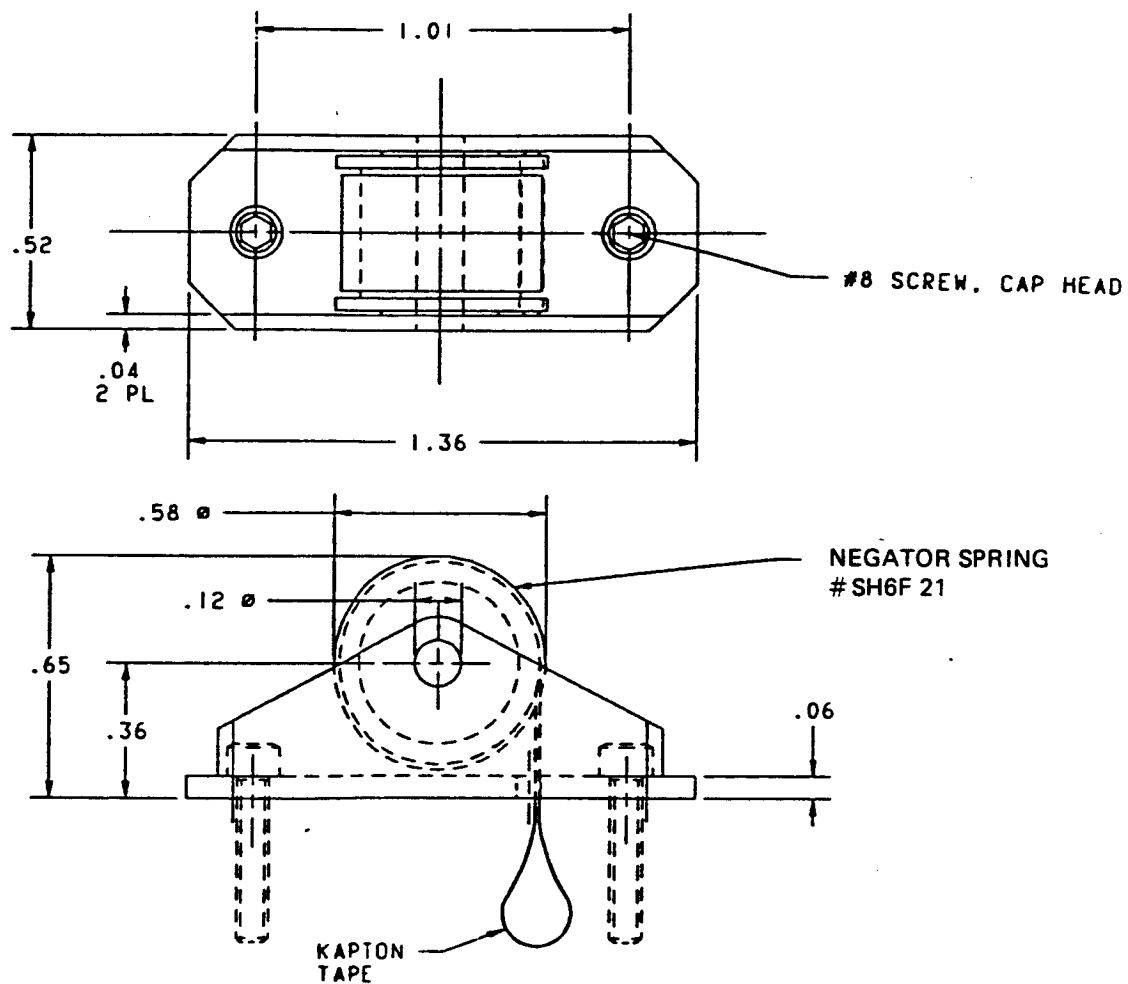


Figure 4-13. Negator Spring Blanket Tension Unit
(Seven Required at 9 N or 2 lbf per Unit)
(dimensions in inches)

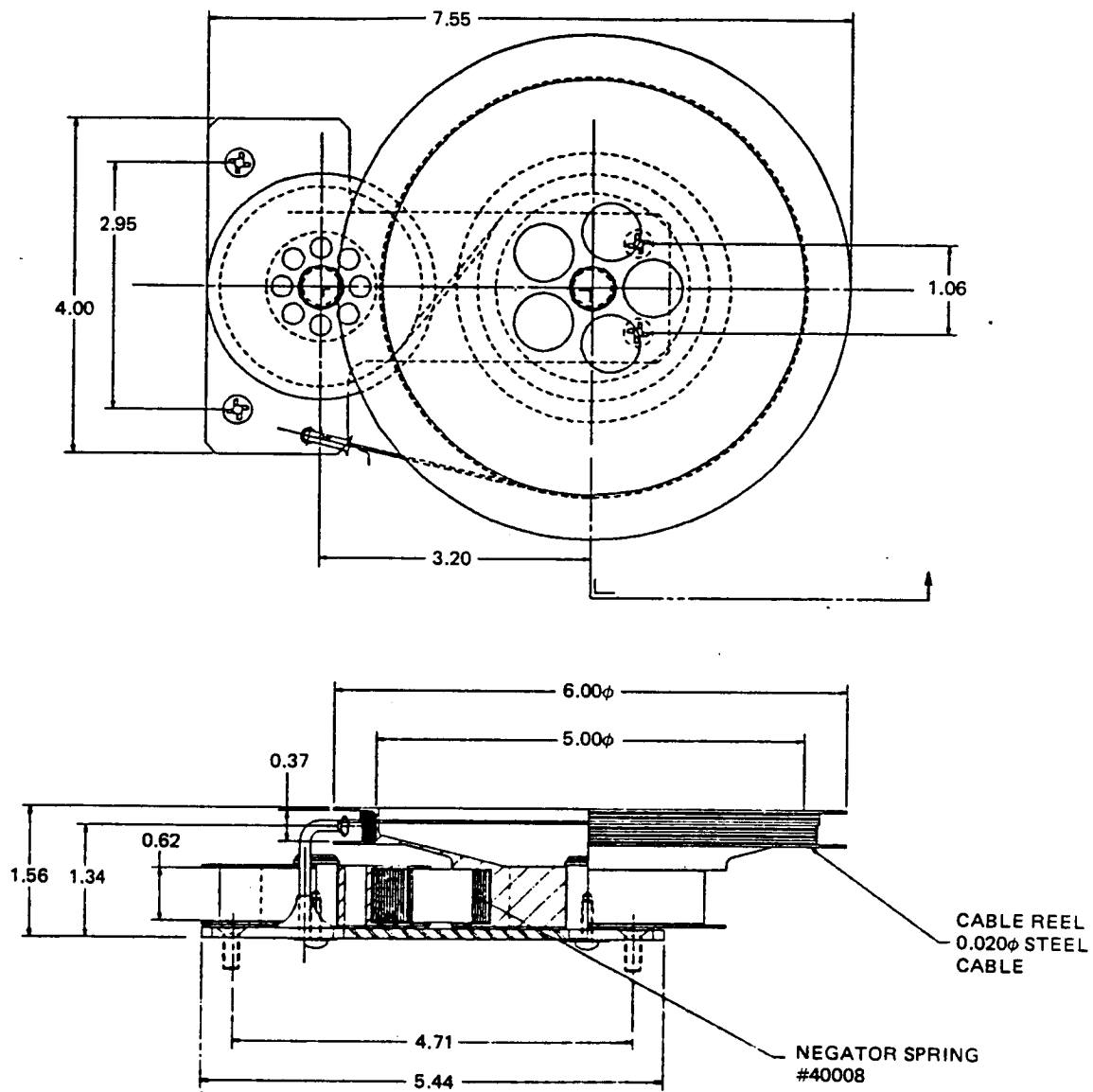


Figure 4-14. Negator Spring Tensioned Guidewire Mechanism
(2 Required at 5 N or 1 lbf per Unit)
(dimensions in inches)

0.01 g (ultimate) as the design requirements for the baseline design. In addition, because of interest from respondents of the market survey on array utility (see Appendix) for even higher levels of deployed strength, it was decided to perform additional trade studies on deployed strength up to 0.05 g. A review of the PDR trades provided by the two mast subcontractors also led to two other decisions: (1) the baseline deployment system would be a motor-actuated canister deployed lattice mast; (2) for purposes of the baseline array design, the data provided by AEC-Able Engineering would be used, although the design recommendations from Astro Aerospace were similar (but their designs were heavier).

Figures 4-15 and 4-16 describe the baseline deployment mast system. The mast element is a continuous tri-longeron lattice structure, 0.21 m (8.2 inches) in diameter, with 3.8 mm (0.15 inch) diameter fiberglass longerons. Batten spacing is 0.12 m (4.7 inches) and the battens are 2.5 mm (0.1 inch) diameter fiberglass. The diagonal lacing is 0.8 mm (30 mil) diameter braided steel cable. The modulus of elasticity for the fiberglass material is 5.2×10^{10} Pa (7.5×10^6 psi). Bending stiffness for the mast is 9.2×10^3 N-m² (3.2×10^6 lb-in²) and torsional stiffness is 4.9×10^3 N-m² (1.7×10^6 lb-in²). The mast stowage section of the canister is constructed from 0.8 mm (30 mil) aluminum and is approximately 0.22 m (8.6 inches) in diameter by 0.56 m (22 inches) long. The 0.13 m (5 inch) high rotating drum-nut section of the canister is constructed from 1.3 mm (50 mil) aluminum with local 5 mm (0.2 inch) protrusions for the 6-degree pitch threads on the inside surface which engage the rollers on the corners of every batten frame. Aluminum flange ring structures, 3.2 mm thick by 0.28 m diameter (0.125 x 11.2 inches), located above and below the drum-nut portion of the canister are used to permit attachment of and reaction of concentrated loads from the blanket housing assembly. The aluminum canister design was about 1 kg (2 pounds) heavier than a graphite/epoxy design; however, the graphite/epoxy design would be much costlier to develop and therefore was not warranted for the prototype wing.

The rotating drum-nut is supported by ring and pinion gears. The pinion gear is driven by a direct current, brushless motor via a planetary gearhead transfer. For flight purposes, the motor would be an electrical redundant version of an Aeroflex 16028 or Sperry 2690903 motor. Deployment time for the 15.4 m (606 inch) long mast is about 20 minutes.

Figure 4-17 and Table 4-1 summarize the impact of deployed wing strength on mast system weight as well as some comparisons for aluminum versus graphite/epoxy canisters, and the weight of the new type of AEC-Able mast system - an articulated four-longeron system termed FASTMast (folding articulated square truss mast). The results show that to achieve a five-fold increase in deployed strength, the mast system weight would only increase about 2.3 kg (5 pounds). The alternate mast design (FASTMast) only becomes weight competitive when made of all graphite/epoxy; otherwise, it is heavier than the fiberglass/aluminum coilable mast/canister design.

4.2.4 Wing Integration Hardware

Figures 4-2 and 4-18 illustrate how the blanket housing assembly and blanket deployment mast system are attached to one another. The pallet structure is attached to the top of the mast canister through an interface ring on the mast canister above the rotating drum-nut. The pallet is stabilized by two graphite/

- COILABLE, CONTINUOUS TRI-LONGERON FIBERGLASS LATTICE MAST DEPLOYED FROM ALUMINUM MOTORIZED CANISTER
- MOTOR-ACTUATED DEPLOYMENT AND RETRACTION CAPABILITY
- 8.2" DIAMETER MAST, 0.15" DIAMETER LONGERON
- SIZED TO PROVIDE 0.1 Hz AND 0.01 G DEPLOYED WING FREQUENCY AND STRENGTH CHARACTERISTICS, RESPECTIVELY

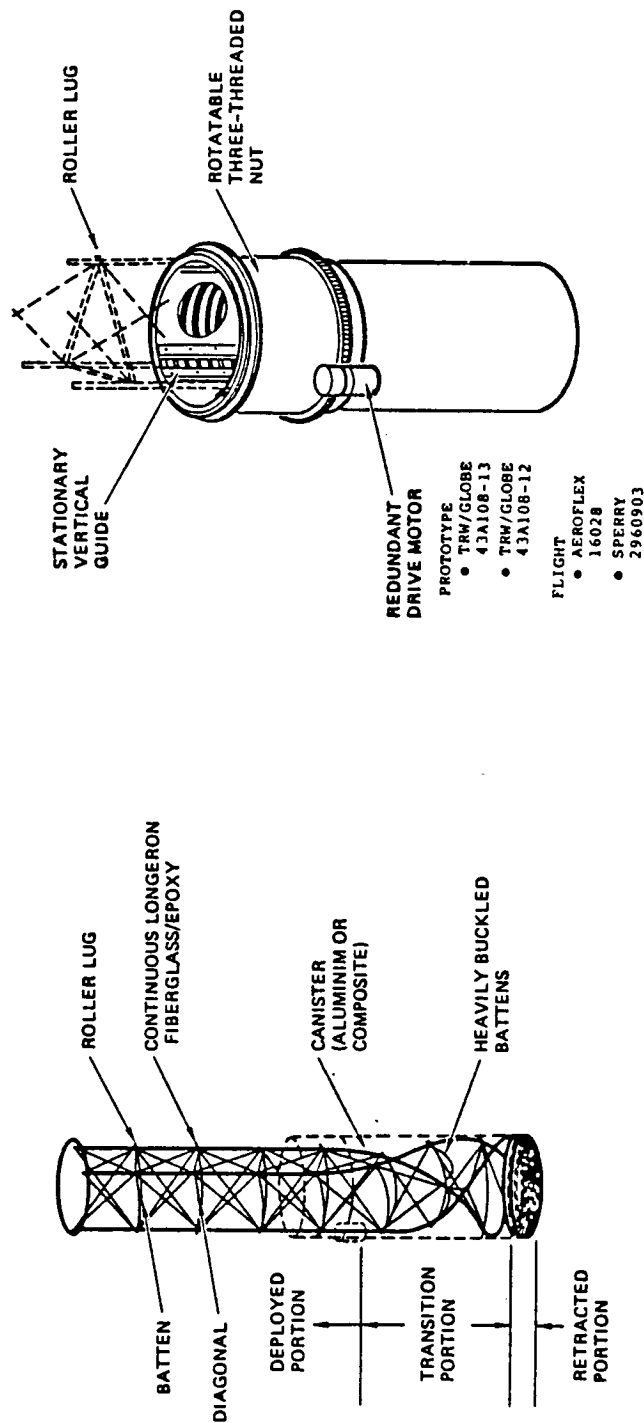


Figure 4-15. Baseline Blanket Deployment Mast System

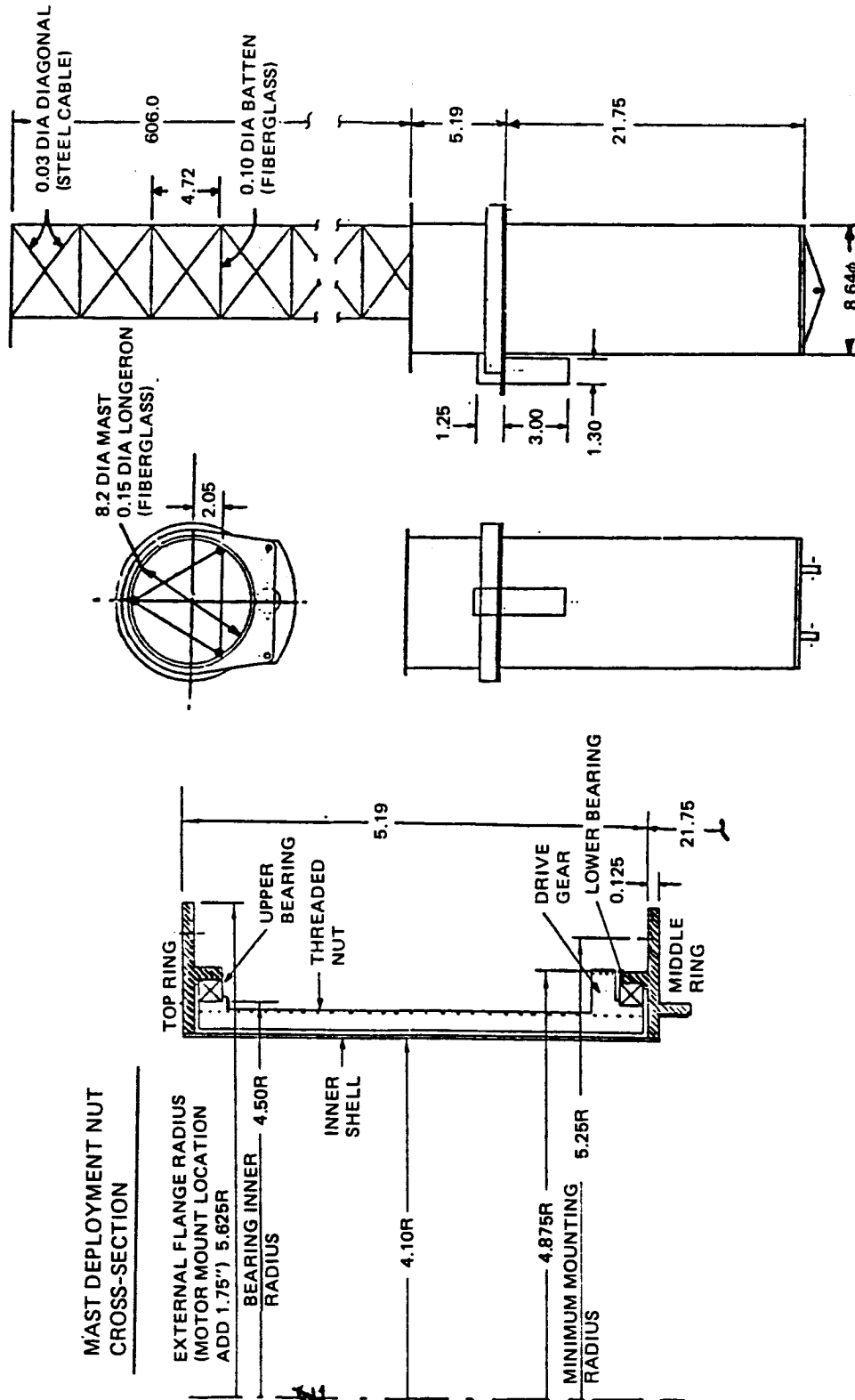


Figure 4-16. Mast System Details (dimensions in inches)

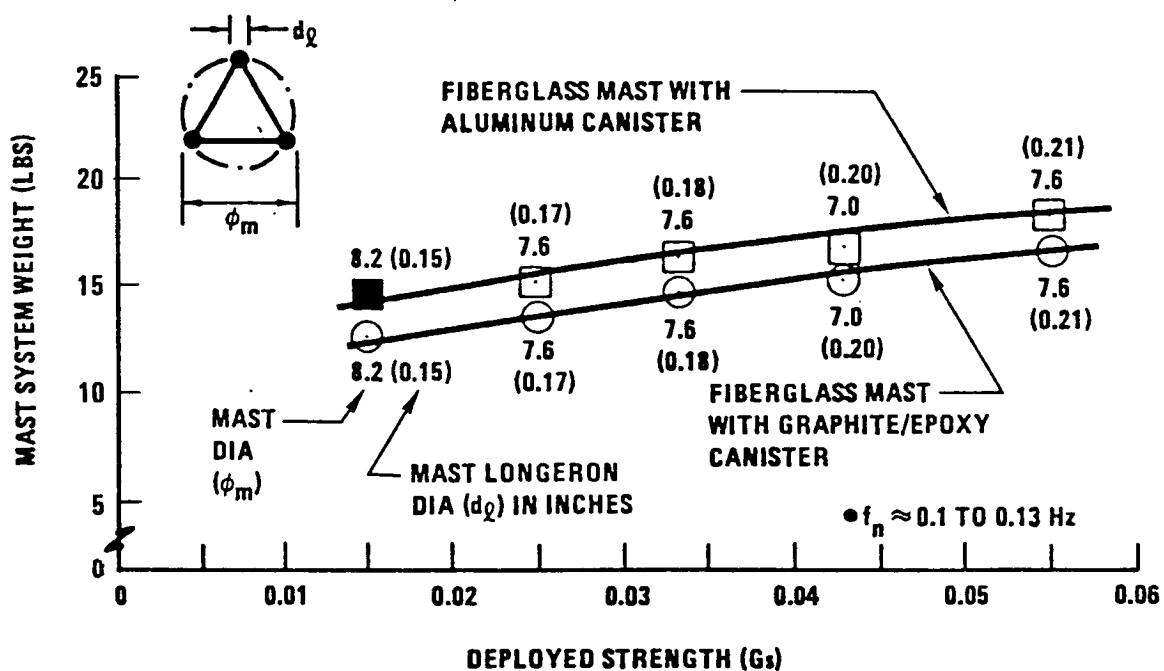


Figure 4-17. Effect of Deployed Wing Strength on Mast System Weight (Canister Deployed Fiberglass Continuous Tri-Longeron ABLEMAST)

Table 4-1. Comparison of Mast Design Options on Mast System Weight

DESIGN	MATERIAL		WEIGHT (LB)	
			ACCELERATION LEVEL	
	MAST	CANISTER	0.01g	0.05g
COILABLE	FIBERGLASS	ALUMINUM	15.6	19.8
	FIBERGLASS	GRAPHITE	14.0	18.1
FASTMAST	FIBERGLASS	ALUMINUM	27.8	37.2
	FIBERGLASS	GRAPHITE	23.3	31.1
	GRAPHITE	ALUMINUM	21.7	25.6
	GRAPHITE	GRAPHITE	17.8	21.1

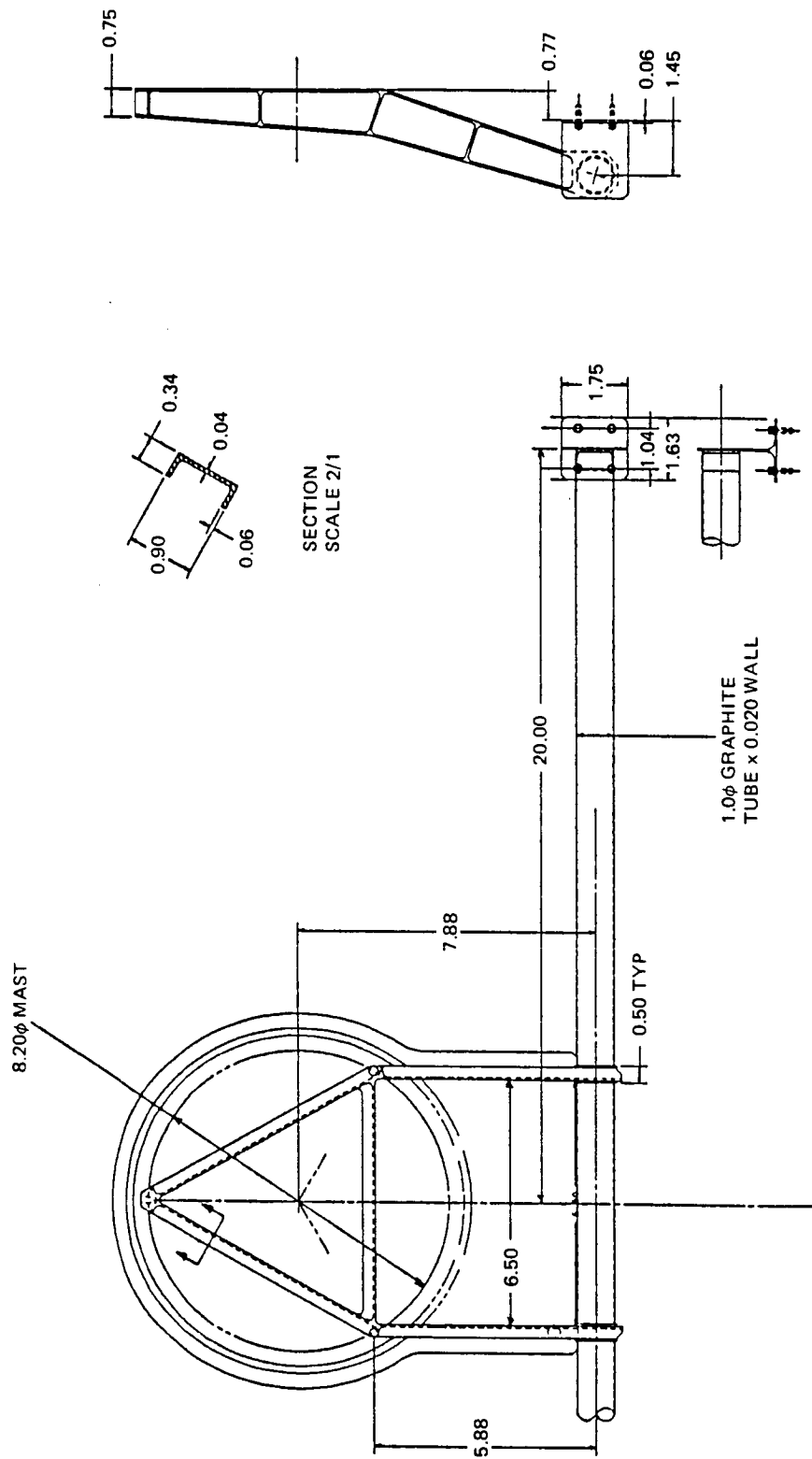


Figure 4-18. Mast Tip Fitting Connecting the Lid Structure to Outboard End of Mast (dimensions in inches)

epoxy tubular struts going from the underside of the pallet structure to an interface ring on the mast canister just below the rotating drum-nut. This creates a stable rigid interface between the pallet structure and mast canister.

The lid is secured to the top of the tri-longeron mast through a tip fitting shown in Figure 4-18. The aluminum triangular-shaped tip fitting is attached via threaded fasteners to inserts integral with the mast upper batten frame corner fittings. The tip fitting, in turn, is attached to the lid through a graphite/epoxy tubular flexure bar which is stiff in torsion. The flexure bar is attached to the lid so that it is in plane with the blanket assembly and guidewires. Thus, the lid can deploy with the mast without tipping. The flexure bar permits the lid to separate away from the pallet about 13 mm (0.5 inch), without the need to activate the mast motor, as the torque tube latch release mechanism is slowly opening the latches. This separation movement is the natural occurrence of the compressed foam padding in the blanket housing assembly returning to its uncompressed state. When the latching mechanism motor is turned off, there will be negligible residual preload on the stowed blanket or lid/pallet structure.

4.3 ELECTRICAL DESIGN

4.3.1 Solar Panel Assembly

The baseline design for the solar panel assembly (SPA) was derived from the preliminary design trades outlined in Sections 3.3.2 and 3.3.3. The major difference in the final configuration is that the packing factor for the solar cell stacks were tightened by reducing the spacing between the cells to 0.64 mm (25 mils) in the series direction and 0.86 mm (34 mils) between rows of cells, thereby slightly reducing the size of each panel within the three-panel SPA to 2.5 by 0.36 m (99.4 x 14.3 inches).

Each cell-covered panel contains eight rows of 2 x 4 cm cells with each row containing 120 cells. The solar cell stack, shown in Figures 4-19 and 4-20, consists of: (1) a 50 μm (2 mil) CMX ceria-doped glass cover coated on the front surface with a UV-rejection filter and an enhanced emittance filter to reduce the operating temperature of the solar cell, (2) a 63 μm (2.5 mil) 10 Ω -cm B-BSF/Al-BSR polished silicon solar cell, (3) two inplane stress relief loop silver-plated Invar interconnectors soldered to the solar cell, and (4) DC93500 silicone adhesive bondlines used to attach the cover glass to the solar cell and the solar cell stack to the carbon-loaded Kapton substrate.

The three-panel SPA configuration is schematically illustrated in Figure 4-21. The first panel of the SPA is illustrated in Figure 4-22. Cells and electrical circuits are arranged on the blanket to create mirror-imaged geometry with respect to the longitudinal centerline of the SPA to minimize current-induced magnetic field effects. Cell rows are arranged in a serpentine manner so string turnaround occurs at the center and the string returns to the outer edge of the panel. An electrical circuit module, consisting of a single parallel cell by 360 cells in series in order to generate a nominal voltage of 150 volts (EOL), requires the first six rows of cells on the left-hand half of the panel. The right-hand half of the panel has an identical but mirror-imaged electrical circuit module. The second pair of imaged electrical circuits requires the last two rows on the first panel plus the first four rows of the middle panel of the three-panel SPA. The third pair of imaged electrical circuits requires the last four rows on the middle panel plus the first two rows on the last of the three

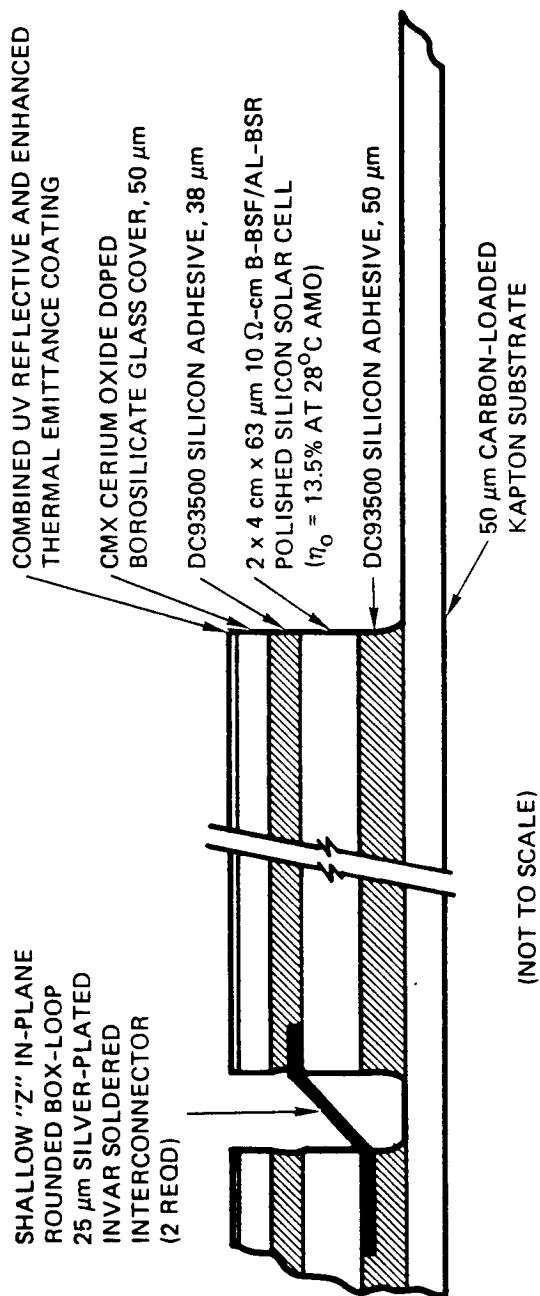
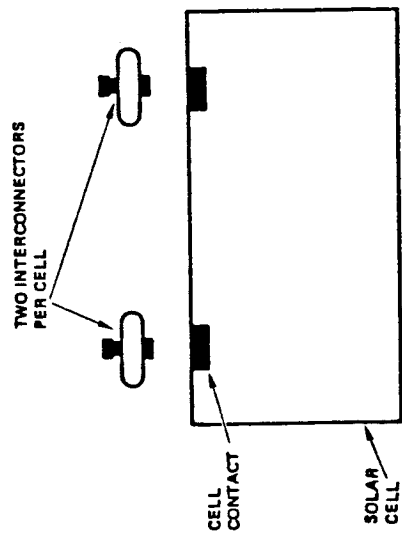


Figure 4-19. Thin Silicon Solar Cell Stack



- 25 μM THICK SILVER PLATED INVAR (TOTAL THICKNESS OF $\approx 45 \mu\text{M}$)
- COMPLIANT EXPANSION LOOPS
- FRONT CONTACT JOINT SANDWICHED BETWEEN CELL AND COVER GLASS
- COMPATIBLE WITH BOTH SOLDERING AND WELDING
- EXTENSIVE THERMAL CYCLE TESTING UNDER TRW IRAD AND JPL CONTRACT

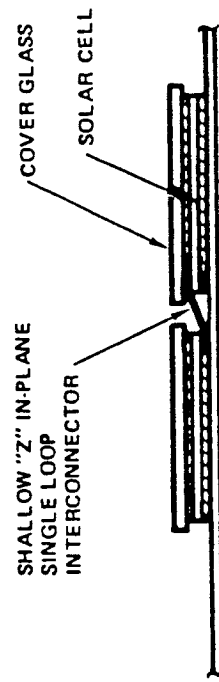
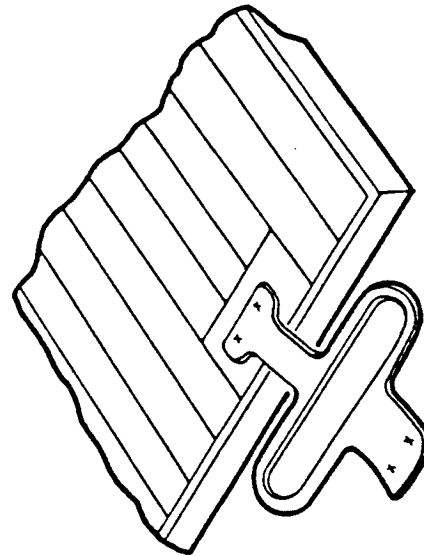


Figure 4-20. In-Plane Single Loop Discrete Interconnector

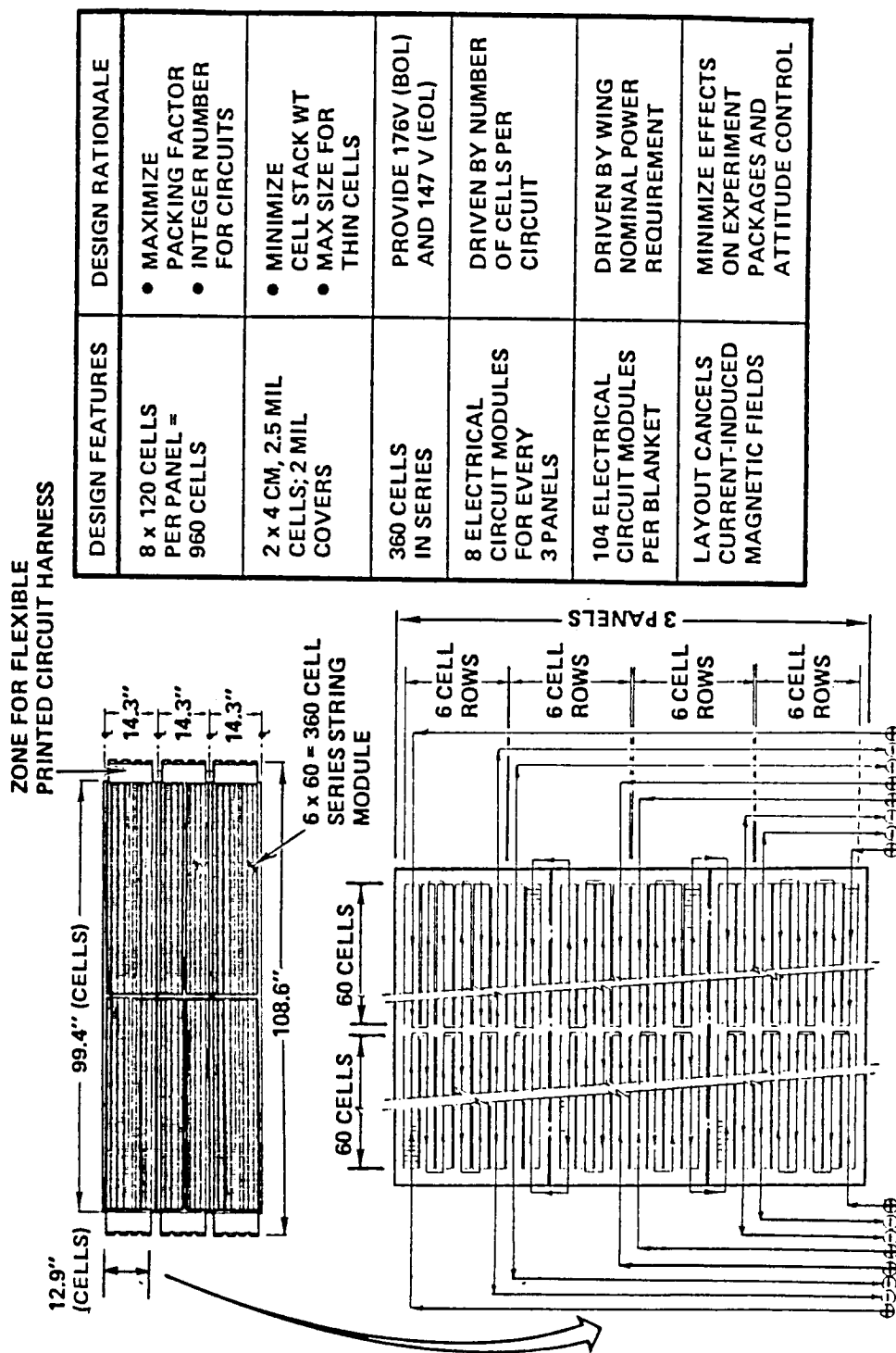


Figure 4-21. Schematic of Three-Panel SPA Electrical Circuitry

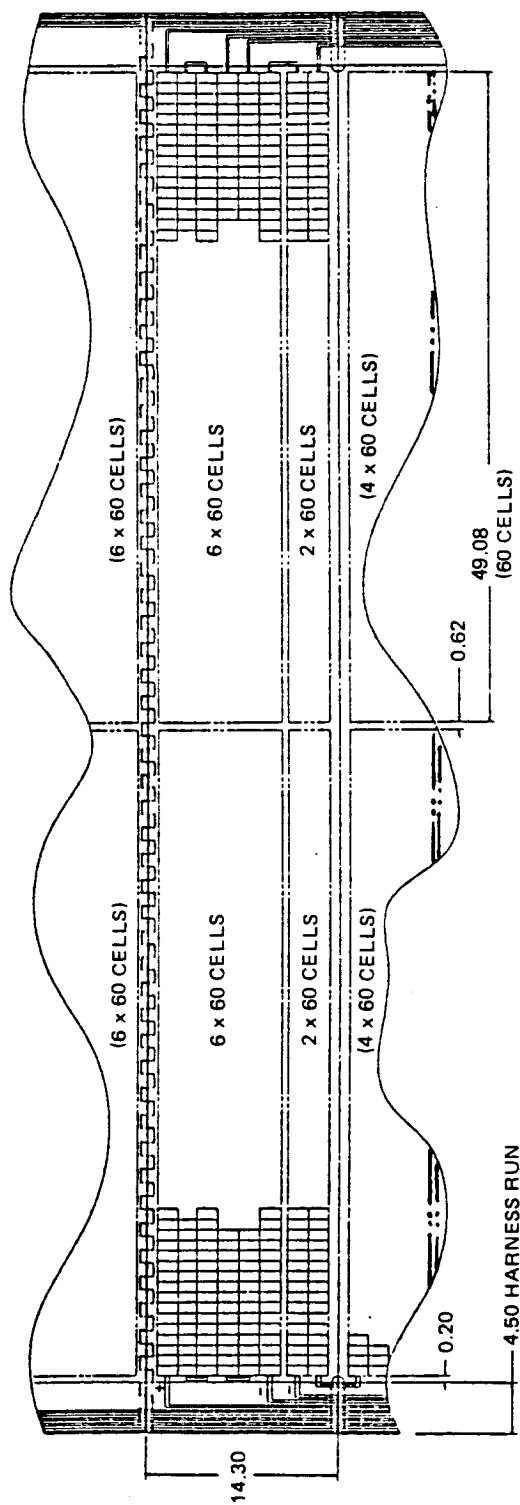


Figure 4-22. Flexible Blanket Solar Panel Assembly (SPA)
(First of Three Panels in SPA Shown)
(dimensions in inches)

panels. The fourth pair of imaged electrical circuits requires the last six rows on the last panel. Thus, on the left-hand side of the SPA are four circuits, and there are four circuits on the right-hand side of the SPA for a total of eight circuits per SPA. Thirteen three-panel SPAs are required to obtain the desired power output.

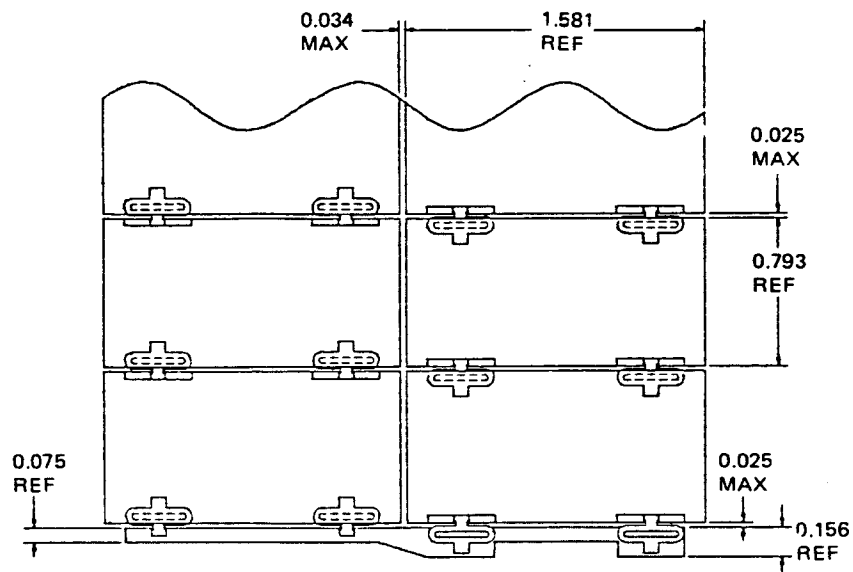
All positive and negative terminations for each of the eight circuits occur along the outside edge of the SPA adjacent to the flexible printed circuit harness segment that is bonded to 0.12 m (4.6-inch) extensions of the basic blanket substrate. The direction of series stringing for each electrical circuit is alternated (i.e., clockwise, counterclockwise, etc.) such that positive terminations for adjacent circuits are next to one another, as are the negative terminations. String terminations and turnarounds are made via silver-plated Invar ribbons shown in Figure 4-23. All electrical connections in the series circuit as well as between the circuit and the harness are soldered.

4.3.2 Blanket Electrical Harness

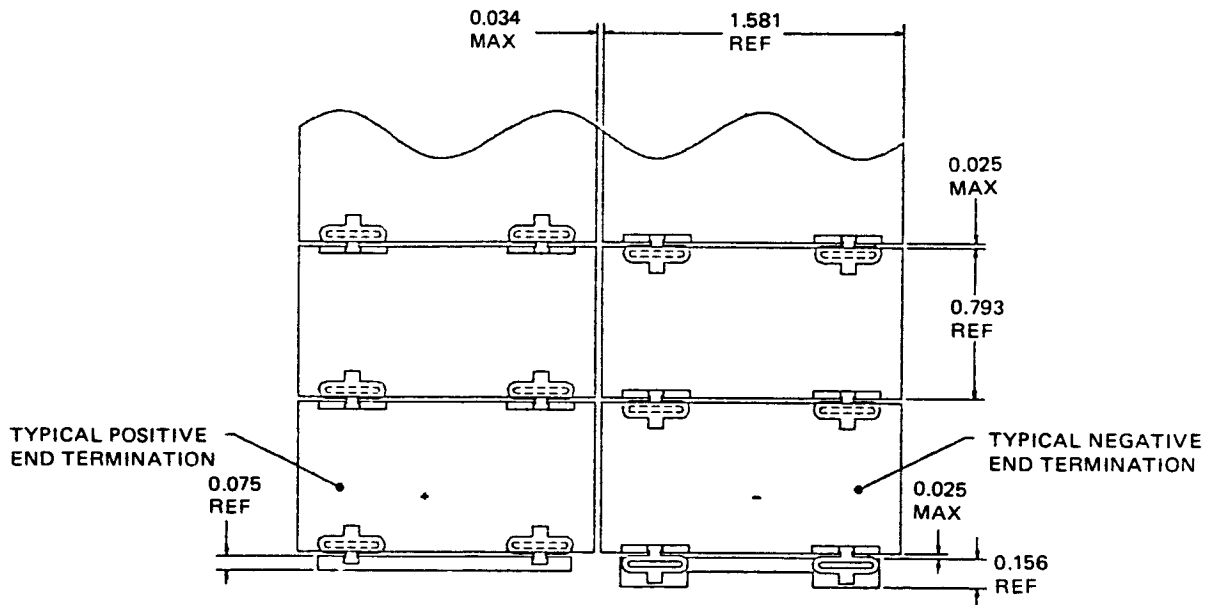
Figures 4-24 through 4-26 illustrate the three types of flexible printed copper Kapton insulated harness segments used on the blanket assembly. The harness, in addition to carrying all power from the 360-cell circuits on the panels to the diode box on the pallet structure, also contains sensor lines and circuit jumpers across fold lines when a circuit carries over from one panel to the next.

The segment shown in Figure 4-24 has no copper traces, just connecting pads to permit attachment to the adjacent harness segment. This segment is used on the outboard leader panel assembly, going from the lid to the most outboard three-panel SPA. It acts as a structural extension of and longitudinal support for the electrical harness at its outboard end. The segment shown in Figure 4-25 is attached to each three-panel cell-covered SPA. Figure 4-26 illustrates the inboard termination segment of the electrical harness. It is attached to the inboard leader panel assembly and goes from the most inboard SPA to the diode box on the pallet. This segment has additional folds and length to permit activation of the blanket Negator spring tensioning system when the blanket is fully deployed and to allow for expansion/contractions of the blanket assembly without inducing loads into the harness.

Each harness segment is approximately 0.11 m (4.5 inches) wide and is bonded with nitryl phenolic adhesive to 0.12 m (4.6-inch) wide extension tabs to the blanket main substrate. The harness is bonded to the cell-side of the blanket to permit direct access to the solar cell circuit terminations located along the outer edge of the main substrate. Printed copper tooling holes are incorporated into the harness segments to permit accurate placement and alignment of the harness segments. The copper traces were sized to be able to carry at least 0.3 ampere (+ traces) and 0.6 ampere (-traces) with a net harness voltage drop of about 2.5 percent (≈ 4.5 volts). The copper traces are 2-ounce copper ($69 \mu\text{m}$ [2.7 mils thick]) by 0.64 mm (25 mil) wide with a 0.51 mm (20 mil) spacing between the traces. The ends of each trace between segments are 1.1 by 2.5 mm (44 x 100 mil) pads (see Figure 4-27). Separation distance between the pads is 0.33 mm (13 mils) which meets the MIL-C-55543 minimum requirement of 0.24 mm (10 mils) for 300-volt applications. At the turnouts along the inside edge of each harness segment, where the harness trace is soldered to the solar cell circuit termination, the trace width is increased in width to about 2.5 mm (100 mils).



a. String Turnaround Details



b. String Termination Details

Figure 4-23. String Turnaround and Termination Details
(dimensions in inches)

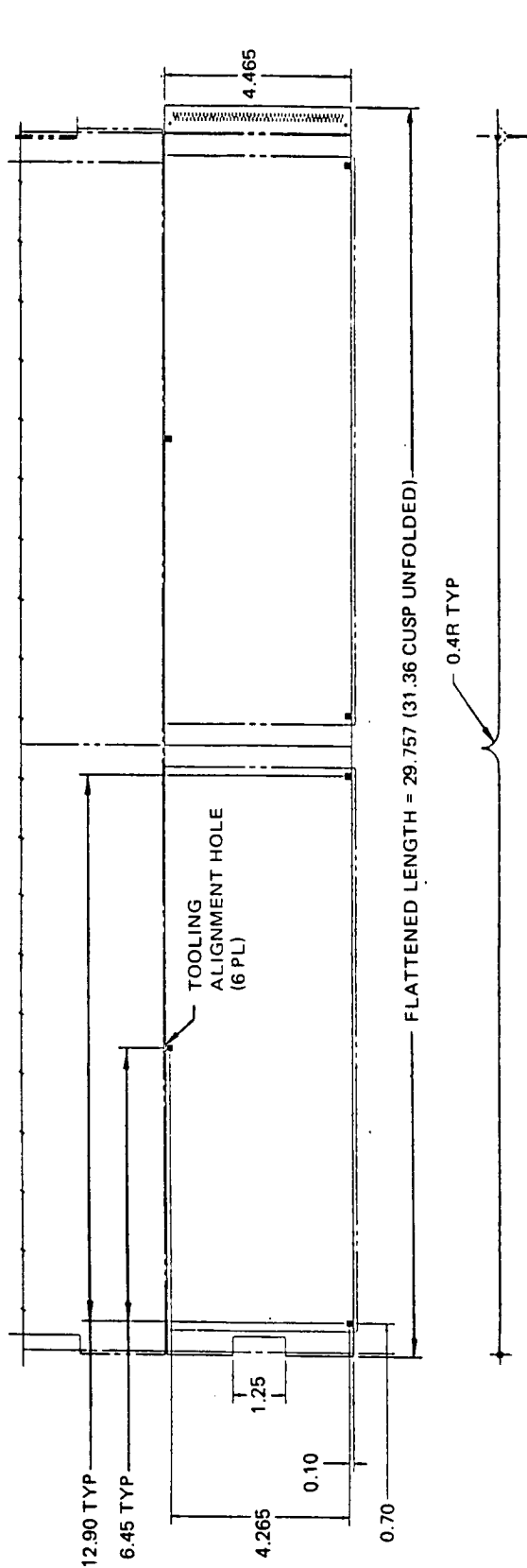


Figure 4-24. Outboard Termination Segment of Electrical Harness (dimensions in inches)

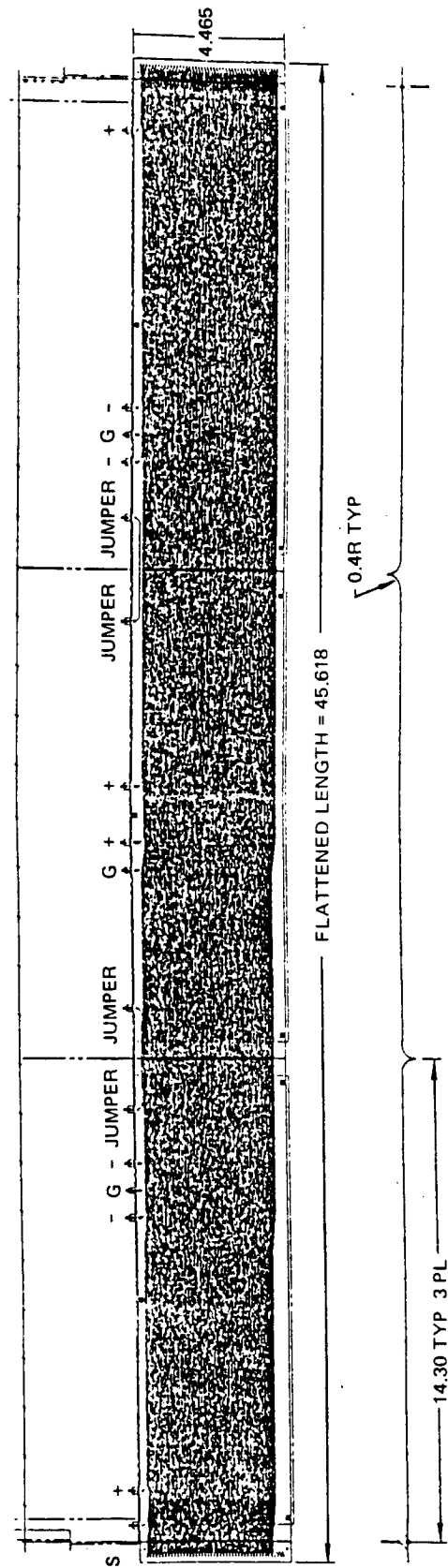


Figure 4-25. Solar Panel Assembly (SPA) Flexible Printed Copper Circuit Electrical Harness Segment (dimensions in inches)

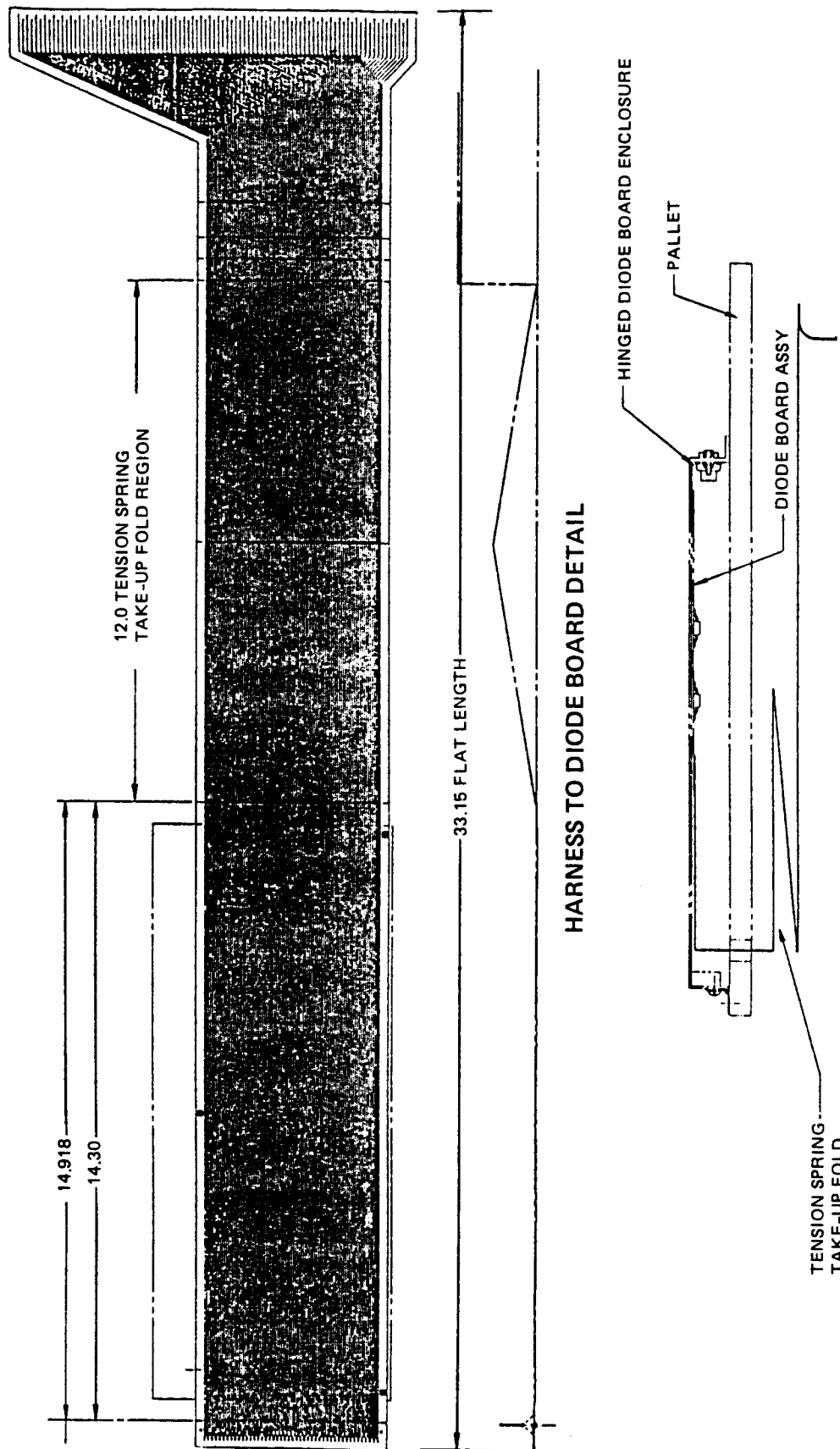


Figure 4-26. Inboard Termination Segment of Electrical Harness (Interface with Diode Box Shown) (Dimensions in inches)

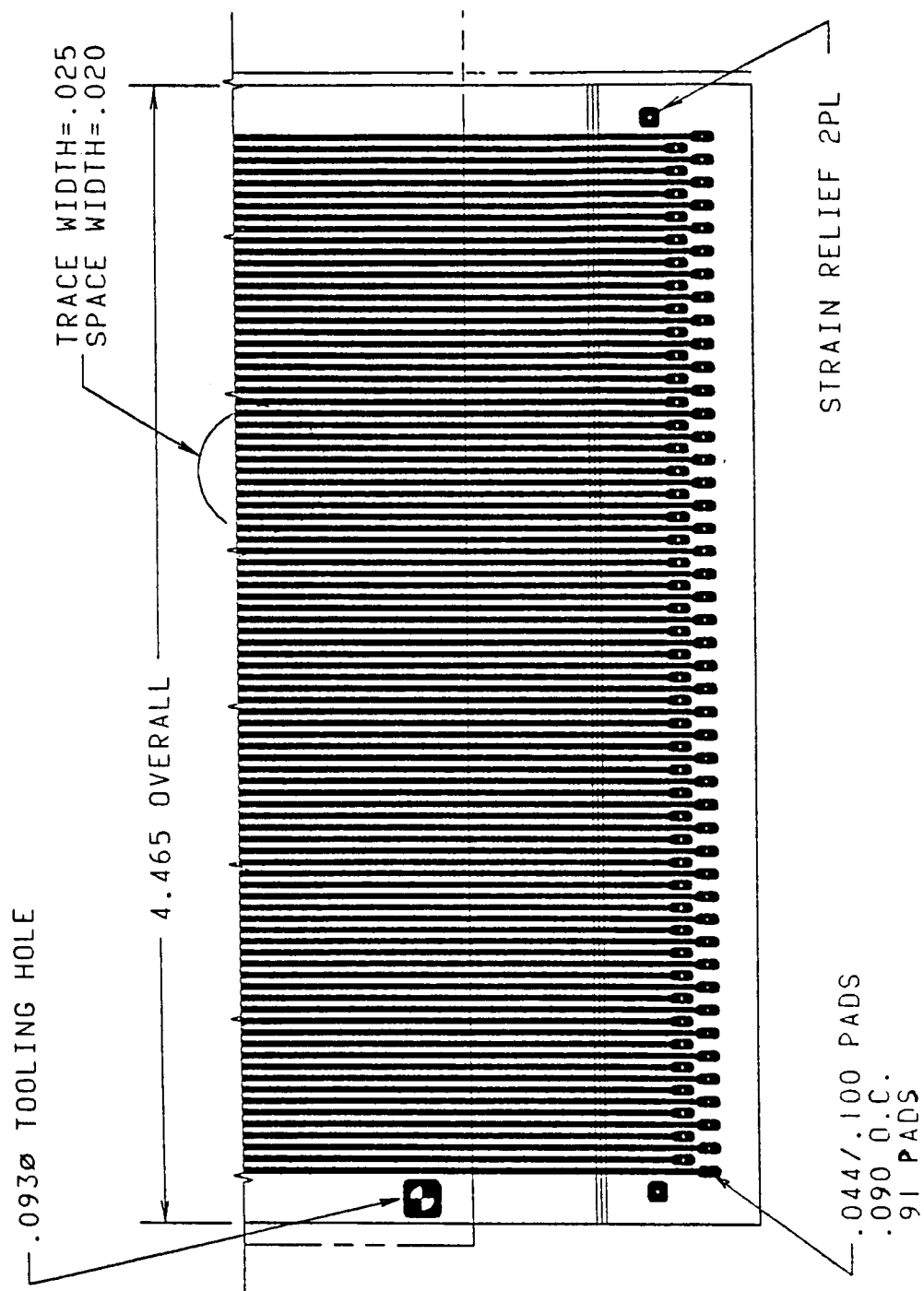


Figure 4-27. Electrical Harness Segment Splice Pad Detail

The harness insulation is conventional Kapton H polyimide film 38 to 50 μm (1.5 to 2 mils) thick. The total harness thickness of a segment with traces is about 191 μm (7.5 mils), making it slightly thicker than the glassed solar cell stack (see Figure 4-28).

When the cell-covered SPAs and leader panels are integrated together to form a complete 42-panel blanket assembly (13 SPAs plus leader panel assemblies), the ends of each harness segment are brought together to form a "cusp" shape and are soldered at each of the 91 pads (plus two stress-relief pads) (see Figure 4-29). In between these locations where the blanket panels are crease-folded to form a hinge line, the harness segment is designed with sufficient length to permit a "cusp" fold in the harness segment. Printed copper tooling holes in the harness segment are used to accurately align the ends for the soldering operation.

As indicated in Section 4.3.1, the series orientation of adjacent cell circuits on the panels are alternated (clockwise, counterclockwise, etc.) such that the positive terminations for adjacent circuits are located next to one another, as are the negative terminations. There are individual copper traces in the harness for each positive termination; however, each adjacent pair of negative terminations are bused together on a common trace. The grounding turnout for each panel is bused to a convenient available negative trace. Also included in the harness is a short jumper trace which permits the continuation of a cell circuit from one panel to the adjacent panel across the fold line of the SPA (refer to Figure 4-30).

In order to minimize the number of unique harness trace patterns for each harness segment (thereby reducing cost and confusion), one trace pattern was used for all SPA segments. Only seven traces in any SPA harness segment terminate with the cell electrical circuits on the SPA (four positive and two negative terminations plus one sensor termination). Since there are a total of 13 SPAs in the blanket assembly, the total number of traces in a harness segment is 91 at the inboard end, with 84 continuing to the outboard end of the harness segment (see Figure 4-30). The trace pattern is indexed (or shifted) towards the inside edge of the harness segment, creating room for seven pads at the outside edge of the outboard end of the harness segment for a total of 91 pads. These 91 pads are soldered to the 91 pads on the inboard end of the next harness segment. Depending on the SPA location, some of the traces in a segment are used to continue the trace run from one outboard SPA down to the base of the blanket and the diode box. Other traces in the segment are not used for electrical purposes but only provide "structural" continuity along the harness run.

4.3.3 Circuit Protection

Each electrical harness run comes off the inboard leader panel at the bottom of the blanket assembly, goes through a slotted hole in the pallet sandwich panel, and terminates in a diode box assembly (see Figure 4-31). The diode box assembly is mounted on the inboard surface of the pallet. The diode assembly box is constructed from aluminum and is approximately 0.25 x 0.30 x 0.025 mm (10 x 12 x 1 inch) in size (see Figure 4-32). The box is attached to a piano hinge

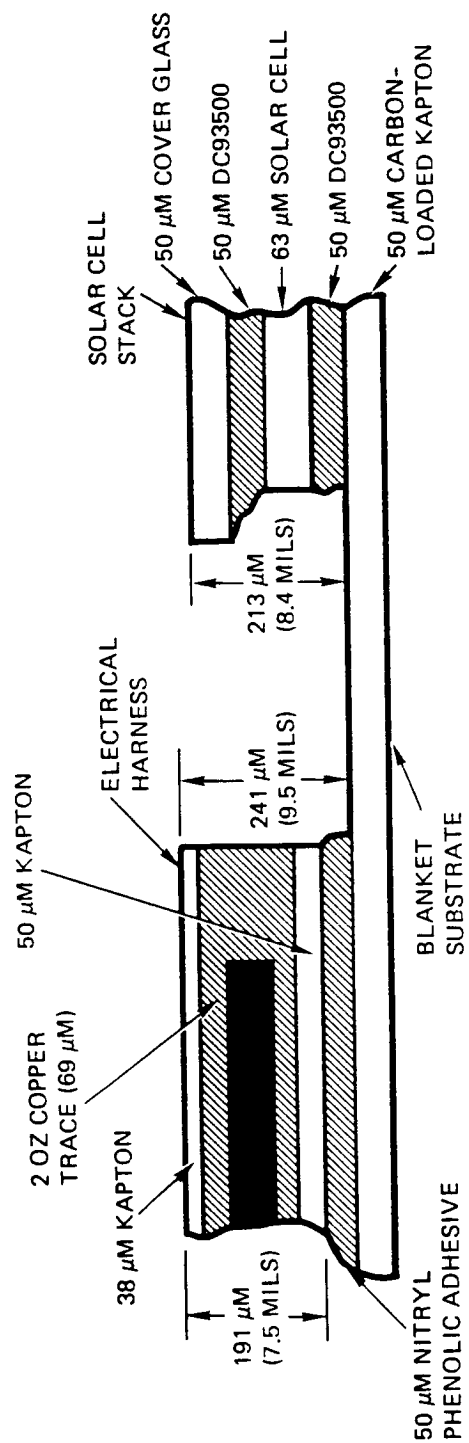


Figure 4-28. Comparative Thickness of Electrical Harness to Solar Cell Stack

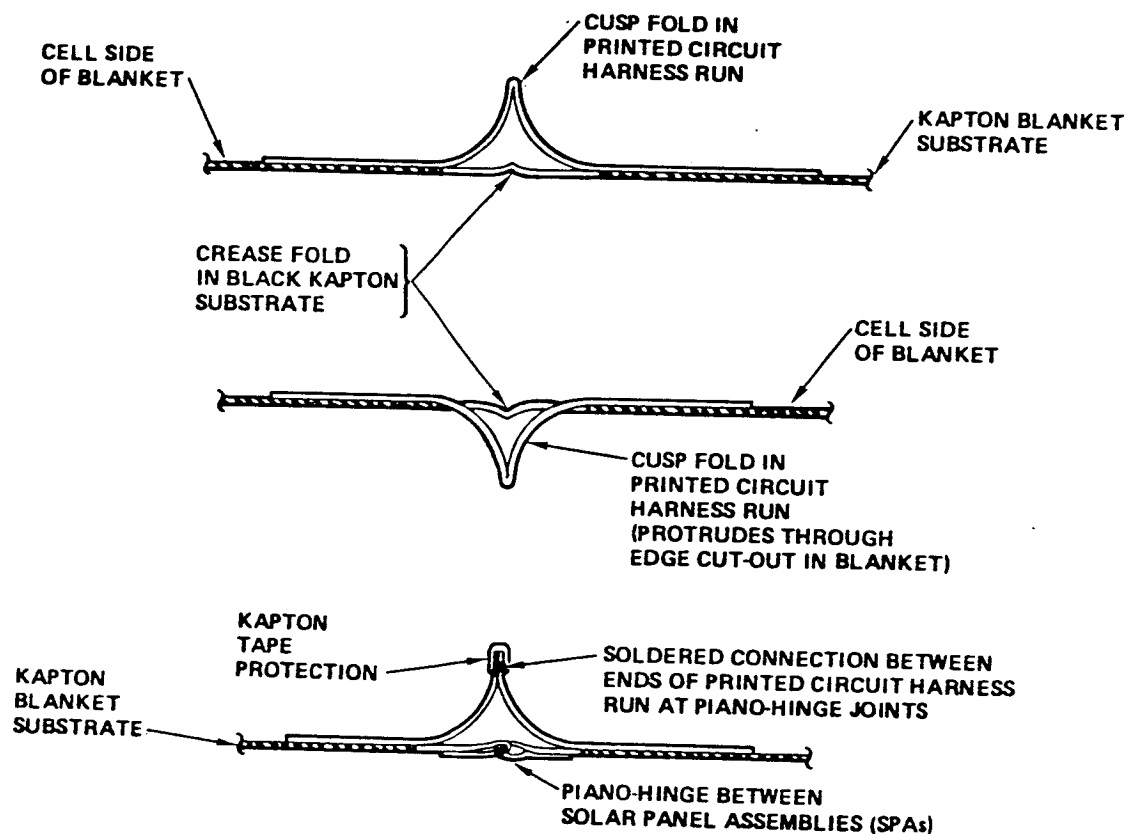


Figure 4-29. Electrical Harness Hinge Line and Splice Details

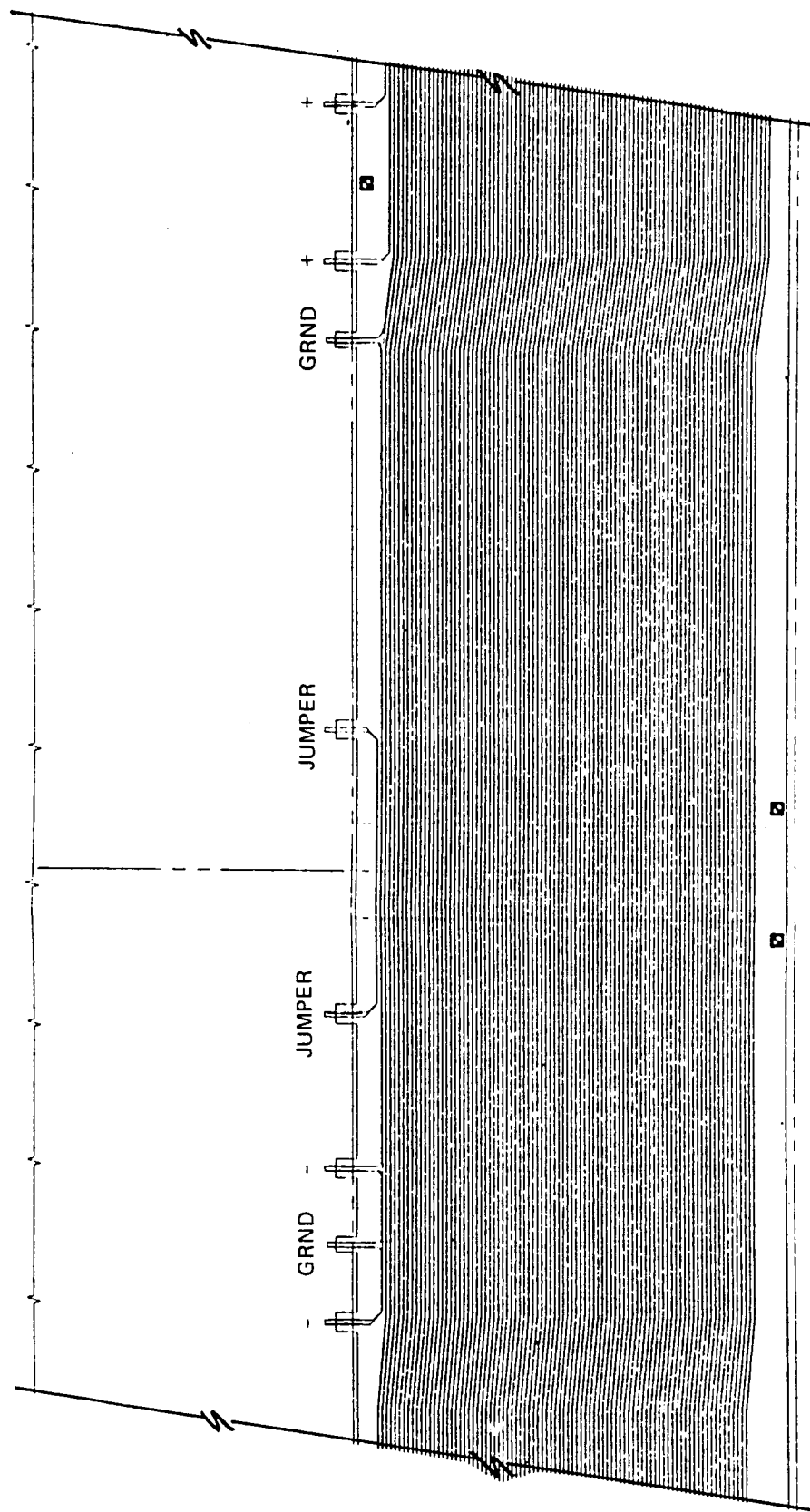


Figure 4-30. Details of Positive, Negative, and Panel Substrate Grounding Terminations for Electrical Harness

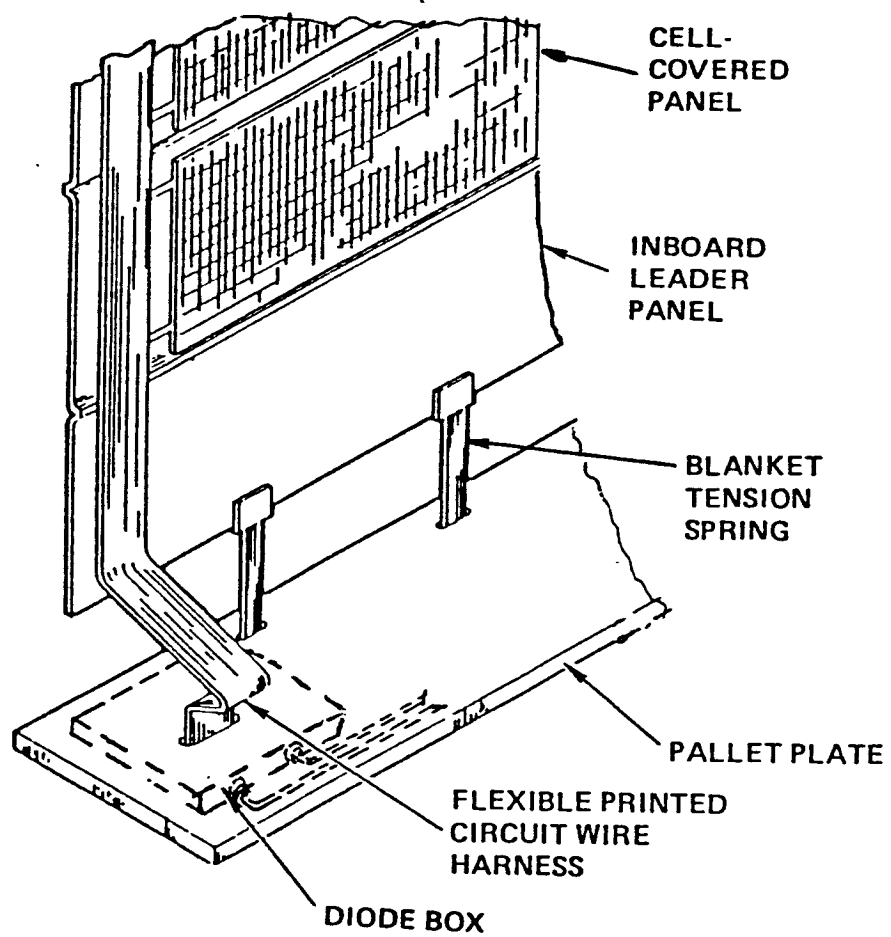


Figure 4-31. Location of Diode Box

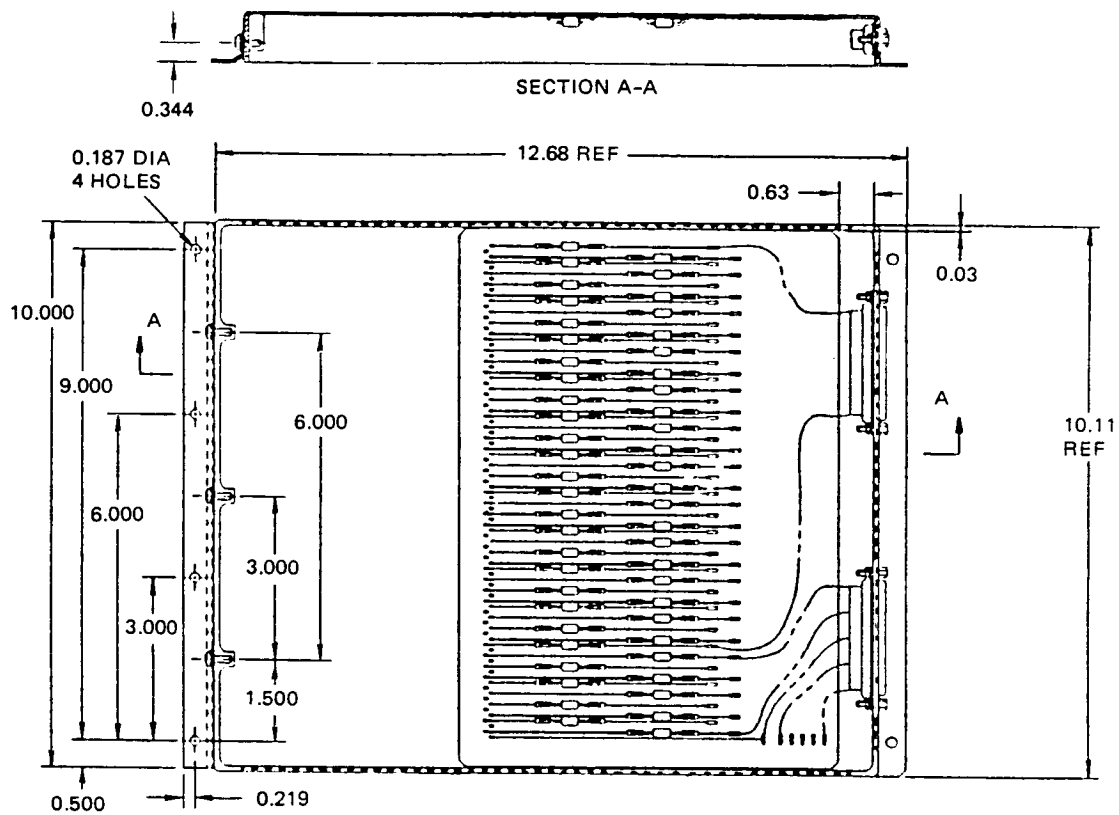


Figure 4-32. Diode Box Assembly

fitting that permits it to swing away from the pallet for easy access to the harness termination on the inside surface of the box.

The diode box circuit diagram is schematically shown in Figure 4-33. Each box contains 52 IN5811 silicon, high-power, fast-recovery, double-plug, solid monolithic diodes (6 amperes, 150 volts), one for each of the 52 circuits that terminates in the box. The diode is mounted to a rigid circuit board that is bonded directly to the inside of the box to maximize the thermal dissipation to space (see Figure 4-34). Each positive termination is connected to a single diode on the board. Pads for the diodes have a thermal path via plated through-holes to the mounting side of the board. Copper land areas were maximized in size for optimum thermal dissipation. Negative terminations are passed electrically from the front to back of the board and are bussed together.

Connection is made via hardwires from each diode and from several points on the negative bus to two 50-pin connectors mounted on the side of the diode box (refer back to Figure 4-32). These electrical connectors represent the electrical interface between the solar array wing and the spacecraft SADA harness.

4.4 ARRAY PERFORMANCE

4.4.1 Electrical Output

Figure 4-35 shows the BOL and EOL electrical performance characteristics for the two-wing array that consists of 39 cell-covered panels per wing blanket assembly. Each panel contains 960 2 x 4 cm cell stacks for a total of 37,440 cells per blanket assembly. Array BOL power is 10,388 watts at 176 volts; EOL power is 7,382 watts at 146 volts. BOL open circuit voltage is 210 volts. All voltage values are with reference to the output of the diode box at the pallet structure. The array as shown is capable of producing slightly more power than indicated. In reality, three-quarters of the second panel of the outboard leader assembly could also be covered with solar cells, thereby adding two 360-cell circuits to each wing. This would increase the array power output by approximately 150 to 200 watts, resulting in BOL power of 10,588 watts and EOL power of 7,524 watts.

The key solar array electrical sizing factors and cell degradation characteristics upon which the electrical performance was derived are in Figure 4-36 and Table 4-2. Total EOL 10-year GEO 1 MEV, equivalent electron fluence (including solar flare radiation) was about 2×10^{15} e/cm², resulting in a power degradation of about 23 percent. Harness and diode losses were assumed to be about 3 percent. The BOL/EOL cell operating temperature was about 27°C/32°C, resulting in very small temperature-induced losses. These operating temperatures were based on non-operating cell solar absorptance of 0.72, cell hemispherical emittance of 0.86, and a substrate hemispherical emittance of 0.86.

The net ratio of EOL to BOL sizing factors of $0.702 \div 0.967 = 0.72$ was less than that inferred from a ratio of the EOL to BOL specific power goals of $105 \div 130 = 0.81$. For minimum weight array designs where the solar cell shielding is reduced to minimum acceptable values (i.e., 50 to 75 μ m [2 to 3 mils] of equivalent fused silica per surface), it is unlikely to be able to achieve EOL/BOL power ratios near 0.80 for a 10-year GEO mission using today's silicon solar cells.

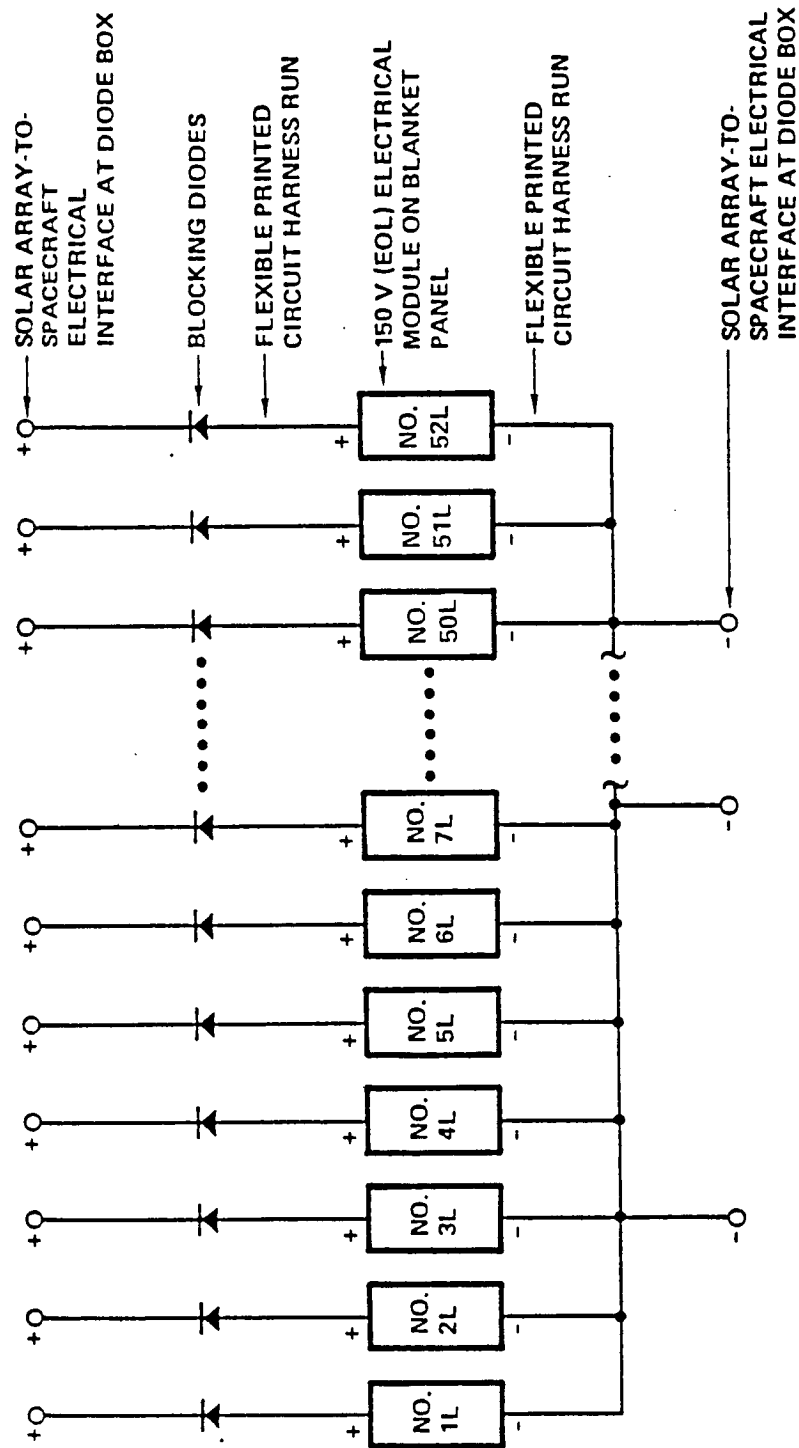


Figure 4-33. Schematic Circuit Diagram of Diode Box
(Left-Hand Harness Run Shown)

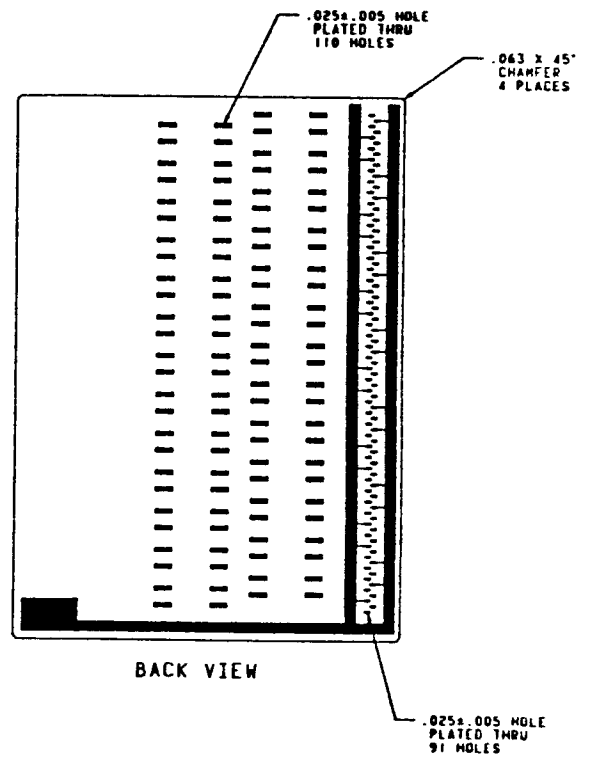
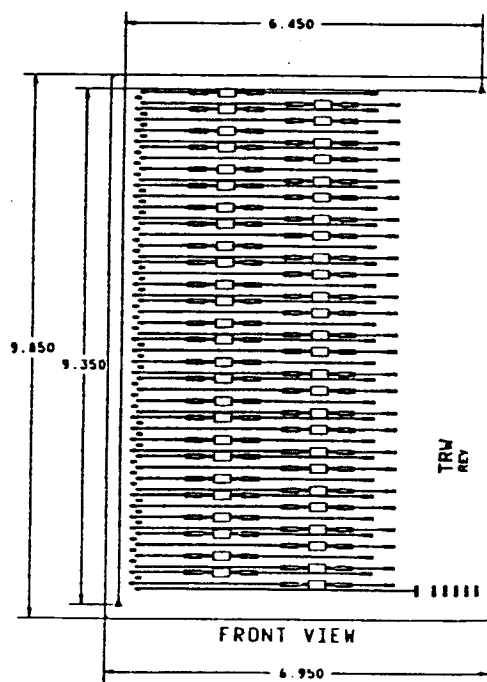


Figure 4-34. Diode Board Assembly Details

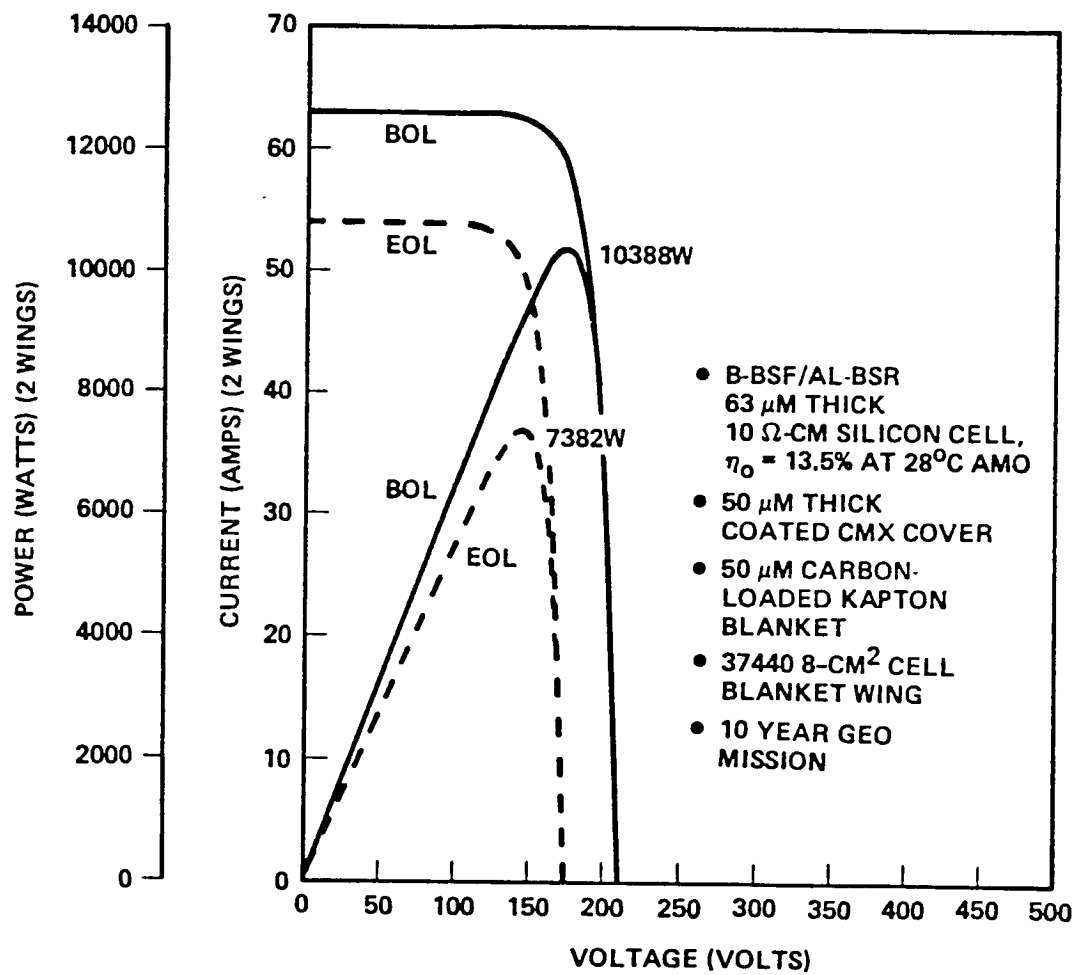


Figure 4-35. BOL and EOL Solar Array Electrical Performance (Two Wings), 10-Year Geosynchronous Mission

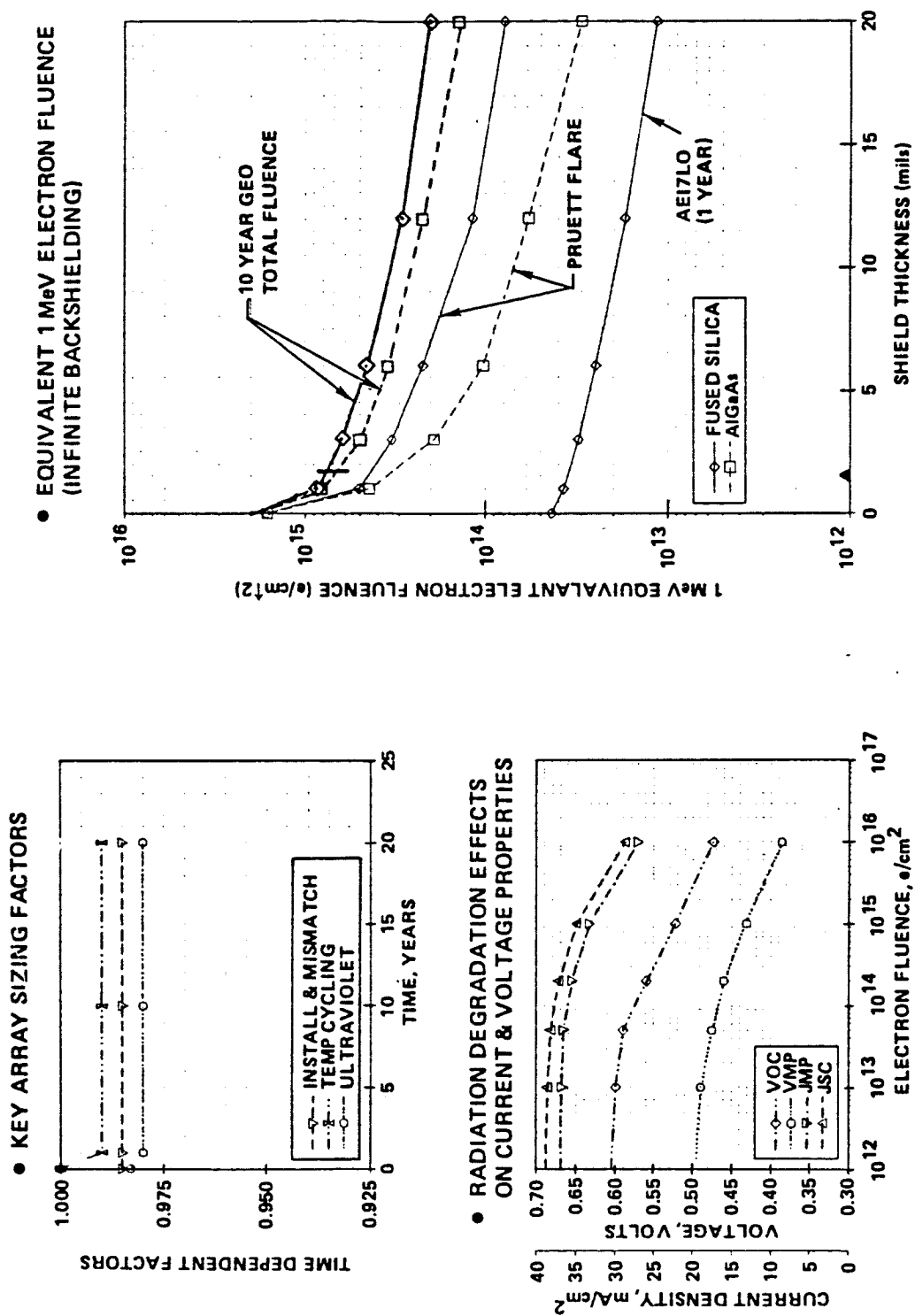


Figure 4-36. Solar Cell Module Design Parameters

Table 4-2. BOL and EOL Design Factors Used for Sizing the Solar Array 10-Year
Geosynchronous Mission (Ceria-Doped Glass-Covered 10 Ω -cm,
B-BSF/Al-BSR, 63 μ m Silicon Cell)

PARAMETER	BOL	EOL
INSTALLATION AND MISMATCH ULTRAVIOLET	0.985 1.000	0.985 0.980
TEMPERATURE CYCLING	1.000	0.990
COVER DARKENING	1.000	1.000
ADHESIVE DARKENING	1.000	1.000
LOW ENERGY PROTONS	1.000	1.000
I _{SC} DEGRADATION	1.000	0.889
I _{MP} DEGRADATION	1.000	0.887
V _{MP} DEGRADATION	1.000	0.886
V _{OC} DEGRADATION	1.000	0.856
P _{MP} DEGRADATION	1.000	0.767
I _{SC} TEMP COEFF	0.048%/°C	0.048%/°C*
V _{OC} TEMP COEFF	-2.10 mV/°C	-2.10 mV/°C*
DIODE AND HARNESS LINE LOSS OPERATING TEMP	0.975 (3.75V) 26.5°C (1.007)	0.975 (3.75V) 31.7°C (0.983)
• NET SIZING PARAMETER AT P _{MP}	0.967	0.702
<ul style="list-style-type: none"> • P_{MP} EOL/BOL = 0.72 • CELL PACKING FACTOR = 0.96 • PANEL PACKING FACTOR (W/O HARNESS) = 0.84 • PANEL PACKING FACTOR (WITH HARNESS) = 0.77 		

*CONSERVATIVELY ASSUMED THAT THE EOL VALUE WAS THE SAME AS BOL VALUE. IN REALITY THE I_{SC} COEFFICIENT INCREASES WITH RADIATION; WHEREAS THE V_{OC} COEFFICIENT REMAINS RELATIVELY CONSTANT. THE NET EFFECT ON EOL POWER IS SMALL SINCE THE OPERATING TEMPERATURE IS NEAR 28°C

4.4.2 Dynamics and Strength Characteristics

4.4.2.1 Deployed Dynamic Characteristics

NASTRAN finite element models of the baseline wing were developed to estimate the dynamic characteristics. Quadrilateral plate elements were used to represent the blanket assembly. The effective stiffness of these plate elements was almost entirely due to the blanket tension load. The distributed mass was based on the weight predictions for the blanket assembly. The pallet and lid structures were modelled as quadrilateral plate elements, using stiffness and mass properties representative of their design. The mast was modeled by individual bar elements, using stiffness and mass properties provided by the mast subcontractors.

The model had 154 nodes, 218 beam elements and 78 membrane/plate elements, with 99 dynamic degrees of freedom. The mast bending stiffness was $9.2 \times 10^3 \text{ N-m}^2$ ($3.2 \times 10^5 \text{ lb-in}^2$), and the torsional stiffness was $4.9 \times 10^3 \text{ N-m}$ ($1.7 \times 10^5 \text{ lb-in}$), which corresponds to an 0.21 m (8.2-inch) diameter tri-longeron mast with 3.8 mm (0.15-inch) diameter fiberglass longerons. Blanket tension was 63 N (14 pounds). The wing was cantilevered from the inboard end of the mast canister. The distance from the plane of the blanket to the mast centerline was about 0.20 m (8 inches), which corresponds to a mast/blanket physical separation of about 0.15 m (6 inches).

Figure 4-37 illustrates the mode shapes and cantilevered frequency levels for the first four modes. The fundamental frequency is about 0.11 Hz and is represented by out-of-plane bending of the wing with mast and blanket in phase. The first torsion mode is at 0.26 Hz. The first blanket flapping mode is at 0.28 Hz. The dynamic characteristics could easily be modified to obtain higher or lower fundamental frequency values by adjusting the stiffness of the mast system.

4.4.2.2 Deployed Strength

Static structural analysis was performed by one of the mast subcontractors (AEC-Able Engineering) for the baseline wing configuration. Design trades were performed to define mast characteristics that would provide sufficient strength to survive 0.01 to 0.05 g static loads when the wing was fully deployed. For the baseline mast size, the deployed wing strength was about 0.015 g. The failure mode for this loading level is buckling of one longeron between batten frames at the root of the mast. With a blanket tension load of 63 N (14 pounds), the relative deflection of the blanket with respect to the mast is about 76 mm (3 inches), thereby leaving 76 mm (3 inches) of clearance between the blanket and mast structure near the mid-length region of the mast. Trade studies also indicated that by using different size masts, deployed strength up to 0.05 g can be obtained for an additional 2.3 kg (5 pounds) weight penalty. Blanket tension level would have to increase to 220 to 270 N (50 to 60 pounds) for the 0.05 g load capability to prevent the blanket from hitting the mast.

Another method of increasing the strength of the mast, without having to change the mast/longeron diameters, is to add batten frames and diagonals between the existing batten frames, thereby reducing the unsupported length of the longeron between batten frames by a factor of 2. This will increase the buckling strength by at least a factor of 3 to 3.5. This approach would increase the mast system weight and reduce the packaging efficiency of the mast.

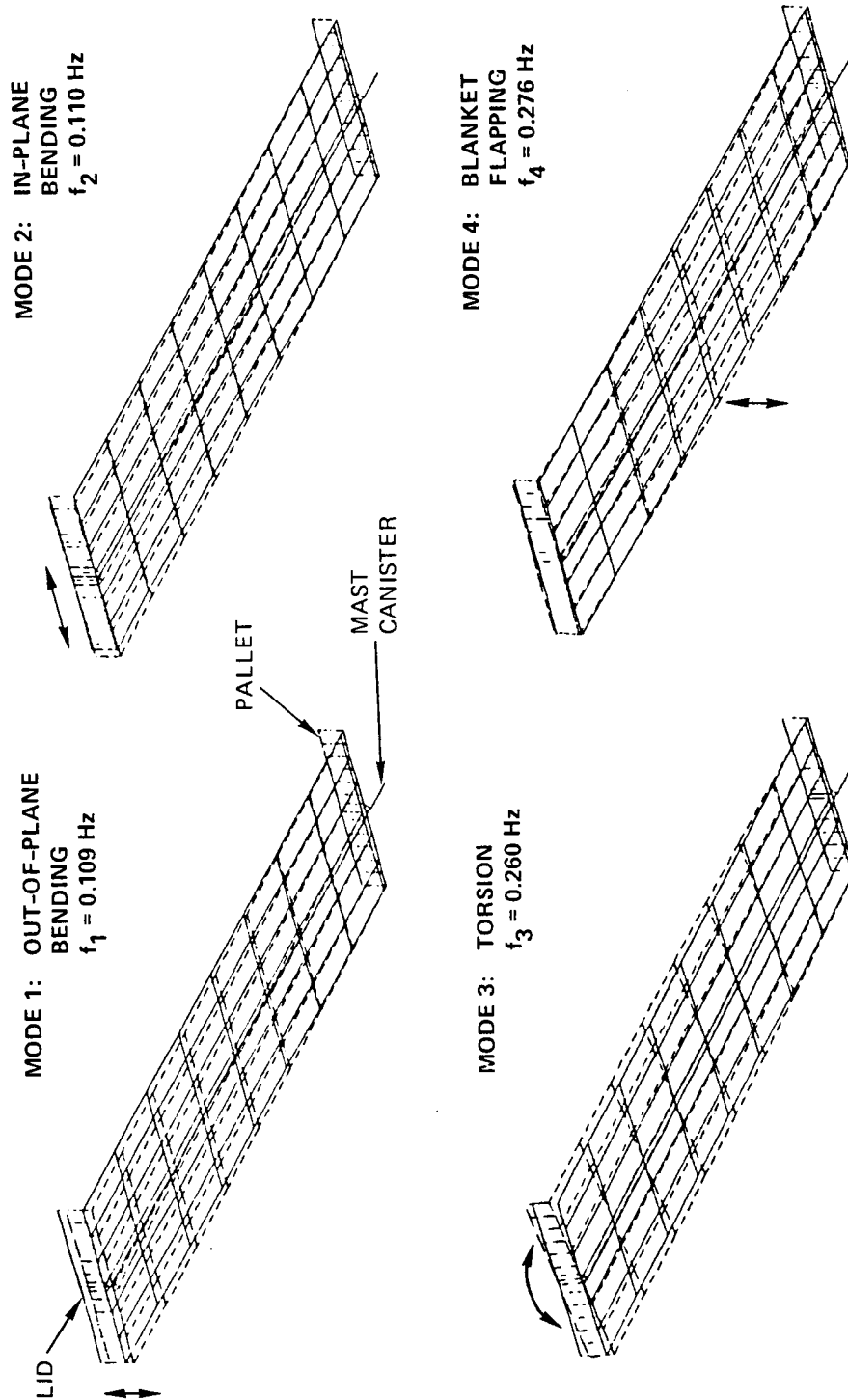


Figure 4-37. Baseline Wing Cantilevered Frequency and Mode Shape Characteristics
 ($EI = 9.2 \times 10^3 \text{ N-m}^2$ [$3.2 \times 10^6 \text{ lb-in}^2$], Blanket Standoff = 0.15 m
 (6 inches), Blanket Tension = 63 N [14 Pounds])

4.4.2.3 Stowed Strength

A NASTRAN finite element model of the stowed solar array wing was developed to determine the interface loads at the spacecraft-to-solar array wing attachment locations and to ensure that the major structural elements and local reinforcements had been properly sized to withstand the shuttle launch loading environment. The calculated interface loads were used by the mast vendor to resize the mast canister structure and to ensure that the attachment flanges on the canister structure could adequately react the loads induced upon it from the blanket housing assembly (with stowed blanket assembly).

The limit static loads were: $N_z = 10.4$ g's, $N_y = 8.04$ g's, $N_x = 7.5$ g's, where the Z-direction is along the mast canister axis, the Y-direction is along the length of the blanket housing assembly, and the X-direction is normal to the YZ plane as illustrated in Figure 4-38. The stowed wing was assumed to be attached to the spacecraft sidewall at four locations: at the base of the mast canister, and at three locations along the outer edge of the pallet structure as indicated in the figure.

Figure 4-38 indicates the magnitude of the interface limit loads determined from the NASTRAN analyses. Localized stress and stiffness analyses were performed on the mast canister, the pallet structure, and diagonal struts to ensure adequate structural integrity of the local structure, using 1.40 as the factor of safety on the limit loads shown.

4.4.2.4 Deployed Deflection Characteristics

Figure 4-39 illustrates the deflected equilibrium shape of the wing under a blanket tension load of 63 N (14 pounds), with no external inertia loads. The blanket off-pointing angle is about 1 degree and the maximum mast tip displacement is +0.18 m (7 inches) relative to the mast root.

Figure 4-40 illustrates the wing deflected shape when subjected to a quasi-static inertia load of 0.01 g (ultimate) uniformly applied normal to the blanket plane. For one condition, the maximum mast tip displacement is 0.43 m (17 inches) relative to the mast root (0.25 m [10 inches] due to the 0.01 g inertia load), with a blanket displacement of 0.15 m (6 inches) thus resulting in a 0.3 m (12-inch) separation between the blanket and mast near the midlength of the mast. For the other condition, the maximum mast tip displacement is 25 mm (1 inch) relative to the mast root (0.15 m [6 inches] due to the 0.01 g inertia load), with a blanket displacement of 25 mm (1 inch) towards the mast thus resulting in a net separation distance of 0.13 m (5 inches) between the blanket and mast near the midlength of the mast.

4.4.3 Specific Power and Power Density

4.4.3.1 Wing Weight

Table 4-3 presents the weight breakdown for the baseline wing. The wing has a deployed frequency of 0.11 Hz and a deployed ultimate static strength of 0.015 g. Without contingency, total wing weight is about 35 kg (77 pounds); with a 10 percent contingency, total wing weight is (38.2 kg) 84 pounds. The weights for the blanket assembly accounts for about 50 percent of the total wing weight. The electrical components weight (solar cell stacks, wiring, electrical harness,

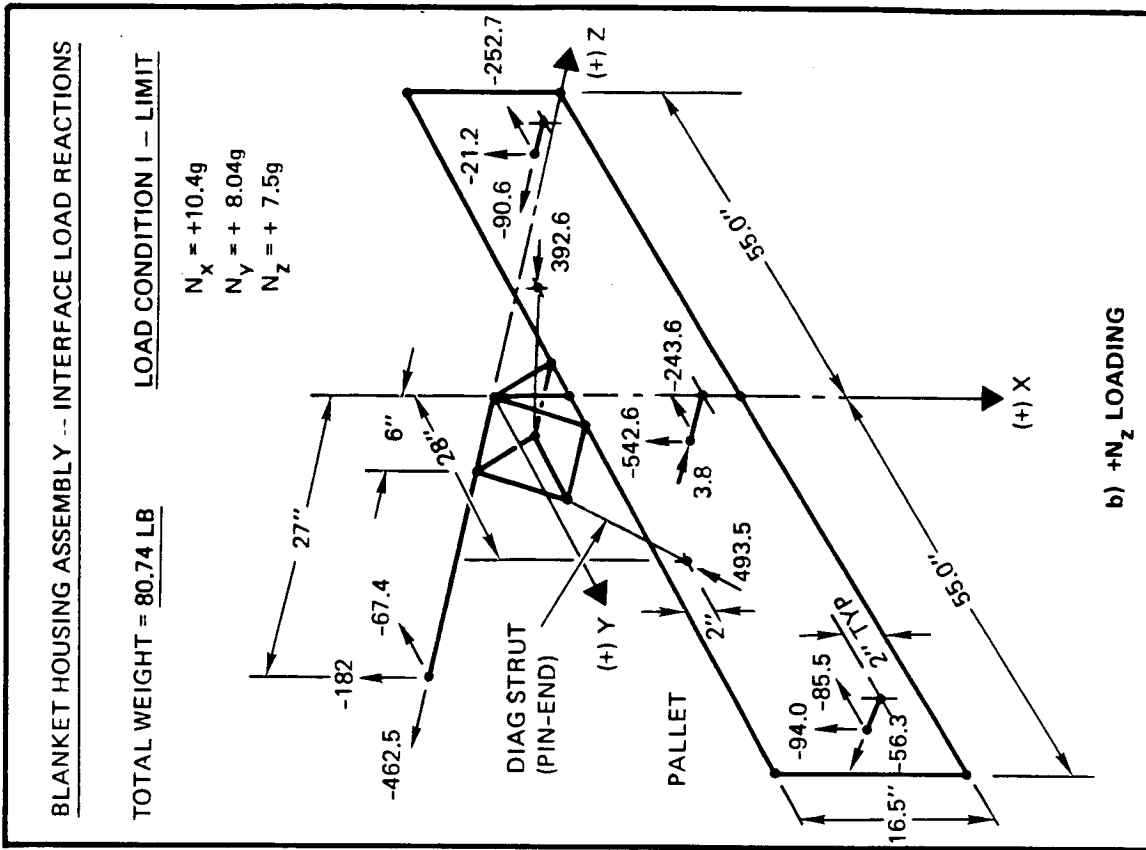
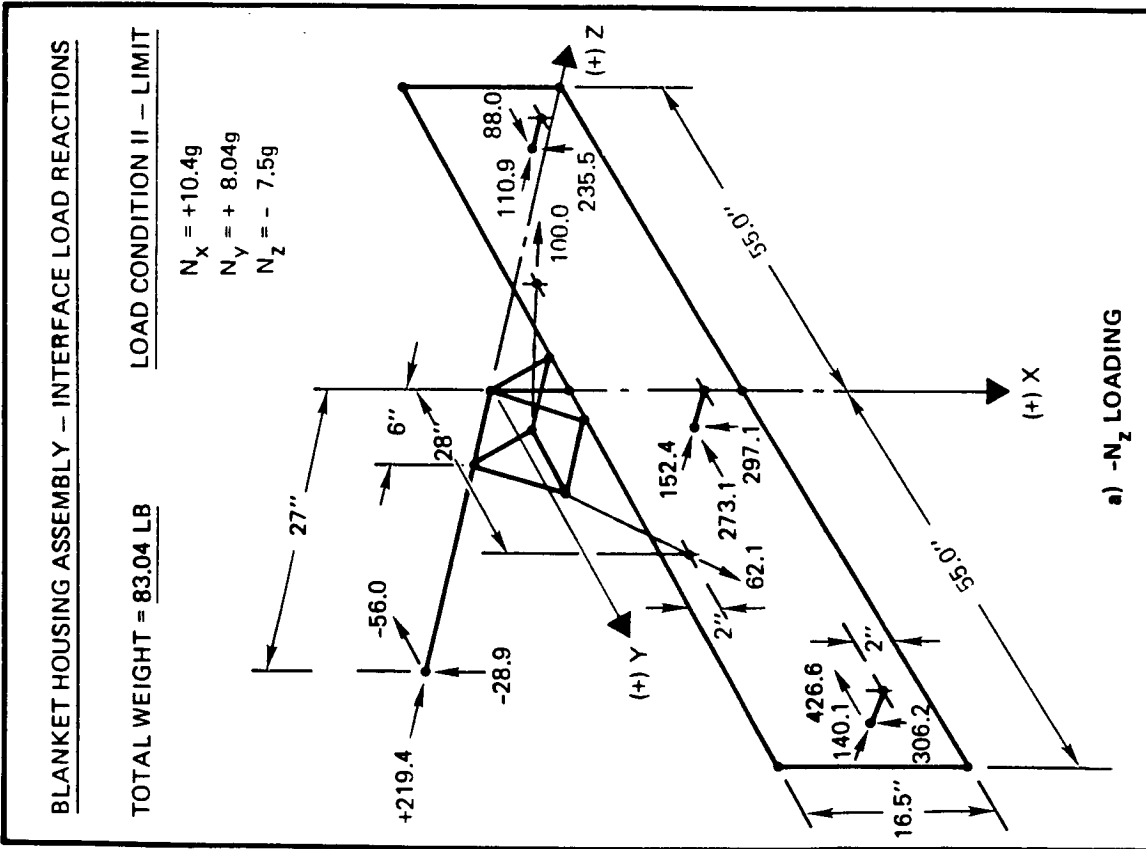


Figure 4-38. Stowed Solar Array Wing, Shuttle Launch Interface Limit Loads (loads in lbs).

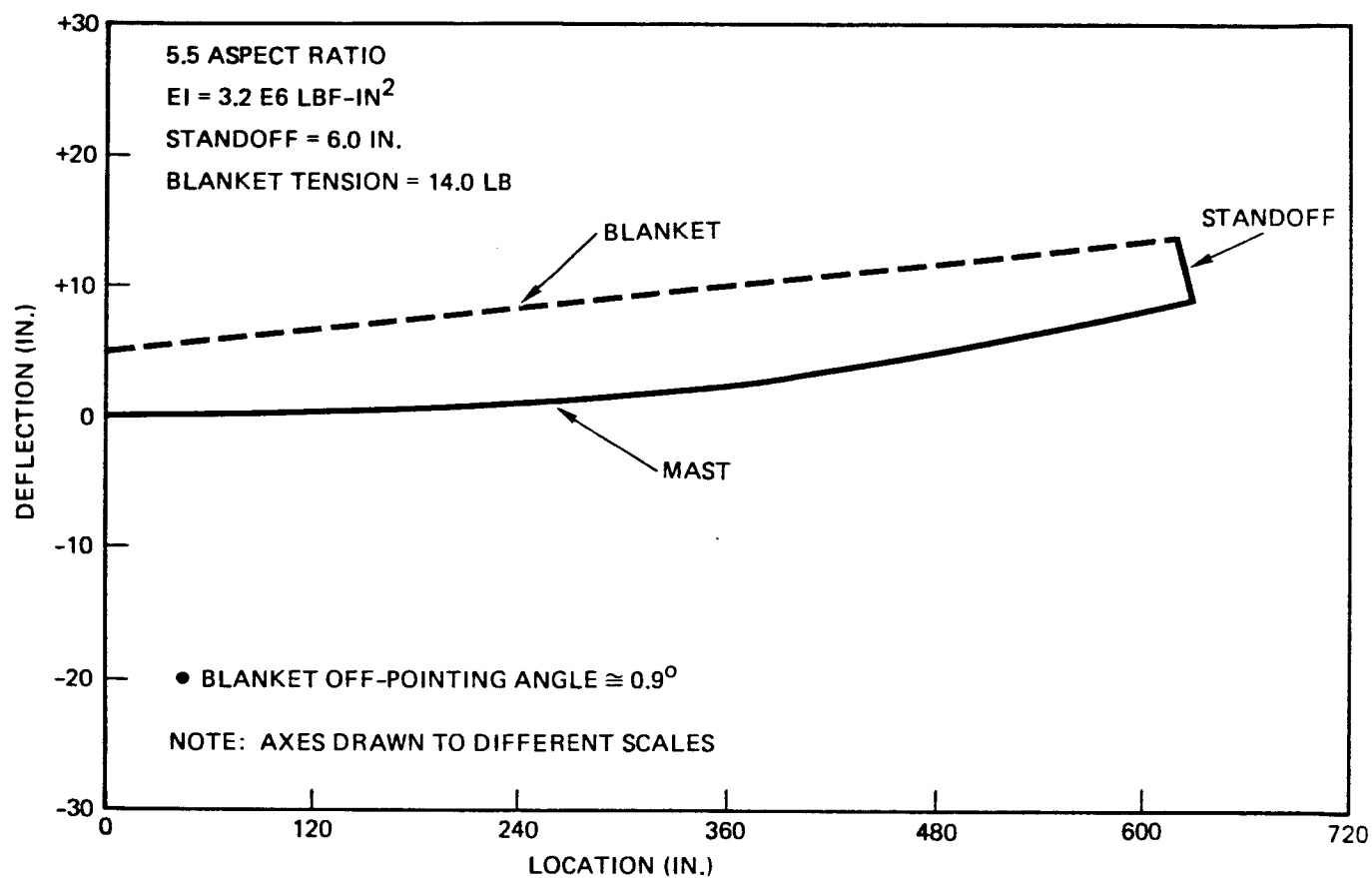
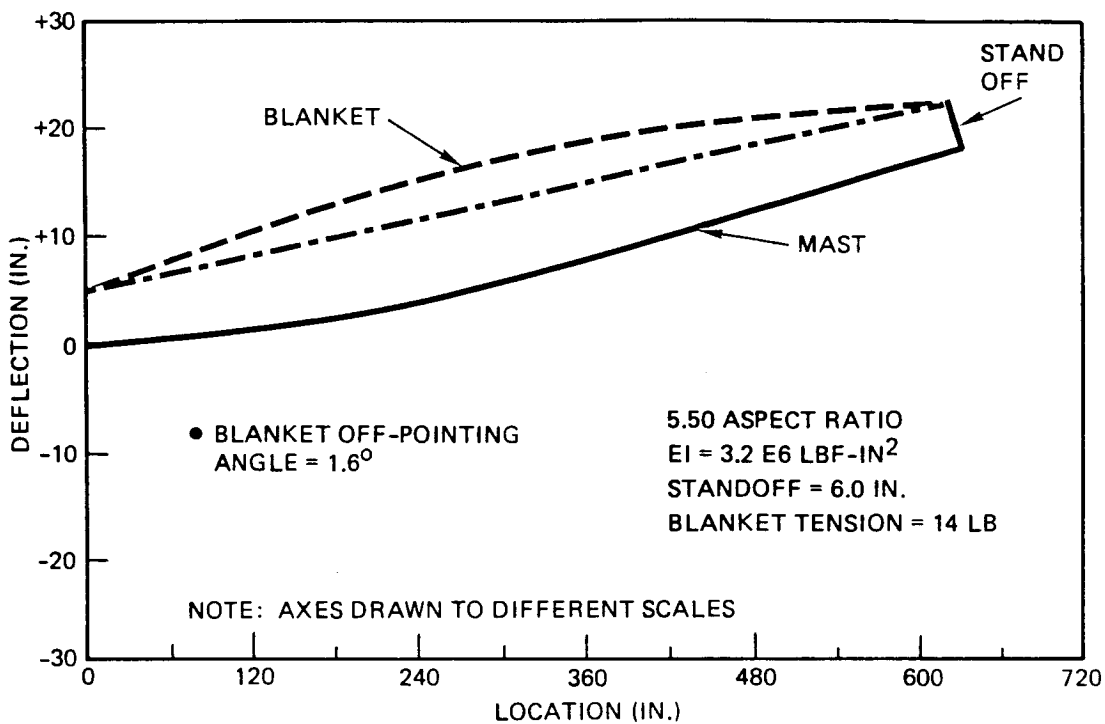
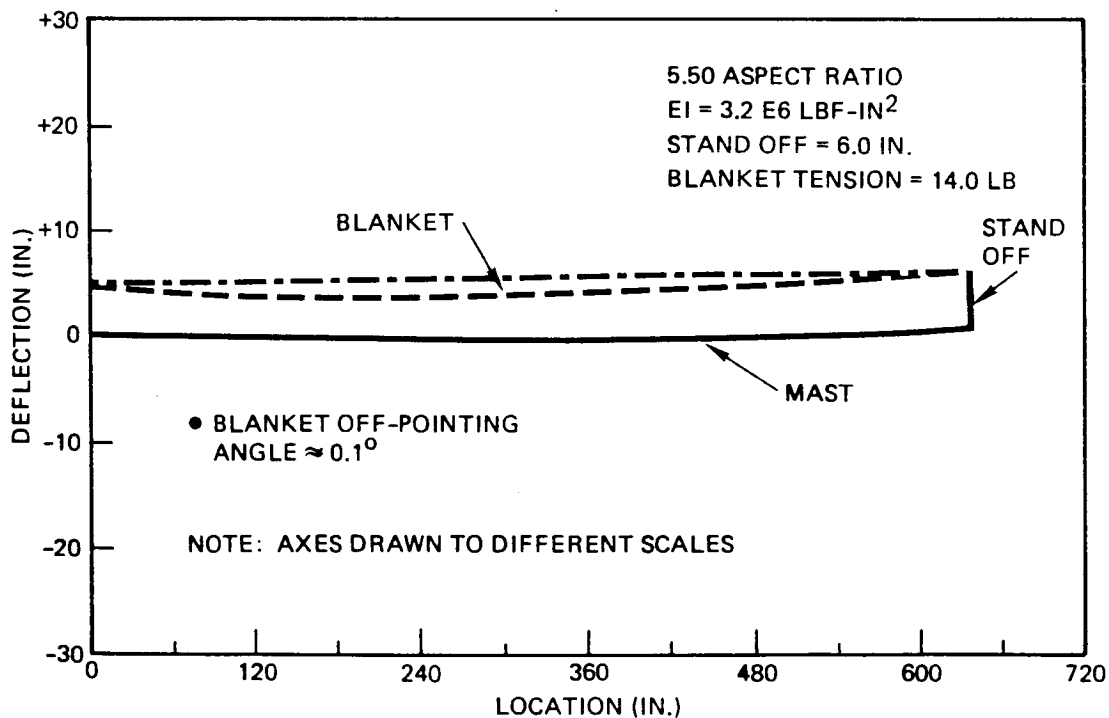


Figure 4-39. Wing Equilibrium Deflection Shape (Wing Deflection Due to Offset Blanket Tension Load)



a. +0.01 g LOADING



b. -0.01 g LOADING

Figure 4-40. Wing Deflected Shape Under Maximum Inertia Loading (0.01 g Ultimate Uniformly Distributed Normal to Blanket Plane)

Table 4-3. Baseline Solar Array Wing Weight Summary, BOL/EOL
Power of 5200/3700 Watts, $F_N = 0.11$ Hz, $N = 0.015$ g

• BLANKET ASSEMBLY (39 CELL-COVERED AND 3 LEADER PANELS; 1 BLANKET)		37.47 LB
SUBSTRATE (2 mil CARBON-LOADED KAPTON, XC10 ¹⁰)	7.55	
HINGE PIN (0.05 IN. DIA G/E ROD; 16 REQD)	0.17	
HINGE REINFORCEMENTS (NYLON RIPSTOP)	0.25	
SOLAR CELL (2.5 mil x 2 x 4 cm; BSF/R; SILICON; 128 mg/CELL; 37440 CELLS)	10.54	
CELL-TO-SUBSTRATE ADHESIVE (1.5 mil DC93500)	2.47	
COVERGLASS (2 mil CMX; 106 mg/COVER; 37440 COVERS)	8.47	
COVERGLASS ADHESIVE (2 mil DC93500)	3.62	
INTERCONNECTORS/TERMINATION STRIPS (1 mil Ag-PLATED INVAR)	0.92	
ELECTRICAL HARNESS (2 OZ CU; PRINTED CIRCUIT; 1 mil KAPTON)	2.88	
HARNESS ADHESIVE (2 mil NITRYL PHENOLIC)	0.60	
• BLANKET HOUSING ASSEMBLY (1 PER WING)		23.69 LB
LID STRUCTURE (0.5 IN. SANDWICH; 10 mil G/E F/S)	4.89	
PALLET STRUCTURE (0.5 IN. SANDWICH; 10 mil G/E F/S)	6.10	
PROTECTIVE FOAM LAYER (0.5 IN. TA-301 POLYIMIDE; 2 REQD)	1.19	
BLANKET PRELOAD/RELEASE MECHANISM (8 LATCHES; AEROFLEX MOTOR)	3.44	
BLANKET TENSION SYSTEM (7 NEGATORS AT 2 LB TENSION EACH)	0.24	
BLANKET GUIDEWIRE SYSTEM (2 UNITS AT 1 LB TENSION EACH)	2.60	
LID/MAST INTERFACE FITTING	0.56	
PALLET/MAST INTERFACE HARDWARE	1.34	
WING/SPACECRAFT ATTACHMENT LUG FITTINGS (3 REQD)	0.15	
DIODE BOX HARDWARE (2 REQD)	1.42	
DIODE BOX BOARD AND DIODES/CONNECTORS (2 SETS REQD)	1.26	
• BLANKET DEPLOYMENT ASSEMBLY (COILABLE F/G LATTICE MAST)		15.35 LB
MAST (F/G 8.2 IN. DIA; 0.15 IN. DIA LONGERONS; 633 IN. LONG)	7.17	
MAST CANISTER WITH S/C ATTACHMENT FTG (ALUM, 27 IN. H x 9 IN. DIA.)	7.22	
ACTUATOR (AEROFLEX DC BRUSHLESS, ELECT REDUNDANT)	0.96	

SPECIFIC POWER CONDITION	W/O CONTINGENCY	WITH CONTINGENCY
BEGINNING-OF-LIFE	149.8 W/kg	136.1 W/kg
END-OF-LIFE*	106.4 W/kg	96.7 W/kg

*10 YEAR GEO

WITHOUT CONTINGENCY	76.5 LB (34.7 kg)
10% CONTINGENCY	7.65 LB
TOTAL WING WEIGHT	84.15 LB (38.2 kg)

diode box, adhesive layers) represents about 40 percent of the total wing weight, with non-electrical components/hardware accounting for 60 percent of the total wing weight.

The weights for the blanket substrate, hinges, diode boxes, electrical harness, and blanket housing assembly were derived from the detail engineering drawings. The weight for the blanket deployment mast system was obtained from detail design analysis by one of the mast subcontractors, AEC-Able Engineering. Solar cell module weight was based on measurements of representative hardware components.

4.4.3.2 Specific Power

Using wing BOL and EOL power of 5194 watts and 3691 watts, respectively, the BOL and EOL specific power, without considering contingency, is 150 W/kg and 106 W/kg, respectively. If a 10 percent contingency on weight is included, the BOL and EOL specific power becomes 136 W/kg and 97 W/kg.

If solar cells are added to a portion of one of the three blank leader panels as discussed in Section 4.4.1, the power output will increase about 2 percent and the wing weight will increase about 1 percent. With this slightly modified design, BOL and EOL specific power become 137 W/kg and 98 W/kg, with a 10 percent contingency.

4.4.3.3 Power Density

The panel area is about 1 m^2 (10.8 ft^2), which includes the area between adjacent fold lines and the electrical harness area. Based on 960 $2 \times 4 \text{ cm}$ cells per panel, with a net EOL output of about 95 watts measured at the diode box, the EOL power density is about 95 W/m^2 .

4.5 DESIGN MATURITY/EQUIPMENT LIST

While the proposed design represents a significant improvement in specific power performance over current solar arrays, it is based on the use of existing or near-term available components such that a prototype wing can be fabricated and demonstration-tested on the ground by late 1987.

Table 4-4 presents a summary equipment list of the key array components. Status of components/materials/subassemblies can be categorized as: off-the-shelf, special order/special fabrication, or developmental. All solar cell stack components (solar cells, cover glass, enhanced emittance filter coating, UV-filter coating, interconnectors, diodes) are presently available from various sources. The fabrication, assembly, installation, and long-term thermal cycle testing of the proposed solar cell stack has been accomplished under NASA-sponsored and TRW IR&D-sponsored programs. The diode box design requires special order using conventional fabrication processes. The flexible printed circuit harness is a special order item; however, there are two suppliers who can produce the parts using existing fabrication processes.

The blanket substrate design uses existing materials and is of a configuration similar to that used on other developmental and flight hardware programs. The major issues with the blanket are: (1) the ability to handle and process the blanket and (2) its kinematic behavior during zero gravity deployment operations.

Table 4-4. Solar Array Wing Equipment List

ITEM (DWG NO.)	DESCRIPTION	QTY PER WING	HERITAGE
SOLAR CELL (X700001)	10 Ω -CM B-BSF/AL-BSR SILICON; 2 x 4 cm x 65 μ m THK; η_p = 13.5% AT 28°C AMO	37440	AVAILABLE FROM 4 CELL VENDORS (ASEC, SL, SOLAREX, AEG); TRW HAS PROCESSED CELLS UNDER JPL CONTRACT
COVERGLASS (X700001)	2.015 x 4.015 cm x 50 μ m THK; CERIA-DOPED GLASS	37440	AVAILABLE FROM PILKINGTON; TRW HAS PROCESSED COVERS UNDER JPL CONTRACT
CELL STACK ADHESIVE	DC93500	—	STANDARD STOCK MATERIAL; AVAILABLE FROM DOW CORNING; USED ON TRW ARRAYS
INTERCONNECTOR	IN-PLANE STRESS RELIEF LOOP; 25 μ m THK Ag-PLATED INVAR COATED WITH SOLDER	74880	STANDARD TRW STOCK ITEM; TRW HAS PROCESSED THESE INTERCONNECTORS ON CONTRACT/IRAD PROGRAMS USING WELDING OR SOLDERING
ELECTRICAL HARNESS (X700006, 7, 8)	KAPTON INSULATED (1 AND 2 MIL) FLEXIBLE PRINTED CIRCUITS (7 MIL THK); 4.5" WIDE x 45" LONG SEGMENTS WITH 91 TWO-OZ COPPER TRACES	2 RUNS OF 15 SEGMENTS EACH	FABRICATED USING STANDARD PROCESSES BY SHELDHAHL
DIODES	SILICON, HIGH POWER, FAST RECOVERY, DOUBLE PLUG, SOLID MONOLITHIC; 6A; 150V	104	STANDARD TRW STOCK ITEM (1D013); (SIMILAR TO IN5811)
DIODE BOX ASSEMBLY (X700010, 13, 15)	10 x 12 x 1" ALUM BOX WITH PRINTED CIRCUIT BOARD FOR DIODE INSTALLATION	2 ASSEMBLIES	PROTOTYPE FABRICATED AND TESTED ON TRW IRAD PROGRAM
BLANKET ASSEMBLY (X142105, 119, 120) (X700000)	3-PANEL SPA ₂ ; 13 SPA ₂ PLUS 3 BLANK LEADER PANELS FOR FULL SIZE BLANKET (109x600")	1 ASSEMBLY	CONFIGURATION SIMILAR TO THAT FLOWN ON CTS, SAFE 1, OLYMPUS ARRAY; HOWEVER DIFFERENT MATERIAL
BLANKET MATERIAL	2 MIL THK CARBON LOADED POLYIMIDE KAPTON	453 FT ²	COMMERCIALY AVAILABLE FROM DUPONT (XC10 ¹⁰ OR XC10 ⁴ OR C601571-37)
BLANKET ADHESIVE	NITRYL PHENOLIC	—	USED IN TRW IRAD PROGRAM ON ULTRA- LIGHTWEIGHT FLEXIBLE BLANKET SOLAR ARRAYS
BLANKET HINGE PINS	50 MIL DIA PULTRUDED GRAPHITE/EPOXY RODS; 100" LONG	16	AVAILABLE FROM DIVERSIFIED FABRICA- TORS (1083-128)
BLANKET HOUSING ASSEMBLY (X142102, 103, 111)	2 — 0.5" THK HONEYCOMB PANEL SUBSTRATES WITH 0.5" THK POLYIMIDE FOAM ON INNER SURFACES	1 ASSEMBLY	STANDARD SPACECRAFT STRUCTURE CONSTRUCTION
COMPOSITE MATERIAL IN BLANKET HOUSING ASSEMBLY	[0/90] LAYUP; 10 MIL TOTAL THK PER FACESHEET; GY70	—	STANDARD SPACECRAFT COMPOSITE MATERIAL
BLANKET PRELOAD AND RELEASE MECHANISM (X142101, 106, 107, 108, 112-118)	TORQUE-TUBE ACTUATED CABLE/LATCH SYSTEM	1 ASSEMBLY OF 8 LATCHES	CONCEPT DESIGNED; KEY PARTS EASILY FABRICATED/ASSEMBLED USING STANDARD PROCESSES
BLANKET PRELOAD ACTUATOR	ELECTRICALLY REDUNDANT DC BRUSHLESS MOTOR	1	AEROFLEX 18028 OR SPERRY 2960903 OR EQUIVALENT, MODIFIED TO DUAL WINDING
MAST SYSTEM (X366-003, 004, 005)	ALUMINUM CANISTER DEPLOYED CONTINUOUS LONGERON LATTICE MAST; 8.2" DIA MAST; 0.16" DIA FIBERGLASS LONGERONS	1 ASSEMBLY	PROTOTYPE UNIT FLOWN ON SAFE 1 WING; UNIT FABRICATED TO FLY ON OLYMPUS ARRAY; REQUIRES LIGHTWEIGHT CANIS- TER DEVELOPMENT; AVAILABLE FROM ABLE ENGRG OR ASTRO AEROSPACE
MAST DEPLOYMENT ACTUATOR	ELECTRICALLY REDUNDANT DC BRUSHLESS	1	AEROFLEX 16028 OR SPERRY 2960903 OR EQUIVALENT MODIFIED TO DUAL WINDING
BLANKET TENSION MECHANISM (X142109)	NEGATOR SPRING UNIT; 2 LB FORCE EACH; HUNTER SPRING SH6F21	7	COMPONENTS AVAILABLE FROM AMETEK; PROTOTYPE UNITS ASSEMBLED/TESTED ON TRW IRAD PROGRAM
BLANKET GUIDEWIRE MECHANISM (X142110)	NEGATOR SPRING TENSIONED CABLE REEL; 0.020" DIA BRAIDED STEEL CABLE HUNTER 40008 SPRING	2	COMPONENTS AVAILABLE FROM AMETEK; PROTOTYPE UNITS ASSEMBLED/TESTED ON TRW IRAD PROGRAM

The blanket housing assembly structure design is based on straightforward standard spacecraft construction using existing materials. Since these structures (lid, pallet, mast interface fittings) don't presently exist, they are classified as special-order items. The blanket preload, latching, and release mechanism is a unique design utilizing conventional materials and a combination of off-the-shelf and special fabrication items. The guidewire mechanism and the blanket tension mechanism are special order assemblies that utilize a combination of off-the-shelf and special fabrication items.

Of all major subassemblies proposed for the solar array, the blanket deployment mast system will need the most development work. The mast system is based on a lattice mast and deployment canister design that has flight experience (Olympus, SAFE I). However, the current hardware is too heavy, primarily the deployment/storage canister. A major development activity required during phase II of the APSA program is to fabricate a lightweight version of the canister structure and rotating drum nut deployment mechanism. Lightweight versions of the lattice mast structure have been built.

For flight hardware, electrically redundant DC brushless motors were proposed for actuation of the blanket housing assembly unlatching operation and for deployment of the mast. There are available non-redundant motor systems. Thus, for flight hardware, the motor designs will have to be modified and requalified. However, for the prototype wing developed under Phase II of APSA, simpler, less costly, off-the-shelf motors will be used.

4.6 UTILITY TO OTHER MISSIONS/REQUIREMENTS

The baseline design was analyzed as to its ability to accommodate other missions and to meet other functional and performance requirements without major modifications. The following sections illustrate that the baseline design has broad utility to meet other missions and requirements.

4.6.1 Scalability to Other Power Levels

Figure 4-41 shows the impact of power level on specific power performance using the baseline thin silicon solar cell module. Power growth (or reduction) is achieved by adding (or removing) SPAs from the blanket assembly, with appropriate redesign of the electrical harness and diode box assembly to account for the different number of electrical circuits. In fact, if less than 5.2 kW per wing is desired, even the electrical harness and diode box assembly do not have to be changed (they would carry the capacity for extra circuits not used).

For the 42-panel, 5.2 kW wing blanket assembly design, the height of the folded blanket assembly is only 11.4 mm (0.45 inch). Thus, the addition or removal of SPAs to increase or decrease power would not have a major effect on the blanket housing assembly. The lid and pallet structure, the folded blanket cushioning provisions, the latching/release mechanism, and the guidewire and tensioning mechanisms would remain virtually unchanged. If the baseline deployed frequency and strength characteristics were to be retained, then the mast system would have to be rescaled for length and diameter (as well as longeron diameter).

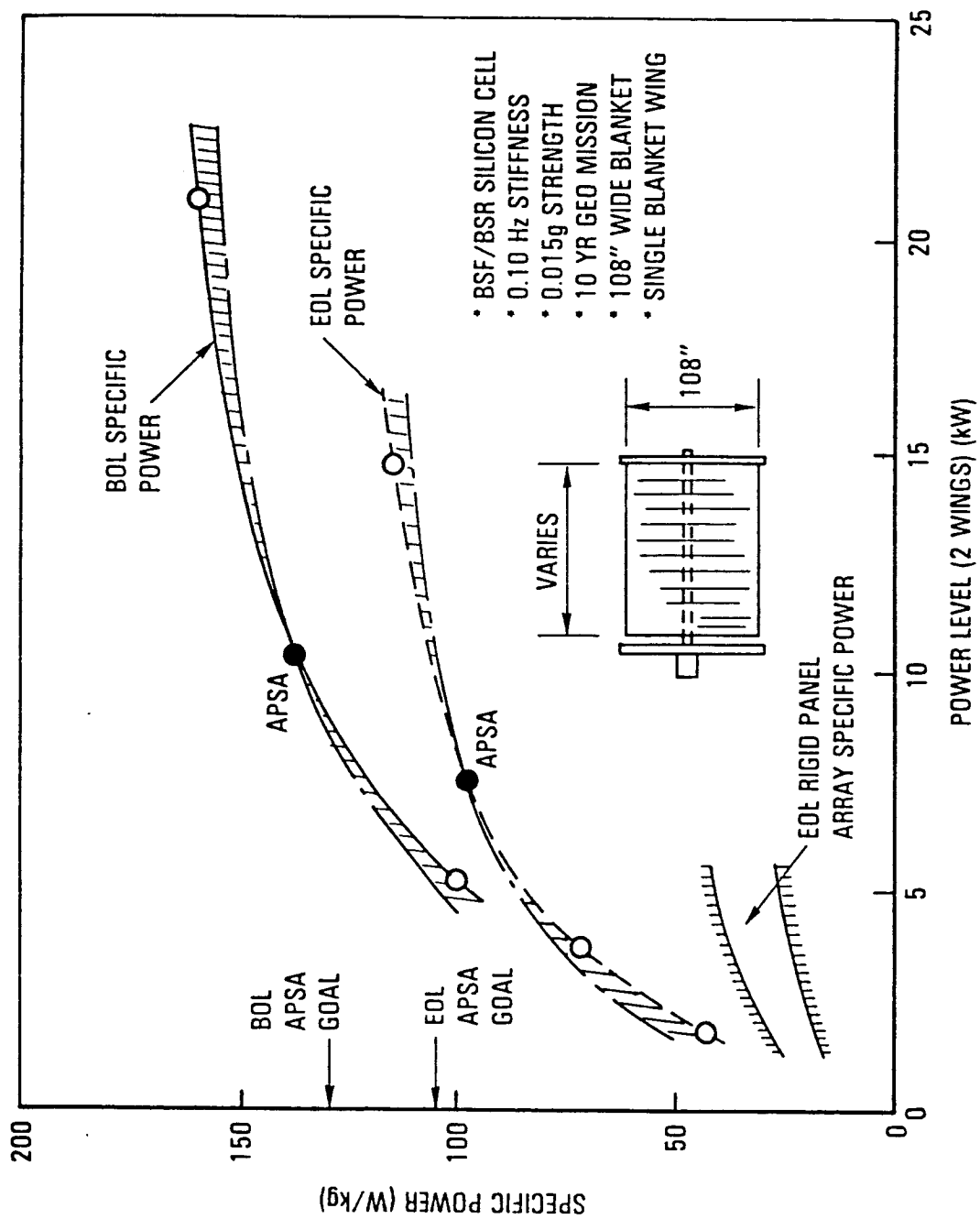


Figure 4-41. Effect of Array Power Level on BOL and EOL Specific Power

Included in Figure 4-41 is the domain for rigid panel array specific power performance. This is based on the performance of U.S.-developed arrays and advanced European arrays. Even at the lower power levels where the flexible blanket array performance is expected to degrade, the specific power is still over 2 times that for the rigid panel arrays.

4.6.2 Accommodation of Advanced Photovoltaic Technology Components

The overall approach to the APSA program was to minimize risk and maximize the space heritage of the components in the array. Certain advanced technology components were investigated to determine their applicability to the APSA program due to their potential for greater efficiency, lighter weight, and lower cost. These technologies were assessed to determine the magnitude of their impact on the performance characteristics of the array. Another aspect of this was to determine the technology readiness and/or lead time for these components for space flight use. This readiness was reviewed with respect to the APSA program schedule requirements.

4.6.2.1 Gallium Arsenide Solar Cells

The attractive aspects of gallium arsenide (GaAs) for the APSA blanket are the higher efficiency and greater radiation resistance than single crystal silicon, both of which lead to a smaller blanket area. GaAs conversion efficiency was studied as a parameter, varying from 16 to 20 percent. This covers the range from the existing to the near-term expectations of the cell suppliers. All cells in this range of efficiency would meet the APSA power density requirement of 110 W/m².

The APSA specific power goal (105 W/kg, EOL) is the design driver with respect to this technology. Figure 4-42 illustrates the relationship between the cell thickness, conversion efficiency, and array performance in terms of W/m² and W/kg. A 16 percent efficient cell could be no thicker than 61 μ m (2.4 mils), an 18 percent cell could be no thicker than 100 μ m (4.0 mils), and a 20 percent efficient cell could be no thicker than 132 μ m (5.2 mils) in order to meet the specific power goal. The GaAs cell thickness currently produced is 305 μ m (12 mils) nominal. Several different approaches are currently being pursued to reduce the thickness (such as the MIT Lincoln Labs CLEFT cell or using a thin Germanium wafer in place of the thick GaAs wafer) but all are in the early stages of development and none would be expected to be commercially available in large quantities for many years, if indeed such approaches prove to be practical.

A complication inherent in the currently available cells is their brittleness. This manifests itself in high cell cost due to low fabrication yields. These cells will incur a yield penalty during panel fabrication, test, and spacecraft integration for the same reason. This situation and the panel assembly process development effort would raise the array cost.

GaAs cells are not recommended for the APSA program due to the cost penalty which would be incurred. In addition, there will be either a weight penalty (existing cells) or a technical risk (thin cells) involved which is not compensated by the near-term performance improvements.

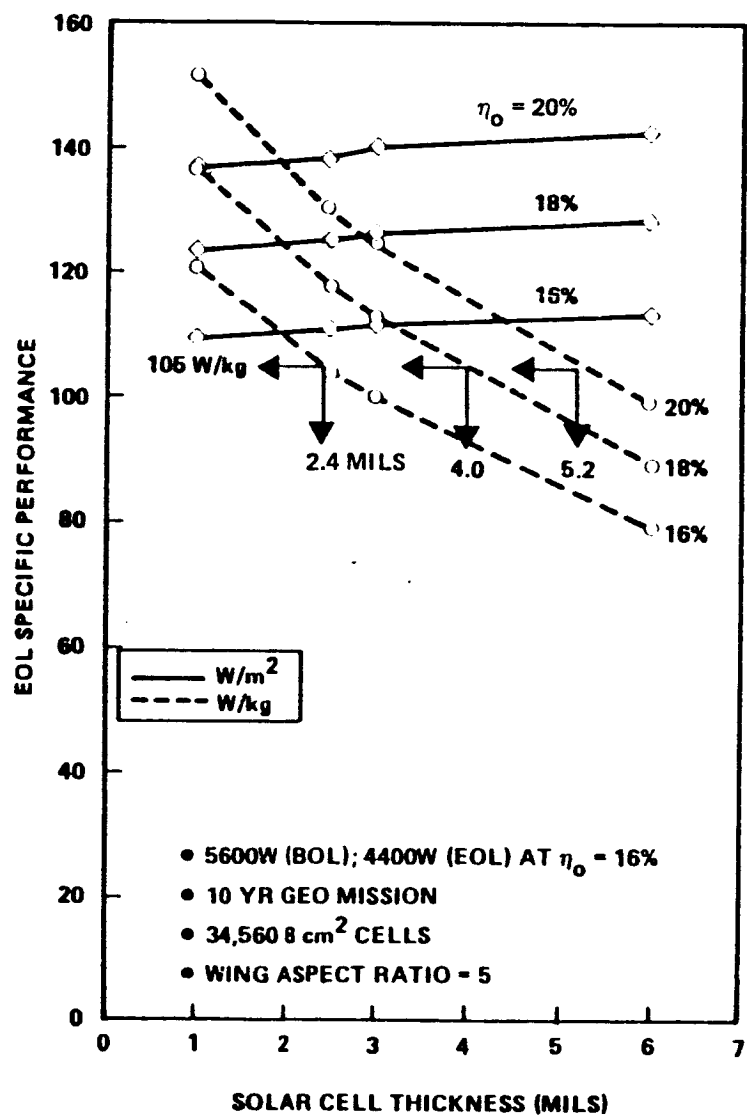


Figure 4-42. Results of Parametric Study of GaAs Solar Cell Thickness and Efficiency

4.6.2.2 Thin Film Amorphous Silicon Cells

Thin film amorphous silicon technology was developed for terrestrial applications using mass production processes to achieve low cost. The terrestrial cells are made of materials which are not suitable for space application. This does not preclude the adaptation of this technology for space use, but it introduces a technology development cost and schedule impact.

This technology was reviewed for potential APSA application due to the potential for reducing the blanket weight and cost. Figure 4-43 demonstrates the relationship between the conversion efficiency of an amorphous cell stack² (without cover glass) and the APSA array performance goals in terms of W/m^2 and W/kg based on the assumption the radiation degradation effects would be negligible and/or that they would be annealed in some manner. A large area cell circuit module would only have to be 5.5 percent efficient at end of life to meet the W/kg goal; however, in order to meet the W/m^2 goal an amorphous module would have to be 10.5 percent efficient.

A review of the state of the art in thin film amorphous silicon technology is shown in Figure 4-44. It is clear from the figure that the module size is inversely related to the conversion efficiency for this technology, and the high conversion efficiency on a large area module, as needed for APSA, has not yet been achieved. This technology is, however, demonstrating rapid performance improvements. A typical present-day module (6 percent efficient) would achieve 120 W/kg but the array would be almost twice the size of the baseline array design using thin, single-crystal silicon cells. If reliable large area circuit modules could be developed that produced EOL 10 percent efficiency, then the array specific power could approach 200 W/kg (or almost twice that now predicted at EOL for the baseline APSA design).

While the high W/kg characteristic of this technology is interesting it must be noted that there is an inherent lack of shielding from particulate radiation. This would require a careful analysis and test program to characterize the radiation effects. Especially important are the high fluence/low energy species which will be absorbed in the cell instead of being absorbed in the cover glass as on existing arrays. There is a growing amount of evidence which supports the possibility of completely annealing the radiation-induced damage. This process will also require development work. Conceptually, it would require array retraction and elevated temperatures.

The conversion efficiency of amorphous silicon is observed to degrade with long-term exposure to sunlight. This so-called Staebler-Wronski effect, or photon degradation, stabilizes in time at 10 to 20 percent for single junction cells and 7 to 8 percent for multijunction cells. There is the possibility that this type of damage could be annealed out in conjunction with the radiation damage annealing at 175°C in a dark condition.

These devices have mutually compensating temperature coefficients for current and voltage which make the efficiency insensitive to temperature. While large variations in both voltage and current would be experienced during a typical geosynchronous mission, and even larger excursions during an interplanetary mission as discussed later, there are existing, space-qualified, peak power trackers which can capitalize upon this characteristic to achieve a net savings for the electrical power system.

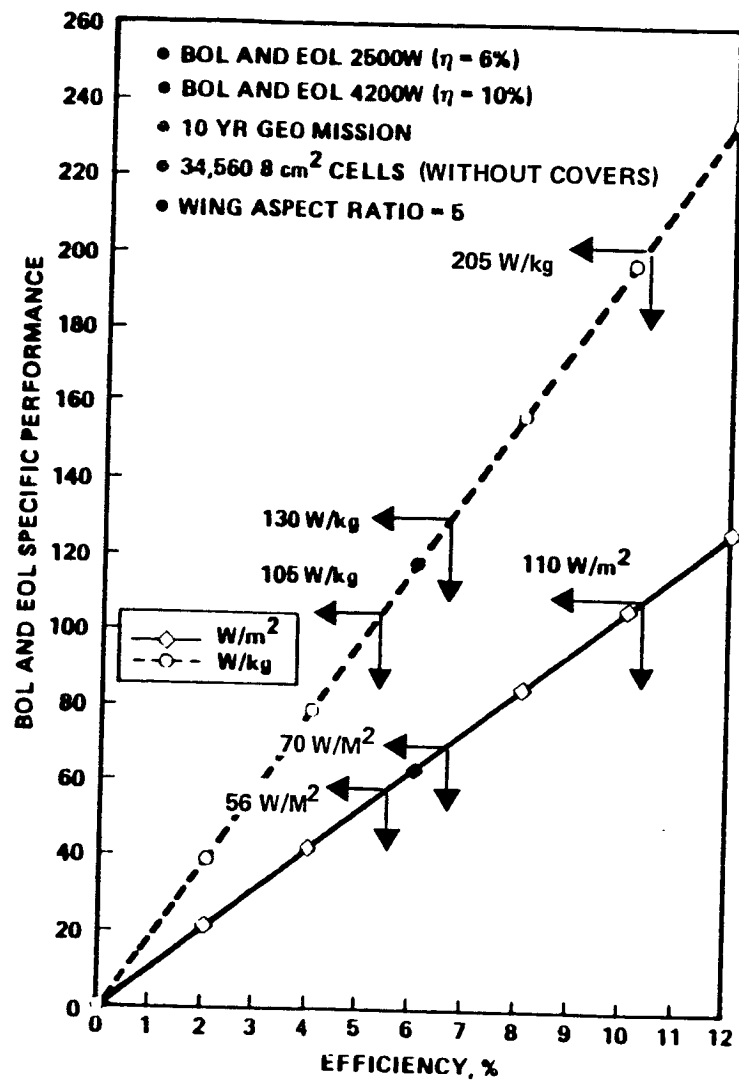


Figure 4-43. Results of Parametric Study of Thin Film Amorphous Silicon Cell Efficiency on Wing Performance

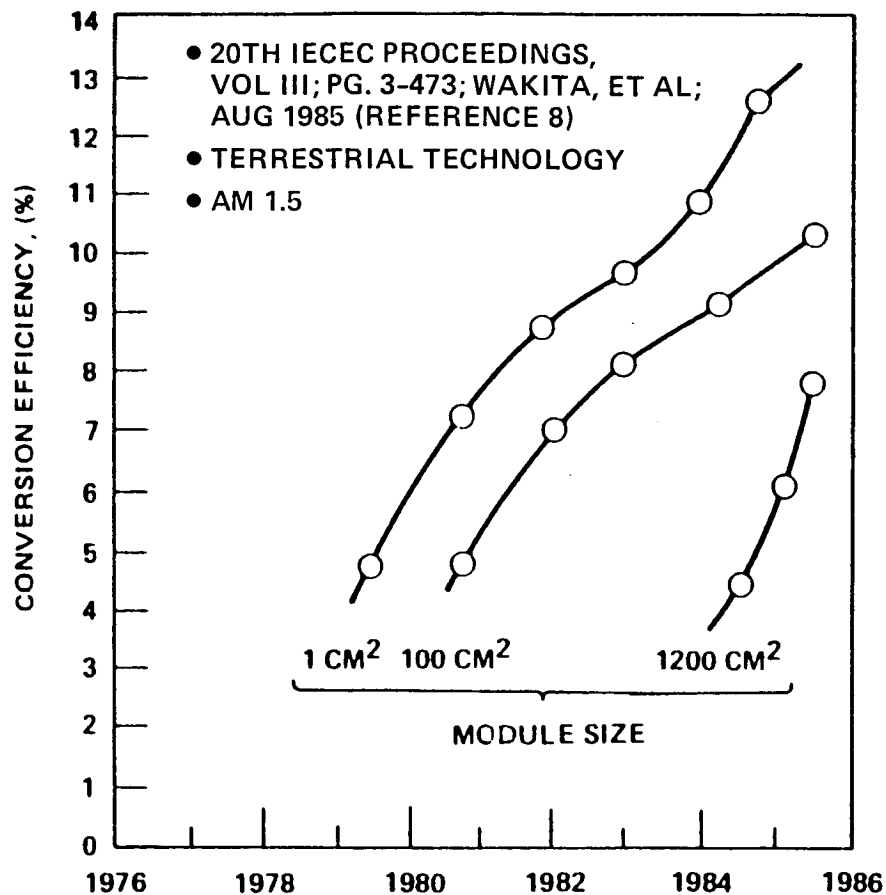


Figure 4-44. State of the Art for Terrestrial Large Area Amorphous Modules in Terms of Conversion Efficiency Versus Module Size

In summary, thin film amorphous silicon technology is new to the aerospace power system and holds tremendous potential for reducing the cost, improving the W/kg performance of solar arrays, and eventually competing with single crystal silicon W/m². At this time, however, it is only considered a potential which will require significant amounts of time and money to fully develop for use on a space flight program. We strongly recommend further study in this area but do not feel it is suitable for use in the baseline APSA design.

4.6.3 Interplanetary Mission Performance

Consideration was given to an interplanetary mission as an appropriate potential application for the APSA solar array design as these missions are extremely sensitive to spacecraft component weights. The two possible mission types, inbound and outbound, are characterized by the solar insolation encountered. The insolation as a function of distance from the sun, overlaid with the locations of some of the likely planetary and asteroidal objectives, is shown in Figure 4-45. There are also several possibilities for a comet rendezvous in the region of interplanetary space encompassed by this figure. The insolation varies from 190 percent to only 4 percent of the near-earth value.

The impact of widely varying solar insolation on solar array operating temperature is shown in Figure 4-46 for two different solar cell types. These cell types represent the APSA baseline cell and a textured front solar cell. The textured cell was considered due to its higher solar absorptance and higher conversion efficiency (under near-earth conditions). The maximum allowable temperature of 150°C for soldered cell modules and 135°C for the fiberglass mast limits inbound missions to about 0.5 AU unless off-pointing of the array is possible. Outbound missions will operate at very low temperatures which do not pose materials problems but will cause anomalies and non-linearities in solar cell performance.

According to the latest information received from the various cell manufacturers and agencies involved in LILT effects testing, the most significant effects are related to cell construction. The types of effects encountered are:

1. band gap energy increase
2. diffusion length decrease
3. Schottky back contacts
4. junction shunting
5. "broken knee" effect
6. low efficiency region surrounding front contact

A potential design solution exists, or has been hypothesized, for each type of LILT effect. However, each cell manufacturer or researcher in this field suggests slightly different approaches or design features to mitigate this problem. The many references on the subject are not conclusive. Furthermore, the nature and magnitude of the LILT effects in p/n or thin or vertical junction single crystal silicon or amorphous silicon cells have yet to be determined. Hence additional development work on the design and evaluation of a LILT cell is required.

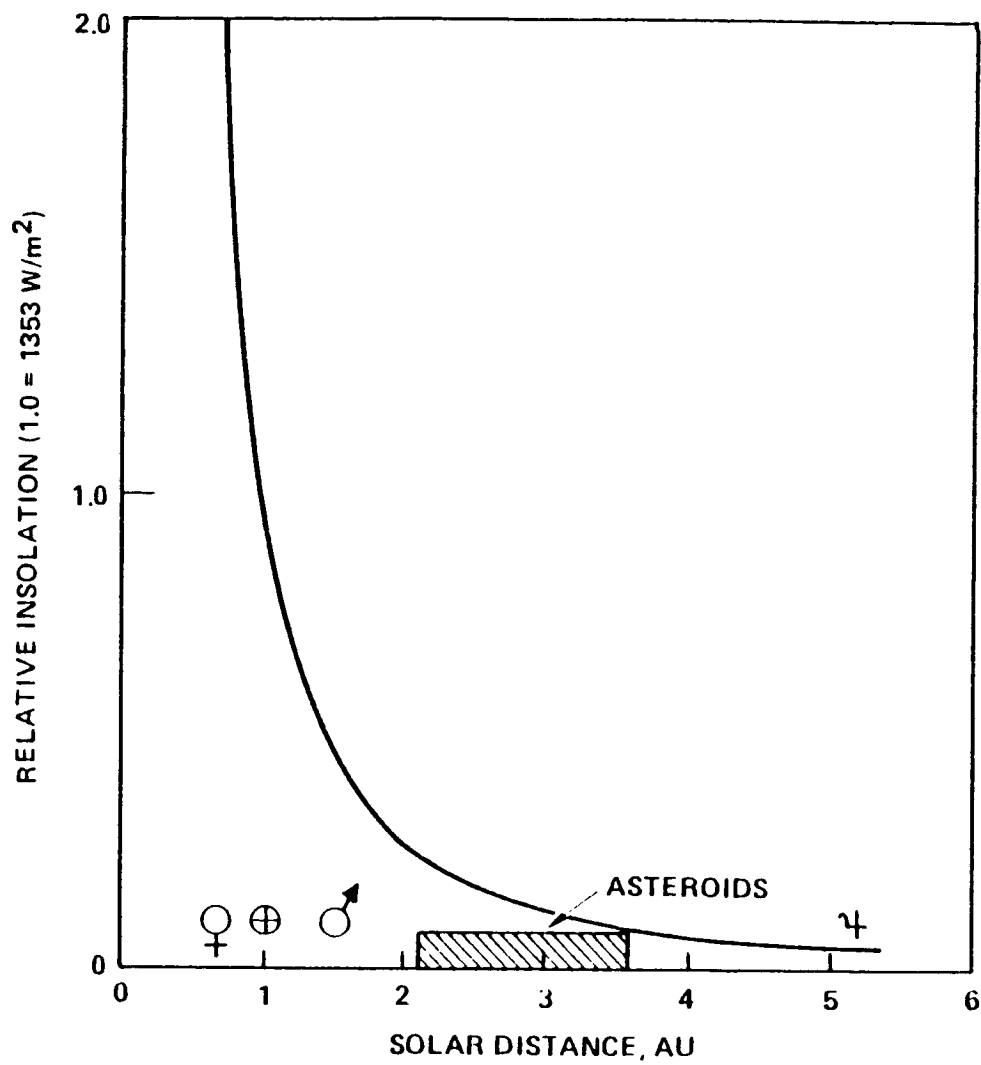


Figure 4-45. Relative Effect of Interplanetary Distance on Solar Array Insolation

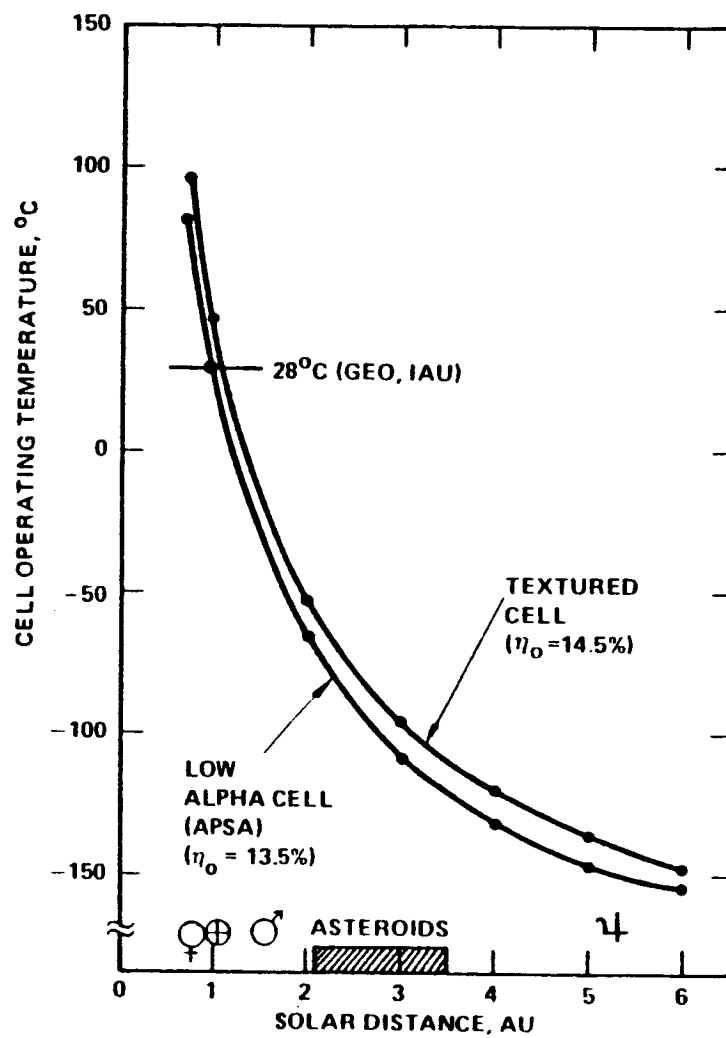


Figure 4-46. Solar Cell Stack Temperature Response of the APSA Array Due to Varying Solar Insolation

An estimate of the impact of the anomalous behavior of existing cell types operating under LILT conditions on the performance of the APSA array was made. This work was based on the results of device testing by NASA/MSFC as reported in References 9 and 10. The LILT behavior of a cell similar to the APSA baseline solar cell (identical except for the thickness) and the textured front solar cell is shown in Figure 4-47. The two curves labeled "best" and "worst" encompass the range of possible output values which can be expected from cells of a given type which would produce equal output in normal light and temperature conditions. The two sets of curves represent the solar insolation levels during a comet rendezvous/asteroid flyby (CR/AF) and a Jupiter encounter. The operating temperatures for the APSA array, taken from Figure 4-46, are shown as vertical arrows. At these temperatures and intensities, the uncertainty in output would represent a design penalty to the array of ± 7 percent (from average measured output) for a typical asteroid mission and ± 16 percent (from average measured output) for a Jupiter mission. In addition, the average measured output differed from the ideally linear response of the solar cell. The effects combine to reduce the array output.

Figure 4-48 shows the impact of the LILT effect on the cell efficiency as a function of distance from the sun when used in an APSA array. The range of values shown represent the best and worst cells as described above. The same two cell types are shown. The APSA baseline cell type is demonstrated to be the better of the two cell types studied.

In summary, it is concluded that the APSA baseline design could probably be utilized for interplanetary missions without major modification. The primary issue is not so much the effect of the potential temperature extremes on the "structural" materials and adhesives as it is the LILT effect on solar cell performance and the potential deviations in array output from nominally predicted performance. The development of a LILT cell is required, after which the APSA design would be fully practical for interplanetary missions.

4.6.4 Low Earth Orbit Mission Performance

The principal design issues for solar array performance in low-earth orbits (LEO) are:

1. Electrostatic charge control
2. Heating from earth and earth albedo
3. Charged particle degradation
4. Atomic oxygen erosion effects
5. Temperature cycling.

Each of these issues is discussed in the following paragraphs.

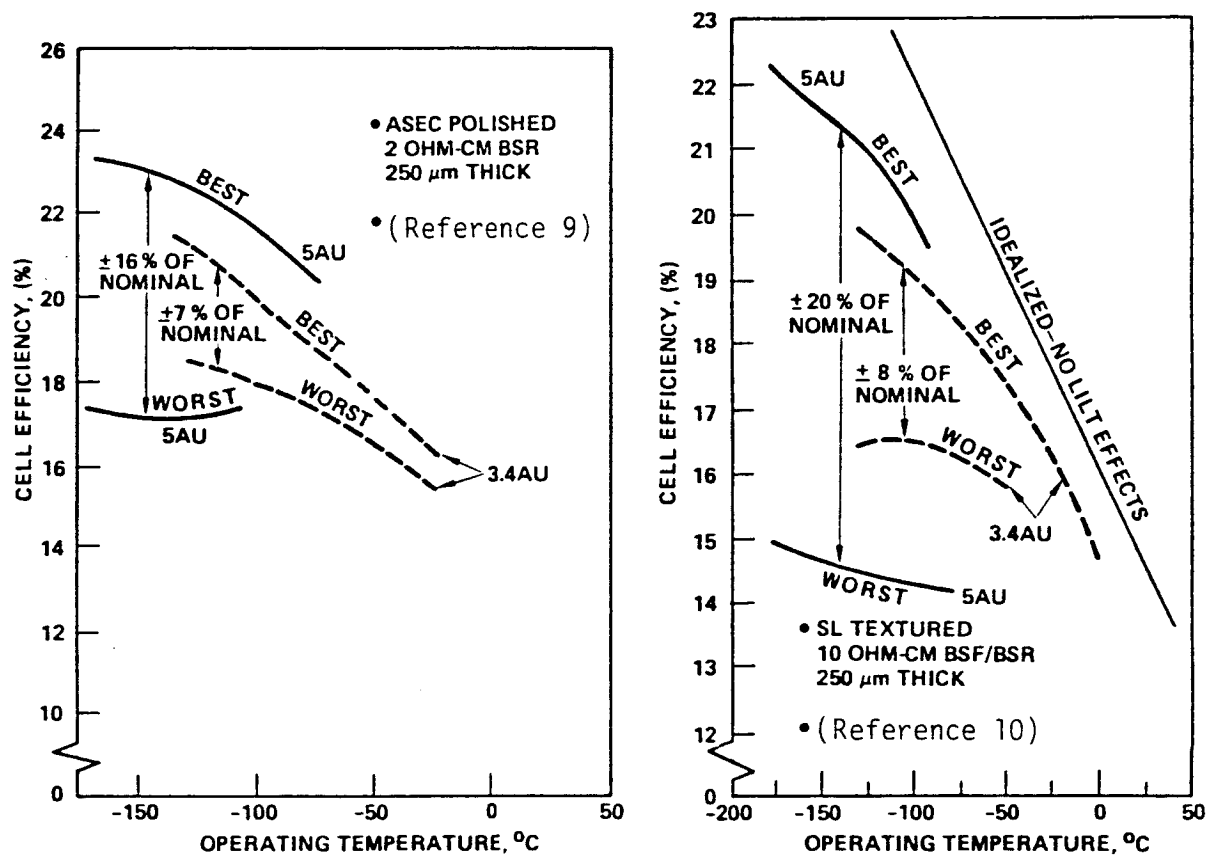


Figure 4-47. The Magnitude of LILT Effects on Cell Performance (Best and Worst Variations) Relative to a Cell Population that Normally Produces Equal Output

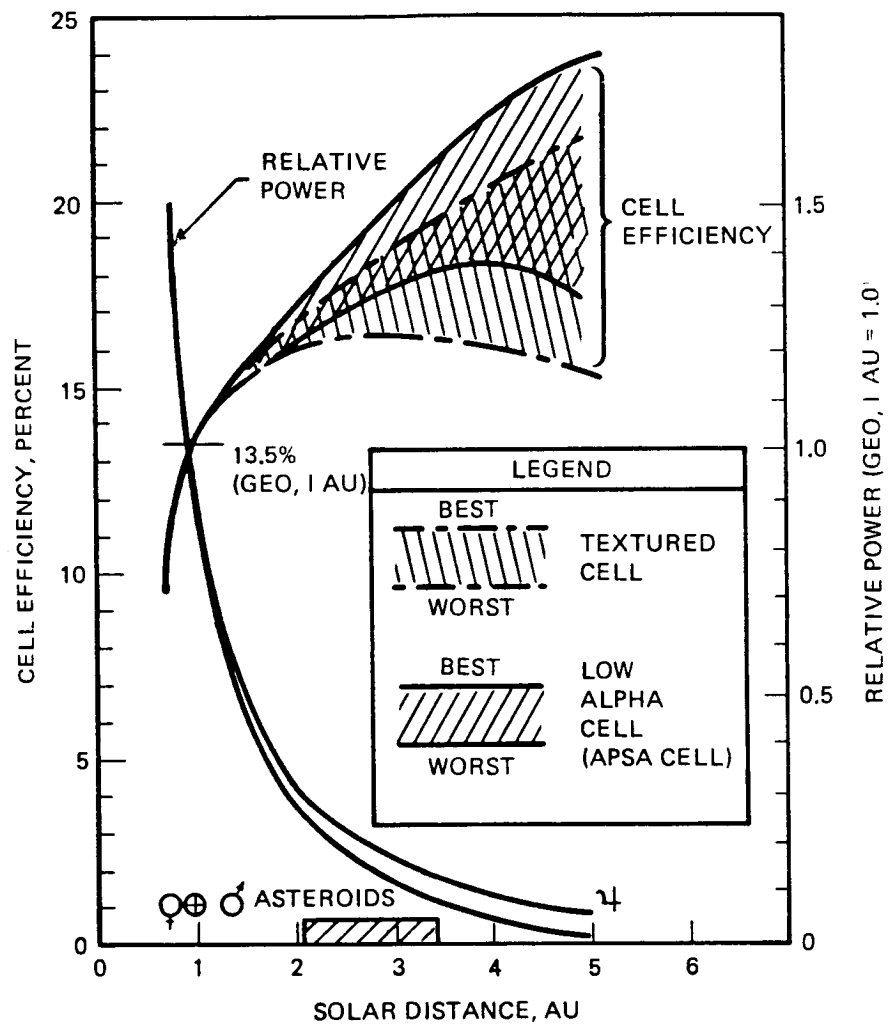


Figure 4-48. The Range of Possible Cell Efficiencies and Relative Power Output Under LILT Conditions for APSA

4.6.4.1 Electrostatic Charging

Electrostatic charging occurs when the environmental plasma particles have sufficient energy and density to charge external surfaces of the array. The hazard from this charging results from the charge deposition reaching a level that either large electric fields are created that affect system operations or discharges occur. Such charging can exist at low altitudes only in polar orbits (above 50 to 60 degrees inclination) and for low inclined orbits in the the radiation belt regions of space above 28,000 km [15,000 nmi]. In polar orbits, the auroral fluxes have been found to charge spacecraft to large negative voltages. Analysis of this phenomenon has indicated that the charging levels can be significantly higher than the -440 volts measured on the DMSP satellites if the spacecraft size is increased to shuttle dimensions and beyond. In the radiation belts, there are fluxes of energetic plasma particles and it is possible for these to charge the array dielectrics either on the surface or buried within. In either case the same charging hazards would exist.

The present APSA design incorporates electrostatic charge control to survive in the geosynchronous substorm environment. The design would be the same for low-earth missions.

4.6.4.2 Heating Effects from the Earth Radiation

Heating from the earth and the earth albedo would become a consideration at lower orbits. The earth represents a heat load of about 0.17 of solar intensity while the albedo is about 0.3. This heat input would result in a 25° to 35°C temperature rise at BOL. Such a temperature increase would result in a 10 to 14 percent reduction in BOL power relative to GEO operations. However, the reduced radiation levels at lower orbits could result in a net 16 to 20 percent increase in EOL power relative to GEO EOL power. For example, the comparison between GEO and LEO power output is given in Table 4-5.

4.6.4.3 Charged Particle Degradation

Charged particle degradation of this solar array must be considered in the radiation belts, polar orbits, and for those orbits crossing the South Atlantic Anomaly (that region of space whose ground track lies between Africa and South America) where there is a concentration of high-energy particle fluxes. In polar orbits there is an additional concern for solar flare proton fluxes. For the polar and radiation belt orbits, the array should be in the radiation environment only for short periods of time.

The array has been designed to tolerate the charged particle environment at GEO which is more severe than in the lower orbits. If the array were to operate for extended periods of time in the radiation belts, additional analysis would have to be done to determine its power output.

Table 4-5. 10-Year LEO APSA Solar Array Power Output Relative to GEO Performance (37,440 2 x 4 cm 10 Ω -CM BSF/BSR η_0 = 13.5 Percent Silicon Cells Per Wing)

Orbit	Altitude (nmi)	Inclination (degrees)	BOL Array Power Output (Two Wings) (watts)	EOL Array Power Output (Two Wings) (watts)
GEO	19,200	0	10,400	7,400
LEO	250	0	9,000 9,300*	8,600 8,800*
LEO	250	32	8,500 8,800*	8,200 8,400*

*Kapton substrate coated on rear surface to reject albedo heating

4.6.4.4 Material Erosion from Atomic Oxygen

As a result of the shuttle flights and experiments, it is now known that various material surfaces facing in the velocity ram direction are eroded by atomic oxygen impacts. This erosion is particularly serious for Kapton which is used in this design for blanket substrate material and harness insulation. A summary of the array components and their susceptibility to oxidation is given in Table 4-6. There are two approaches that can be used to alleviate this effect. The first approach is to establish a criterion for acceptable mass loss over the mission life. This criterion would be based on the available information on the energy dependence of the reaction (see Figure 4-49), the orientation of the surface relative to the velocity (as illustrated in Figure 4-50) and the atomic oxygen number density (see Figure 4-51). Since the number density is a function of solar activity (see Figure 4-52), this also has to be factored into these considerations.

These considerations result in the projected Kapton losses illustrated in Figure 4-53. As shown, a $6.4\text{ }\mu\text{m}$ (0.25-mil) loss in a $50\text{ }\mu\text{m}$ (2-mil) Kapton film over a 10-year lifetime would require operating at the following orbits:

- No lower than 450 km (240 nmi) for standard conditions
- No lower than 650 km (350 nmi) for active conditions.

For the composite materials in the mast and blanket housing structure, the erosion rates are similar to that for Kapton. However, the permissible sacrificial loss over the lifetime can be larger because these materials are used in substantially thicker components/elements.

The second approach is to coat the susceptible materials if erosion cannot be tolerated. For the susceptible exposed silvered surfaces (i.e., interconnectors) solder coating appears to be effective. Possible coatings suggested for Kapton and composite materials are silicones, SiO/Teflon, or ITO. Each of these coatings will have to be qualified for flight application and their impact on thermophysical properties and electrostatic charge buildup would have to be evaluated in more depth. For the polar orbit LEO missions, the use of coatings may complicate the control of electrostatic charge buildup because the present carbon-loaded Kapton substrate material would not be directly exposed. The use of coatings to counter atomic oxygen material erosion effects would also complicate the manufacturing of the array because of the desire to obtain crack-free coatings and to be able to obtain coated surfaces with reliable thickness.

4.6.4.5 Thermal Cycling

Low-earth orbits result in substantially more eclipse cycles than GEO. In a 10-year mission at low orbits there can be 60,000 thermal cycles over the temperature range -80° to 80°C , whereas in GEO a 10-year mission results in only 1000 cycles over a temperature range of -160° to 30°C . Such cycling could induce fatigue failure in cell interconnects and cell contacts. Recent TRW and NASA/LeRC temperature cycle test data on welded and soldered conventional thickness and thin silicon cell modules indicate that there was negligible electrical degradation after 60,000 to 90,000 cycles (References 4 and 5).

Table 4-6. Susceptibility of Array Components to LEO Atomic Oxygen Erosion

COMPONENT	MATERIAL	EFFECTS	OPTIONS
• COVERGLASS OPTICAL COATINGS	MgF ₂	NEGLECTIBLE	-
• COVERGLASS	FUSED SILICA, CMX	NEGLECTIBLE	-
• ADHESIVES	DC 93500, DC 6-1104, RTV-142	NEGLECTIBLE	-
• DIODES	COPPER LEADS	MODERATE EROSION	SOLDER PLATING PROTECTS COPPER
• HARNESS INSULATION	KAPTON	SEVERE EROSION	<ul style="list-style-type: none"> • FLY UNPROTECTED ABOVE CERTAIN ALTITUDE; • SILICONE COATED; • SiO₂-PTFE COATED; • ITO COATED;
• BLANKET MATERIAL	KAPTON	SEVERE EROSION	
• INTERCONNECTORS	SILVERED INVAR	SEVERE Ag EROSION	
• HARNESS LEADS	COPPER	MODERATE EROSION	
• TERMINATION STRIPS	SILVERED INVAR	SEVERE Ag EROSION	<ul style="list-style-type: none"> SOLDER PLATING PROTECTS COPPER, SILVERED INVAR • FLY UNPROTECTED ABOVE CERTAIN ALTITUDE; • SILICONE COATED; • SiO₂-PTFE COATED
• DEPLOYMENT MAST	FIBERGLASS/EPOXY	SEVERE MATRIX EROSION	
• DEPLOYMENT MAST CANISTER	ALUMINUM; OR GRAPHITE/EPOXY	NEGLECTIBLE; OR SEVERE MATRIX EROSION	
• BLANKET BOX STRUCTURE	GRAPHITE/EPOXY	SEVERE MATRIX EROSION	
• MISCELLANEOUS FITTINGS	ALUMINUM	NEGLECTIBLE	-
• THERMAL CONTROL PAINT	ST3G-10	NEGLECTIBLE	-
			(SAME AS MAST STRUCTURE)
			(SAME AS MAST STRUCTURE)

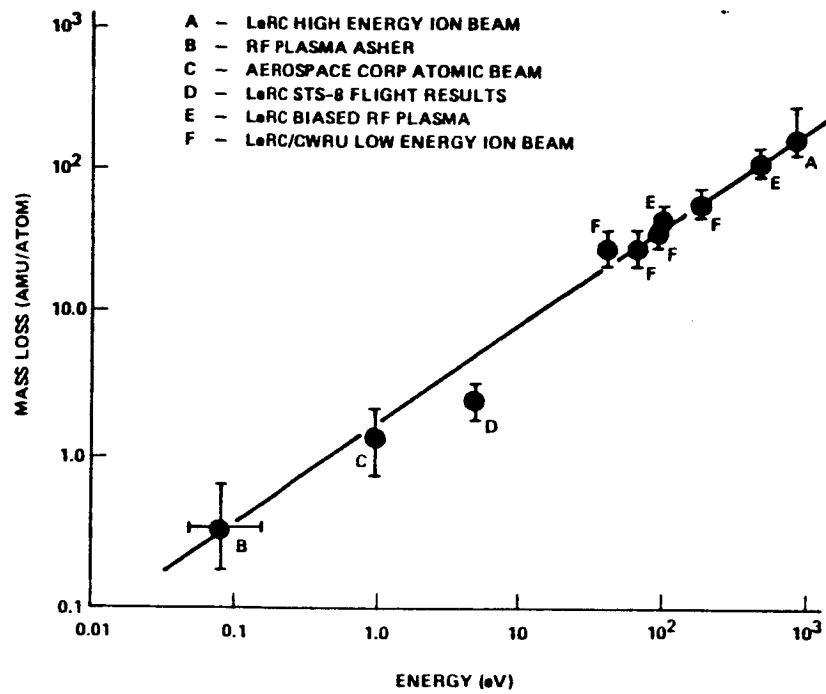


Figure 4-49. Kapton Mass Loss Weights (Reference 11)

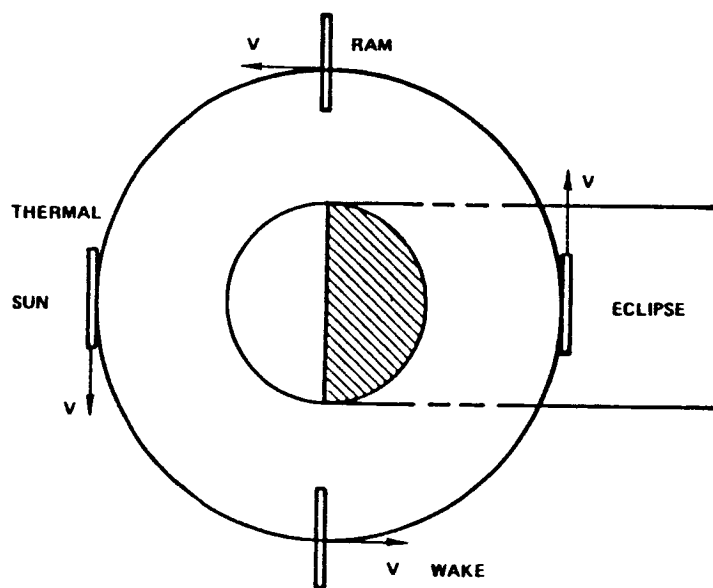


Figure 4-50. Changes in Environmental Conditions Over Orbit

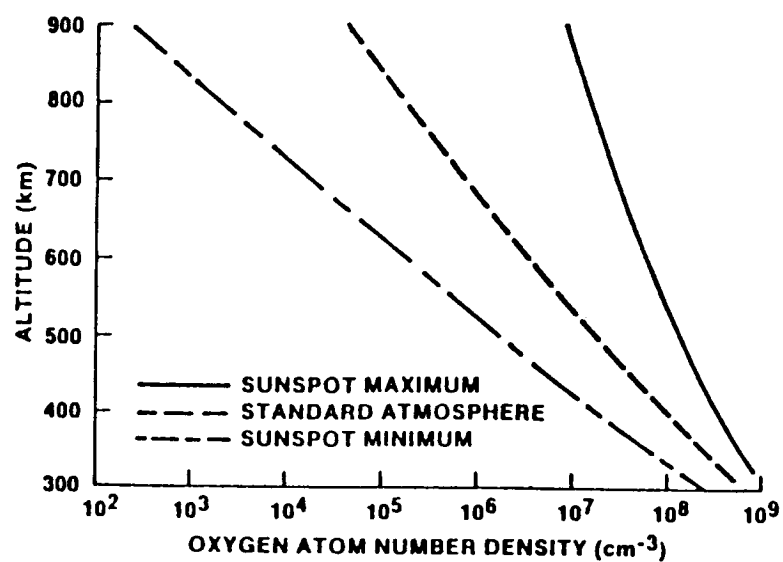


Figure 4-51. Atomic Oxygen Density Profiles

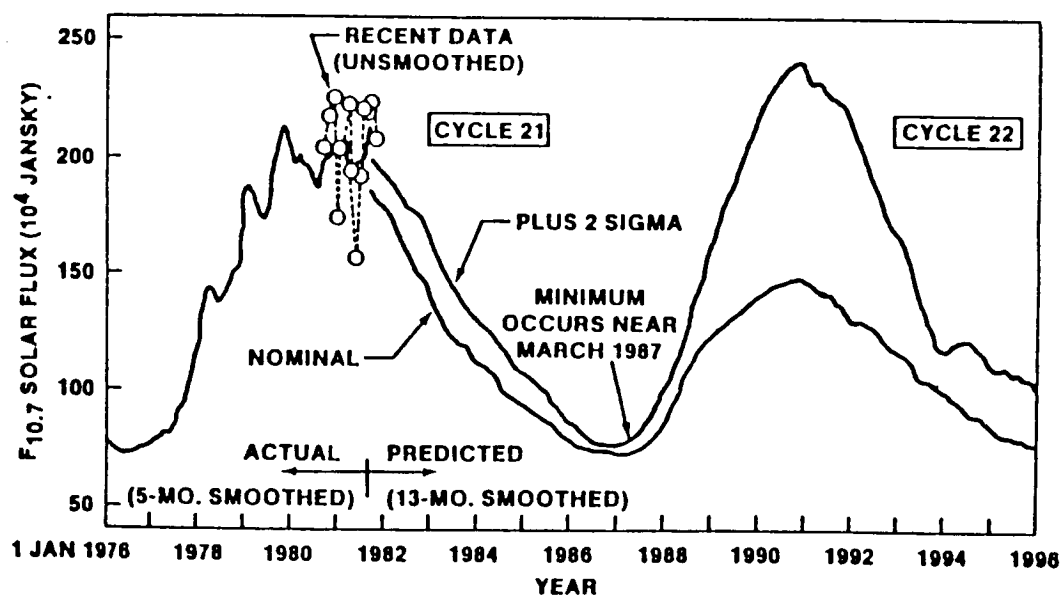


Figure 4-52. Solar Activity Predictions

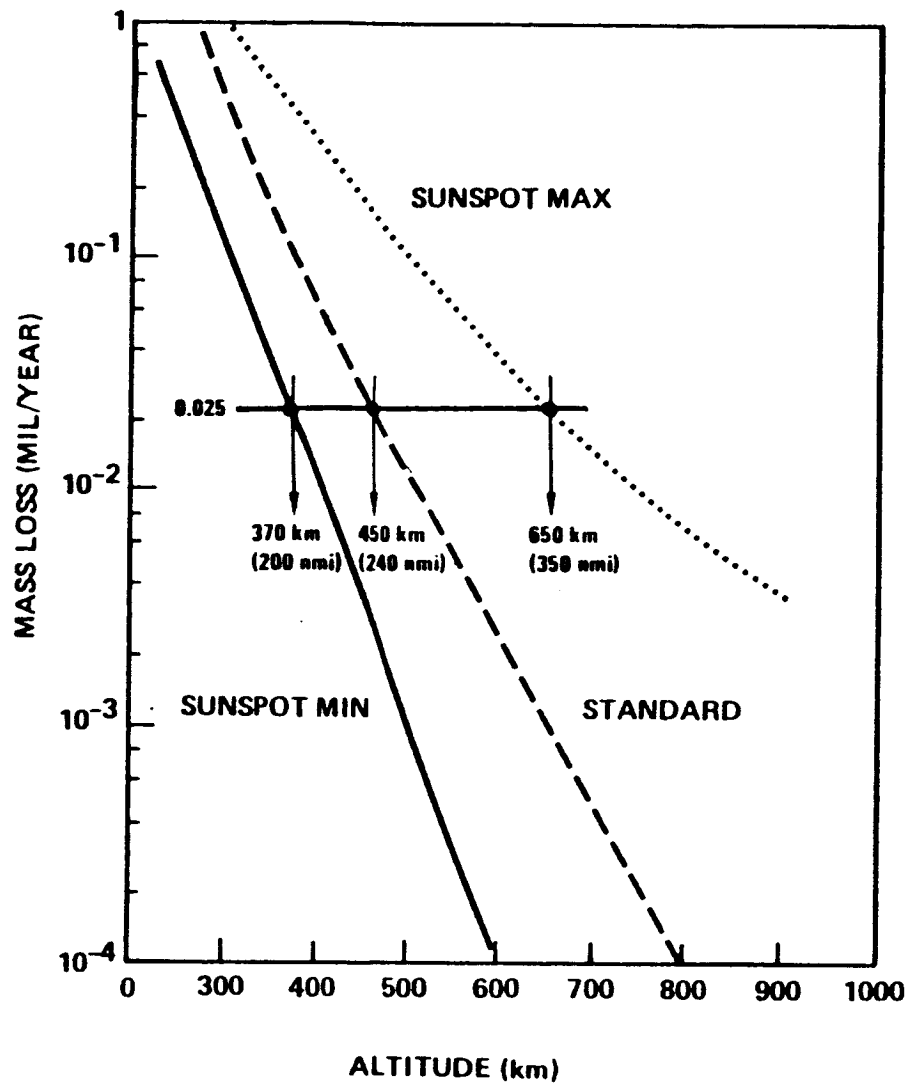


Figure 4-53. Projected Kapton Mass Loss per Year in Orbit Based on Velocity Effects, One-Side Erosion

4.6.4.6 LEO Mission Suitability Summary

In summary, the APSA could probably support a 10-year LEO mission without major modification at most orbits of interest. Atomic oxygen material erosion at the lower LEO altitudes is the primary design issue of concern, although a LEO mission that was at a high inclination would require both the atomic oxygen issue and electrostatic charge control issue to be compatibly resolved.

The performance characteristics for the present APSA design (39 cell-covered panels per wing, without coatings on the potentially susceptible Kapton and composite material surfaces) for a 460 km (250 nmi), 0-degree inclined orbit would be: 120 W/kg (BOL) specific power, 114 W/kg (EOL) specific power, 110 W/m² (EOL) power density. If the inclination were changed to 32 degrees, the performance would decrease about 5 percent because of the added radiation degradation.

4.6.5 Spacecraft Integration Issues

Issues about integrating the wing to the spacecraft were discussed in Section 3.1. The primary issues deal with the size and shape of the stowed wing relative to the size and shape of the available stowage volume on the spacecraft. The results of the trade-off studies (illustrated in Figures 3-3 to 3-7) showed that the "single blanket with offset mast" configuration for the baseline design would be compatible with a wide range of spacecraft sizes and geometries.

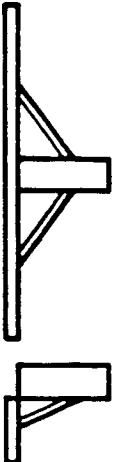

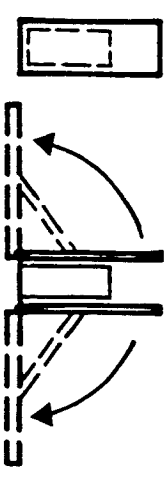
Nevertheless, situations could exist that would require a different stowed wing size and geometry to fit the available stowage volume on the spacecraft. In many cases, this would require the introduction of secondary, but complicating deployment operations prior to the blanket unfolding/extension operation. Table 4-7 conceptually illustrates some possible modifications to the baseline wing configuration, along with the potential impact on wing performance characteristics. Departure from the baseline design (which is considered the most straightforward and least complex) will increase design complexity and weight (5 to 10 percent). The ability to perform ground testing of the wing deployment operations will also be greatly complicated.

4.6.6 Automatic Retraction Capability

The baseline array design incorporates a mast system that is self-retractable. Also included are guidewire mechanisms that help control the blanket assembly out-of-plane motions during deployment operations. While the need for guidewires is marginal for deployment operations, the results from CTS and SAFE I solar array experience, as well as from SEPS array technology and TRW flexible blanket prototype wing tests, clearly shows that guidewire mechanisms would be required for automatic retraction operations.

The major deficiency in the present array design that would not permit automatic retraction lies in the design of the blanket assembly hinge lines between the SPAs and within the SPAs. Past experience has shown that the hinge lines require two characteristics to permit automatic retraction capability: (1) the unfolded hinge line requires some type of restoring torque distributed along the length of the hinge line to initiate refolding (or rotation) of the hinge line in the proper direction; (2) the hinge line needs to be stiffened along its length to eliminate the possibility of localized out-of-plane deflections developing across the hinge line, thereby preventing the hinge from refolding.

Table 4-7. Effect of Stowed Wing Configuration on Wing Performance
(BOL/EOL Wing Power of 5200/3700 Watts, AR = 5.5,
 $F_N = 0.10$ Hz, $N = 0.01$ g)

FIXED	SINGLE FOLD	DOUBLE FOLD
		
<p>84.2 LB (38.2 kg) PER WING</p> <p>136.1 W/kg (BOL) 96.7 W/kg (EOL) 94.7 W/M² (EOL)</p>	<p>87.5 LB (39.7 kg) PER WING</p> <p>131.0 W/kg (BOL) 93.2 W/kg (EOL) 94.7 W/M² (EOL)</p>	<p>92.7 LB (42.0 kg) PER WING</p> <p>123.9 W/kg (BOL) 88.1 W/kg (EOL) 94.7 W/M² (EOL)</p>
<ul style="list-style-type: none"> • LEAST COMPLEX DESIGN • COMPATIBLE WITH GROUND DEPLOYMENT TESTING 	<ul style="list-style-type: none"> • INCREASE IN WEIGHT DUE TO ADDED MECHANISMS • COMPATIBLE WITH GROUND DEPLOYMENT TESTING 	<ul style="list-style-type: none"> • INCREASE IN WEIGHT DUE TO ADDED MECHANISMS AND STRUCTURE • COMPLICATED GROUND DEPLOYMENT TESTING BECAUSE OF 2 BLANKETS AND SECONDARY BLANKET BOX DEPLOYMENT

Several hinge line designs possessing the required characteristics were successfully developed under the NASA SAFE I wing program and by TRW for its prototype retractable flexible blanket solar array wing. Some of these hinge line designs were shown in Figure 3-9.

With the use of the existing mast and guidewire mechanism design, in conjunction with the modified blanket assembly hinge lines, the wing can be retracted from its fully deployed state until the blanket is completely refolded and contained between the lid and pallet structure of the blanket housing assembly. This condition would be satisfactory for most mission needs. However, if the lid must be resecured to the pallet, then the torque-tube latching mechanism must be changed. Such latching mechanisms have been designed and demonstrated under the SAFE I array program and by TRW for its prototype flexible blanket wing.

In summary, the incorporation of automated wing retraction capability greatly complicates the overall design and introduces further risk into the system functional performance. Nevertheless, such capability has been successfully demonstrated. The wing weight would increase about 10 percent with a concomitant reduction in specific power. There would be negligible impact on power density.

4.7 RISK ASSESSMENT

Achieving a three- to four-fold improvement in specific power performance over current array systems is not without some developmental risk. Except for the development of a lightweight version of the blanket deployment lattice mast system (primarily the canister structure), all other materials and hardware components are available from suppliers and/or they can be developed by straightforward application of conventional/available design techniques and manufacturing processes.

The risk areas deal primarily with weight growth and failure to achieve acceptable structural and functional behavior as the result of launch environments and deployment operations. Handling and producibility of the blanket assembly needs to be demonstrated, although there is previous experience on other flexible blanket prototype and flight hardware programs to suggest that it can be done. Cell/circuit integrity during the vibro-acoustic launch phase and deployment phase needs to be demonstrated, although SEPS technology and SAFE I hardware experience suggest the proposed protection features incorporated into the design should be acceptable.

Depending on the nature and number of problems uncovered during Phases II and III of the program, the potential reduction of specific power (i.e., weight growth) could lie between 5 and 15 percent; the reduction of power density could be about 5 percent. The key risk areas cannot be eliminated by analytical means alone. The key risk areas can only be assessed by fabricating and testing component-level and system-level hardware.

5. PROTOTYPE WING IMPLEMENTATION PLAN

During Phase II of the APSA program, a prototype version of the baseline wing design will be fabricated. In Phase III of the APSA program, the prototype wing will be subjected to a series of functional tests and environmental exposures on the ground to demonstrate the feasibility of the design. The prototype wing must satisfy certain requirements:

1. Demonstrate the form, fit, and function of the baseline design.
2. Demonstrate the ultralightweight characteristics of the baseline design.
3. Demonstrate the producibility of the baseline design.
4. Capable of ground testing.
5. Fabrication of the prototype wing should be completed within 15 months after start of Phase II.
6. Target cost of \$500K to \$600K.

5.1 PROTOTYPE WING DESCRIPTION

Figure 5-1 illustrates the prototype wing. The wing is a high-fidelity representation of the baseline 5.2 kW wing, except for the reduced length and percentage of live interconnected solar cell modules.

The wing includes: (1) full-scale graphite/epoxy blanket housing assembly with a complete working stowed blanket preload/latching/release mechanism; (2) a lightweight full-scale version of the blanket deployment mast system with a canister capable of storing over 15 m (50 feet) of mast, but with only 4.6 m (15 ft) of mast installed; (3) a full-width blanket assembly consisting of three of the 13 solar panel assemblies (SPA), along with the necessary leader panel assemblies. The blanket assembly would contain 1100 live thin silicon solar cell modules distributed into 120- to 360-series connected cell circuits, with mass-simulated aluminum chip cells covering the remaining area. The live solar cell circuits would be connected to representative flexible printed circuit harness runs installed along each edge of the shortened blanket assembly. One of the harness runs would terminate into a prototype diode box assembly on the pallet structure.

The prototype wing will permit ground deployment testing to be performed. The stowed wing will provide a representative test article for evaluation of launch loading response, structural integrity of the wing under vibro-acoustic and thermal environments, and the protection afforded to the stowed solar cell modules. The fidelity of the prototype blanket assembly (SPAs, leader panels electrical harness, solar cell modules) will permit the weight of the full-size 5.2 kW blanket assembly to be derived from the weight of the prototype components. The weight of the prototype blanket housing assembly will provide a direct measurement of the flight hardware weight, except for a few components such as a flight-qualified electrically redundant motor and some thermal insulation blankets. The prototype full-scale aluminum mast canister and reduced length of fiberglass mast will permit the weight of the flight version of the mast system to be derived.

- FULL SIZE WING EXCEPT FOR TRUNCATED LENGTH
- 12-PANEL BLANKET COVERED WITH LIVE THIN CELL MODULES (10%) AND CELL MASS-SIMULATED ALUMINUM CHIPS WITH FLEXIBLE PRINTED CIRCUIT HARNESS RUNS
- FULL SIZE LIGHTWEIGHT VERSION OF MAST SYSTEM CANISTER WITH TRUNCATED LENGTH MAST (AT 15 FT)
- LIGHTWEIGHT VERSION OF BLANKET HOUSING ASSEMBLY

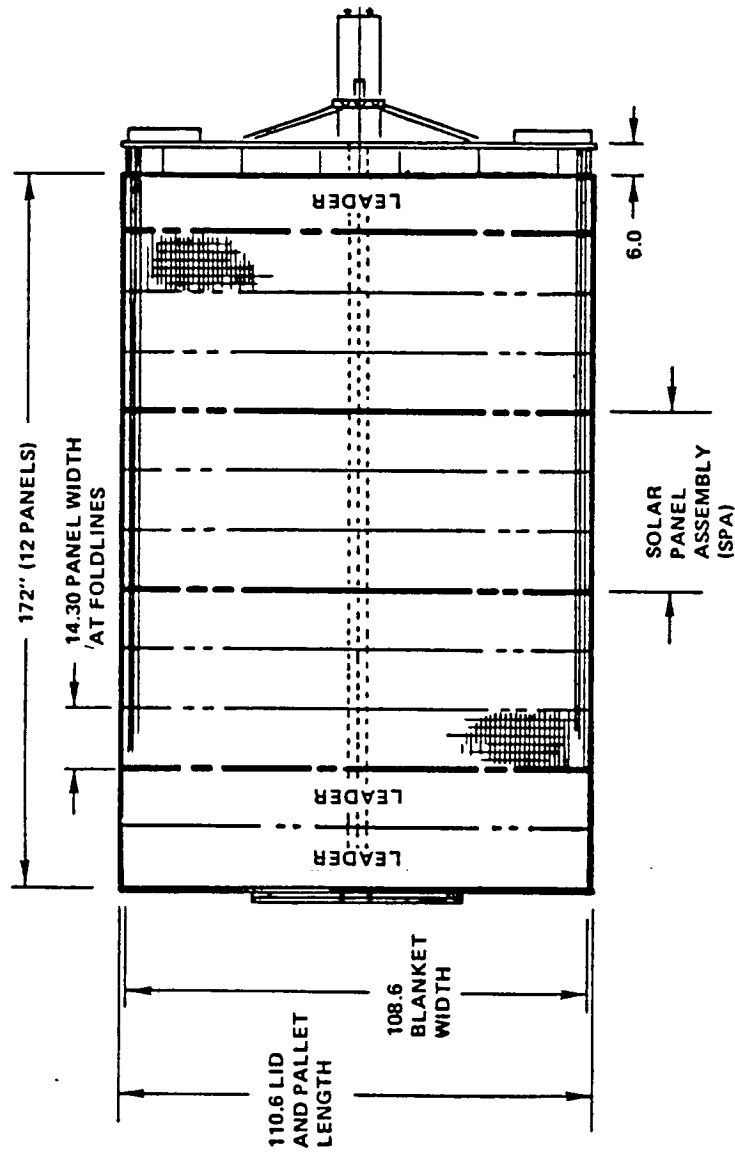


Figure 5-1. Prototype Wing Configuration (Option A)

Because prototype wing cost is an important factor, other less costly options were also developed. These options include: (1) Option B - reduce the number of live interconnected thin silicon solar cell modules to 600 instead of 1100 as previously indicated; (2) Option C - reduce the number of panels in the shortened full-width blanket assembly to eight, consisting of two three-panel SPAs and two blank leader panels; the number of live cells would be reduced to 700; and (3) Option D - use the eight-panel blanket assembly version, except with 500 live cell modules. For each of these three options, the blanket housing assembly and deployment mast system essentially would be the same as the Option A 12-panel prototype configuration.

Budgetary and planning (B&P) cost estimates for Option A were about \$750K for fabrication and assembly of the prototype wing. The B&P cost estimates for the other options were as follows: Option B - \$700K; Option C - \$680K; Option D - \$650K.

The Option A prototype wing (or any other option) is compatible with an existing ground deployment test fixture that was developed under TRW IR&D to support deployment/retraction testing of a similar configuration flexible blanket wing (see Figure 5-2). The blanket housing assembly (excluding the lid) and mast canister are rigidly attached to a peripheral framework and the blanket assembly and lid are attached to air-bearing supports along the top and bottom edges of the wing. The air-bearing supports ride on a high-pressure air linear manifold system. Tests with earlier versions of a flexible blanket wing indicate negligible friction or interaction between the test fixture that supports the blanket assembly and the kinematic motions of the deploying flexible blanket, thereby assuring a realistic means of evaluating the deployment operations/characteristics of the wing. This fixture will also be used for final integration of the prototype wing.

5.2 FABRICATION FLOW PLANS

5.2.1 Mechanical Subassemblies

5.2.1.1 Blanket Solar Panel Assembly Substrate

Figure 5-3 illustrates the blanket SPA substrate manufacturing flow plan. The SPA substrate will be fabricated from 50 μm (2 mil) thick carbon-loaded Kapton polyimide sheet material obtained from DuPont. The material is available in roll form 1.5 m (60 inches) wide. The hinge pins will be pultruded graphite/epoxy rods 1.3 mm (50 mil) diameter by 2.5 m (99.4 inches) long. The electrical harness will be a prefabricated flexible printed copper circuit approximately 0.11 m (4.5 inches) wide. The harness insulation will be 38 to 50 μm (1 to 2 mil) conventional Kapton polyimide which, along with the nominal 1 oz copper conductors (35 μm [2.5 mils] thick), results in a nominal harness thickness of 150 μm (6 mils). The adhesive used to assemble the SPA substrate and bond the harness segments to the SPA substrate will be 50 μm (2 mil) thick nitryl phenolic. In order to control the dimensional accuracy and alignment of the assembly, tooling holes and pins will be used when assembling the SPA substrate and harness segments.

The SPA substrate segments and tabs on which the harness will be attached will be cut to size from net width rolls of the carbon-loaded Kapton material. Trim templates will be used to cut the material to size. The SPA segments will

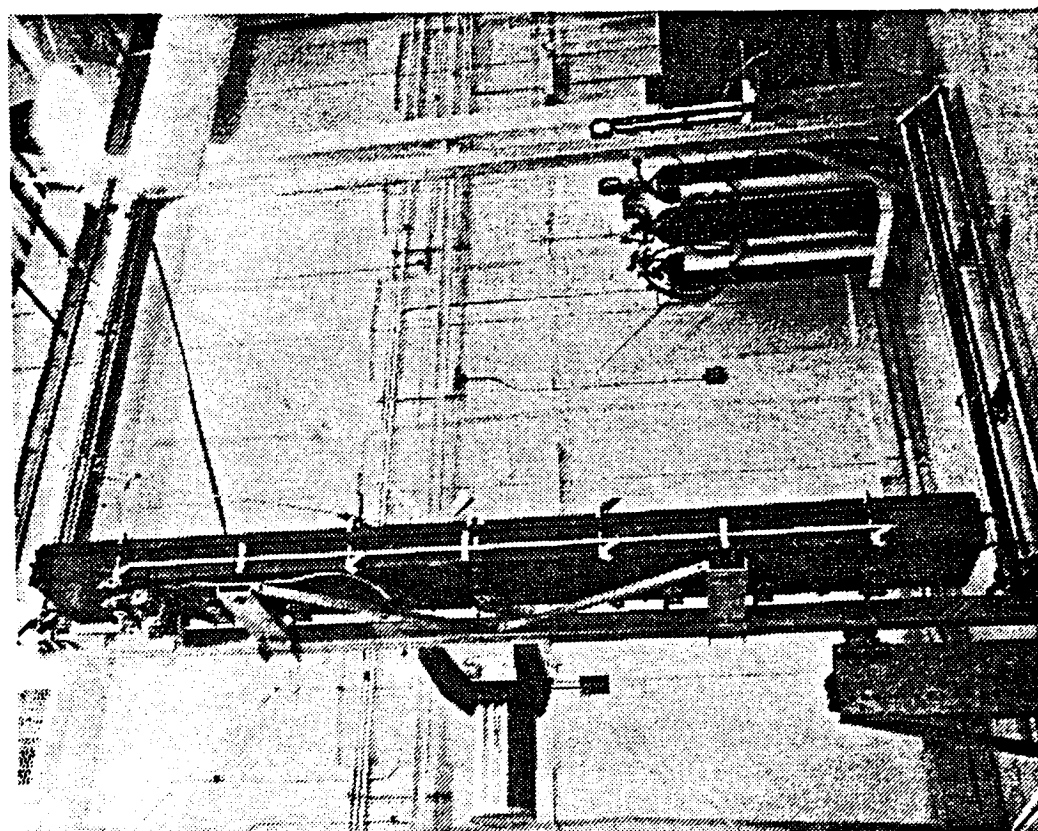
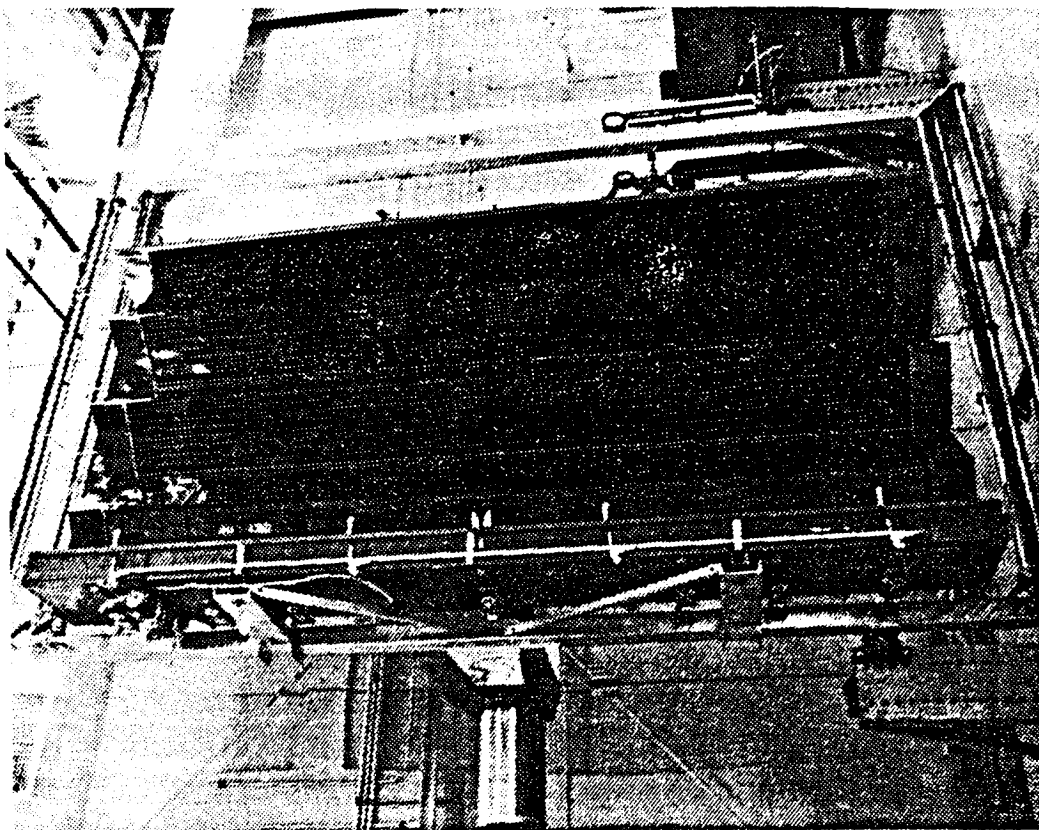


Figure 5-2. Solar Array Prototype Integration and Deployment Test Fixture

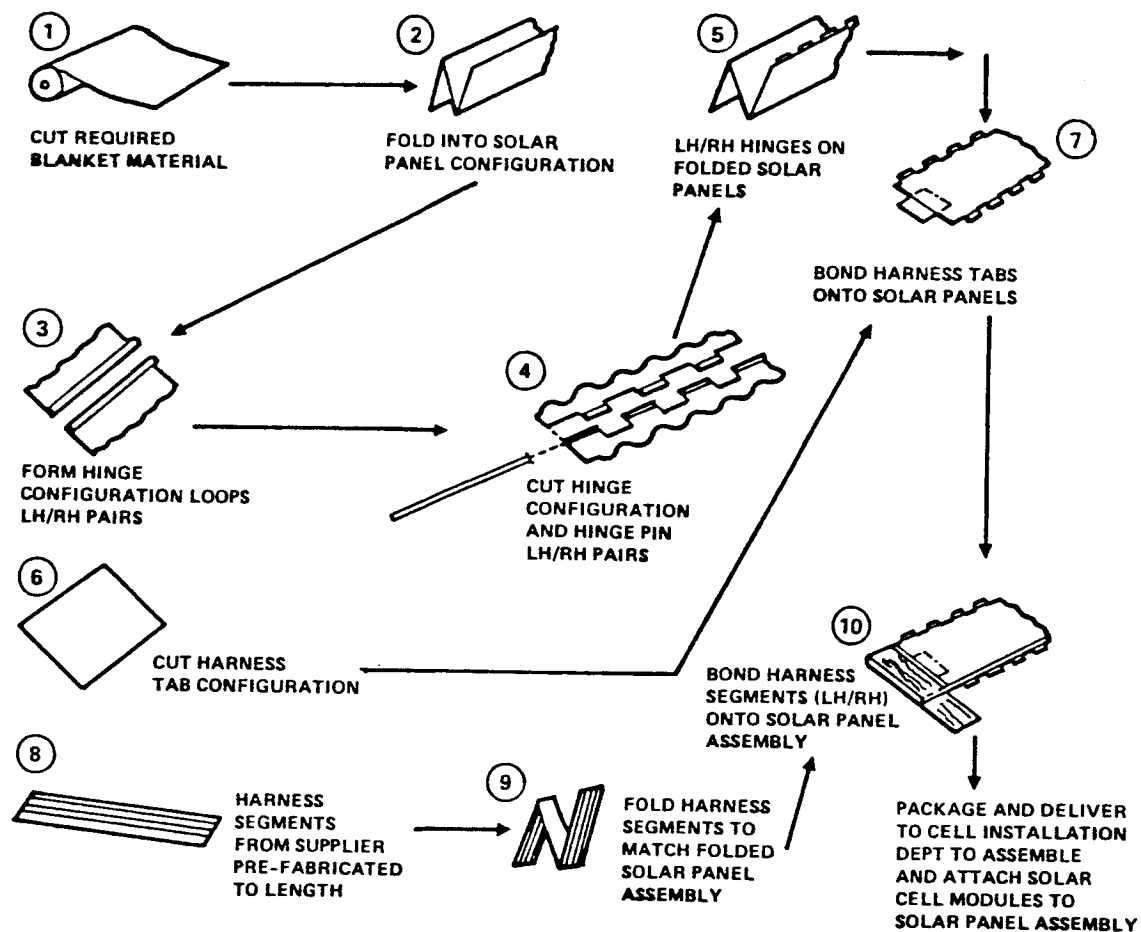


Figure 5-3. Blanket Manufacturing Flow Diagram

be cut to make a three-panel, two-fold configuration approximately 1.1 m (43 inches) long by 2.5 m (99 inches) wide. The material will be cut to allow for folding and bonding the piano hinge loop. Templates will be used to size and control the fold and forming of the panels to ensure interchangeability of the SPAs. After inspection of the folded panel segment, the hinge loops will be formed and bonded. The cutouts in the hinge loops will be blanked out using a specially designed punch and die set. Next, the pre-cut harness tabs will be located with tooling holes in the bonding fixture, and the tabs will be bonded to the three-panel SPA substrate.

Next, the left-hand and right-hand prefabricated electrical harness segments will be folded using a tooling jig. The folded harness segments will be positioned on their respective harness tabs with tooling holes and pins and bonded using nitril phenolic adhesive. After completing installation of the harness segments, the SPA will be unfolded to ensure that the harness and substrate work together to create a flat SPA without wrinkling or distortion. Following inspection, the SPA will be refolded, identified, packaged, and sent to the solar cell module assembly and installation line (see Section 5.2.2).

5.2.1.2 Blanket Housing Assembly

Unlike the SPA substrate, the design of the blanket housing assembly incorporates straightforward structures and mechanisms using conventional spacecraft materials. The pallet and lid are constructed from graphite/epoxy facesheet aluminum honeycomb sandwich panels. The isolation padding will be cut from 13 mm (0.5 inch) thick flexible polyimide foam sheets and encased in 12 μ m (0.5 mil) thick Tedlar polyvinylfluoride film. The folded blanket preload/latch/release mechanism consists of a graphite/epoxy torque tube and aluminum fittings. The mast tip fitting is machined from aluminum and integrated to a graphite/epoxy torque/flexure tube with aluminum end fittings. The pallet support struts are constructed from graphite/epoxy tubes with aluminum end fittings. The blanket tensioning units and guidewire mechanism are assembled from a mixture of plastic and aluminum components, steel Negator springs, and braided stainless steel cable.

The approach is to fabricate the various components, assemble the preload/latch/release mechanism and mast tip fitting, and attach the mechanism to the lid and pallet structure. Next, the foam padding will be bonded to the lid and pallet structure. Then the blanket tension units and guidewire mechanisms will be attached to the pallet structure. Finally, the lid assembly and pallet assembly will be shipped to final wing integration.

5.2.2 Electrical Subassemblies

Over the last 27 years, TRW has acquired extensive solar cell stack assembly and installation experience. In the last 8 years, we have had the opportunity to apply that experience and equipment to the fabrication of flexible blanket assemblies, including the processing of 50 μ m thin cell stacks of a design similar to that proposed for the APSA baseline system (under JPL Contract 956402). Figure 5-4 illustrates the semiautomatic equipment line that would be used to process the solar cell stacks for the prototype wing as well as for future flight hardware.

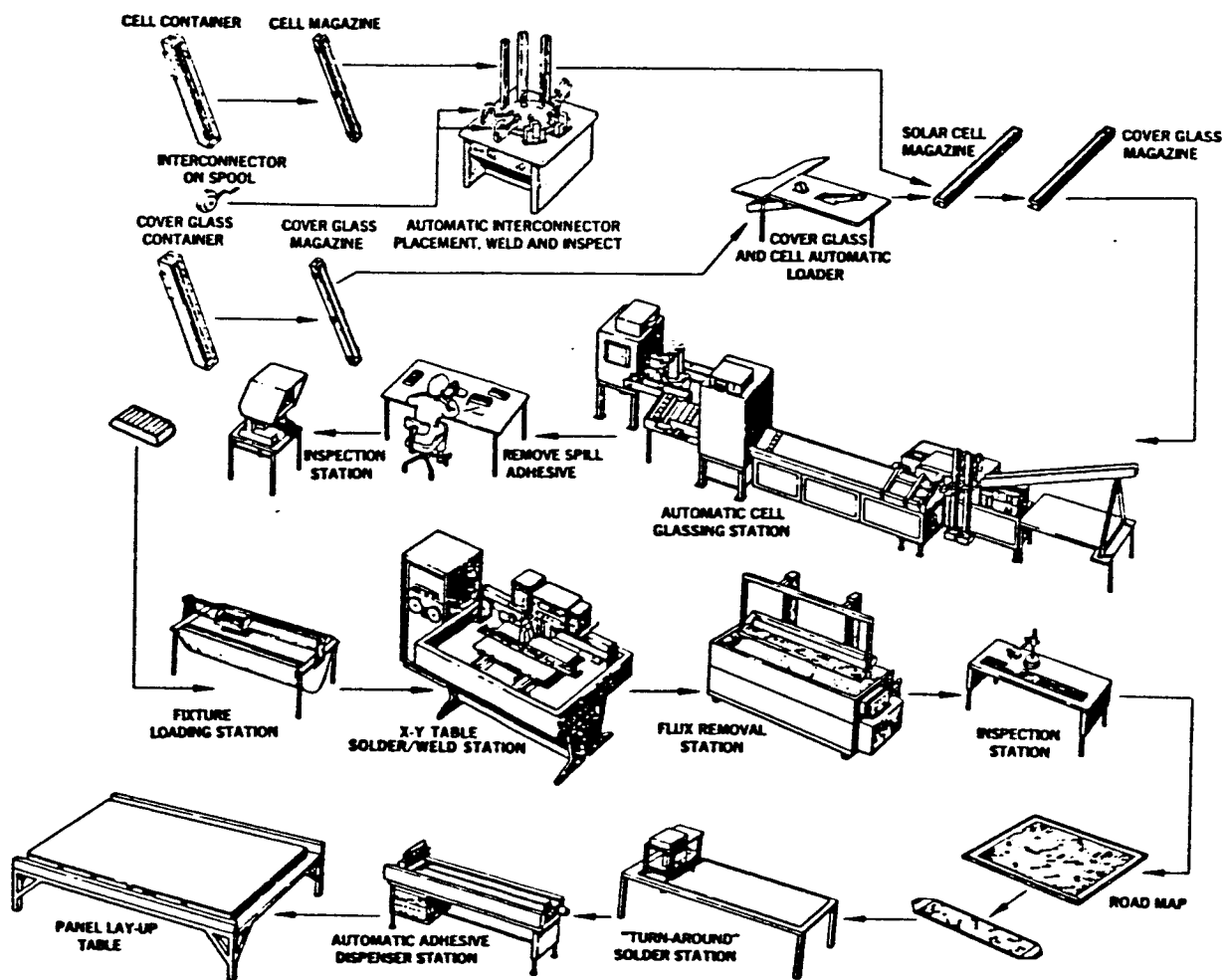


Figure 5-4. Semiautomated Solar Cell Stack Assembly and Panel Installation Line

Figure 5-5 shows the flow diagram for the proposed assembly of the solar cell stacks and installation of the glassed interconnected circuit modules onto the Kapton blanket substrate. Included in the flow diagram are both live modules and mass-simulated modules. The blanket subassembly on which the cells will be installed is a three-panel SPA unit. The SPA will have the flexible printed circuit electrical harness segments adhesively bonded along the two outer (non-hinged) edges.

The 12 major steps in the assembly/installation flow are summarized below:

- Step 1. Transfer thin cells from cell vendor styrofoam boxes to automated magazines.
- Step 2. Insert magazine with the thin cells into the Interconnector Attachment Station where two silver- and solder-plated in-plane stress relief loop interconnectors are soldered to the silver-plated negative cell front contracts. Completed cells with the two attached interconnectors are then automatically loaded into a second magazine. The flux is removed with solvent (vapor phase cleaner).
- Step 3. The solder joints are inspected for uniform solder flow and fillet as the cells are shifted out of and back into the holding magazine by the semiautomatic inspection station.
- Step 4. Thin solar cells with interconnectors are glassed in individual alignment fixtures using the Automated Glassing Station. A metered amount of DC93500 adhesive is first applied to the front of the solar cell. Then a cover glass is automatically transferred from a holding magazine and placed on top of the solar cell. The cover glass is positioned to overhang the cell on all four sides.
- Step 5. The cover glass adhesive is cured in a temperature-controlled oven, followed by removal of any excess adhesive.
- Step 6. Glassed cell stacks are inspected for proper cover glass alignment and overhang and for cracks. The cell stacks are then grouped by electrical grade. Completed stacks are then stored in plastic containers.
- Step 7. Completed stacks are placed into a module fixture in which they are series connected by means of soldering the interconnector from one stack to the silver-plated positive cell rear contact of another stack, employing one of three automated X-Y solder (or weld) stations. Completed series strings are transferred with vacuum pickup bars from the assembly fixture to a Flux Removal Station.
- Step 8. The rear solder joints are inspected for uniform solder flow and fillet. The series strings are then transferred to a panel "circuit roadmap." Strings are then jointed together to obtain a total circuit module.

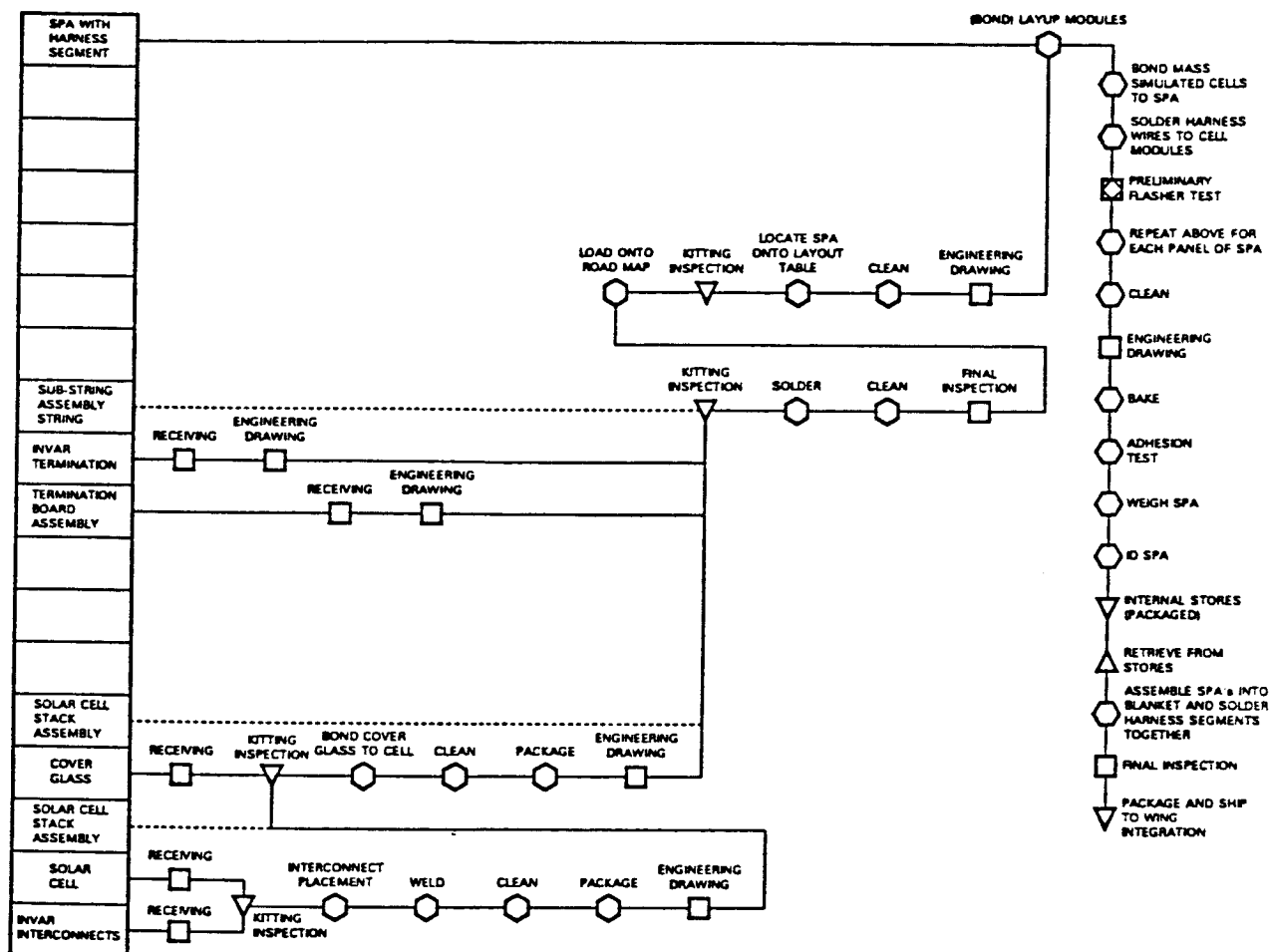


Figure 5-5. Solar Cell Module Assembly and Installation Flow Diagram

- Step 9. The SPA substrate is positioned onto the panel layup fixture (Figure 5-6). The substrate dielectric insulator is cleaned and inspected. Straight edge tooling is positioned and DC93500 adhesive is applied to the substrate with a doctor blade. Circuit module layup follows by transferring the module with a vacuum pickup to the adhesive-coated area. As the vacuum is removed, the pickup tool is replaced with weights to hold the circuit module in place during the adhesive curing cycle. Subsequent progressive repositioning of straight edges, adhesive application, and module transfer is continued until the total panel (and SPA) is covered with cells.
- Step 10. The flexible printed circuit harness terminations are cut to length and are soldered to the circuit module termination strips. This is repeated for each circuit module.
- Step 11. Each completed circuit module, while remaining on the layup fixture, is flash tested using the Xenon lamp Large Area Pulsed Solar Simulator to measure electrical performance and check the integrity of each module.
- Step 12. Any other wiring required for the prototype SPA is added.

The above 12-step process is repeated for each SPA. For the prototype wing, some of the SPAs or portions of the SPA will have 150 μ m (6 mil) thick anodized aluminum chip mass-simulated solar cells as well as live interconnected 120- to 360-series cell circuit modules. The aluminum chips would be added during Step 9 above.

Each SPA is folded and stored. Then the folded SPAs are retrieved, stacked on top of each other, and the hinge pin is inserted into the piano-hinge assembly, thereby mechanically connected one SPA to the next. Next the end of each flexible printed circuit harness run is accurately positioned to its counterpart from the next SPA and soldered together to form a "cusp" fold and to create an integrated electrical harness. The blank leader panels are also integrated to the cell-covered SPAs in a similar manner.

The resulting hardware is a completed blanket assembly ready for integration to the blanket housing assembly (lid and pallet structure).

5.2.3 Wing Integration

Figure 5-7 illustrates the overall wing fabrication and integration flow plan. The blanket assembly will be assembled per the discussions of Sections 5.2.1 and 5.2.2. The blanket housing assembly components, including the lid structure, pallet structure, folded blanket assembly cushioning structure, blanket preload/latch/ release mechanism, blanket tensioning units, guidewire mechanisms, and mast tip fitting, will be fabricated.

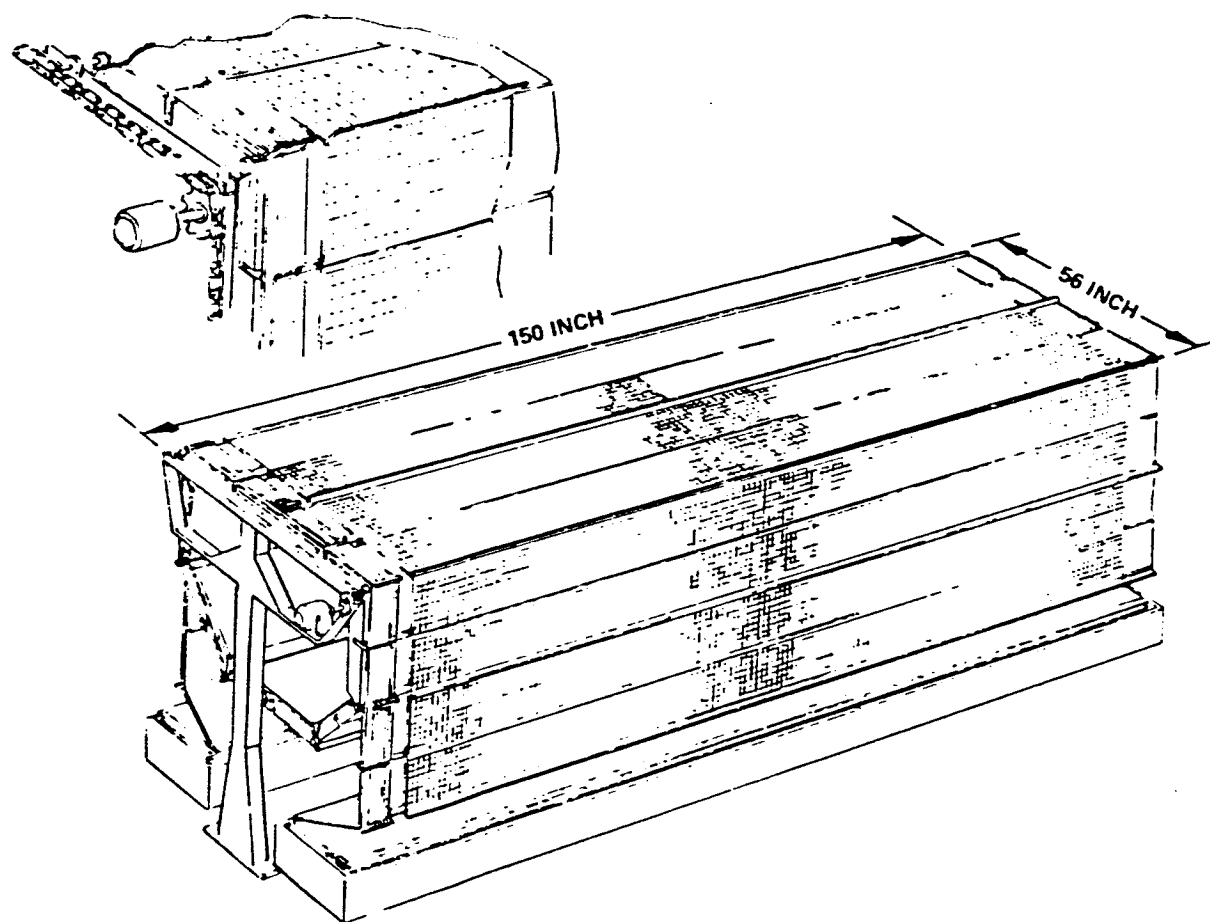


Figure 5-6. Cell Laydown Fixture (Concept Shown)

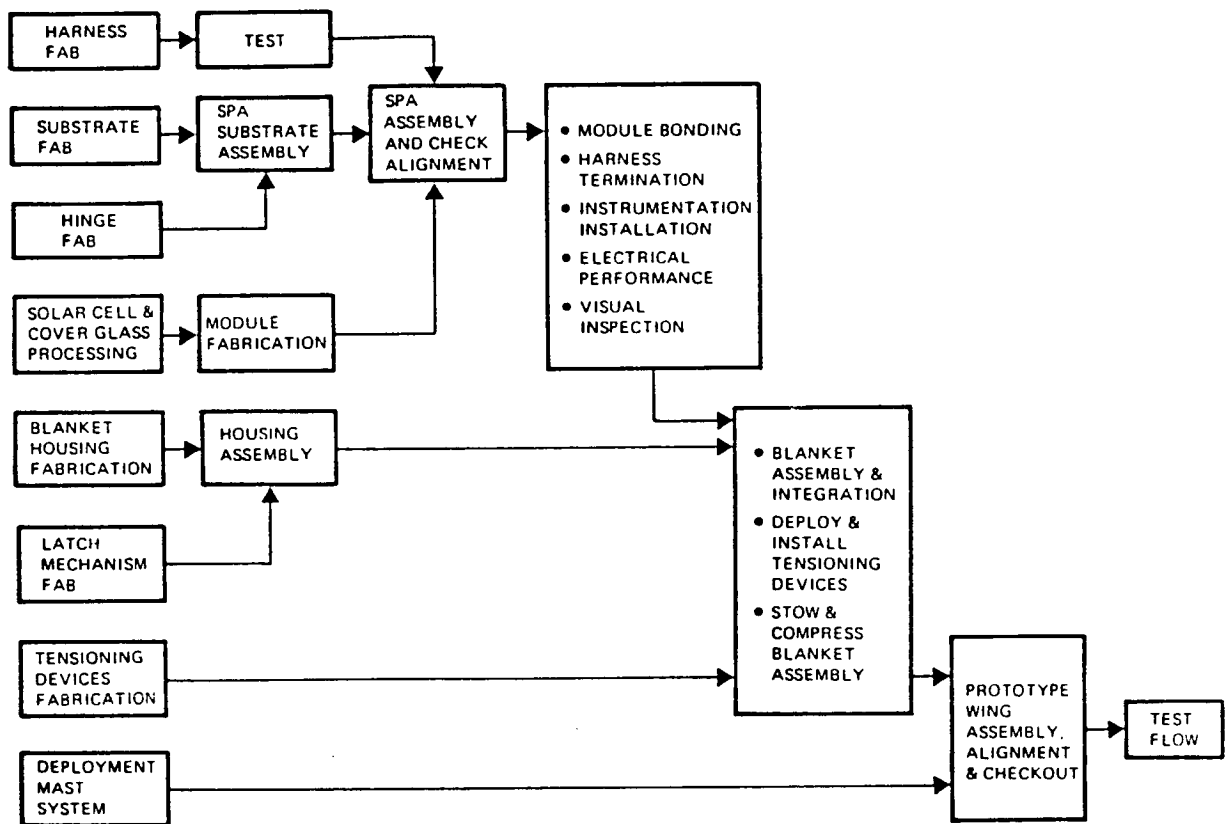


Figure 5-7. Wing Fabrication and Integration Flow Plan

The preload/latching release mechanism and diode box will be assembled and integrated to the lid and pallet structure. The mast tip fitting will be assembled and integrated to the lid structure. The blanket tensioning units and guidewire mechanisms will be integrated to the pallet structure. The folded blanket assembly will be installed between the lid and pallet structure and attachments made to the lid and to the tensioning units. However, the guidewire cables will not be attached to the blanket assembly or to the lid.

The blanket deployment mast system will be provided by the mast supplier fully assembled and ready for integration to the blanket housing assembly structure. The blanket deployment mast system will consist of the motorized mast canister and the appropriate length of tri-longeron lattice mast stowed in the canister.

The integration and deployment test fixture shown in Figure 5-2 will be used for final integration of the major subassemblies (blanket assembly, blanket housing structure, mast system) to form a wing system. The blanket housing assembly with installed folded blanket assembly will be rigidly secured to the integration/test fixture framework. Pickup points on each panel outer edge and on the lid will be attached to the air-bearing sleds that ride on the linear air manifold tubes. The blanket will then be unfolded to its full length. Then the guidewires will be extended from the pallet and attached to the blanket assembly at each rear fold line and secured to the lid structure. The blanket assembly will then be carefully retracted and blanket housing assembly latches resecured. The mast system will be integrated to the blanket housing assembly by: (1) attaching the pallet structure to the upper flange ring of the mast canister, (2) installing the two strut braces from the pallet structure to the flange ring below the drum nut on the mast canister, and (3) attaching the lid to the mast through the mast tip fitting that was already attached to the lid. The wing will be carefully deployed and aligned, then retracted and readied for deployment checkout tests.

5.3 COMPONENT DEVELOPMENT TESTS

There are a whole series of key component-level or subsystem tests that could be performed before committing to full-scale prototype wing hardware. These include:

- a. Electrical performance of the solar cell module under standard conditions
- b. Measurement of key solar cell module and substrate thermophysical properties from which predictions of operating temperature can be confirmed
- c. GEO simulated thermal vacuum life-cycle demonstration test of the solar cell module/substrate/harness
- d. Vibro-acoustic launch environment tests of the stowed folded blanket (or sections thereof) to evaluate protection of the solar cell modules
- e. Swarm tunnel tests on sections of the blanket assembly to demonstrate electrostatic charge control for GEO and polar orbit missions

- f. Demonstration of function and stiffness/strength characteristics of the mast system
- g. Functional demonstration of stowed blanket preload disengagement and release mechanism on the blanket housing assembly
- h. Where practical, measurement of weight of components and major subassemblies to help confirm predictions for wing weight and specific power.

Some of the tests listed above are more critical than others to support the demonstration of design feasibility for the baseline wing design. It is proposed to include all tests except Items a, b, and c as part of the Phase II activities. Items a, b, and c have been excluded because, in one form or another, such tests have been performed in the past. The evaluation of cell protection under launch environments is very critical and will be performed on a multiple-panel section of folded blanket (five to 10 panels, 0.1 to 0.2 m² [1 to 2 ft²] each) with live interconnected and mass simulated solar cells stowed within a section of the lid/pallet structure. Electrostatic charge control tests will be performed on a section of the blanket panel and harness in a swarm tunnel at TRW. Demonstration of deployment mast stiffness/strength/functional characteristics will be done by the mast subcontractor on a section of the mast structure and on a structural model of the canister unit as part of his development program prior to delivery of the prototype mast system to TRW. Functional checkout of the blanket housing assembly preload and lid release mechanism will be performed as part of the buildup activities associated with the blanket housing assembly. Component tests on key aspects of the mechanism will be done on structural mock-ups of the mechanism. Weight of prototype components and/or major subassemblies will be measured during the fabrication and assembly period prior to full integration of the prototype wing.

5.4 DEVELOPMENT SCHEDULE

Figure 5-8 shows the schedule for fabrication, assembly, and integration of the prototype wing (Option A) to be performed during Phase II of the APSA program and for subsequent ground demonstration testing to be performed during Phase III of the APSA program. The schedule was developed based on inputs from key suppliers (blanket material, cover glass, solar cell, deployment mast, electrical harness), a review of the wing design by manufacturing and integration engineering personnel at TRW, and engineering judgment based on the previous flexible blanket prototype wing development experience at TRW.

The maturity of the design, the availability of key components, and past experience in fabricating a prototype flexible blanket wing support the contention that Phase II would be completed within 10 months, starting September 1986, and Phase III could be completed within a subsequent 5-month period. Option B, with fewer live cells on the 12-panel blanket, would require the same total time period as Option A. Options C and D, with the eight-panel blanket, would require 1 month less (namely, 9 months for Phase II, 5 months for Phase III). Phase II does include some functional testing of the wing mechanisms and wing deployment to verify correct alignment and assembly prior to the start of more detailed ground demonstration and design verification activities under Phase III.

The critical path items for Phase II include: (1) delivery of the thin solar cells, electrical harness segments, and deployment mast system from the

- PHASE II (WING FABRICATION/ASSEMBLY) – 10 MONTHS
- PHASE III (DESIGN VERIFICATION TESTING) – 5 MONTHS

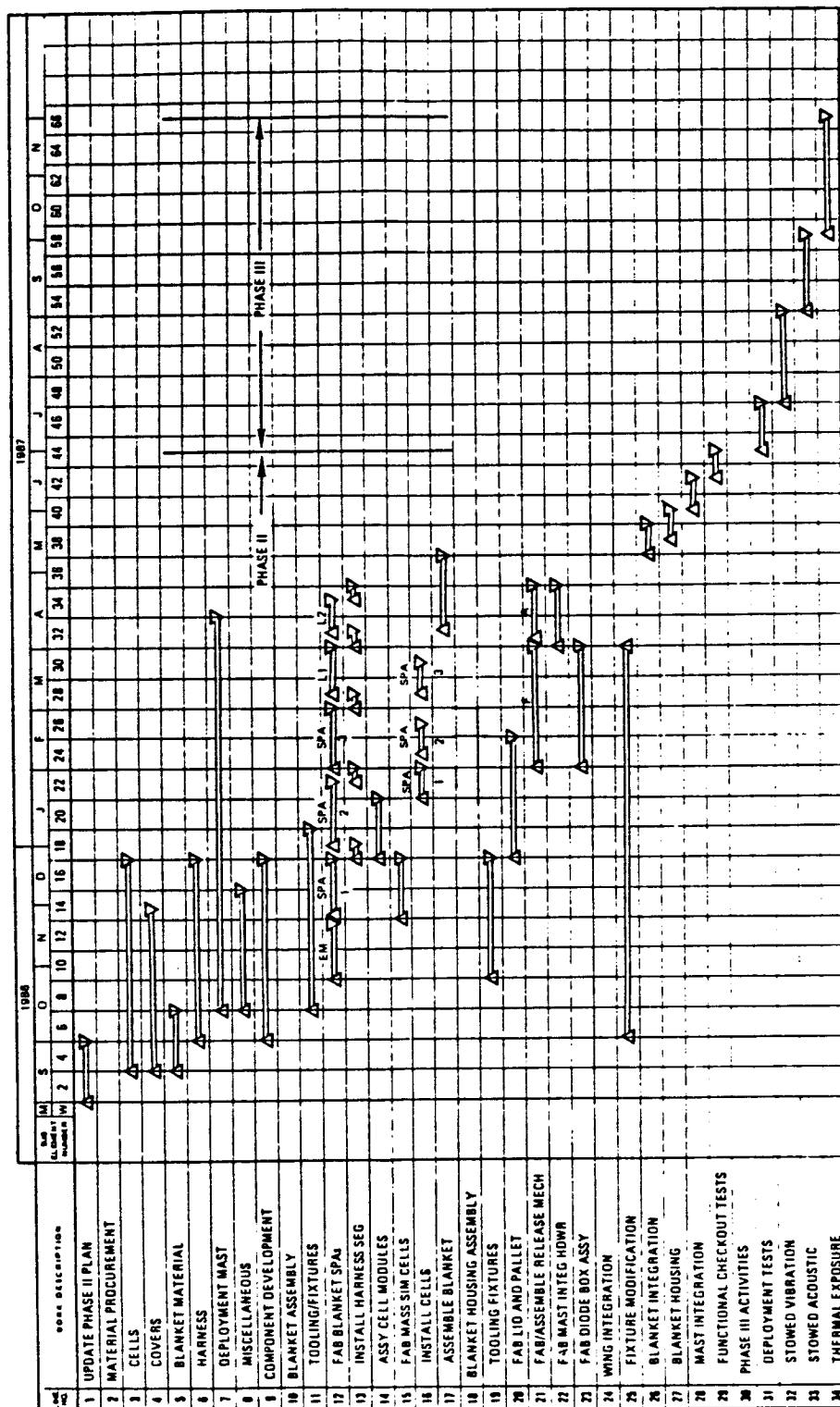


Figure 5-8. Prototype Wing Development Schedule, Option A Wing Configuration, Phase II and Phase III Activities

respective suppliers; (2) fabrication of the solar cell covered SPAs and assembly of the SPAs into an integrated 12-panel blanket; and (3) integration of the major subassemblies to create the prototype wing. The other major assumption is that the component development activities (line item 9) do not uncover any design deficiencies that would require major redesign. Such occurrences could add 2 to 4 months to the Phase II schedule. The existing integration and deployment test fixture will be modified (lengthened to accommodate the longer test article) in parallel with fabrication of the major wing subassemblies such that it will be ready for final wing integration activities.

6. CONCLUSIONS AND RECOMMENDATIONS

6.1 CONCLUSIONS

Results from Phase I of the Advanced Photovoltaic Solar Array (APSA) design study lead to the basic conclusion that the goals and objectives of the program are realistic and achievable within the time period set forth by JPL. The program can result in the development of a solar array with three to four times the specific power performance of current, comparable power-level arrays and have over twice the specific power performance of the SAFE I prototype flexible blanket array developed by NASA/OAST in the early 1980s.

The major conclusions about the flatpack, foldout flexible blanket array design are as follows:

1. The array wing configuration is based on a design similar to that used on SAFE I, CTS and Olympus flexible blanket arrays - a one blanket wing with a deployment mast structure located behind the blanket plane.
2. Two-wing array specific power characteristics of 136 W/kg (BOL) and 97 W/kg (EOL) at 10.4 kW (BOL) and 7.4 kW (EOL) for a 10-year geosynchronous mission.
3. Power density of 133 W/m² (BOL) and 95 W/m² (EOL) for a 10-year geosynchronous mission.
4. The design is sized for a deployed fundamental natural frequency of 0.10 Hz, and a deployed strength of 0.015 g; however, this easily can be easily increased five-fold for less than a 10 percent increase in array weight and concomitant decrease in specific power.
5. The array design is based on existing and emerging technology to permit prototype wing fabrication and ground test demonstration within 15 months. With a focused effort, flight hardware arrays could be available for spacecraft integration in early 1990. The key existing technologies include:
 - 13.5 percent efficient, 63 μ m (2.5 mil) thick, 10 Ω -cm B-BSF/Al-BSR silicon solar cells
 - 50 μ m (2 mil) thick coated ceria-doped coverglass
 - Flexible printed circuit copper electrical harness
 - 50 μ m (2 mil) thick carbon-loaded, partially conductive, Kapton polyimide blanket substrate material.
6. The major component that needs further development is a lightweight version of a canister-deployed continuous tri-longeron fiberglass lattice mast system that was used on the SAFE I wing.
7. The wing design can be verified by ground-based testing without the need for complex test fixtures and equipment.

8. The array has broad utility to meet other mission and functional requirements without major changes in the proposed design.
- Can be scaled in size to accommodate a wide range of power levels with improved specific power performance at the higher power levels up to 12 kW (BOL) per wing (for a one-blanket wing).
 - Can easily accommodate advanced photovoltaic components ranging from gallium arsenide cells, IR-reflective cells, IR transparent cells, indium phosphide cells, amorphous silicon film technology.
 - Can be used for interplanetary missions with negligible modifications.
 - Can be used for LEO missions with minimum modifications (primary related to atomic oxygen protection).
 - Can incorporate partial extension and full retraction capability with minimum modification and minimum increase in complexity and weight (10 percent decrease in specific power).
 - Is compatible with most spacecraft configurations/sizes and with shuttle environments.

Other important conclusions derived from the Phase I study include:

1. For the power ranges studied, wing aspect ratio (blanket length divided by blanket width) does not have a major impact on specific power or power density. For a nominal 5kw (BOL) wing, the specific power varied less than 10 percent over the aspect ratio range 2.5 to 10, for given deployed stiffness and strength requirements. The wing should be as wide as possible consistent with limitations imposed by spacecraft stowage and interference with other appendages and sensor fields of view on the spacecraft.
2. For low inclined orbits above 15,000 nmi and polar orbits above 50 to 60 degrees inclination at any altitude, grounding of the array structure, especially the blanket assembly, is required to minimize the effects of electrostatic charge buildup from substorm environments.
3. The array can operate in LEO down to 460 to 650 km (250 to 350 nmi) orbits with acceptable performances under the erosive effects from atomic oxygen at those altitudes; however, there are coatings and material substitutions that will improve the long lifetime performance in LEO atomic oxygen environments.

4. At LEO, the array has a specific power of 120 W/kg (BOL) and 114 W/kg (EOL), with an EOL power density of 110 W/m² for a 10-year mission at 460 km (250 nmi) (0 degrees inclination); BOL/EOL array power would be 9 kW/8.6 kW for the identical size array defined for GEO operations. Performance decreases 5 percent if the inclination is 32 degrees for the same LEO altitude.
5. The array can withstand the temperature extremes from an interplanetary mission covering the solar distance range from Jupiter (5.2 AU) to near Mercury (0.5 AU). The major issue for interplanetary missions is the large deviations from nominal performance experienced by the solar cells due to the low-intensity-low-temperature (LILT) problems for outward bound missions.
6. To provide substantial improvements in specific power over that associated with the thin silicon solar cell module design, the higher efficiency advanced solar cells such as gallium arsenide, indium phosphide, multijunction cascade types, etc., must be less than 100μm (4 mils) thick. If reduced array size is more important than specific power and cost, then the use of the higher efficiency advanced solar cells will provide substantial improvements in power density over the baseline thin silicon solar cell.
7. Thin film amorphous silicon cell technology merits further evaluation/development because of its potential to obtain array specific power performance of 200 W/kg (EOL). This is predicated on being able to demonstrate space radiation tolerant 10 percent operating efficiency modules with high manufacturing reliability. The present operating efficiency of 5 to 6 percent results in an array with comparable specific power as the baseline array, but 70 to 100 percent larger in size.

6.2 RECOMMENDATIONS

Based on the results and technology status of the proposed design, the following recommendations are made:

1. The baseline design has sufficient technical and design readiness to warrant implementation of the prototype demonstration phase of the APSA program in order to verify the producibility and predicted performance of the array. The prototype wing can be fabricated within 10 months for about \$700K to \$800K.
2. The technical feasibility of utilizing thin film amorphous silicon solar cells for long-term space missions should be seriously evaluated because of the potential to provide even greater specific power performance at lower cost than the baseline design. A major program is need to develop large-scale production of high-performance modules and to demonstrate high performance (10 percent efficiency) after long-term space radiation and thermal cyclic environments.

3. The design defined for this study was for a long-term, geosynchronous mission. Since the design appears to have broad application to other near-earth and interplanetary missions, these specific missions should be addressed in greater depth to obtain a better determination of the required design modifications and array performance characteristics.

7. NEW TECHNOLOGY

No items of new technology were developed by TRW Space & Technology Group under this contract.

The technique proposed to protect the flexible blanket assembly from accumulated electrical charge from the space plasma, without degrading the blankets' thermophysical heat emissivity properties, is covered under a TRW patent application submitted in June 1986. A serial number has yet to be issued by the U.S. Patent Office. The technique was developed under TRW Independent Research and Development activities and documented in 1981 and 1984. The disclosure is contained in TRW Docket Numbers 160097 and 160137.

The wing integration and deployment test fixture was designed, developed, and demonstrated under two TRW IR&D programs during 1981 through 1983 in support of an IR&D prototype flatpack, foldout, flexible blanket wing development program. The features of the fixture permit zero and partial gravity deployment and retraction tests to be performed on flexible blanket wings which replicate the blanket kinematic behavior characteristics obtained on KC-135 aircraft simulated partial gravity tests.

APPENDIX

MARKET SURVEY RESULTS FOR UTILITY OF AN ADVANCED PHOTOVOLTAIC SOLAR ARRAY

As part of the Phase I statement of work, TRW was required to assess the potential market and array design utility for near term (10 to 15 years) NASA, commercial, and military missions. In addition, the data obtained could be useful in highlighting more specific design and performance requirements and potential mission applications that could have an impact on the evolving array design.

A 19-question survey and data package was prepared and sent to over 100 engineering and management personnel in 33 NASA, industry, and DoD organizations 3 months before the study preliminary design review. The data package included some conceptual design information about the generic wing configuration and performance trends so that the respondents would understand something about the potential design. Also included were the array design goals/requirements established by JPL at the start of the study.

Table A-1 lists the recipients of the survey package. Responses were obtained from twelve organizations (listed under Question 1 and coded A through L in terms of their summary responses listed under the subsequent questions). Table A-2 presents the survey conclusions. Also included in this appendix on the subsequent pages are the survey questions along with the summary responses to each of the questions.

Most responses indicated "recurring cost" to be more important than array performance in terms of specific power (W/kg) or power density (W/m^2), with a willingness to give up 20 to 50 percent of the specific power goal in exchange for low cost. There appeared to be a need for high-power arrays in the 5 to 12 kW range, with a few applications above 50 kW. The need for partial extension and full retraction of the array was identified as a requirement for some missions. The deployed frequency characteristics and deployed strength requirements were generally at the high end of the APSA study range or above. There was almost no information forthcoming on stowage volume or array size/geometry constraints.

In conclusion, the survey results were of marginal value to the design definition of the advanced photovoltaic solar array. For some mission applications, the solar array will be a critical subsystem, where performance requirements are closely defined. However, for many missions, the solar array is not considered a critical subsystem and the performance requirements are specified such that weight efficiency is sacrificed for some other performance parameter or for some other spacecraft subsystem.

Table A-1. Recipients of APSA Survey Package

<u>Company/Agency</u>	<u>Quantity</u>
TRW	12
Fairchild Space and Electronics	2
MDAC/Huntington Beach	5
MDAC/St. Louis	1
Rockwell International	3
Ball Aerospace	1
Ford Aerospace	1
General Dynamics	2
Lockheed Missile & Space Company	7
Martin Marietta Company	1
Hughes	12
Boeing	2
General Electric	6
RCA Astroelectronics	7
RCA American Communications	2
Grumman Aerospace Corporation	2
Satellite Business Systems	2
Comsat Corporation	4
Intelsat Corporation	1
NASA/JPL	3
NASA/LeRC	6
NASA/JSC	4
NASA/MSFC	6
NASA/GSFC	1
NASA/LaRC	2
NASA Headquarters	2
Aerospace Corporation	6
AF Aero Propulsion Laboratory	4
AF Space Technology Center	1
AF/SAMSO	1
AF Cambridge Research Laboratory	1
MIT Lincoln Laboratories	3
Navy Research Laboratory	1
	<hr/>
	114

Table A-2. Survey Conclusions

1. MOST RESPONSES INDICATE RECURRING COST MORE IMPORTANT THAN ARRAY PERFORMANCE (W/KG, W/M²); I.E., WILLING TO GIVE UP 20 TO 50 PERCENT OF W/KG GOALS TO ACHIEVE LOWER COST
2. EOL SPECIFIC POWER OF 15 TO 100 W/KG, WITH MOST RESPONSES LESS THAN 50 W/KG
3. POWER RANGE OF 5 TO 12 KW, WITH A FEW MISSIONS AT 50 KW AND ABOVE
4. VOLTAGE LEVEL OF 50 TO 200 VOLTS (EOL)
5. ABOUT 50 PERCENT OF MISSIONS ABOVE NOMINAL LEO (\approx 300 NM)
6. MOST MISSIONS SHUTTLE LAUNCHED
7. PRIMARY MILITARY MISSIONS: A FEW COMMUNICATION MISSIONS
8. PARTIAL EXTENSION, FULL RETRACTION, FULL RESTOWAGE ARE OTHER PERFORMANCE REQUIREMENTS INDICATED FOR SOME MISSIONS
9. CRITICAL DYNAMIC MODE IS THAT WHICH CAUSES SPACECRAFT ROTATION RATHER THAN TRANSLATION
10. DEPLOYED FREQUENCY REQUIREMENT NOT WELL DEFINED; GENERALLY RANGE FROM 0.05 TO 0.2 HZ WITH A FEW AT >0.5 HZ
11. DEPLOYED LOADING REQUIREMENT NOT WELL DEFINED; GENERALLY RANGE FROM 0.01 TO 0.1 GS (LIMIT) WITH MOST ABOVE 0.05 GS
12. DEPLOYED WING SIZE: SHORT AS POSSIBLE CONSISTENT WITH STOWAGE LIMITATIONS OF WING WIDTH
13. LITTLE INFORMATION AVAILABLE ON ACTUAL SPACECRAFT BODY CONFIGURATIONS AND AVAILABLE ARRAY STOWAGE VOLUME; STOWAGE ON N/S OR E/W WALLS PREFERRED OVER NADIR/ZENITH FACES OF SPACECRAFT
14. STOWED WING CONFIGURATION WITH BLANKET HOUSING STRUCTURE RIGIDLY ATTACHED TO MAST PREFERRED OVER OTHER CONCEPTS REQUIRING SECONDARY PIVOTING OF BLANKET HOUSING STRUCTURE PRIOR TO WING DEPLOYMENT
15. ONE OR TWO BLANKETS PER WING
16. ARRAY WING STANDOFF DISTANCE RANGES FROM 2 TO 10 FEET
17. SHADOW PROTECTION REQUIRED DUE TO TRANSIENT SHADOWS
18. LASER/NUCLEAR HARDENING FOR SOME APPLICATIONS

1. RESPONDING COMPANIES

- A. Ford Aerospace & Communications Corporation
Western Development Labs Division
Supervisor, Mechanisms and Solar Arrays
- B. Hughes Aircraft Company
Space and Communications Group
Manager, Power Sources Department
- C. U.S. Air Force
Air Force Wright Aeronautical Labs
Technical Manager
- D. NASA/Johnson Space Center
Power Branch/EP-5
Aerospace Technologist
- E. TRW
Military Space Systems-Systems Engineering
Member Technical Staff
- F. Rockwell International
Satellite Systems Division
Senior Engineer Specialist
- G. RCA Corporation
RCA-Astro Electronics Division
Manager, Conceptual Design
- H. Fairchild Space Company
Systems and Advanced Missions
Staff Engineer
- I. Martin Marietta Aerospace
Power Sources
Senior Engineer
- J. NASA Langley Research Center
Space Station Office
AST, Technical Management (Systems)
- K. TRW Defense Projects Division
Space Transportation
Manager, SLD Advanced Applications
- L. McDonnell Douglas Corp.
Space Transportation
Manager, SLD Advanced Applications

2. What organizational function does your opinion reflect?

Advanced or corporate planning -

Advanced studies - B, C, D, E, F, G, H, J, K, L

Engineering design - A, B, C, F, G, I, J

Manufacturing -

Integration and Test -

Other -

3. Is your organization interested in this solar array technology for potential applications during the 1988 to 2000 time period?

Yes - A, B, C, D, E, F, G, H, I, J, K, L

No -

4. If your answer to Question 3 is NO, please identify major reasons for not considering this type of solar array. Answer Questions 5 through 19 to identify your requirements/preferences and illustrate/describe type of array being considered on supplemental sheet.

Current photovoltaic array technology acceptable for your mission requirements - J

Non-photovoltaic power generation being considered - E

Other - E, photovoltaic power generation as well as DIPS and nuclear power are being considered for spacecraft.

A photovoltaic power generation is being studied for spacecraft B and C.

5. IF YOUR ANSWER TO QUESTION 3 IS YES, PLEASE DESCRIBE CANDIDATE MISSIONS IN THE TABLE BELOW AND ANSWER QUESTIONS 6 THROUGH 19 TO IDENTIFY YOUR REQUIREMENTS/PREFERENCES.

COMPANY	SPACECRAFT* NAME	MISSION* OBJECTIVE	LAUNCH VEHICLE	ORBIT ALT. (NMI)	MISSION DURATION (YEARS)	NEED DATE FOR S/A FLT. H/W
A	A	COMMERCIAL COMMUN.	SHUTTLE OR ARIANE	GEO	10	MID 1990s
	B	INTERPLANET EXPLORATION	SHUTTLE	---	MANY	MID 1990s
B		NO RESPONSE				
C	SBR SDI	RADAR SURVEIL. SPACE DEFENSE	SHUTTLE SHUTTLE, TAV	5000 MANY	5 2-10	--- 2000
D	SPACE STATION	PERMANENTLY MANNED SPACE STATION	SHUTTLE	275	30	OCT '87
	SPACE STATION PLATFORM	PLATFORM F/ EXPERIMENTS	SHUTTLE	275	30	AFTER '87
E	A	SPACE SURVEIL. & TRACKING	STS	---	10	1990
	B	SDI	SDLV	---	10	1990
	C	SDI	STS	---	10	1990
F	SSTS	ADVANCED SURVEILLANCE	SHUTTLE	---	CLASSIFIED	---
	BSTS	ADVANCED SURVEILLANCE	SHUTTLE	---	CLASSIFIED	---
	ADV. GPS#	GPS	SHUTTLE	---	TBD	1990
G	A	GEO COMMUN. S/C	STS OR ARIANE 4	GEO	12	1990
	B	LEO DEDICATED MISSION	STS	380	15**	1989
	C	LEO SPACE STAT. PLATFORM	STS	215 TO 485	15**	1993
H	RADARSAT	OCEAN OBSERVA- TIONS	STS	1007	5.	1992
I	A	A	STS	650	5	1990
J	(SEE BACK)					
K	A	CLASSIFIED	STS	5400	4+	1990-1992
	B	CLASSIFIED	STS	GEO	7-10	1990-1995
L	A	---	STS	325	3	1990
	B	---	STS	600	3	1992
	C	---	STS	300	5	1992

** SERVICEABLE SPACECRAFT; DESIGN LIFE INDEFINITE. DURATION SHOWN IS SUGGESTED INTERVAL BETWEEN ARRAY REPLACEMENTS.

* ADV. GPS - MODIFIED GPS BUS FOR ADVANCED FUTURE SPACE MISSIONS.

6. WHAT ARRAY POWER LEVEL AND VOLTAGE LEVEL ARE YOU INTERESTED IN?

COMPANY	SPACECRAFT NAME	NO. OF WINGS PER ARRAY*	ARRAY BOL PWR LEVEL (KW)	ARRAY EOL PWR LEVEL (KW)	BOL OPEN CIRCUIT VOLTAGE (V)	EOL VOLTAGE (V)
A	A	2	12 SUMMER SOLSTICE	10 SUMMER SOLSTICE	120	100
	B	1 OR 2	---	5 TO 10	120	100
B	NO RESPONSE					
C	SBR	NOT DEFINED	--	50	NOT DETERMINED	
	SDI	NOT DEFINED	300	---	NOT DETERMINED	
D	SPACE STATION		---	300	200	200
	SPACE STATION PLATFORM	2	725	25	775	75+
E	A	2	20-40	10-20	50-200	28-120
	B	2	N/A	2-4	N/A	28
	C	2	N/A	1-2	N/A	28
F	SSTS	1-2	7-50	6-40	120-220	100-200
	BSTS	2	2.3-7	~2-6	30-120	28-100
	ADV. GPS	2	2	~1.5	27.4	
G	A	2	6	5	---	40-120*
	B	1	4	3	--	40-120
	C	2	12	8	-	40-120
H	RADARSAT	1	10	6	125 MAX	44 PEAK POWER POINT MINIMUM
I	A	2	5	4	60	53
J	SEE BACK					
K	A	2	---	5-50	---	250-300
	B	1 OR 2	--	3.5-5	---	30-50 BUS VOLTAGE
L	A	2	1.5	1.3	30	28
	B	2	12	11	75-85	70-80
	C	2	0.7	0.6	30	28

* EITHER 35V OR 100V BUS (BOTH TYPES PLANNED)

J. Supplemental Information for Question # 5 & 6

Langley would be interested in advanced technology development possible in support of Space Station activity in the future. These missions or experiments (ground and on-orbit) are not currently defined to the detailed requirement level. Current activities have included preliminary definition activities like the ACCESS experiment (deployment and dynamic response measurements) as well as future planned structural verification experiments (such as the COFS project testing of MAST beams and arrays and generic space station models). Of course, as advanced PV arrays become available, they will be tested at Langley, since savings of mass and drag while allowing increased power availability will always be a worthwhile power system up-grade.

7. WHAT ARE YOUR SOLAR WEIGHT ALLOCATION AND SPECIFIC POWER REQUIREMENTS?

COMPANY	SPACECRAFT NAME	ARRAY WEIGHT REQUIREMENTS (KG)	BOL SPECIFIC POWER (W/KG)	EOL SPECIFIC POWER (W/KG)
A	A	---	---	35 TO 50
	B	---	---	35 TO 50
B	NO RESPONSE			
C	SBR	BEING STUDIED	---	---
	SDI	BEING STUDIED	---	---
D	SPACE STATION SPACE STATION PLAT.			
E	A	---	200	100
	B	---	NOT AVAILABLE	NOT AVAILABLE
	C	---	NOT AVAILABLE	NOT AVAILABLE
F	SSTS	TBD	20*	15*
	BSTS	TBD	25*	20*
	ADV. GPS	TBD	25*	20*
G	A	50	---	100**
	B	40	---	75**
	C	110	---	75**
H	RADARSAT	250	---	---
I	A	150	33	27
J	SEE BACK			
K***	A	225 TO 2250	22.2 OR MORE	27
	B	234	15 OR MORE	15
L	NO RESPONSE			

* INCLUDING SMATH HARDENING CAPABILITY

** THESE ARE GENERAL GUIDELINES. BASICALLY WE ARE LOOKING FOR THE BEST PERFORMANCE CONSISTENT WITH THE LOAD AND FREQUENCY REQUIREMENTS AT REASONABLE COST.

*** SPECIFIC POWER: THE HIGHER THE BETTER. NUMBERS USED FOR EVALUATED MISSION FEASIBILITY AREAS FOLLOWS.

J. Supplemental Information for Question #7

The specific power goals for the APSA project appear to be very ambitious indeed. The Space Station PV arrays are designed for approximately 17 w/kg, so that numbers larger than 100 w/kg would be a fantastic increase in power availability (or decrease in structure mass, volume, size, etc. for the same power). In fact, a six-fold increase in specific power would possibly have some impact on the selection of the space station power generation system (PGS). Be certain to consider all implications of the changes made to the PGS, since trading one approach with known limitations for another approach with unknown limitations may not be an acceptable option (for example, GaAs for Si solar cells may cause additional problems that have to be evaluated).

8. How important are the APSA specific power goals (i.e. 105 to 130 w/kg) relative to array recurring flight hardware cost?

1. Array specific power substantially more important than cost (i.e., BOL and EOL goals are critical to the success of the mission).
2. Recurring cost somewhat more important than achieving stated specific power goals (i.e., BOL and EOL goals can be reduced 10 to 20 percent to achieve lower cost array).
3. Recurring cost substantially more important than achieving stated specific power goals (i.e., BOL and EOL goals can be reduced 30 to 50 percent or more to achieve lower cost array).

1. C, E, F (survivability is most important issue), J, L
2. D*, G (S/C A), I, K
3. A, G (S/C B & C), H

No Response - B

* of importance is the total cost of the system over the life of the mission

10. What dynamic mode shape is critical to the determination of minimum frequency for the deployed array listed in Question 9?

1. Mode shapes that result in translation disturbances to the spacecraft body.
2. Mode shapes that result in rotation or angular disturbances to the spacecraft body.
3. Other:
 1. D, E (S/C A), F, K
 2. A, D, E (S/C A), G, I, K, L
 3. E (S/C B & C undetermined), H (TBD), J (both rotational and translational response could affect pointing and control).

No Response: B, C

9. WHAT ARE YOUR DEPLOYED ARRAY DYNAMIC FREQUENCY REQUIREMENTS? WHAT FACTORS OR MISSION OPERATIONS DRIVE THE REQUIREMENT?

	SPACECRAFT COMPANY NAME	WING DEPLOYED FUNDAMENTAL	KEY REASONS FOR THIS FREQUENCY REQUIREMENT
A	A	0.05-0.1	ATTITUDE CONTROL INTERACTIONS
	B	0.05-0.1	ATTITUDE CONTROL INTERACTIONS
	NOTE: FOR VERY LARGE ARRAYS OUR ATTITUDE CONTROL ENGINEERS MAY NEED TO LEARN HOW TO DEAL WITH LOWER FREQUENCIES		
B	NO RESPONSE		
C	NO RESPONSE		
D	SPACE STATION	<0.1	CONTROLLABILITY ARRAYS AND SPACE STATION STABILITY PLATFORM
	SPACE STATION PLATFORM		
E	A	0.2	POINTING CONTROL
	B	UNDETERMINED	
	C	UNDETERMINED	
F	SSTS	TBD	TBD
	BSTS	TBD	TBD
	ADV. GPS	TBD	TBD
G	A	>0.05	CONTROL SYSTEM INTERACTIONS
	B	>0.05	CONTROL SYSTEM INTERACTIONS
	C	>0.05	CONTROL SYSTEM INTERACTIONS
H	RADARSAT	TBD	---
I	A	>1.0	WILL COUPLE WITH CONTROL SYSTEM FREQS.
J	SEE BACK		
K	NOTE: ARRAY FREQUENCY MUST BE THE SAME FOR ALL ORIENTATIONS TO AVOID S/C DYNAMICS BEING DEPENDENT ON ARRAY ORIENTATION.		
	A	N/A	
	B	<0.15 HZ	DE TUNE EFFECT OF ARRAY BY PLACING ITS FREQUENCY LOWER THAN OTHERS.
L	A	2 HZ	NONE
	B	0.2-0.5 HZ	NONE
	C	3 HZ	NONE

J. Supplemental Information for Question #9

The deployed array natural frequencies (consider all of them in the frequency range) should be such that they do not interact or otherwise adversely effect the control system and controllability of the structure. There also could be several closed loop control systems in operation at one time, each influencing structural motions of different locations (or each other) in a different manner. Careful response to all applied forces is necessary.

11. WHAT ARE YOUR DEPLOYED LOADING ENVIRONMENTS? WHAT FACTORS OR MISSION OPERATIONS DRIVE THIS REQUIREMENT?

COMPANY	SPACECRAFT NAME	LIMIT LINEAR ACCELERATION LOAD)* (IN/SEC ²)	LIMIT ANGULAR ACCELERATION LOAD)* (RAD/SEC ²)	KEY REASONS FOR THIS LOADING ENVIRONMENT
A	A	<0.1g	?	THRUSTER FIRING
	B	<0.1g	?	THRUSTER FIRING
B	NO RESPONSE			
C	LOADING ENVIRONMENTS DETERMINED BY WEAPON SURVIVABILITY REQUIREMENTS TYPICALLY 0.1g.			
D	SPACE STATION	TBD	TBD	TBD
	SPACE STATION PLATFORM	TBD	TBD	TBD
E	A	---	UNDETERMINED	---
	B	---	UNDETERMINED	---
	C	---	UNDETERMINED	---
SUPPLEMENTAL INFORMATION: THESE LIMIT ACCELERATIONS HAVE NOT BEEN DETERMINED. HOWEVER, DUE TO MISSION REQUIREMENTS IN MOST OF THE SPACECRAFT DISCUSSED, IT IS BELIEVED THAT EVASIVE MANEUVERS WILL BE AN IMPORTANT FACTOR IN ESTABLISHING THE LIMIT LOADS. THIS KIND OF MANEUVER SUGGESTS THAT SUCH LIMITS MUST BE HIGHER THAN IN OTHER NON-MILITARY MISSIONS.				
F	SSTS	116	TBD	MANEUVERING AND FAST ARRAY RETRACTION
	BSTS	39	TBD	"
	ADV. GPS	39	TBD	"
G	A	1	0.001	STATIONKEEPING REQ'T'S.
	B	20	.01	ORBIT BOOST & DEBOOST
	C	20	.01	"
H	RADARSAT	0.01g	TBD	---
I	A	N/A	N/A	N/A
J	MANY VARIOUS LOADINGS POSSIBLE FROM ORBITAL INSERTION OR CHANGE (DEBOOST FOR EXAMPLE) TO OPERATIONAL LOADS FROM MOTIONS OF WHATEVER STRUCTURE IS ATTACHED.			
K	A	N/A		
	B	0.15	0.00018	ATTITUDE & ORBIT CORRECTION
L	A	4.0	0.03	ORBIT KEEPING AND
	B	0.1	0.005	ATTITUDE CONTROL
	C	0.3	0.02	

12. ARE THERE ANY REQUIREMENTS THAT WOULD LIMIT THE WING DEPLOYED LENGTH OR WIDTH? IF NO, THEN LEAVE THE APPROPRIATE SPACE BLANK. IF YES, THEN IDENTIFY THE DIMENSIONAL LIMITATIONS AND REASON BEHIND THE LIMITATION.

COMPANY	SPACECRAFT NAME	WING LENGTH (INCHES)	WING WIDTH (INCHES)	KEY REASON FOR THIS LIMITATION
A	B	AS SHORT --- AS PRACTICAL		MINIMIZE SOLAR PRESSURE TORQUE WITH ONE WING
B	NO RESPONSE			
C	NO RESPONSE			
D	NO RESPONSE			
E	NO RESPONSE			
F	SSTS	TBD	TBD	P/L-SENSOR FIELD OF VIEW, ARRAY
	RSTS	TBD	TBD	STIFFNESS FOR MANEUVERING
	ADV. GPS	TBD	TBD	"
G	A	---	~120	F OF V AND PLUME* INTERACTION EFFECTS
	B	---	~150	
	C	---	~200	
H	RADARSAT	---	<120	STOWAGE ON S/C IN SHUTTLE
I	NO RESPONSE			
J	YES, LIMITATIONS WILL EXIST IF CONSIDERTION IS GIVEN TO HAVING FLEXIBLE ARRAYS ATTACHED TO A FLEXIBLE, CONTROLLABLE VEHICLE			
K	A	---	207	SHUTTLE CONSTRAINTS
L	A			PACKAGING VOLUME
	B			WEIGHT
	C			PACKAGING VOLUME

* NUMBERS ARE ROUGH GUESSES. DEPEND ON MISSION OPERATION DETAILS.

13. BASED ON YOUR PRESENT UNDERSTANDING OF HOW YOU WOULD PREFER TO INTEGRATE THE SOLAR ARRAY WINGS TO THE SPACECRAFT BODY, PLEASE IDENTIFY FROM FIGURE 3* THE STOWED WING CONFIGURATION MOST LIKELY REQUIRED. IF NONE OF THOSE FIGURE 3 ARE APPLICABLE, PLEASE INDICATE YOUR CONFIGURATION BY A SKETCH ON A SUPPLEMENTAL SHEET.

COMPANY	SPACECRAFT NAME	WING STOWAGE CONFIGURATION. CIRCLE THE APPROPRIATE ANSWER BASED ON APPROACHES SHOWN IN FIGURE 3.*						
		3A	3B	3C	3D	3E	3F	OTHER
A	A	3A						
	B	3A						
B	NO RESPONSE							
C		NO CLEAN DRIVER- TOO EARLY TO TELL						
D	SPACE STATION	3A						
	SPACE STATION PLATFORM	3A						
E	A		3B					
	B		3B					
	C		3B					
F	SSTS					3E		
	BSTS		3B					
	ADV. GPS		3B					
G	A		3B	3C				
	B	3A						
	C	3A						
H	RADARSAT	3A						
I	A					3E		
J	JPL'S PREVIOUS STUDY MAY HAVE REVIEWED THESE OPTIONS AND RECOMMENDED 3A. SPACE STATION USES 3B NOW.							
K	A		3B					
	B						3F	
L	A		3B					
	B						3F	
	C							OTHER

* SEE NEXT PAGE FOR CANDIDATE WING STOWAGE CONFIGURATION

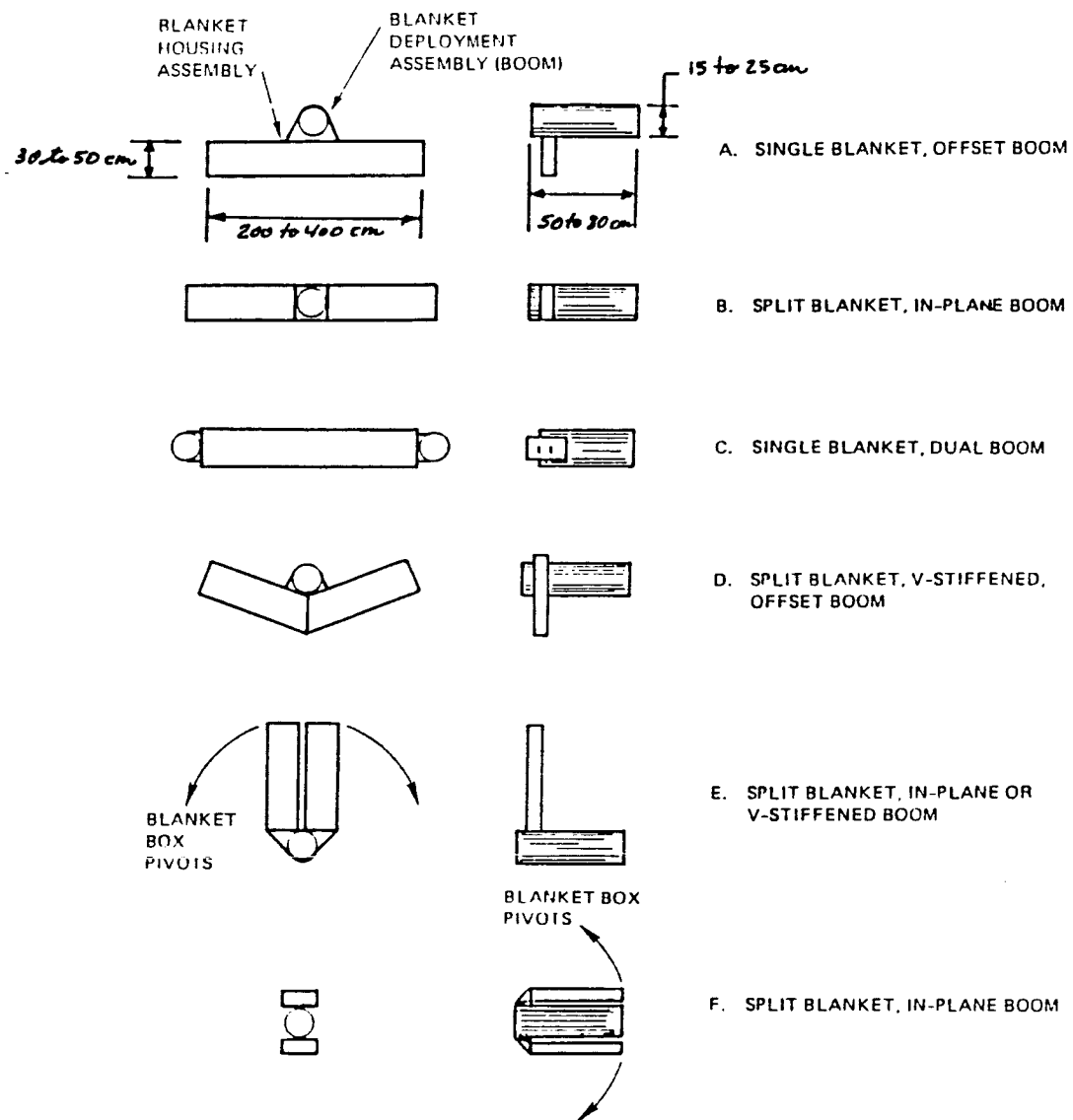
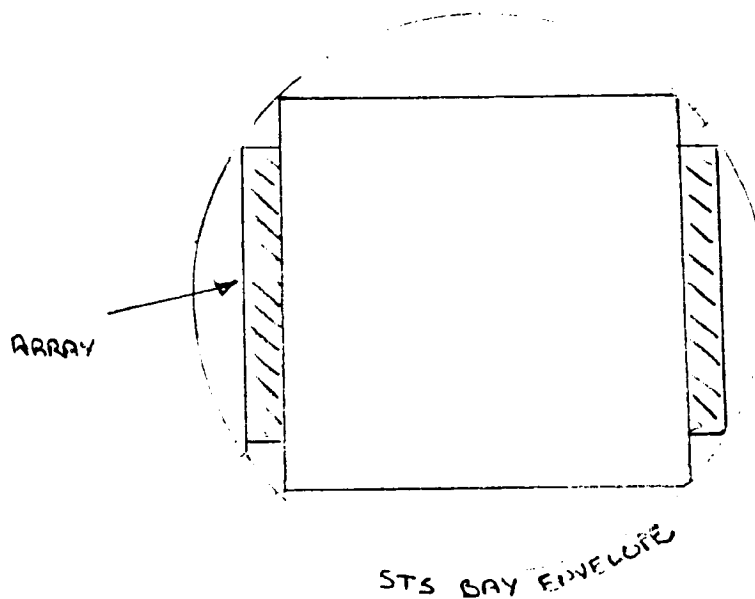


Figure 3 Candidate Wing Stowage Configurations

14. Based on your present understanding of your spacecraft and launch vehicle integration, can you provide the size and shape of the stowage volume available for each stowed wing? Please use a supplemental sheet to answer this question identifying the spacecraft name with each sketch.

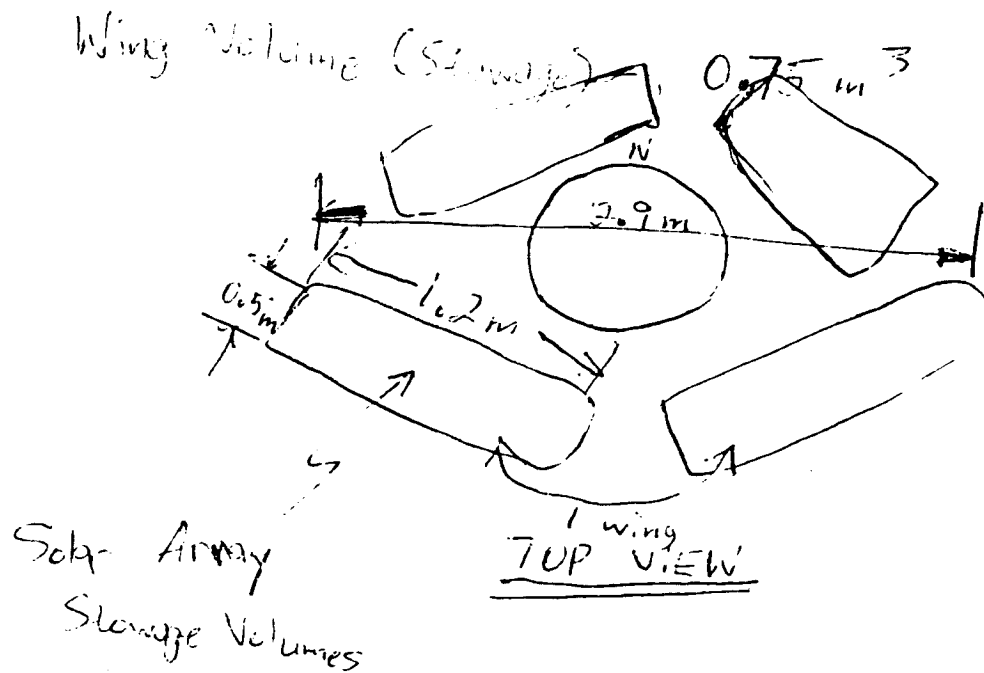
- A. No
- B. No Response
- C. No Response
- D. Shuttle Payload Bay
- E. Not Available for Any Spacecraft Discussed
- F. N/A
- G. Supplemental Information for Question #14

It is difficult to provide a specific answer for generic spacecraft. In general, the array should be stowable within the chordal segments shown in the sketch. Length (into paper preferably less than 5 feet).

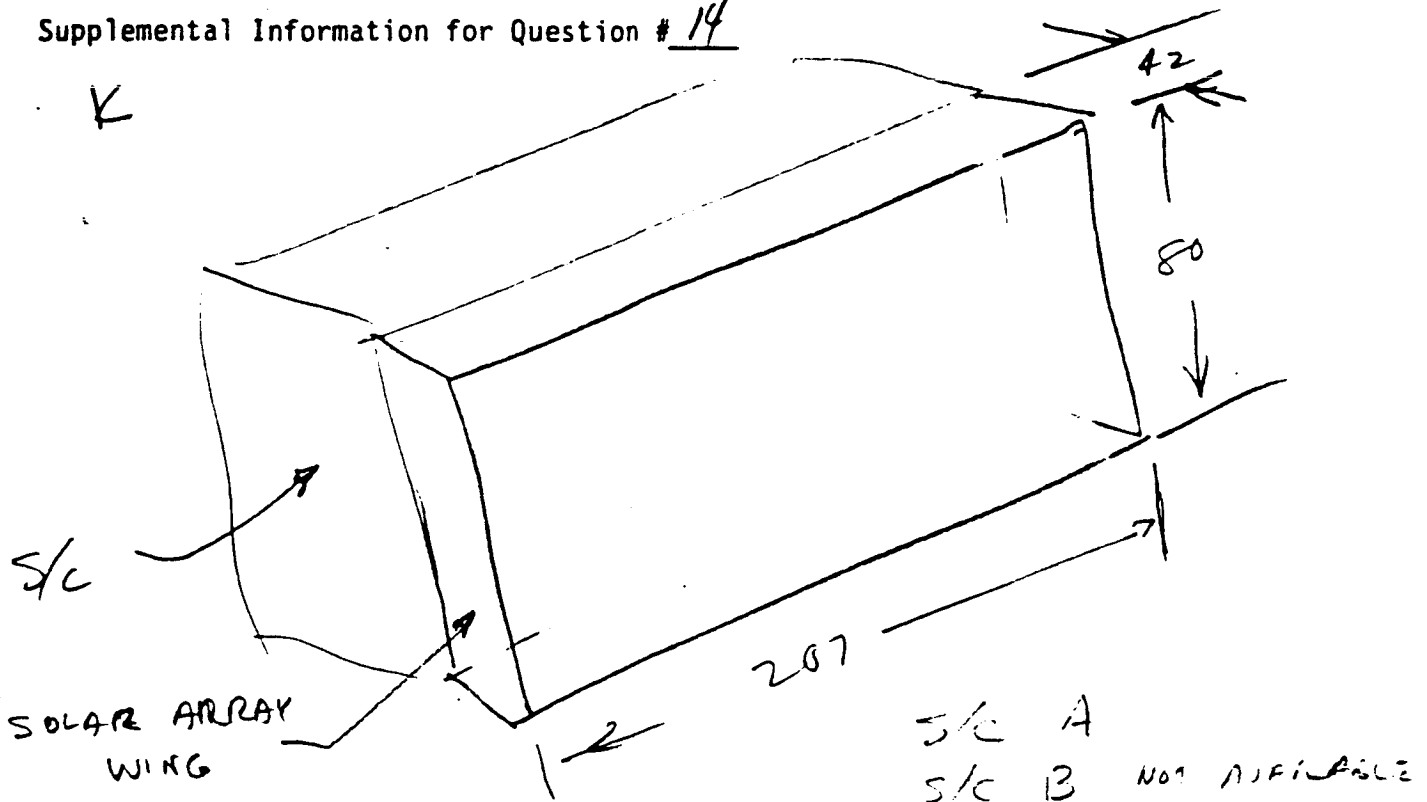


- H. Stowage Volume Approximately 120x87x32 inches
- I. (supplemental info on back)
- J. No. Details Not Available in General
- K. No Response

I
Supplemental Information for Question # 14



K
Supplemental Information for Question # 14



15. ON WHAT SPACECRAFT BODY SURFACES CAN THE STOWED WINGS BE LOCATED? PLACE AN (X) IN THE APPROPRIATE SPACE. THE ANSWER TO THIS QUESTION CAN BE INCLUDED ON SKETCHES PROVIDED FOR QUESTION 14.

COMPANY	SPACECRAFT NAME	ON THE NORTH & SOUTH FACING SIDES	ON THE EAST & WEST FACING SIDES	ON THE NADIR FACING SIDE	ON THE ZENITH FACING SIDE	PARTICALLY WITHIN THE SPACECRAFT BODY VOLUME*
A	A	X				POSSIBLY
B	NO RESPONSE					
C	NO RESPONSE					
D	SPACE STATION SPACE STATION PLATFORM	ASTRONOMY EXPERIMENTS			X GRAVITY EXPERIMENTS	
E	A B C		X INERTIAL STABILIZED, SUN POINTING SIDE INERTIAL STABILIZED, SUN POINTING SIDE			
F	SSIS BSIS ADV. GPS	X X X	X X X			
G	A B C	X* X* X*				PARTIALLY YES YES
H	RADARSAT		ONE PAGE ONLY			
I	A	X	X			
J	NO DETAILED INFORMATION AVAILABLE					
K	A	X				
L	A B C				X X	X X
				X		

*THE TERMS N/S AND S/W ARE AMBIGUOUS FOR LEO S/C. STOWAGE ON THE FACE NORMAL TO THE DEPLOYED BOOM AXIS IS PREFERRED.

16. WHAT STANDOFF OR CLEARANCE DISTANCE IS REQUIRED BETWEEN THE ADJACENT SPACECRAFT BODY SURFACE AND MOST INBOARD LOCATION OF SOLAR CELLS OR BLANKET HOUSING ASSEMBLY STRUCTURE? INDICATE THE REASON FOR THE REQUIREMENT.

COMPANY	SPACECRAFT NAME	STANDOFF DISTANCE (INCHES)	KEY REASON FOR REQUIREMENT. PLACE AN (X) IN THE APPROPRIATE BOX.			
			PREVENT PERMANENT SHADOWS ON CELLS	REDUCE INTER-ACTION WITH RADIATOR SURFACES	PREVENT PHYSICAL INTERFERENCE WITH OTHER APPENDAGES	OTHER*
A	A	30-80**	X			
	B	30-80**	X			
B	NO RESPONSE					
C	SBR	---	X		X	ANTENNAE
D	SPACE STATION	---	X			
	SPACE STAT. PLAT.	---	X			
E	A	NOT AVAIL.				
	B	0				CONFIGUR. D/N REQ. STANDOFF
	C	0				"
F	SSTS	36" MIN.	X		X	
	BSTS	36" MIN.	X		X	
	ADV. GPS	36" MIN.	X		X	
G	A	100				TO MINIMIZE PLUME IMPINGEMENT
	B	25			X	
	C	25			X	
H	RADARSAT	120	X		X	
I	A	6			X	
J	(SEE BACK)					
K	A	48				
L	A	5 FT			X	
	B	10 FT			X	
	C	5 FT	X			

** DEPENDS ON MAIN BODY CONFIGURATION

17. IS SHADOW PROTECTION REQUIRED BECAUSE OF TRANSIENT OR QUASI-STEADY STATE SHADOWS ON THE SOLAR CELLS FROM OTHER SPACECRAFT STRUCTURES? PLACE AN (X) IN THE APPROPRIATE SPACE AND PROVIDE ADDITIONAL DATA IF APPLICABLE.

COMPANY	SPACECRAFT NAME	TRANSIENT SHADOWS	QUASI-STEADY STATE SHADOWS	DESCRIPTION OF SHADOWS (I.E., RATE OF MOVEMENT AND SIZE, SHAPE)
A	A	YES		{ DEPENDS ON MAIN BODY GEOMETRY.
	B	YES		{ VARIOUS TYPES OF SHADOWS POSSIBLE
B	NO RESPONSE			
C	NO RESPONSE			
D	SPACE STATION		X	
	SPACE STAT. PLAT.		X	
E	NO RESPONSE			
F	SSIS	X	X	TBD
	BSIS	X	X	TBD
	ADV. GPS	X	X	TBD
G	A		X	POSSIBILITY OF PARTIAL SHADOWING BY A MESH ANTENNA
	B			
	C		X	MAIN BODY SHADOWING TRANSVERSING AT ORBITAL RATE
H	RADARSAT	X	X	
I	A	X		LINES APPROX. 1 INCH WIDTH, 1 FT/MIN. VELOCITY
J	(SEE BACK)			
K	B	X		N/A
L	A	X		
	B	X		
	C	X		

J. Supplemental Information for Question #16 & 17

Clearance distance is used on the space station for provision of an alpha joint, power distribution equipment, and a "reasonable" number of five meter bays of truss structure. How much space is needed for shadowing purposes is a subject of intensive study by the power system contractors (TRW and Rocketdyne). Shadows are caused by the regular rotation of the solar arrays to face the sun and the subsequent shadowing of the arrays by the various payloads on the station. These are very regular, transient shadowing requirements estimated at 5 percent or less.

18. PLEASE LIST OTHER PERFORMANCE REQUIREMENTS, FOR YOUR POTENTIAL SOLAR ARRAY APPLICATIONS. PLACE AN (X) IN THE APPROPRIATE BOX AND PROVIDE ADDITIONAL DATA IF APPLICABLE IN THE FOLLOWING TWO TABLES.

COMPANY	SPACECRAFT NAME	PARTIAL* EXTENSION	PARTIAL* RETRACTION	FULL* RETRACTION	FULL* RESTOWAGE	KEY REASONS FOR THE REQUIREMENT
A	NO RESPONSE					
B	NO RESPONSE					
C	RESTOWAGE MAY BE NEEDED FOR PLANE CHANGE OR ROTATION FOR SURVIVABLE REQUIREMENTS					
D	SPACE STATION				TBD	{ COST EFFECTIVENESS OF REPAIRING DEFECTIVE SOLAR ARRAY WINGS.
	SPACE STATION PLATFORM				TBD	
E	A				X	
F	SSIS	X	X	X	X	{ MANEUVERING, SURVIVABILITY P/L REQMS.
	BSIS	X	X	X	X	
	ADV. GPS	TBD	TBD	TBD	TBD	
G	A	X ONCE, 25%		X	X	{ PROVIDE POWER IN TRANSFER ORBIT FOR SERVICING* (3 CYCLES) & FOR REPLACEMENT (1 CYCLE)
	B			X	X	
	C			X	X	
H	RADARSAT			X	X	RETRIEVAL, SERVICING
I	A	X		X		VARIOUS POWER REQMS FOR DIFFER. MISSION PHASES
J	SPACE STATION PLATFORM WILL USE "SHORTENED" VERSIONS OF REGULAR SOLAR ARRAYS, AND THEY HAVE TO FULLY RETRACT FOR SERVICING					
K	NO RESPONSE					
L	A					
	B	X				
	C				X	

* EXCLUDING GROUND TEST

QUESTION 18. CONT.						
COMPANY	SPACECRAFT NAME	STOWED WING FREQUENCY (HZ)	DEPLOYMENT DURING TRANSFER ORBIT	TRANSFER ORBIT PWR (KW) & VOLTAGE LEVEL (V)	MINIMIZE CURRENT-GENERATED MAGNETIC FIELDS	MILITARY HARDENING OR SURVIVABILITY*
A	A B	>50HZ FOR THE TYPE OF ARR. YOU HAVE DESCR. TO SHOW COMPACTITY	YES YES	{ DEPENDS	YES YES	NO NO
B	NO RESPONSE					
C	A B					SCOPA HARDENING GOALS SDI HARDENING GOALS
D	SPACE STATION SPACE STATION PLATFORM				X X	
E	A B C	NOT AVAIL. NOT AVAIL. NOT AVAIL.	NO NO NO	0 KW, 0V 0 KW, 0V 0 KW, 0V	X NO NO	X PROJECT DOCUMENTS PROJECT DOCUMENTS
F	SSTS BSTS ADV. GPS	TBD TBD TBD	MAYBE NO NO			DOD SSTS-MRDA CONTRACT DOD BSTS-MRDA CONTRACT IN-HOUSE STUDY & IR&D
G	A B C	>50 >50 >50	X(PARTIAL) X(FULL) X(FULL)	1.0 KW, 40V --- ---	X X X	DMSS-SVR-250 15 MARCH '82 ---
H	RADARSAT		X		X	
I	NO RESPONSE					
J	NO RESPONSE					
K	NO RESPONSE					
L	A B C		NO NO NO			

19. Provide other comments or information that would be helpful to the design development and demonstration of the JPL Advanced Photovoltaic Solar Array.
- C. Experiments are planned to study environment interactions on solar arrays at high voltages. Data should be available in the 1989 time period.
- D.
 - Current criticism of solar arrays is the large area required for 300 kw, therefore (kw/m^2) is a little more important than (kw/kg). Also ($\text{\$/kg}$) has not been brought up. This might limit the size of the space station.
 - Currently the space station is under study and there are no firm hardware requirements.
 - Systems engineers are uneasy about orienting large area solar arrays with respect to the sun and spacecraft.
 - Criticism of Figure 2B. A split blanket in-plane boom would increase array area a little.
Criticism of Figure 2C. The slanted V-stiffened blanket would require a larger area array.
Criticism of Figure 2D. A double boom will increase array weight.
- E.
 - Military missions require laser hardened solar arrays.
 - Deployed stiffness and strength are orders of magnitude higher than the proposed for APSA.
 - 1987 technology seems to be too near term for consideration today on the advanced systems we are involved with.
- F. Our future military application missions require high ICS & SMATH level design or/and fast retraction array rate.
- G. Thermal shock characteristics (upon entering or leaving eclipse) could be important for precision attitude control applications. Preliminary data should be issued to potential users ASAP.
- H. Replaceability on orbit.
- J. Detailed information on photovoltaic array design for space station use (primary user in the near term) must be obtained from the Lewis Research Center Space Station Office. They should coordinate with OAST and JPL on this development and testing program.

REFERENCES

1. Advanced Photovoltaic Solar Array Design, "Preliminary Design Review Data Package (CDRL 003)," JPL Contract 957358, TRW Report No. 46810-6001-UT-00, 11 March 1986.
2. Advanced Photovoltaic Solar Array Design, "Final Design Review Data Package (CDRL 005), Volume 1: Design Summary and Implementation Plan," JPL Contract 957358, TRW Report No. 46810-6003-UT-00, 25 June 1986.
3. Advanced Photovoltaic Solar Array Design, "Final Design Review Data Package (CDRL 005), Volume 2: Prototype Wing Configuration Drawings," JPL Contract 957358, TRW Report No. 46810-6003-UT-00, 25 June 1986.
4. R. E. Patterson, "NASA Welding Assessment Program," Final Test Report on JPL Contract 956042, TRW Report No. 38512-6003-UT-00, January 1985.
5. R. E. Patterson, et al., "Development of Flight-Ready 50-Micron-Thick Silicon Solar Cell Array Module Technology," to be presented at the 21th IECEC, San Diego, CA, 25-29 August 1986.
6. R. M. Kurland, et al., "Ultralightweight Solar Array Technology," Proceedings of the Third European Symposium on Photovoltaic Generators in Space, Bath, England, May 1982.
7. C. K. Purvis, et al., "Design Guidelines for Assessing and Controlling Spacecraft Charging Effects," NASA TP 2361, September 1984.
8. T. Wakita, et al.; "Development of Large-Area Amorphous Silicon Solar Cells," Proceedings of the 20th IECEC, Volume 3, pp 3-470 to 3-475, Miami Beach, Florida, August 1985.
9. A. F. Whitaker, et al., "Characterization of Three Types of Silicon Solar Cells for SEPS Deep Space Missions, Volume 1: Current-Voltage Characteristics of OCLI BSF/BSR 10 Ω -cm and BSR 2 Ω -cm Cells as a Function of Temperature and Intensity," NASA TM 78253, November 1979.
10. A. F. Whitaker, et al., "Characterization of Three Types of Silicon Solar Cells for SEPS Deep Space Mission, Volume 3: Current-Voltage Characteristics of Spectrolab Sculptured BSR/Pt (K7), BSR/Pt (K6.5) and BSR (K4.5) Cells as a Function of Temperatures and Intensity," NASA TM 78305, August 1980.
11. D. F. Ferguson, "The Energy Dependence and Surface Morphology of Kapton Degradation Under Atomic Oxygen Bombardment," Proceedings of the 13th Space Simulation Conference, pp 205 to 221, NASA/GSFC, October 1984.